



*Smart system of renewable energy storage based on **IN**tegrated **EV**s and **bA**tteries to empower mobile, **D**istributed and centralised **E**nergy storage in the distribution grid*

Deliverable n°:	<b>D5.4</b>
Deliverable name:	<b>Advanced Optimal Battery operation and control algorithm</b>
Version:	<b>1.0</b>
Release date:	<b>17/12/2018</b>
Dissemination level:	<b>Public</b>
Status:	<b>Submitted</b>
Author:	<b>Pol Olivella-Rosell, Pau Lloret, Leon Haupt and Sara Barja – UPC</b> <b>Sigurd Bjarghov, Venkatachalam Lakshmanan, Hossein Farahmand, Magnus Korpås – NTNU</b> <b>Juha Forsström, Victor Mukherjee, Ari Hentunen – VTT</b> <b>Stig Ødegaard Ottesen, Terje Lundby – eSmart</b>



**Document History:**

Version	Date of issue	Content and changes	Edited by
0.1	24/11/2018	Executive summary	Hossein Farahmand
1.0	17/12/2018	Updated based on reviewers comments	Hossein Farahmand, Venkatachalam Lakshmanan

**Peer reviewed by:**

Partner	Reviewer
SIN	Jayaprakash Rajasekharan
ElaadNL	Patrick Rademakers

**Deliverable beneficiaries:**

WP / Task
WP5 / Task 5.3 and 5.4
WP8 / Task T8.3
WP6
WP10, Pilots

## Executive summary

The renewable energy source (RES) penetration in the electricity network is highly depend on the ways to manage the variations in their energy production, and many methods including demand-side management are available. Maturing battery technologies and decreasing price of batteries creates special interest in mitigating the fluctuations in RES energy production by adding electrical storage in electric network. The main focus of the INVADE project is to study possibilities to increase RES penetration and integration in the power system by adding storage. In this respect, the analysis within the project centres on the flexibility services from different types of batteries, namely: centralized, distributed and mobile (EVs). The focus of the work package 5 (WP5) is to manage several distributed flexible, and find cost-effective investment decision to install batteries. Deliverable D5.4 provides an advanced optimal battery operation and planning algorithm, and it is a complement to the D5.3.

The report is split into two documents. The first document details the modelling framework for the flexibility management algorithm. Detailed model of batteries based on D6.2, EV model, and thermal load models are explained. The overall framework of optimization and the variable fixing issues and their solution approaches are presented in order to deal with uncertainties during operation planning. Finally, aggregated flexibility services that can be offered to external agents, i.e., BRPs and DSOs are elaborated. This document contains a detailed description of the algorithms that will be used in the daily operations of flexibility assets.

The second document deals with a detailed explanation of the bi-level robust algorithm for optimal investment decisions on battery storage systems including optimal sizing and placement. In order to deal with the uncertainty modelling in the storage planning problems, robust optimization of storage investment is adapted. The robust optimization framework represents a tractable uncertainty modelling structure, which has a potential to be applied in large-scale systems. The proposed scheme is applied to 19-bus LV CIGRE benchmark grid to investigate the capability and efficiency of the model. However, it is not applied in INVADE pilots since our information about the relevant pilots is limited.

Deliverable 5.4 presents the necessary methods and models for the development of the integrated INVADE platform to serve 5 pilots based on the framework described in D4.3.



*Smart system of renewable energy storage based on **IN**tegrated **EV**s and **bA**tteries to empower mobile, **D**istributed and centralised **E**nergy storage in the distribution grid*

Deliverable n°:	<b>D5.4 A</b>
Deliverable name:	<b>Flexibility management algorithms</b>
Version:	<b>1.0</b>
Release date:	<b>17/12/2018</b>
Dissemination level:	<b>Public</b>
Status:	<b>Submitted</b>
Author:	<b>Pol Olivella-Rosell, Pau Lloret, Leon Haupt and Sara Barja – UPC</b> <b>Sigurd Bjarghov, Venkatachalam Lakshmanan, Hossein Farahmand, Magnus Korpås – NTNU</b> <b>Juha Forsström, Victor Mukherjee, Ari Hentunen – VTT</b> <b>Stig Ødegaard Ottesen, Terje Lundby – eSmart</b>



**Document history:**

Version	Date of issue	Content and changes	Edited by
0.1	01/10/2018	First draft, proposing outline and structure of the document	H. Farahmand, S. Bjarghov, V. Lakshmanan, P. Olivella-Rosell, P. Lloret
0.2	10/10/2018	Adding space heating model	V. Lakshmanan and H. Farahmand
0.3	15/10/2018	Adding Pilot structure based on internal documents provided by Stig Ødegaard Ottesen	H. Farahmand
0.4	16/10/2018	Adding electric water heater and EV model	P. Olivella-Rosell
0.4	20/10/2018	Adding Battery Model	S. Bjarghov
0.5	1/11/2018	Adding Information structure and the planning process	V. Lakshmanan
0.6	10.11.2018	Chapter on Aggregated flexibility services	P. Olivella-Rosell, P. Lloret
0.7	10/11/2018	Chapter on Variable fixing technique	V. Lakshmanan and S. Bjarghov
0.8	12/11/2108	Improve the domestic space heating model based on feedback received from Prof. Magnus Korpås	V. Lakshmanan and H. Farahmand
0.9	15/11/2018	Inputs from VTT to battery model	Juha Forsström, Victor Mukherjee, Ari Hentunen
0.91	20.11.2018	Improve battery modelling	S. Bjarghov, J. Forsström, V. Mukherjee, A. Hentunen
0.92	24.11.2018	Final Edit	V. Lakshmanan, S. Bjarghov, H. Farahmand, P. Olivella-Rosell and P. Lloret
0.93	27.11.2.18	Chapter 11 and section 10.5 is completed	P. Olivella-Rosell, P. Lloret and V. Lakshmanan,
1.0	14.12.2018	Addressing the reviewers' comments	V. Lakshmanan and H. Farahmand

**Peer reviewed by:**

Partner	Reviewer
SIN	Jayaprakash Rajasekharan
ElaadNL	Patrick Rademakers

**Deliverable beneficiaries:**

WP / Task
WP5 / Task 5.3 and 5.4
WP8 / Task T8.3
WP10, Pilots

## Table of contents

<b>Executive summary .....</b>	<b>12</b>
<b>1 Introduction .....</b>	<b>13</b>
<b>2 Simplified models and advanced models .....</b>	<b>14</b>
2.1 Battery model	14
2.2 EV model	15
2.3 Thermal load model	15
2.3.1 Electric Water heater model	15
2.3.2 Space heating model	15
<b>3 Battery model .....</b>	<b>16</b>
3.1 Simple battery model	16
3.2 Advanced battery model	16
3.2.1 Constant voltage charging constraint	16
3.2.2 Piecewise linearized battery efficiency	17
3.2.3 Battery degradation	23
3.2.4 Degradation modelling	27
<b>4 EV model .....</b>	<b>31</b>
4.1 Introduction	31
4.2 EV mathematical formulation	31
<b>5 Electric water heater model .....</b>	<b>34</b>
5.1 Introduction	34
5.2 Thermal load modelling – Electric water heater	35
5.3 Electric Water Heaters (EWH), Shiftable Energy Volume	35
<b>6 Space Heating Model .....</b>	<b>43</b>

6.1	Introduction	43
6.2	Thermal load modelling - Space heating	43
6.3	Control limitations	44
6.4	Flexibility	47
6.5	Mathematical formulation	48
6.6	Runtime constraints	49
6.7	Time restriction of flexibility activation	50
6.8	Identification for 'start', 'run' and 'end' of flexibility activation	51
6.9	Maximum duration of flexibility activation constraint	51
6.10	Minimum duration between successive flexibility activation constraint	52
6.11	Maximum number of flexibility activation constraint	52
6.12	Flexibility contract cost	53
6.13	The complete model	53
6.14	Illustrative example	55
<b>7</b>	<b>Information structure and the planning process.....</b>	<b>58</b>
7.1	Introduction	58
7.2	Length of planning horizon	58
7.3	Time resolution	59
7.4	Receding and rolling process	59
7.5	Overall framework	60
	7.5.1 Program control flow	61
<b>8</b>	<b>Variable freezing techniques.....</b>	<b>64</b>
8.1	Problem description	64
8.2	Variable freezing approaches	68
	8.2.1 Approach 1: Running constraints for the entire time horizon	68



8.2.2	Approach 2: Running constraints (only) for current and future time periods	73
8.3	The t-1 issue	75
8.4	Overall evaluation of approaches	76
8.4.1	Approach 1	76
8.4.2	Approach 2	76
<b>9</b>	<b>Pilot structures .....</b>	<b>77</b>
9.1	Introduction	77
9.2	Norwegian case study	78
9.2.1	Structure information and historic meter values	78
9.2.2	Commercial/agreement information	79
9.2.3	Grid contract	79
9.2.4	Retail contract	81
9.2.5	Flexibility	81
9.2.6	An illustrative example	84
9.3	Dutch case study	88
9.3.1	Introduction	88
9.3.2	Structure information and historic meter values	89
9.3.3	Objectives	90
9.3.4	Flexibility and decisions	93
9.4	Bulgaria case study	101
9.4.1	Introduction	101
9.4.2	Structure information and historic meter values	101
9.4.3	Real-time meter values in general	102
9.4.4	Commercial/agreement information	103
9.4.5	Flexibility	103
9.4.6	An illustrative example	106

<b>10 Prosumer objective functions .....</b>	<b>109</b>
10.1 Norwegian case study	109
10.1.1 Periods smaller than 1 hour	110
10.2 Dutch pilot	110
10.2.1 Pilot 1: Home charging	111
10.2.2 Pilot 2: Large scale offices and parking lots	113
10.2.3 Pilot 3 Small scale office	114
10.2.4 Pilot 4 Large scale public	115
10.3 Bulgarian pilot	116
10.4 Spanish pilot	116
10.5 Illustrative prosumer results	116
<b>11 Aggregated flexibility services .....</b>	<b>122</b>
11.1 Introduction	122
11.2 Flexibility request prioritization	122
11.3 Flexibility availability algorithm	123
11.4 Centralized mathematical formulation	124
11.5 Distributed mathematical formulation	125
11.6 Objective functions in pilots	126
11.6.1 Spanish objective function	126
11.6.2 German objective function	126
11.7 DSO case study	127
11.7.1 Spanish case study	127
11.7.2 German case study	132
11.8 BRP case study	132
11.8.1 Spanish case study	132
<b>12 Conclusions.....</b>	<b>133</b>

<b>13 Appendix: Offline software testing manual .....</b>	<b>135</b>
13.1 Introduction	135
13.2 Building a test case and running	135
13.3 Solver selection and MIP gap input	137
13.4 Automatic model building	137
13.5 Site implementation	138
13.6 Input data file structure	140
13.6.1 “TestCaseData.xlsx”	140
13.6.2 Site configuration and resource information	141
13.6.3 Prosumer.xlsx	142
13.6.4 Storage_x.xlsx	143
13.6.5 Charging_x.xlsx	144
13.6.6 Generation_x.xlsx	146
13.7 Running a test case	146
13.8 Output file format	147
13.8.1 Site_x_control_signals.xlsx	147
13.8.2 Site_x_prosumer_costs_and_energy_balance.xlsx	148
13.9 Testing the RH code including variable fixing	152
13.9.1 Changes into the main code file	153
13.9.2 To copy applied values of the current execution time to the next period	153
13.9.3 To fix the variables for the past periods	155
13.9.4 To add metered values from past periods to the baseline	156
<b>14 Appendix: Overview of sets, parameters and variables .....</b>	<b>158</b>
14.1.1 Sets	158
14.1.2 Parameters	159
14.1.3 Variables	166



## Abbreviations and Acronyms

Acronym	Description
AHES	AMI Head End system
API	Application programming interface
BMS	Battery Management System
BRP	Balance Responsible Party
BS	Balance Scheduling
CEM	Customer energy management system
CPO	Charge point operator
DER	Distributed Energy Resources
DMS	Distribution management system
DOD	Depth of discharge
DSO	Distribution System Operator
EMG	Energy Management Gateway
EOL	End Of Life
ESS	Energy Storage System
EV	Electric Vehicle
EVSE	Electric Vehicle Supply Equipment
EWH	Electric water heater
FEP	Front End Processor
FO	Flexibility Operator
IEC	International Electrotechnical Commission
IED	Intelligent Electronic Device
IIP	Integrated INVADE Platform
LV	Low Voltage
MDC	Meter Data Concentrator
MDM	Meter data management
MR	Meter Reader
MV	Medium Voltage
NA	Not Applicable
OCHP	Open Clearing House Protocol
OCPI	Open Charge Point Interface
OCPP	Open Charge Point Protocol
OCMP	Open Charge Management Protocol

<b>Acronym</b>	<b>Description</b>
OM	Operation meter
OSCP	Open Smart Charging Protocol
PCS	Power Conversion System
PRIME	PowerLine Intelligent Metering Evolution
PV	Photovoltaic
RTU	Remote Terminal Unit
SCADA	Supervisory control and data acquisition
SDC	Smart device controller
SGAM	Smart Grid Architecture Model
SM	Smart Meter
SOH	State of Health
TBD	To Be Determined
ToU	Time-of-Use
TSO	Transmission System Operator
USEF	Universal Smart Energy Framework
V2G	Vehicle to Grid
WP	Work Package

## Executive summary

Flexibility management algorithm comprises the necessary methods and models for the development of integrated INVADE platform. The platform will support many different functional areas, but the main development in the INVADE project is the cloud based flexibility management system, which will be used in the daily operations of the different flexibility services. A first, simplified version of the developed algorithm has been delivered to the integrated INVADE platform in June 2018. The output of the algorithm includes the decision support for the optimal operation of flexibility assets. The algorithm can be integrated into real-time control for managing several distributed flexible resources such as a fleet of EVs and other consumer flexibility assets. The platform incorporate flexibilities from a local to a regional perspective by introducing Flexibility Operator. Flexibility Operator is in charge of flexibility management at integrated INVADE platform.

In this document we formulate the flexibility management algorithm both from prosumer perspective and from BRP and DSO perspective, which is an aggregated level. The aggregated flexibility algorithm ensures that each prosumer providing flexibility to external agents will be economically rewarded and the FO will schedule the minimum cost flexibility sources at the same time.

This document contains a detailed description of the algorithms that will be used in the daily operations and it is a complement to the D5.3. First, the mathematical formulation of available flexibility assets at INVADE pilots are reviewed. Secondly, chapter eight presents the program framework and it constitutes a general overview about the files structure with special attention to the input and output files. It presents the receding horizon approach used to reproduce the daily operations. Finally, the document explains aggregated flexibility services that can be offered to external agents, i.e., BRPs and DSOs.

Overall, the document encompasses methodologies for improved management of the flexibility resources based on forecasting information of the system.

# 1 Introduction

According to the DoA the deliverable D5.4 is Advanced Optimal Battery operation and control algorithm. This report contains the final version of the flexibility management allocation and operation algorithms from T5.3 and T5.4. This version includes more technical parameters and detailed use case scenarios for operating the INVADE platform. This version will be implemented in the INVADE Platform. The work in this document is built upon the content in several other deliverables in different work packages: D4.1 [1], D4.2 [2], D5.1 [3], D5.2 [4], D5.3 [5] and D10.1[6].

The main purpose with this document is to provide advanced optimization models for the flexibility resources used in the flexibility algorithms defined in D5.3 [5]. These models are the extension of simplified models used in the Integrated INVADE platform through the task T8.3. The task T5.4 has implemented the simplified battery operation and control algorithm described in D5.3 [5].

An overview of different flexibility services and how they will be implemented in the different pilots are defined in D4.3 [7].

**Table 1: Overview of flexibility services to be used in each pilot (Y: yes; N: no).**

Flexibility customer	Flexibility services INVADE	Norwegian pilot	Dutch pilots	Bulgarian pilot	German pilot	Spanish pilot
DSO	Congestion management	N	Y	N	Y	Y
	Voltage / Reactive power control	N	Y	N	Y	Y
	Controlled islanding	N	N	N	N	Y
BRP	Day-ahead portfolio optimization	N	N	N	N	N
	Intraday portfolio optimization	N	N	N	N	N
	Self-balancing portfolio optimization	N	N	Y	N	Y
Prosumer	ToU optimization	Y	Y	Y	N	N
	kWmax control	Y	Y	Y	N	N
	Self-balancing	Y	Y	Y	Y <sup>1</sup>	N
	Controlled islanding	N	N	N	N	N

---

<sup>1</sup> Prosumer self-balancing service is going to be supplied by local home management system product from SMA (<https://www.sma.de/en.html>) outside the scope of the INVADE project



The rest of this document is organized as follows: Chapter 2 describes the main differences between the simple models described in D5.3 and the advanced models presented in this document. A detailed model of battery, which the main source of flexibility in INVADE project is detailed in Chapter 3. Updated EV models are described in Chapter 4. Chapter 5 and 6 describes both thermal loads water heater and space heating in detail in the respective chapters. Chapter 7 – Information structure and the planning process, Chapter 8 presents the possible variable fixing methods and their advantages and disadvantages. The 5 different pilot structures and detailed in Chapter 9. The objective functions related to prosumer services are presented in Chapter 10 and the objective functions related to aggregated flexibility services are presented in Chapter 11. Finally the Chapter 12 presents the concluding remarks.

## **2 Simplified models and advanced models**

In D 5.3 [5], simplified models of all flexible resources were discussed with generalised perspective. This chapter outlines the specific characteristics of model for each flexible resources and highlights the differences compared to the simple model.

### **2.1 Battery model**

The proposed simple battery model in D5.3 considers the battery to have constant charging and discharging efficiency for all values of the charging and discharging power. In reality, the efficiency changes in a nonlinear way for different charging and discharging power values. Also, the model considers the battery capable to charge with constant current in the whole region of its state of charge. The simple model doesn't consider different types of battery degradation.

The advanced model includes the nonlinear change in efficiency with charging and discharging power by splitting the charging and discharging power regions in multiple parts and linearizing the efficiency by adopting piecewise linearization technique.

The battery degradation is accounted separately for its calendar ageing and cycle ageing. More technical descriptions are detailed in the Chapter 3.

## 2.2 EV model

In D5.3, the EV models proposed considers that the EVs charging power can be controlled to any value between zero and their maximum charging power. But in reality, the charging power has a much higher non-zero minimum value below which the next possible value is zero. Moreover, in the communication protocol between charger and car the low non-zero values are not allowed, and experience shows that most cars stop charging below 11 amps. Therefore, the variable corresponding to the charging power cannot be continuous variable. This expanded model allows to set the charging power between a maximum and minimum charging levels or on/off regulation, depending on case.

In D5.3, the V2G model is included. However, there are several uncertainties about the available information and the final plan for the application of this technology in INVADE platform, which makes it difficult to decide, what would be the improvement to that model.

## 2.3 Thermal load model

For thermal loads, in D5.3 a state queue model and black box approach with temperature prediction were proposed. Both methods assumes that there minimum two measurement parameters namely temperature and power consumption are available. But in reality, only power consumption measurements are available. Therefore, the thermal loads were classified into two different categories as space heaters and water heaters.

### 2.3.1 Electric Water heater model

The electric water heaters can be treated as a curtailable disconnectable load models. The main problem is that the energy curtailed will never be recovered. Therefore, shiftable energy volume model is proposed which can consider the re-bound effect to consume the energy curtailed during flexibility activation.

### 2.3.2 Space heating model

The new space heating model assumes that there are three different temperature states possible. And there is a possibility to predict the energy requirement to achieve the three different temperature states using machine learning. The flexibility available between the upper and lower energy levels are captured in the new model proposed. More technical details are elaborated in the Chapter 6.

### 3 Battery model

In this chapter we briefly present the simplified battery model, followed by a detailed description of what is new in the advanced battery model.

#### 3.1 Simple battery model

The constraints needed to model the energy capacity and state of energy have been presented in D5.3 but will be repeated here. This simple model contains the basic equations needed to operate a battery, but lacks features such as degradation costs (both cycle and calendar ageing), non-linear efficiency and non-constant-current charging regions. These new features will be presented in the following subsections.

#### 3.2 Advanced battery model

The advanced battery model contains new functionalities such as cyclic ageing, calendar ageing, piecewise linearized efficiency and constant voltage charging constraints. These are presented in the following subsections. All notation that is new is listed in this deliverable, but notation that is similar to the notation used in D5.3 is not repeated.

##### 3.2.1 Constant voltage charging constraint

In order to avoid reaching minimum and maximum cell voltages during operation, additional constraints are needed. As described in D6.5, the CC (constant current) charging region of a battery does not apply to the full SOC area of a battery. The following constraints reduces the allowed charging power when approaching the minimum and maximum energy levels. This will prevent scenarios where we calculate the state of charge to reach its maximum value in time step  $t$ , when actually the battery management system restricted the charging power, resulting in a lower state of charge than expected.

$$\sigma_{b,t}^{B,dis} \leq Q_b^{B,dis} \cdot \frac{[\sigma_{b,t-1}^{B,SOC} - O_b^{B,min}]}{(1 + w_b^B) N^{hour}}, \forall b \in B, t \in T \quad (1)$$

$$\sigma_{b,t}^{B,ch} \leq Q_b^{B,ch} \cdot \frac{[O_b^{B,max} - \sigma_{b,t-1}^{B,SOC}]}{(1 + w_b^B) N^{hour}}, \forall b \in B, t \in T \quad (2)$$

The tuning parameter  $w_b^B$  can be used to tune to which extent the charging has to be slowed down when approach minimum or maximum state of charge. This is more thoroughly explained in D6.5.

### 3.2.2 Piecewise linearized battery efficiency

The efficiency of the energy storage system is a combination of the battery efficiency and the inverter efficiency. Inverter efficiencies are normally very strong (>98%) around the rated power, but can be weak at low power. The battery efficiency mostly depends on ohmic losses inside the battery.

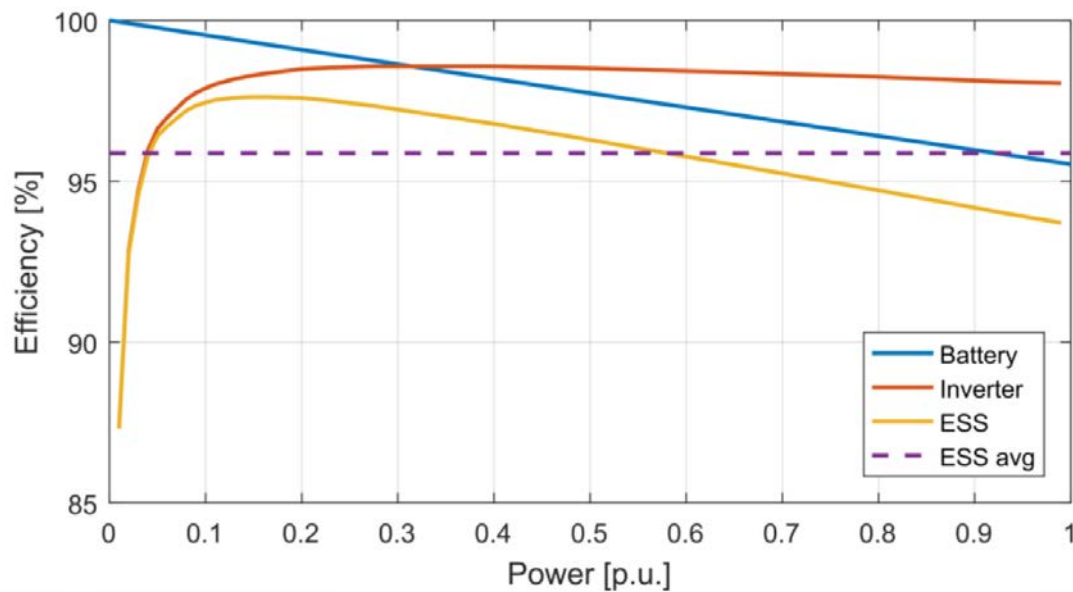


Figure 1: Energy storage system efficiency curves.

Figure 1 shows that the inverter efficiency is high and stable around 98 % for most segments of the rated power capability (red curve), except for the low power segment (< 5% of rated power). The battery losses are close to zero for low power, and linearly increases to around 4 % at full power (blue curve). The combined efficiency of the storage system is shown as the yellow line and has an average efficiency of 96 % as indicated by the purple line. The easiest approach is to model the efficiency as a constant with 96 % efficiency (or any other constant efficiency of an ESS), however, as the curve shows, this could lead to an error of about 2%, and even more if the discharge/charge power is low. One approach is piecewise linearization, which means creating segments of efficiencies which are dependent on the rated power used in the optimization.

Table 2: (Dis)advantages with both efficiency modelling methods

	Advantages	Disadvantages
<b>Constant efficiency</b>	<ul style="list-style-type: none"> <li>• Solves fast</li> <li>• Easy to implement</li> <li>• If degradation cost is modelled properly, efficiency is a minor cost factor in comparison</li> </ul>	<ul style="list-style-type: none"> <li>• Very bad ESS efficiency in low power segments</li> <li>• Real measurement values have to be used constantly due to error in most steps</li> </ul>
<b>Piecewise linearized efficiency</b>	<ul style="list-style-type: none"> <li>• More precise approach</li> <li>• Adaptable to different types of ESS with different efficiency characteristics</li> </ul>	<ul style="list-style-type: none"> <li>• Solve time increases drastically with increased amount of segments</li> <li>• Convex dependency between injected and received power is required</li> <li>• Complex implementation</li> </ul>

In Table 2, the evaluation of the two approaches is presented. Of course, the advantage of one is the disadvantage of the other. Whereas piecewise linearization is more precise, it does not necessarily capture the low efficiency at low power, due to the need for convex dependency. A possible approach would be to set the lowest possible charging power to 10 % of the rated charging capacity. However, this makes our optimization problem a MIP (mixed integer programming) problem, which could increase the solving time drastically. It should also be mentioned that errors made in such low power areas also makes up a very low volume of the total energy input and output, and hence is not responsible for any significant part of the revenue related to the battery. Thus it could also be ignored for simplicity.

### 3.2.2.1 Piecewise linearized efficiency with binary representation model

Because the efficiency of the battery depends on the power input, we have to model a power dependent efficiency. As shown in Figure 1, this dependency is not linear, which complicates the model solving. Therefore, we make a linear approximation by segmenting the efficiency into J segments. The more segments, the higher precision. In Figure 2 it is shown how  $\sigma_{b,t}^{B,ch}$  and  $\sigma_{b,t}^{B,dis}$  are split into two variables each<sup>2</sup>.

<sup>2</sup> Note that if this model is used, the energy balance and state of charge equations have to be changed accordingly. The variables with superscript *inv* represents the

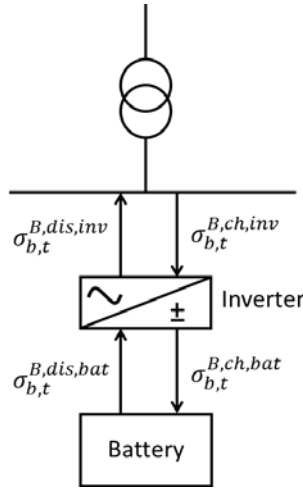


Figure 2: Overview of variables when using piecewise linearized efficiency.

Firstly, the power that goes into the inverter has to be divided into segments.

$$\sigma_{b,t}^{B,ch,inv} = \sum_{k \in K} \sigma_{b,t,k}^{B,ch,inv}, \forall b \in B, t \in T, k \in K \quad (3)$$

Then, segments are given boundaries  $B_{b,k}^B$  which represents the end of the segment x-axis value. The following equation allocates the correct amount of charging power to each segment by using this value.

$$\left( B_{b,k}^B - B_{b,k-1}^B \right) \cdot \gamma_{b,t,k+1}^{B,ch} \leq \sigma_{b,t,k}^{B,ch,inv} \leq \left( B_{b,k}^B - B_{b,k-1}^B \right) \cdot \gamma_{b,t,k}^{B,ch}, \forall b \in B, t \in T, k \in K \quad (4)$$

Next, each segment is given a binary value  $\gamma_{b,t,k}^{B,ch}$  which represents whether or not a segment has a value (is activated). The following equation says that a segment  $\gamma_{b,t,k+1}^{B,ch}$  cannot be activated unless the previous segment  $\gamma_{b,t,k}^{B,ch}$  also is activated. This will ensure that segments are enabled in the correct order (sequentially). Segments are activated if  $\gamma_{b,t,k}^{B,ch} = 1$  and are not activated if  $\gamma_{b,t,k}^{B,ch} = 0$ .

$$\gamma_{b,t,k}^{B,ch} \geq \gamma_{b,t,k+1}^{B,ch}, \forall b \in B, t \in T, k \in K \quad (5)$$

Finally, the output of the inverter which is then received by the battery is shown in Eq.

(6)

---

power that is exchanged between the main meter node and the inverter, whereas the variables with superscript *bat* represents the power exchanged between the inverter and the battery.

$$\sigma_{b,t}^{B, ch, bat} = \sum_{k \in K} \mu_{b,k}^B \cdot \sigma_{b,t,k}^{B, ch, inv}, \forall b \in B, t \in T, k \in K \quad (6)$$

Similarly for discharging, all equations are repeated. However, as shown in Figure 2, we are now trying to find the power out of the inverter as a function of what was withdrawn from the battery.

$$\sigma_{b,t}^{B, dis, bat} = \sum_{k \in K} \sigma_{b,t,k}^{B, dis, bat}, \forall b \in B, t \in T, k \in K \quad (7)$$

$$\left( B_{b,k}^B - B_{b,k-1}^B \right) \cdot \gamma_{b,t,k+1}^{B, dis} \leq \sigma_{b,t,k}^{B, dis, bat} \leq \left( B_{b,k}^B - B_{b,k-1}^B \right) \cdot \gamma_{b,t,k}^{B, dis}, \forall b \in B, t \in T, k \in K \quad (8)$$

The same rule of segment enabling applies, but now for discharging.

$$\gamma_{b,t,k}^{B, dis} \geq \gamma_{b,t,k+1}^{B, dis}, \forall b \in B, t \in T, k \in K \quad (9)$$

Finally, the power going into the main meter node is shown in (EQREF).

$$\sigma_{b,t}^{B, dis, inv} = \sum_{k \in K} \mu_{b,k}^B \cdot \sigma_{b,t,k}^{B, dis, bat}, \forall b \in B, t \in T, k \in K \quad (10)$$

In Figure 3 the relation between output and input power,  $\mu_{b,k}^B$  is shown. The relation is almost completely proportional except for some deviances for low powers. When charged with full power, the efficiency is 98 % in this example. A more clear efficiency curve can be shown in Figure 4.

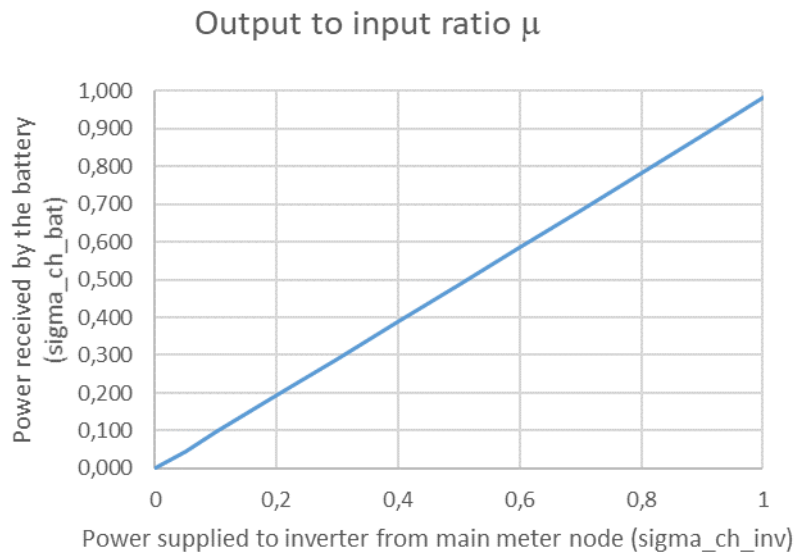


**Figure 3: Relation between the power received by the battery and input power to inverter represented by slope  $\mu$  for different segments.**

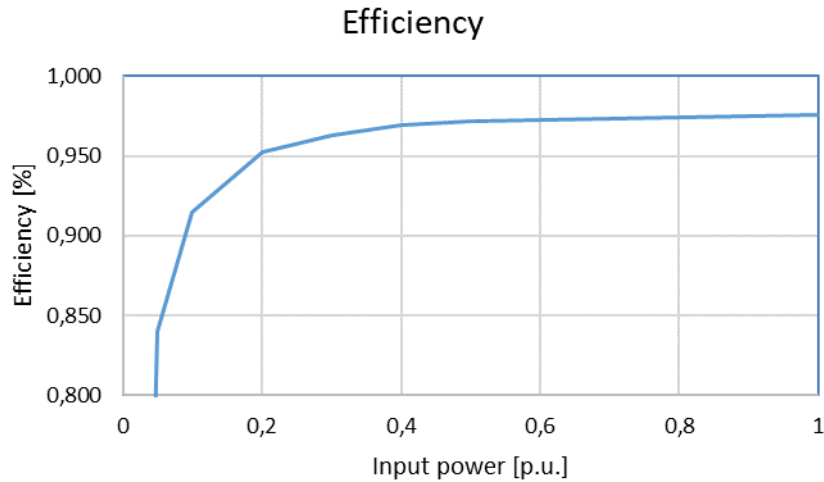


Figure 4: Efficiency for different input powers.

### 3.2.2.2 Piecewise linearized efficiency with “special order set 2” variables

Another way of implementing piecewise linearized efficiency is by utilizing special order sets (SOS). SOS1 and SOS2 variables allow us to create segments where only one or two segments can have a non-zero value, respectively. This can be used to create a piecewise approximation where different power inputs results in different efficiencies for the battery.

The mathematical formulation of the SOS2 approach is explained in D6.5. However, this approach is not directly translatable to Pyomo. Therefore, this subsection will focus on how to implement the SOS2 approach, and does not go in-depth on the mathematical formulation.

Two things are needed for implementation

- The x and y coordinates which represent the selected values which constitutes the piecewise linear approximation of the battery inverter efficiency. This is shown in Figure 6.
- The built-in pyomo function called Piecewise, which takes 6 inputs described below:
  - Time index, model.t
  - X-axis variable,  $\sigma_{b,t}^{B,ch,inv}$
  - Y-axis variable,  $\sigma_{b,t}^{B,ch,bat}$



- The reserved pyomo library call, “pw\_repn”. This can call different piecewise approximation methods. Example: pw\_repn='SOS2' or pw\_repn='CC'.
- X-coordinates of the selected values using the reserved pyomo library call: “pw\_pts”. In Figure 6, the input would be  $\text{pw\_pts}=[0, 0.1 \cdot Q_b^{B, ch}, 0.5 \cdot Q_b^{B, ch}, Q_b^{B, ch}]$ .
- What type of mathematical operator to be used. Typically these are equal, greater than or equal or less than or equal. The type is called by the reserved pyomo library call: “pw\_constr\_type”. Because we want a value on the line in-between the x and y axis values, we use pw\_constr\_type='EQ'.
- Function rule representing the relation between x and y coordinates. f\_rule=\_function\_name\_. Example: “f\_rule=f\_efficiency”.

Finally, an example of the code needed is shown in Figure 5.

```
def f_efficiency(model,t,sigma_ch_inv):
    if (sigma_ch_inv == model.Q_max*0):
        return 0
    elif (sigma_ch_inv == model.Q_max*0.1):
        return 0.9 * model.Q_max
    elif (sigma_ch_inv == model.Q_max*0.5):
        return 0.97 * model.Q_max
    else:
        return 0.98 * model.Q_max

model.A_inv_ch = Piecewise(model.t,\
                           model.sigma_ch_inv,\
                           model.sigma_ch_bat,\
                           pw_repn='SOS2',\
                           pw_pts=[0, 0.1*model.Q_max, 0.5*model.Q_max, model.Q_max],\
                           pw_constr_type='EQ',\
                           f_rule=f_efficiency)
```

Figure 5: Example of how piecewise linearized efficiency using SOS2 variables is implemented.

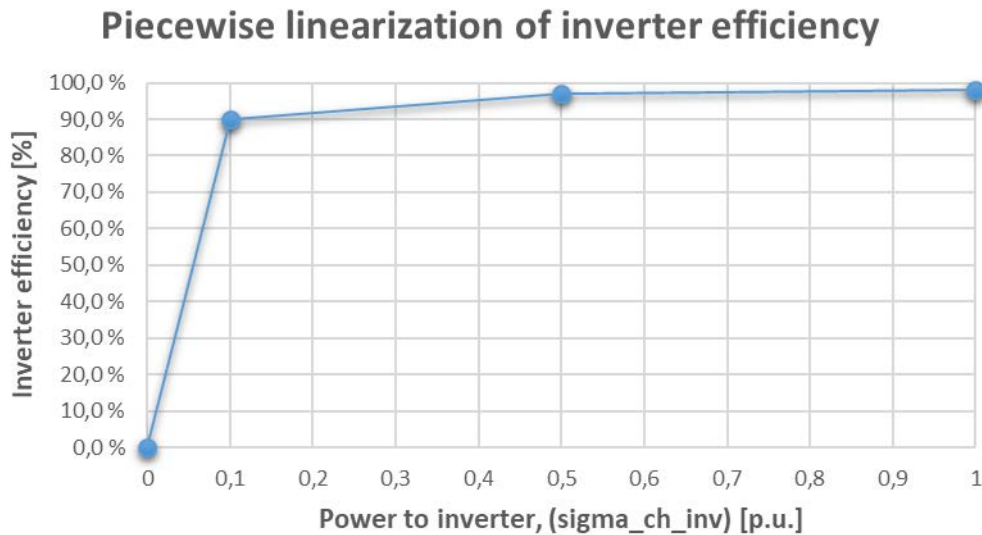


Figure 6: x and y coordinates needed to create an SOS2 piecewise linear approximation.

Note that the solver GLPK does not handle SOS2 constraints. If to be solved by GLPK, the approach described in 3.2.2.1 should be used, or a different type of approximation should be utilized. The other types of approximations and their results can be found in D6.5, along with an evaluation of the methods comparing solving speed.

### 3.2.3 Battery degradation

Degradation processes were described in detail in D6.3 *Simplified battery state of health diagnostics tool*. In brief, the degradation process in a lithium ion battery is a complex combination of electrochemical and mechanical processes, which lead to capacity decrease and power fading. Most of these processes cannot be studied independently as they occur simultaneously at similar timescales and interact with each other. Ageing processes can be divided into two groups: ageing during use and ageing during storage. In other words: ageing related to cycle life and ageing related to calendar life.

#### 3.2.3.1 Performance degradation

The performance of a battery degrades as a result of ageing. The main characteristics that are affected by the ageing are the capacity and the internal impedance. As a consequence, the ageing degrades also the efficiency and the heat generation characteristics as well as lengthens the duration of charging due to longer duration of constant-voltage operation. For repetitive use at constant operating conditions, the capacity degradation rate is typically almost linear. A change in the typical use pattern or ambient temperature may change the degradation rate too because of degradation

stress factors. For impedance increase, the rate of degradation is more difficult to predict. For some batteries, the impedance increases in a linear manner, whereas for other batteries the impedance remains nearly constant for almost the whole lifetime.

Degradation stress factors are all the operation practices or circumstances that accelerate the degradation in battery and thus shorten the lifetime of the cell. By identifying the stress factors, the battery operating conditions and practices can be optimized within the application limits so that the degradation of the battery is minimized and longer lifetime is achieved.

A summary of the degradation stress factors addressed in the lifetime tests of the reviewed articles in D6.4 is shown in Figure 7. Results vary widely depending on the chemistry and even among different studies regarding the same chemistry. The values in the low-stress and optimal-range columns are very coarse generalisations based on the results.

Stressor	High stress	Low stress	Optimal range
Cycle depth ( $\Delta$ DOD)	High $\Delta$ DOD	< 50%	< 30%
Temperature	High and low temperature	10–35 °C	15–30 °C
Current (C-rate)	High rate	< 1C	< C/2
SOC / voltage	High SOC / voltage	< 4 V	< 70% SOC

Figure 7: High, low and optimal stress ranges.

### 3.2.3.2 Cost of degradation

In D6.2, the operational optimization algorithm included the Levelized Cost of Degradation (LCOD) in the objective function to address the costs that are related to the battery degradation. The LCOD was obtained by calculating the marginal degradation caused by cycling and by utilizing either the investment cost or the replacement battery cost. The cycle depth stress factor was incorporated into the algorithm by applying the equivalent rainflow counting algorithm proposed by Xu et al. [8]. This approach has three drawbacks: (i) The future benefits are not discounted, (ii) the battery lifetime and the replacement battery cost are not known initially, and (iii) the operational decisions are solely based on the technical and economical parameters, and therefore, the battery may

be totally unused or overused in some cases. For example, a battery with high investment cost or low cycle lifetime may be used very little in cases where the benefits are low. However, even in that case, it is not meaningful not to use the battery at all, because the investment has already been made, and the battery has a limited calendar life as well. Therefore, it would be better to use the battery to obtain the available benefits to minimize the losses.

In a recent article by He et al. [9] [10] an intertemporal decision framework for the management of a storage was proposed, in which the optimal usage of the storage in the economic sense is first planned for the long term, which is followed by the formulation of the operational decision-making in the short term. The operational algorithm includes the battery degradation in the objective function, but it excludes the investment cost of the battery, because the investment cost is a sunken cost that should not affect the operational decision making. This approach is intuitive and solves the main problems of the LCOD method. However, it requires additional efforts to first determine the optimal usage and later on to manage the utilization of the battery and the associated rate of degradation according to the predefined plan.

### 3.2.3.3 End of life

End of life of a battery is when it no longer meets its performance requirements. As long as safety is maintained, the limit of performance requirements can be decided internally, but normally EOL is when the performance is about 60–80 % of its rated performance.

In order to identify when the EOL of a battery is reached, the State of Health (SOH) of the battery needs to be tracked. Many BMSs and EMSs provide some SOH indication, which can be based simply on coulomb-counting or on more advanced methods. In INVADE, a SOH diagnostics tool was developed in T6.2. The tool is an Excel-based offline tool that can be used locally by the pilots. The tool incorporates a detailed battery degradation model that addresses the degradation stress factors to the historical usage data of the battery system. Time-series data is given as an input, and the estimated SOH is provided as an output. The system operator can then update the battery capacity parameter to the IIP. It is suggested to update the parameters on a monthly basis.

The EOL is highly dependent on the application-specific performance requirements and the techno-economics of the use case. At some point, a critical performance requirement cannot be anymore achieved, or the flexibility profit no longer exceeds the marginal cost of operation. A default EOL criterion of 70 % of the original capacity (i.e., 70 % SOH) will be used for INVADE pilot batteries, but it can be adapted for each pilot based on the

application-specific requirements, battery technical specification and warranty terms and conditions, and techno-economic evaluations.

#### 3.2.3.4 Model parameters

The input parameters that are needed to run the model are shown in Table 3. Some parameters are used directly in the model or constraints, whereas some parameters are used indirectly to calculate or define other parameters or characteristics of the model. Note that this is not a complete list, but a general overview of some general assumptions made in order to fine-tune the operation of the battery.

**Table 3: Parameters that are needed to run the battery model.**

Parameter	Unit	Default	Info	Source
Energy capacity	kWh		Updated regularly	Specification
Discharging power capacity	kW		Continuous rating	Specification
Charging power capacity	kW		Continuous rating	Specification
Battery charging and discharging efficiency	%	98.5%	At typical rate in the application	Calculated based on specification
PCS maximum efficiency	%	98.5%	Maximum value	Specification
Cycle lifetime	FCE		Convert to full cycles equivalent	Specification or warranty terms
Calendar lifetime	years	10 years		Specification or warranty terms
End of life	%	70%	Percentage of the original capacity	Specification or warranty terms
Replacement battery cost	€	500 €/kWh	Battery system only	Estimation
Cost of degradation tuning parameter		1	Updated regularly	SOH diagnostics
Typical operating temperature	°C	25 °C		Application-specific
Minimum SOC	%	5%		Application-specific
Maximum SOC	%	95%		Application-specific
Power constraint coefficient for charging		0.8		Application-specific
Power constraint coefficient for discharging		0.8		Application-specific

### 3.2.4 Degradation modelling

#### 3.2.4.1 Cycle ageing

In INVADE, the cycle depth is considered as the most influential degradation stress factor, and therefore, it is included in the calculation of the cost of degradation. An equivalent rainflow counting algorithm is implemented that calculates the marginal cost of degradation caused by the cycle depth [8]. Additionally, the temperature stressor is included indirectly as a parameter. The operating temperature data is not collected in the IIP, and hence, actual temperature data cannot be used in the optimization. The selected approach is to use historical long-term average temperature from the local SCADA system, which can be updated regularly by the system operator. In this way, the long-term average temperature is used to calibrate the degradation rate of the battery. If the temperature data is not available in the SCADA system, the parameter shall be set to resemble the average ambient temperature or the expected average operational temperature of the battery.

In order to model cycle ageing, the battery has to be divided into segments. These segments are virtual and are used by the optimization model to allocate costs to charging/discharging decisions segment by segment. The cost of discharging a segment increases the deeper the cycle<sup>3</sup>.

The mathematical formulation requires some additional variables and parameters. First,  $J$  segments need to be defined. From there we have the following new maximum SOC per segment;

$$O_{b,j}^{B,\max} = \frac{O_b^{B,\max}}{J}, \forall b \in B, j \in J \quad (11)$$

To model marginal cost of cycle ageing, further input parameters are needed such as the battery cell replacement cost  $R_b^B$  (€) the battery size  $O_b^{B,\max}$  and the discharge efficiency  $A_b^{B,\text{dis}}$ . Since the cycle depth ageing stress function is non-linear, the marginal cost is linearized with different numbers of segments  $j$  with  $j \in J$ .

$$c_{b,j}^B = \frac{R_b^B}{A_b^{B,\text{dis}} O_b^{B,\max}} J \left[ \phi\left(\frac{j}{J}\right) - \phi\left(\frac{j-1}{J}\right) \right], \forall b \in B, j \in J \quad (12)$$

---

<sup>3</sup> Note that this is independent of which segment is being discharged. A cycle from 80-60-80% SOC has an equal cost of a cycle from 60-40-60% SOC.

Where we have a near quadratic function to calculate the stress function:

$$\phi(\delta) = a\delta^c \quad (13)$$

For NMC batteries,  $a = 5.24 \times 10^{-4}$  and  $c = 2.03$ , which represent the stress function for NMC performing approximately 3000 cycles at 80% cycle depth [8].

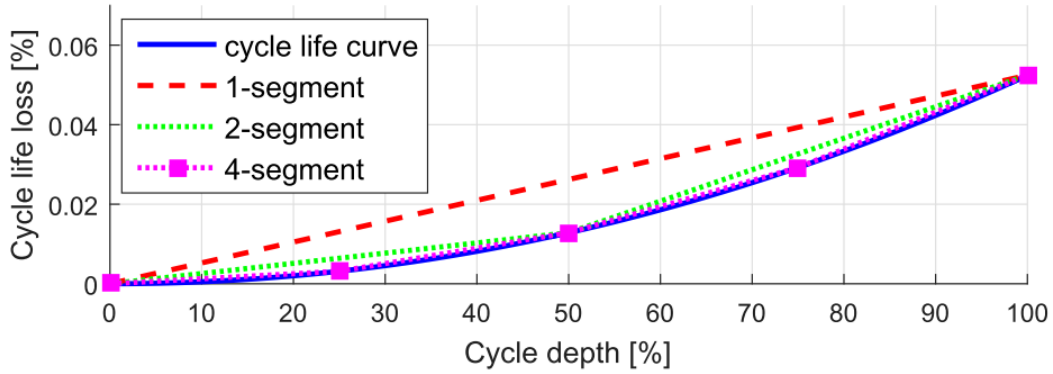


Figure 8: Example of an upper-approximated cycle depth ageing stress function [8].

To allocate the correct initial and final SOC,  $\sigma_b^{B,SOC,init}$  and  $\sigma_b^{B,SOC,final}$  are given their respective SOC values for  $t = 0$  and  $t = t_{end}$  by summing the energy for all segments.

$$\sum_{j \in J} \sigma_{b,j}^{B,SOC,init} = \sigma_b^{B,SOC,init}, \forall b \in B, j \in J \quad (14)$$

$$\sum_{j \in J} \sigma_{b,j}^{B,SOC,final} = \sigma_b^{B,SOC,final}, \forall b \in B, j \in J \quad (15)$$

When using segmented variables, the new SOC evolution equation looks as following. Note that  $A_b^{B,ch}$  represents the battery efficiency, whereas the inverter efficiency described in 3.2.2 is already incorporated in  $\sigma_{b,t,j}^{B,ch}$ .

$$\sigma_{b,t,j}^{B,SOC} = \sigma_{b,t-1,j}^{B,SOC} + \sigma_{b,t,j}^{B,ch} \cdot A_b^{B,ch} - \frac{\sigma_{b,t,j}^{B,dis}}{A_b^{B,dis}}, \forall b \in B, t \in T, j \in J \quad (16)$$

The sum of charging/discharging power in all segments equals the total charging/discharging power of the battery.

$$\sigma_{b,t}^{B,ch} = \sum_{j \in J} \sigma_{b,t,j}^{B,ch}, \forall b \in B, t \in T, j \in J \quad (17)$$

$$\sigma_{b,t}^{B,dis} = \sum_{j \in J} \sigma_{b,t,j}^{B,dis}, \forall b \in B, t \in T, j \in J \quad (18)$$

The total charging from all segments also has to stay below the maximum charging and discharging power. Additionally,  $\delta_{b,t}^B$  ensures that charging and discharging does not happen at the same time.

$$\sigma_{b,t}^{B,ch} \leq Q_b^{B,ch} \cdot \delta_{b,t}^B, \forall b \in B, t \in T \quad (19)$$

$$\sigma_{b,t}^{B,dis} \leq Q_b^{B,dis} \cdot (1 - \delta_{b,t}^B), \forall b \in B, t \in T \quad (20)$$

Next, the SOC in each segment has to be between zero and the maximum SOC per segment.

$$\sigma_{b,t,j}^{B,SOC} \leq O_{b,j}^{B,max}, \forall b \in B, t \in T, j \in J \quad (21)$$

In addition, the accumulated SOC in all segments cannot exceed the maximum nor go below the minimum battery SOC.

$$\sum_{j \in J} \sigma_{b,t,j}^{B,SOC} \leq O_b^{B,max}, \forall b \in B, t \in T, j \in J \quad (22)$$

$$\sum_{j \in J} \sigma_{b,t,j}^{B,SOC} \geq O_b^{B,min}, \forall b \in B, t \in T, j \in J \quad (23)$$

Finally, the cost of degradation in each segment is allocated in the following constraint. The marginal cost of degradation from each segment is allocated to the corresponding discharging segment. Because the marginal cost of cycling reflected by  $c_{b,j}^B$  is a non-linear parameter, the cost will be higher the deeper the cycle.

$$\beta_{b,t,j}^{B,cyc} = c_{b,j}^B \cdot \sigma_{b,t,j}^{B,dis}, \forall b \in B, t \in T, j \in J \quad (24)$$

#### 3.2.4.2 Calendar ageing

Also the degradation caused by the calendar life has been addressed in D6.5. The calendar life degradation model includes the SOC stress factor and the temperature stress factor. The calendar ageing was initially included to add cost for not using the battery and to control the SOC to be at the optimal level to achieve long calendar life. The disadvantage is the ambiguity of the parameterization, because typically the battery specifications and warranty terms provide very generic statements about the calendar lifetime, which cannot be used to parameterize the model properly without making substantial assumptions. At a later phase, when the long-term planning and the associated coefficient was added to the cost of degradation model, the original need was no longer valid, as the average rate of degradation could now be forced to track the target



degradation. Both degradation models have been implemented and tested. The final decision on which of these models will be used in the pilots will be made at a later stage.

The calendar ageing is modelled by the following equation:

$$\beta_{b,t}^{B,cal} = \frac{1}{T_{Lf}^B \cdot D_Y \cdot H_d \cdot S_h} \cdot \left[ S_b^{B,0} + S_b^{B,SOC} \frac{1}{2} \cdot \left[ \sigma_{b,t}^{B,SOC} + \sigma_{b,t-1}^{B,SOC} \right] \right], \forall b \in B, t \in T \quad (25)$$

In general, a higher SOC leads to a higher calendar ageing cost. This cost depends on the parameterization factors  $S_b^{B,SOC}$  and  $S_b^{B,0}$ . Because these factors are hard to tune correctly, it should be noted that it can be difficult to get a good representation of the real battery characteristics.

### 3.2.4.3 Battery degradation tuning factor

Finally, we create a variable  $\beta_{b,t}^{B,tot}$  which sums the degradation in each time period  $t$ . It is to be used in the minimization objective function if battery degradation is to be taken into account. The total degradation cost per time step is then given by Eq. (26).

$$\beta_{b,t}^{B,tot} = \rho_b^B (\beta_{b,t}^{B,cal} + \sum_{j \in J} \beta_{b,t,j}^{B,cyc}), \forall b \in B, t \in T, j \in J \quad (26)$$

Although the model proposed in this section keeps the algorithm from making decisions that does not result in revenue higher than the degradation cost of the battery, a factor  $\rho_b^B$  is added if it is necessary to tune down the degradation costs that are used in the algorithm. Especially the cycle degradation cost is quite high, and if correct values are used, the battery could end up not being used much at all because each cycle has a very high cost. Still, the batteries are already invested in and they are there to be used. By giving  $\rho_b^B$  a value between 0 and 1, degradation costs can be tuned from 0 to full depending on the owner's wish. It is recommended to start by setting this parameter to 1, and tune it if the battery is not serving its purpose in the eyes of the owner.

## 4 EV model

### 4.1 Introduction

The simple EV model assumes continuous control of EV charging between 0 and maximum power. In this chapter we present detailed description of advanced EV model which has ON-OFF control and charging between minimum and maximum power.

### 4.2 EV mathematical formulation

For fully controllable EV charging points ( $v \in V^c$ ) we can delay, interrupt and set the charging power of the EV charging process. This model allows to set the charging power between a maximum and minimum charging levels or on/off regulation, depending on each case. An example is given in the Table 4 for the adjustable control between 3 and 1 kWh. Therefore, the model cannot set a charging power below 1 kWh.

**Table 4. Illustrative example controllable EV charging.**

	1	2	3	4	5	6	7	8
$W_{v,t}^{EV}$	3	3	2					
$\theta_{v,t}^{ch}$		2	1	0	2	2	1	

This model controls charging stations and does not include EV driver charging needs or the EV battery state-of-charge as input due to the lack of information exchange. Some references in the literature assume to have this information as Mohseni [11] and Mouli [12]. However, this is not possible in the INVADE project. Departure times, EV battery capacity and the energy requested for the following periods are not known and the model relies upon the forecasting inputs.

The inputs are:

- EV charging demand forecasted ( $W_{v,t}^{CP}$ ) per period  $t$  and charging point  $v$ . It is the energy consumption baseline in the charging point  $v$  without flexibility activation.

This input parameter is used for defining the EV charging demand parameter  $\theta_{v,n}^{CP,cd}$  as (27) shows.

$$\sum_{t=T_{v,n}^{EV,start}}^{T_{v,n}^{EV,end}} W_{v,t}^{CP} = \theta_{v,n}^{CP,cd} \quad \forall v \in V^c, \forall n \in N(v) \quad (27)$$

- 3 EV charging point status possibilities: connected and consuming, connected but not consuming and not connected. The  $n$  number of sessions between connection and disconnection periods  $[T_{v,n}^{EV,start}, T_{v,n}^{EV,end}]$  are extracted from the EV charging point status.

The decision variable  $\theta_{v,t}^{CP,ch}$  represents the energy supplied to the EV charging point  $v$  in each time period  $t$ . The amount of energy charged out of the session scope is zero. Therefore, if an EV reaches a charging point before  $T_{v,n}^{EV,start}$ , the charging point reports the event and the platform re-calculates the optimal scheduling before starting the charging process.

$$\theta_{v,t}^{CP,ch} = 0, \quad \forall v \in V^c, \forall n \in N(v), t \notin [T_{v,n}^{EV,start}, T_{v,n}^{EV,end}] \quad (28)$$

The decision variable  $\theta_{v,t}^{CP,es}$  represents the total energy supplied to the EV during the charging session  $n$  from  $T_{v,n}^{EV,start}$  until time period  $t$ . Each charging session is independent and  $\theta_{v,t}^{CP,es}$  is zero at the beginning of each session  $n$ . The following constraint calculates the total energy supplied to the EV  $v$  until the period  $t$  ( $\theta_{v,t}^{CP,es}$ ) within the charging session  $n$ .

$$\theta_{v,t}^{CP,es} = \theta_{v,t-1}^{CP,es} + \theta_{v,t}^{CP,ch} \quad \forall v \in V^c, \forall n \in N(v), t \in [T_{v,n}^{EV,start}, T_{v,n}^{EV,end}] \quad (29)$$

Notice there is no charging efficiency parameter included in Eq. (29) because the energy effectively stored in the EV battery is not known. Additionally, the forecast tool predicts the energy measured in the charging point so no need to include any efficiency.

$$Q_v^{CP,min} / N^{hour} \leq \theta_{v,t}^{CP,ch} \leq Q_v^{CP,max} / N^{hour} \quad \vee \quad (\text{OR}) \quad \theta_{v,t}^{CP,ch} = 0, \quad \forall v \in V^c, t \in T \quad (30)$$

Eq. (30) is a disjunctive constraint that limits the charging power in a charging point. It ensures that the charging power scheduled per charging point is between  $[Q_v^{CP,min}, Q_v^{CP,max}]$  or it is disconnected.

$$\sum_v^{V^c} \theta_{v,t}^{CP,ch} \leq Q_{v,t}^{CP,ch} / N^{hour}, \quad t \in T \quad (31)$$

Eq. (31) ensures that the total charging power per charging station is limited to a given value ( $Q_v^{CS,ch}$ ).

$$\theta_{v,t}^{CP,es} \leq \theta_{v,n}^{CP,cd}, \quad \forall v \in V^c, \forall n \in N(v), t = T_{v,n}^{EV,end} \quad (32)$$

Finally, Eq. (32) sets the maximum energy supplied per session  $n$  and charging point  $v$  and it is equal or less than the forecasted EV energy demand  $\theta_v^{CP,cd}$ .

The following cost function compensates for the difference between the expected EV charging demand estimated by the FO ( $W_{v,t}^{CP}$ ) and the result of applying the set-points ( $\theta_{v,t}^{CP,ch}$ ). Additionally, this difference is relative to the total charging demand expected ( $\theta_v^{CP,cd}$ ). Notice that an EV could be rewarded even in cases that the EV is not fully charged when it leaves. This is included in the compensation fee ( $P_v^{CP,ns}$ ) for every kWh not supplied

$$\zeta^{EV,control} = \zeta^{EV,shift} + \zeta^{EV,non-supplied} + \zeta^{EV,charging\ cost} \quad (33)$$

$$\zeta^{EV,shift} = \sum_{v \in V^c} \sum_{n \in N(n)} \sum_{t=T_{v,n}^{EV,start}}^{T_{v,n}^{EV,end}} P_v^{CP,shift} \sum_{T_v^{EV,start}}^t (W_{v,t}^{CP} - \theta_{v,t}^{CP,ch}) \quad (34)$$

$$\zeta^{EV,non-supplied} = \sum_{v \in V^c} \sum_{n \in N(v)} P_v^{CP,ns} (\theta_{v,n}^{CP,cd} - \theta_{v,T_{v,n}^{EV,end}}^{CP,es}) \quad (35)$$

$$\zeta^{EV,charging\ cost} = \sum_{v \in V^c} \sum_{t \in T} P_t^{buy} \cdot \theta_{v,t}^{CP,ch} \quad (36)$$

Notice that the Eq. (36) is not necessary if the objective function already includes the electricity consumption cost.

Model assumptions and limitations:

- 1) Charging power: The power input from the EV charger is assumed to be independent of the state of charge. This assumption holds true for chargers with a small power-rate which are very popular in residential installations. As this model is meant for mainstream and cheap charging technologies, the charger is assumed to have a small to medium power available. Typically, 3.3 kW and up to 11 kW.
- 2) Flexibility contracts: The information from flexibility contracts for EV in households are the shifting and non-supplying costs. Additionally, the EV owner can declare the periods when the EV can be shifted forward if necessary. In case of public charging stations, it depends on the EV driver information available. This should be discussed case by case.

Input data:

This model relies upon the forecasting tools capable to create the input data requested to execute the EV flexibility model for scheduling purposes.

- 1)  $W_{v,t}^{EV}$ : The expected EV energy consumption without external signals of each EV  $v$  at time period  $t$  [kWh]. From this value,  $V_v^{EV,start}$  and  $V_v^{EV,end}$  are known.
- 2) Charging point status. This information allows to create the expected arrival and departure times  $[T_v^{EV,start}, T_v^{EV,end}]$ .

Additionally, the following information is needed:

- 1)  $P_{v,t}^{CP,flex}, P_v^{CP,ns}, P_t^{buy}$ : Flexibility costs if available
- 2)  $Q_v^{CP,ch}, Q_v^{CS,ch}$ : Charging point and station maximum capacities

Model limitations:

- It requires an accurate forecasting system for knowing the EV energy consumption and departure times in case of not having this information.
- Even though the aggregated services for energy delivery is satisfied there might be a chance that individual EV's energy delivery requirements are not met.

## 5 Electric water heater model

### 5.1 Introduction

Flexible loads are one of the flexibility resources considered in the INVADE project. In the D5.3 document, the flexible loads were classified as curtailable and shiftable loads and different ways of handling such loads were described. However, thermal loads were considered as a special case and their description is not sufficiently covered. The purpose of this chapter is to propose a possible solution for one such loads namely electric water heater.

## 5.2 Thermal load modelling – Electric water heater

Controllable water heaters will be involved in some of the Norwegian households. Each water heater will have fixed parameter for installed capacity (kW). All the water heaters in the pilot will have 1.95 kW.

The water heater control is based on a set of timing restrictions that will be input to the optimization algorithm:

- a. For each period, a parameter says whether it is allowed to disconnect the water heater or not (e.g. disconnection is allowed at any time, except from between 1900 and 2200).
- b. A maximum disconnection duration is given (e.g. if the water heater is disconnected, it must at the latest be reconnected after 1 ½ hour)
- c. A minimum duration (rest time) between two disconnections is given (e.g. if a water heater is reconnected after a disconnection, it cannot be disconnected again before at least 3 hours)

The parameters above will be provided by a local home automation facility in the Norwegian pilot.

The output from the optimization algorithms is a set of disconnection and reconnection periods. The control signals will be off and on with a given time (e.g. off at 12:15, on at 12:45). This information will have the granularity equal to the length of the periods, mainly 15 minutes, which means that the connections and disconnections will be set to these time points, and not at any minute inside a 15 minutes' interval.

## 5.3 Electric Water Heaters (EWH), Shiftable Energy Volume

In order to represent the above described behaviour, it is developed an improved shiftable energy volume model that is able to disconnect the EWH when needed and it considers the re-bounce effect. Therefore, if there is a load curtailment, it will always supply the exactly same amount of curtailed energy afterwards, within the corresponding shifting interval  $i \in [T_{L,i}^{EWH,start}, T_{L,i}^{EWH,end})$ . The main improvement from the previous shiftable energy volume model described in D5.3 has to do with including two new timing constraints:  $D_i^{EWH,max}$  (maximum disconnection duration) and  $D_i^{EWH,min}$  (the minimum

time between two disconnections) to let the EWH to recover temperature inside the water tank.

It is good to clarify that in this present case,  $T_{l,i}^{EWH,start} = V_{l,i}^{EWH,start}$ , since it is not possible to move load backwards. From now on, the parameter  $T_{i,l}^{EWH,start}$  will be used.

In order to simplify, let's consider a EWH installed capacity of 2 kW. Each time interval lasts 15 minutes, making a 0.5 kWh of maximum energy consumed each time period.

These two new timing restrictions are explained below:

- $D_l^{EWH,max}$ : Parameter that indicates the maximum number of time periods available for disconnection during each load shift interval. The number of disconnections, unlike the curtailable loads model, do not have to be followed.
- $D_l^{EWH,min}$ : Parameter that ensures the minimum duration between successive activations.

A minimum number of consecutive time periods is established in which the EWH cannot be disconnected under any circumstances. This restriction is imposed due to uncertainty, since the water temperature inside the EWH is an unknown value because the temperature sensor inside is not sending information outside.

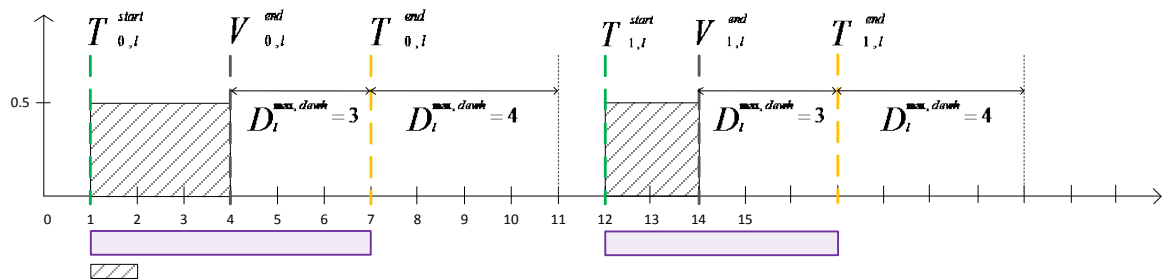


Figure 9: Graphic explanation of  $D_l^{EWH,min}$ ,  $D_l^{EWH,max}$  and the shifting intervals I.

$D_l^{EWH,min}$  is the minimum rest periods between two EWH shift intervals, but as you can see in the graphic example above, the duration can be more than  $D_l^{EWH,min}$  time intervals.

The model is divided in three big steps that are going to be explained.

**STEP 1:** Automatic generation of shift interval set and parameters. Figure 10 shows the sub steps to follow:

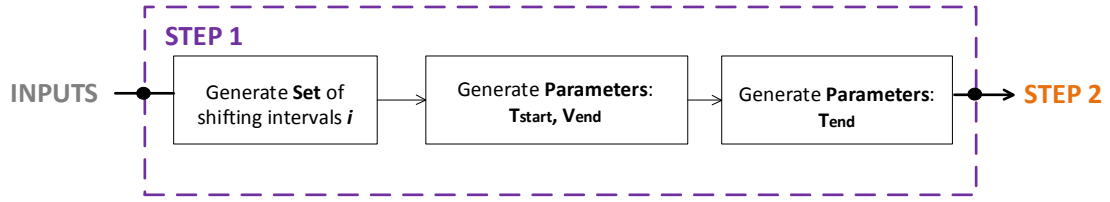


Figure 10 Step1 graphic diagram

Another graphic example is given below in order to explain Step1 procedure. A baseline EWH consumption  $W_{l,t}^{EWH}$  is shown in Figure 11. In this example, it is allowed to disconnect in all the planning horizon between  $T_{i,l}^{EWH,start}$  and  $T_{i,l}^{EWH,end}$ . (This means  $C_{l,t}^{EWH,allow} = 1 \quad \forall t \in T$ ). So the  $W_{l,t}^{EWH}$  is going to be the same that  $W_{l,t}^{EWH,restrict}$ , since:

$$W_{l,t}^{EWH,restrict} = W_{l,t}^{EWH} \cdot C_{l,t}^{EWH,allow} \quad \forall l \in L^{ewh} \quad (37)$$

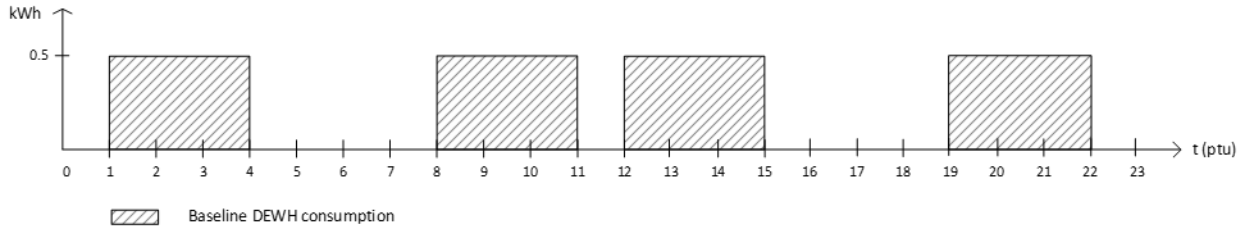


Figure 11: Baseline Forecast EWH consumption  $W_{l,t}^{EWH,restrict}$

The following parameters values are given:  $D_l^{EWH,min} = 3, D_l^{EWH,max} = 2$

Firstly, it is needed to know the set of EWH shift intervals  $i$ . Then, the following parameters,  $T_{l,i}^{EWH,start}$  and  $V_{l,i}^{EWH,end}$ , can be calculated automatically.

Once  $T_{l,t}^{EWH,start}$  and  $V_{l,t}^{EWH,end}$  are already found,  $T_{l,i}^{EWH,end}$  is imposed by the following restriction Eq. (38)

$$T_{l,i}^{EWH,end} = V_{l,i}^{EWH,end} + D_l^{EWH,max} \quad \forall l \in L^{ewh}, \forall i \in I \quad (38)$$

Figure 12 shows visually the automatically estimated  $T_{l,i}^{EWH,start}$  and  $T_{l,i}^{EWH,end}$  values.



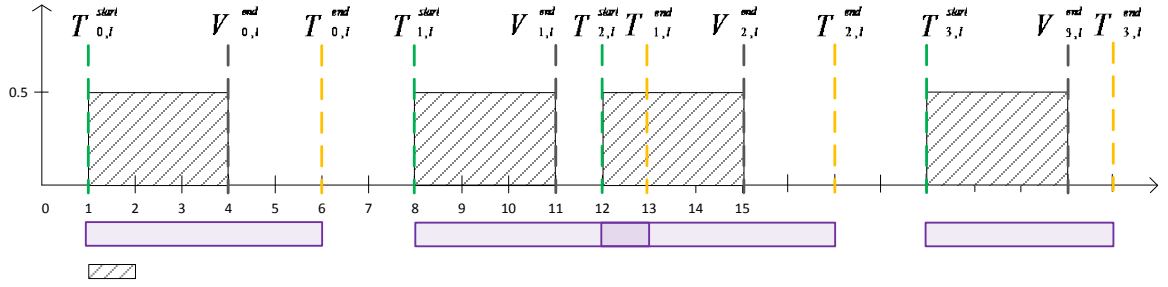


Figure 12: Set of shifting intervals  $I$  and parameters found automatically in Step1

As can be seen in Figure 12, some arrangements need to be done. For example,  $T_{l,2}^{EWH,start}$  can never start before the end of the previous load shift interval  $T_{l,1}^{EWH,end}$ .

Step2 arranges all these inconsistencies.

**STEP 2:** Ensures that all the following restrictions (Restriction 1 and Restriction 2) are met.

Once all the parameters needed for the model are established ( $T_{l,i}^{EWH,start}$  and  $T_{l,i}^{EWH,end}$ ), we make sure now to meet the two restrictions. If they do not meet, the  $T_{l,i}^{EWH,end}$  assigned value in Step1 must be changed.

**Restriction 1:** there is at least  $D_t^{EWH,min}$  time intervals where the EWH cannot be controlled or shifted.

$$T_{l,i+1}^{EWH,start} - T_{l,i}^{EWH,end} \geq D_t^{EWH,min} \quad (39)$$

**Restriction 2:** ensures that there is, at most,  $D_t^{EWH,max}$  time periods where the baseline consumption can be shifted/controlled in each time shift interval  $i$ .

$$V_{l,i}^{EWH,end} \leq T_{l,i}^{EWH,end} \leq V_{l,i}^{EWH,end} + D_t^{EWH,max} \quad (40)$$

In the example proposed in Figure 12, it can be seen that the **Restriction 1** does not meet in any case: all the shifting intervals  $i \in I$  are separated less than  $D_t^{EWH,min}$  periods. For example, between shifting intervals  $i = 1$  and  $i = 2$  there is less than 3 periods.

Notice also that the last shifting interval ( $i = 3$ ),  $T_{l,i}^{EWH,end}$  is equal to 23 because there is no more periods in the planning horizon in this present example.

If **Restriction 1** ( $T_{l,i+1}^{EWH,start} - T_{l,i}^{EWH,end} \geq D_l^{EWH,min}$ ) does not meet,  $T_{l,i+1}^{EWH,start} - T_{l,i}^{EWH,end}$  value can be positive or negative:

**Positive value:**  $0 \leq T_{l,i+1}^{EWH,start} - T_{l,i}^{EWH,end} < D_l^{EWH,min}$

Solution proposed: Move  $T_{l,i}^{EWH,end}$  backwards.

The parameter  $T_{l,i+1}^{EWH,start}$  maintains the same time interval position, while  $T_{l,i}^{EWH,end}$  is brought backwards in order to meet the  $D_l^{EWH,min}$  restriction.

As a result, the previous shift interval have less time periods available for flexibility, because  $[T_{l,i}^{EWH,start}, T_{l,i}^{EWH,end})$  is shortened.

The new  $T_{l,i}^{EWH,end}$  value would be Eq. (41)

$$T_{l,i}^{EWH,end} = T_{l,i+1}^{EWH,start} - D_l^{EWH,min} \quad \forall l \in L^{ewh}, \forall i \in I \quad (41)$$

It does not make sense that  $T_{l,i}^{EWH,end} < V_{l,i}^{EWH,end}$ , so if this happens, we equal values  $T_{l,i}^{EWH,end} = V_{l,i}^{EWH,end}$ , becoming that shift interval  $i$  is non-flexible.

Figure 13 shows the new  $T_{i,l}^{end}$  values after applying the formulation explained above

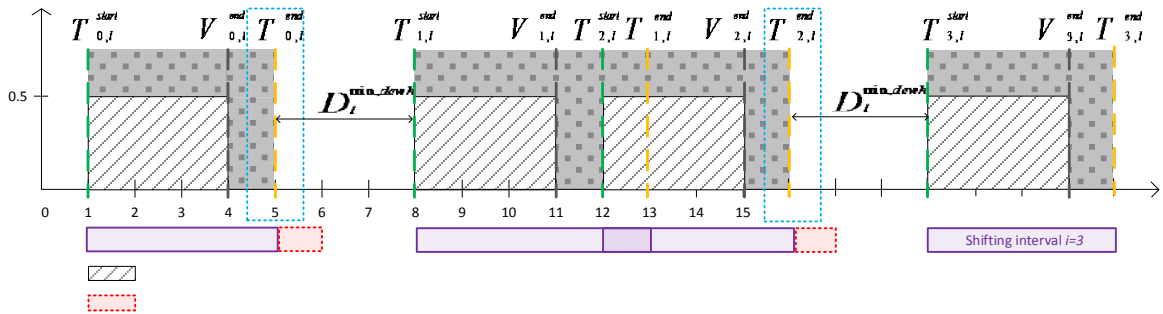


Figure 13 New Tend values that meet Restriction 1 for  $0 \leq T_{i+1,l}^{EWH,start} - T_{i,l}^{EWH,end} < D_l^{EWH,min}$

**Negative value:**  $T_{l,i+1}^{EWH,start} - T_{l,i}^{EWH,end} < 0$

Solution proposed: Move  $T_{l,i}^{EWH,end}$  backwards. Eq. (42)

$$T_{l,i}^{EWH,end} = T_{l,i}^{EWH,end} - |T_{l,i+1}^{EWH,start} - T_{l,i}^{EWH,end}| - D_l^{EWH,min} \quad \forall l \in L^{ewh}, \forall i \in I \quad (42)$$

Like it has been explained before, if  $T_{l,i}^{EWH,end} < V_{l,i}^{EWH,end}$ , values are equal  $T_{l,i}^{EWH,end} = V_{l,i}^{EWH,end}$ .

In Figure 14, it can be seen how shifting interval  $i=1$  becomes inflexible, this means no curtailments are allowed within that shift interval.

This meets **Restriction1**, because there are more than  $D_l^{EWH,min}$  periods between two possible disconnections.

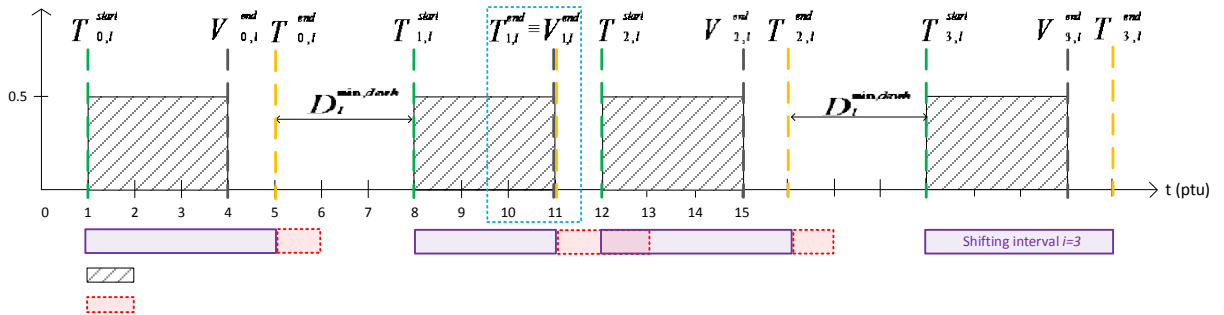
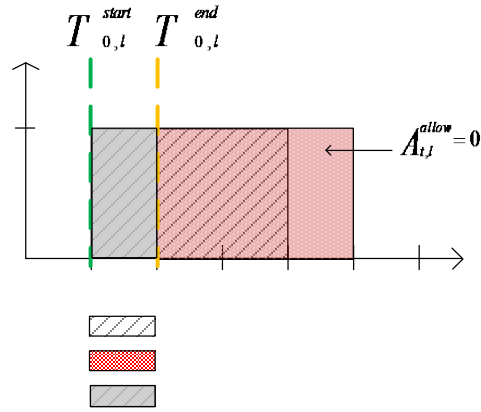


Figure 14 New Tend values that meet Restriction 1 for  $T_{l,i+1}^{EWH,start} - T_{l,i}^{EWH,end} < 0$

**STEP 3:** ensures that there is no  $W_{l,t}^{EWH,restrict}$  consumption shifted to periods when  $C_{l,t}^{EWH,allow} = 0$ .

Another different graphic example is shown in Figure 15 in order to explain the present step. In that example,  $C_{l,t}^{EWH,allow} = 0$  during time intervals [2,5), where the algorithm is not allowed to control the EWH consumption. The  $W_{l,t}^{EWH}$  consumption is [1,4). As a result, the baseline restrict  $W_{l,t}^{EWH,restrict}$  is [1,2).

So during the periods where  $C_{l,t}^{EWH,allow} = 0$ , it is not allowed to control the EWH consumption. Due to this, we cannot shift EWH consumption from time interval 1 to period 2 or 3, for instance. Because of this, there must be set an inflexible shift interval, so load is not shifted to periods where there is a consumption already.



**Figure 15 Step3 graphic explanation: there must be set an inflexible shift interval, so load is not shifted to periods where there is a consumption already**

So, if  $C_{l,t}^{EWH,allow} = 0$  and during the time interval before there is a consumption and the present time interval does too, then:  $T_{l,t}^{EWH,end} = V_{l,t}^{EWH,end}$ .

Once the algorithm procedure has been explained, all the optimization equations are described below:

For each period, the parameter  $C_{l,t}^{EWH,allow}$  says whether it is allowed to disconnect the water heater or not (e.g. in Figure 16 disconnection is allowed at any time, except from between 19:00 and 22:59, where  $C_{l,t}^{EWH,allow} = 0$ ).

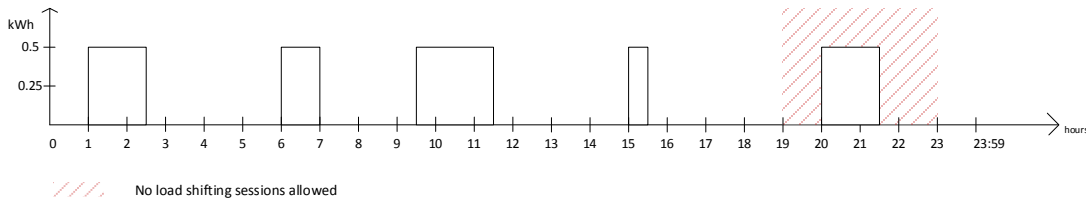


**Figure 16 Red shading represents the periods when it will not be possible to disconnect EWH consumption under any circumstances ( $C_{l,t}^{EWH,allow} = 0$ ).**

Power levels can be controlled between a minimum  $E_t^{EWH,min}$  and a maximum  $E_t^{EWH,max}$  value. In this EWH particular case, we want an ON/OFF control type, and in order to do so,  $E_t^{EWH,min}$  and  $E_t^{EWH,max}$  are set to the same value Eq. (43)

$$E_t^{EWH,min} = E_t^{EWH,max} \quad \forall l \in L^{ewh} \quad (43)$$

The final amount of energy consumed  $\omega_{l,t}^{EWH}$  is a semi-continuous variable Eq. (44)

$$E_t^{EWH,min} \leq \omega_{l,t}^{EWH} \leq E_t^{EWH,max} \quad \text{OR} \quad \omega_{l,t}^{EWH} = 0 \quad \forall l \in L^{ewh}, t \in T \quad (44)$$

For each load shift interval  $i$  the sum energy volume delivered to the load unit must equal the sum baseline forecast. Eq. (45)

$$\sum_{t=T_{l,i}^{EWH,start}}^{T_{l,i}^{EWH,end}} \omega_{l,t}^{EWH} = \sum_{t=T_{l,i}^{EWH,start}}^{T_{l,i}^{EWH,end}} W_{l,t}^{EWH,restrict} \quad \forall l \in L^{ewh}, t \in T \quad (45)$$

There could be inflexible intervals (for example, during the periods where  $C_{l,t}^{EWH,allow} = 0$  and there could be a baseline consumption during that periods), where the forecast load cannot be shifted/controlled.  $W_{l,t}^{EWH,c\_allow}$  is a parameter that indicates the baseline consumption when  $C_{l,t}^{EWH,allow} = 0$ . The energy delivered to the EWH unit must equal the baseline forecast during the periods where there is **no** shifting interval / Eq. (46)

$$W_{l,t}^{EWH,c\_allow} = W_{l,t}^{EWH} \quad \forall l \in L^{ewh}, t \notin T(i) \quad (46)$$

In order to know the final and real EWH consumption, the parameter  $W_{l,t}^{EWH,c\_allow}$  must be added to the optimized  $\omega_{l,t}^{EWH}$  Eq. (47)

$$\omega_{l,t}^{EWH\_realconsumption} = W_{l,t}^{EWH,c\_allow} + \omega_{l,t}^{EWH} \quad \forall l \in L^{ewh}, t \in T(i) \quad (47)$$

For EWH units, we introduce the concept of weighted average delay, already defined in other sections Eq. (48):

$$\tau_{l,i}^{EWH} = \frac{\sum_{t=T_{l,i}^{EWH,start}}^{T_{l,i}^{EWH,end}} ((\omega_{l,t}^{EWH} - W_{l,t}^{EWH,restrict})t)}{\sum_{t=T_{l,i}^{EWH,start}}^{T_{l,i}^{EWH,end}} W_{l,t}^{EWH,restrict}} \quad \forall l \in L^{ewh}, t \in T(i) \quad (48)$$

This weighted average delay will never be negative, because it is not allowed to shift volume backwards. It is reminded that  $T_{i,l}^{EWH,start} = V_{i,l}^{EWH,start}$ .

The total costs for shifting EWH volume is then Eq. (49)

$$\zeta^{EWH} = \sum_{l \in L^{ewh}} \sum_{i \in T} (P_l^{EWH,shift} \cdot \tau_{l,i}^{EWH}) \quad \forall l \in L^{ewh}, \forall i \in I \quad (49)$$

## 6 Space Heating Model

### 6.1 Introduction

Follow up the description of the thermal loads from previous chapter, the purpose of this chapter is to propose a possible solution for space heating.

### 6.2 Thermal load modelling - Space heating

Assume that the site is a household and has a main meter to measure the consumption at the household level as shown in Figure 17. Beneath the main meter, it has a set of inflexible loads and one flexible/controllable load unit, which is a panel oven that heats a living room. The energy consumption of the panel oven is metered separately as shown in the Figure 17. The living room has temperature control, and the people living in the household can enter a temperature setpoint for the room, and the heating system will ensure that the temperature always stays in a small bandwidth around this setpoint. The temperature setpoints can have different values for different days and for different times of the day.

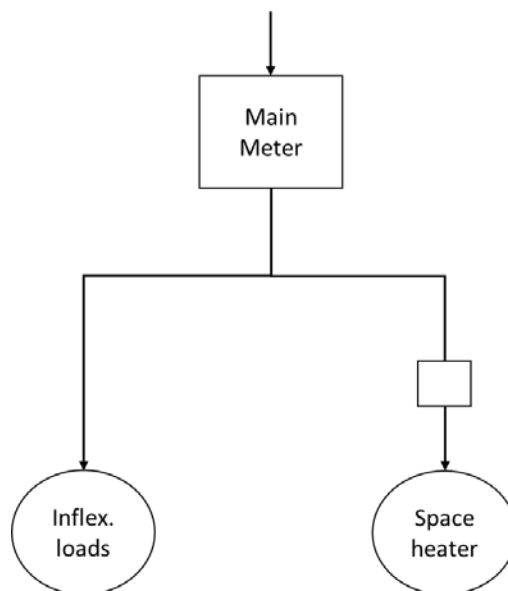


Figure 17. Household with space heating system.

### 6.3 Control limitations

A Flexibility Operator (FO) sells services to households, where the energy costs are reduced by utilizing available flexibility. Through an agreement with a FO the user is willing to deviate from the temperature setpoints to save total energy costs. The temperature deviations are allowed with some predefined limitations:

- 1) The temperature deviation is only allowed from midnight until 16.00 (hours 1 – 15). From 16.00 to 24.00 deviations are not allowed.
- 2) The temperature deviation must be limited to +/- 2°C
- 3) The temperature is not allowed to deviate for any longer time than three hours, then the temperature must return to the setpoint
- 4) Deviations are allowed maximum twice a day

For example, in a given day, the temperature setpoints are 21°C from 16.00 to 24.00 and 19 °C for the rest of the day as shown in Figure 18. The green curve shows the setpoints. The red curve shows the upper limit when deviation is allowed, and the blue shows the corresponding lower temperature limit. Notice that the timing constraints – maximum three hours' deviation and maximum twice a day, is not visible in Figure 18. By selecting between the three temperature levels, consumption can be shifted away from high price hours.

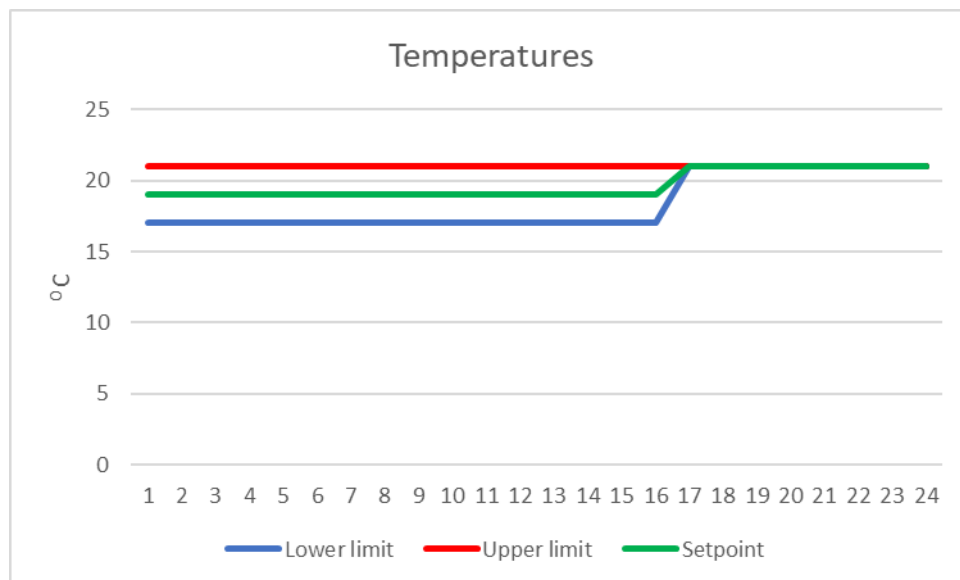


Figure 18. Temperature variation during a day in a house

The temperature inside the room is proportional to the thermal energy level inside the room. If the energy level is high, the room temperature is high and vice versa. The

required energy level for given temperature and the energy demand can be predicted in multiple ways [13-16]. Article [13] proposes a grey-box modelling technique to identify suitable model for the heat dynamics of buildings. Article [14] presents a method for heat load forecasting for single family houses. This model can be used to estimate the energy level to maintain the temperature in the room. Power capacity profile estimation for building heating and cooling in demand-side management is presented in [15]. A review of different energy models for demand forecasting is presented in [16].

The space heating model presented in this chapter relays on the energy levels predicted by prediction algorithms provided by eSmart in INVADE Integrated Platform (IIP). The algorithms should estimate the needed energy if the temperature in one hour is increased to the upper limit (21°C) or reduced to the lower limit (17°C) in the allowed time interval (hour 1 – 15). More energy is needed to deliver the upper temperature limit and less to deliver the lower limit, compared to the setpoint.

However, if the temperature in one hour is deviating from the setpoint, it will also influence the energy needed in the next hour. If the temperature in one hour is raised to the upper limit, the need in the next hour is smaller, compared to a situation where the temperature in the same hour is at the setpoint. And contrary: if the temperature in one hour is reduced to the lower limit, the energy needed to reach the setpoint or the upper limit will be larger.

Let us say the inside temperature at any time period is  $T_{l,t}^{SH,in}$  and the corresponding energy level inside the room is  $w_{l,t}^{SH,r}$ . The setpoint temperature values entered by the user is  $T_{l,t}^{SH,s}$ . The upper and lower limit of the temperature are denoted by  $T_{l,t}^{SH,u}$  and  $T_{l,t}^{SH,l}$ . The energy level in the room  $w_{l,t}^r$  corresponding to the temperature  $T_{l,t}^{SH,s}$  is predicted to be  $W_{l,t}^{SH,s}$ . Similarly the energy level in the room  $w_{l,t}^{SH,r}$  corresponding to the temperature at upper limit  $T_{l,t}^{SH,u}$  is predicted to be  $W_{l,t}^{SH,u}$  and energy level in the room  $w_{l,t}^{SH,r}$  corresponding to the lower upper limit  $T_{l,t}^{SH,l}$  is predicted to be  $W_{l,t}^{SH,l}$ . The additional energy  $(W_{l,t}^{SH,u} - W_{l,t}^{SH,s})$  delivered can be used for compensating the energy required for heating in the future time periods. The energy difference  $(W_{l,t}^{SH,s} - W_{l,t}^{SH,l})$  can be used for heat storage for the energy available in the future time periods.

As the temperature outside the house  $T_{l,t}^{SH,out}$  is lower than  $T_{l,t}^{SH,in}$ , there is a heat loss  $W_{l,t}^{SH,out}$  from the house to outside environment as shown in the Figure 19. The space heater has to compensate for the heat loss by adding the heat energy  $\omega_{l,t}^{SH}$  to maintain



the temperature between  $T_{l,t}^{SH,u}$  and  $T_{l,t}^{SH,l}$ . If energy provided by  $\omega_{l,t}^{SH}$  is less than  $W_{l,t}^{SH,out}$  the temperature inside the house will continue to drop from  $T_{l,t}^{SH,in}$  in the next time periods and vice versa. The relation between  $T_{l,t}^{SH,in}$ ,  $T_{l,t}^{SH,out}$ ,  $\omega_{l,t}^{SH}$  and  $W_{l,t}^{SH,out}$  is not linear.

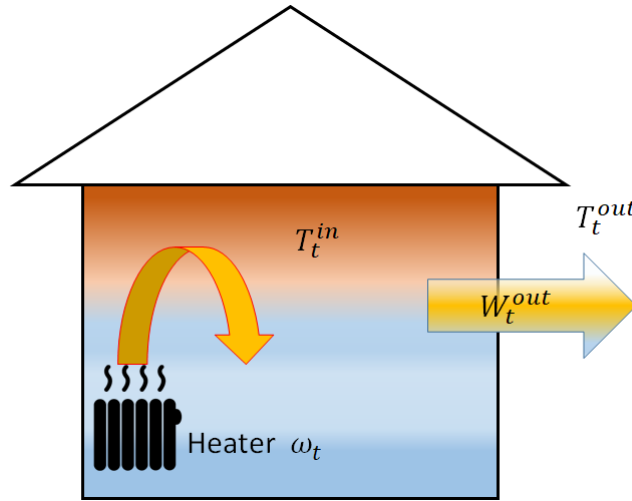


Figure 19. Heat flow and temperature in a house

Let us say when  $T_{l,t}^{SH,in} = T_{l,t}^{SH,s}$ , the heat loss  $W_{l,t}^{SH,out} = W_{l,t}^{SH,out(s)}$ . Similarly the heat loss at  $T_{l,t}^{SH,in} = T_{l,t}^{SH,u}$  is  $W_{l,t}^{SH,out(s)} + \alpha_{l,t}$ , where  $\alpha_{l,t}$  is the additional heat loss due to increase in room temperature, and the heat loss at  $T_{l,t}^{SH,in} = T_{l,t}^{SH,l}$  is  $W_{l,t}^{SH,out(s)} - \beta_{l,t}$ , where  $\beta_{l,t}$  is the reduction in heat loss due to decrease in room temperature.

For the model simplicity, let us assume that  $\alpha_{l,t}$  and  $\beta_{l,t}$  are considerably small when compared to  $W_{l,t}^{SH,l}$ ,  $W_{l,t}^{SH,s}$  and  $W_{l,t}^{SH,u}$  and the total heat capacity of the room, and errors due to disturbances like unexpected air exchange on door openings and change in number of occupants. Therefore the heat loss in whole temperature range ( $T_{l,t}^{SH,l}$  to  $T_{l,t}^{SH,u}$ ) is assumed to be  $W_{l,t}^{SH,out}$ .

Table 5 explains an example case of energy requirement for the first 7 time periods, each representing 1 hour, within the controllable period 0 and 16 hours as shown in Figure 18. These values will be provided by eSmart prediction algorithms in IIP, for a constant outside temperature  $T_{l,t}^{SH,out}$ . This means that for the hours where the temperature can deviate (1 – 15), we can decide between three different options: The temperature can be at the lower limit, at setpoint or at upper limit and required energy to maintain the temperature are predicted accordingly.

**Table 5: Predicted heater energy consumption to reach the temperatures**
 $T_{l,t}^{SH,u}$ ,  $T_{l,t}^{SH,s}$  and  $T_{l,t}^{SH,l}$  from  $T_{l,t}^{SH,s}$ .

Temperature	Energy required	Time period						
		1	2	3	4	5	6	7
$T_{l,t}^{SH,u}$	$W_{l,t}^{SH,u}$ (kWh)	1.5	1.5	1.5	1.5	1.5	1.5	1.5
$T_{l,t}^{SH,s}$	$W_{l,t}^{SH,s}$ (kWh)	1	1	1	1	1	1	1
$T_{l,t}^{SH,l}$	$W_{l,t}^{SH,l}$ (kWh)	0.7	0.7	0.7	0.7	0.7	0.7	0.7

## 6.4 Flexibility

The heat capacity  $W_{l,t}^{SH,u} - W_{l,t}^{SH,s}$  provides heat storage for preheating the room and the heat capacity  $W_{l,t}^{SH,s} - W_{l,t}^{SH,l}$  provides the heat storage that can be availed by cooling the room to  $T_{l,t}^{SH,l}$ . The reasons for flexibility usage could be

1. **To minimize the energy cost with time varying prices:** The space heaters can consume more by preheating the room during the low price periods or if high energy price is anticipated in the following hours. Also cooling the room by reduced consumption during the high energy price periods, or if low energy price is anticipated in the following hours can reduce total energy cost for heating.
2. **To avoid the total power consumption to exceed the subscribed power limits:** The combined power consumption of other loads (mainly inflexible loads) and the load due to regular heating (without optimization) by space heaters may exceed the subscribed power limit. In such scenarios, the flexibility provided by the space heaters can be used to avoid power peaks by shifting their consumption.
3. **To provide flexibility in aggregated flexibility services:** In case of DSO or BRP requesting flexibility, thermal space heaters can provide up and down regulation.

## 6.5 Mathematical formulation

As described earlier, the electrical energy delivered to the heater at any time period is  $\omega_t$  which is in the demand part of the energy balance equation. As the resistive electric space heaters has a coefficient of performance (COP) 1, the amount of kWh of electricity consumed equals to the kWh of heat emitted. Since  $w_{l,t}^{SH,r}$  is energy level in the room at any time period and the heat loss at any time period is  $W_{l,t}^{SH,out}$ . The relation between  $w_{l,t}^{SH,r}$ ,  $w_{l,t-1}^{SH,r}$ ,  $W_{l,t}^{SH,out}$  and  $\omega_t$  are as given by Eq. (50). If  $\omega_t^{SH} = W_{l,t}^{SH,out}$ ,  $w_{l,t}^{SH,r}$  will remain at the same value as in the previous time period  $w_{l,t-1}^{SH,r}$  and the room temperature also maintained in the same level as the temperature at previous time period. If  $\omega_t^{SH} > W_{l,t}^{SH,out}$ , then  $w_{l,t}^{SH,r}$  will be higher than  $w_{l,t-1}^{SH,r}$  and the room temperature also will increase. Similarly if  $\omega_t^{SH} < W_{l,t}^{SH,out}$ , then  $w_{l,t}^{SH,r}$  will be lower than  $w_{l,t-1}^{SH,r}$  and the room temperature also will decrease. As the temperature inside the room has to be maintained between  $T_{l,t}^{SH,u}$  and  $T_{l,t}^{SH,l}$ ,  $w_{l,t}^{SH,r}$  has to take a value between  $W_{l,t}^{SH,u}$  and  $W_{l,t}^{SH,l}$ . The maximum value of  $\omega_t^{SH}$  is limited by the space heater capacity  $W_l^{SH,H}$ .

$$w_{l,t}^{SH,r} = w_{l,t-1}^{SH,r} + \omega_t^{SH} - W_{l,t}^{SH,out}, \quad \forall l \in L^{sh}, \forall t \in T \quad (50)$$

$$0 \leq \omega_t^{SH} \leq W_{l,t}^{SH,h}, \quad \forall l \in L^{sh}, \forall t \in T \quad (51)$$

$$W_{l,t}^{SH,l} \leq w_{l,t}^{SH,r} \leq W_{l,t}^{SH,u}, \quad \forall l \in L^{sh}, \forall t \in T \quad (52)$$

Where

$W_l^{SH,h}$ : is the maximum power rating of the space heater,

$W_{l,t}^{SH,l}$  is the energy level of the room corresponding to temperature  $T_{l,t}^{SH,l}$

$W_{l,t}^{SH,u}$  is the energy needed to achieve  $T_{l,t}^{SH,u}$

Let us consider the following simple example case shown in the Table 6, with the initial condition  $w_{l,0}^{SH,r} = 1$ , heat loss  $W_{l,t}^{SH,out}$  is 0.5 kWh for all time periods and maximum power rating of the space heater  $W_l^{SH,H}$  equals to 4 kW. The electricity prices are shown in the fourth row, represent by parameter, i.e.,  $P_t^{buy}$ . At the low price period 't = 3',  $P_t^{buy} = 5$  € cent /kWh the room is preheated to the maximum level

( $w_3^r=1.5$  kWh) to avail the flexibility. Similarly, as there is high price seen at the period 't = 7', the room is preheated to the maximum level at the period 't = 5' ( $w_{l,5}^{SH,r}=1.5$  kWh) to avail the flexibility and reduce the total cost from 47.5 to 35 € cent.

**Table 6: Example case flexibility activation at low price period.**

Parameters	Time period						
	1	2	3	4	5	6	7
$W_{l,t}^{SH,u}$ (kWh)	1.5	1.5	1.5	1.5	1.5	1.5	1.5
$W_{l,t}^{SH,s}$ (kWh)	1	1	1	1	1	1	1
$W_{l,t}^{SH,l}$ (kWh)	0.7	0.7	0.7	0.7	0.7	0.7	0.7
$W_{l,t}^{SH,out}$ (kWh)	0.5	0.5	0.5	0.5	0.5	0.5	0.5
$P_{l,t}^{buy}$	10	10	5	10	10	20	30
$\omega_{l,t}^{SH}$ (kWh)	0.5	0.5	1	0	1	0.5	0
$w_{l,t}^{SH,r}$ (kWh)	1	1	1.5	1	1.5	1.5	1

## 6.6 Runtime constraints

Like other flexibility resources, there should be a provision to limit the number of flexibility activations, maximum duration of each activation and minimum resting time between two successive activations

To implement the timing constraints for flexibility activations, the 'start', 'end' and 'run' conditions of the flexibility activations have to be defined. The start condition is represented by a binary variable  $\delta_{l,t}^{SH,start}$ , the end condition is represented by a binary variable  $\delta_{l,t}^{SH,end}$  and the run condition is represented by another binary variable  $\delta_{l,t}^{SH,run}$

$\delta_{l,t}^{SH,start}$  will take a value 1 at the first period of the flexibility activation and will be 0 for the rest of the periods.  $\delta_{l,t}^{SH,run}$  will take a value 1 for all the periods in which flexibility is activated, including the first period of flexibility activation (This case is different from other flexible load). The  $\delta_{l,t}^{SH,end}$  will take a value 1 one period after the flexibility activation is ended and will be 0 for the rest of the time periods. For example, if the flexibility is activated for the periods 3,4,5 and 6,  $\delta_{l,t}^{SH,start}$  will be 1 only for period 3,  $\delta_{l,t}^{SH,run}$  will 1 for the periods 3, 4, 5 and 6, and  $\delta_{l,t}^{SH,end}$  will be 1 only for period 7. A detailed example is given in the Table 7.

With the binary variables, equation Eq. (52) can be rewritten as follows to enable flexibility only when  $\delta_{l,t}^{SH,run} = 1$ .

$$\delta_{l,t}^{SH,run} \cdot W_{l,t}^{SH,l} + (1 - \delta_{l,t}^{SH,run}) \cdot W_{l,t}^{SH,s} \leq w_{l,t}^{SH,r} \leq \delta_{l,t}^{SH,run} \cdot W_{l,t}^{SH,u} + (1 - \delta_{l,t}^{SH,run}) \cdot W_{l,t}^{SH,s}, \quad \forall l \in L^{sh}, \forall t \in T \quad (53)$$

$$\delta_{l,t}^{SH,run} \in \{0,1\}, \quad \forall l \in L^{sh}, \forall t \in T \quad (54)$$

## 6.7 Time restriction of flexibility activation

The flexibility activation can be restricted to certain time periods as shown in Figure 20.

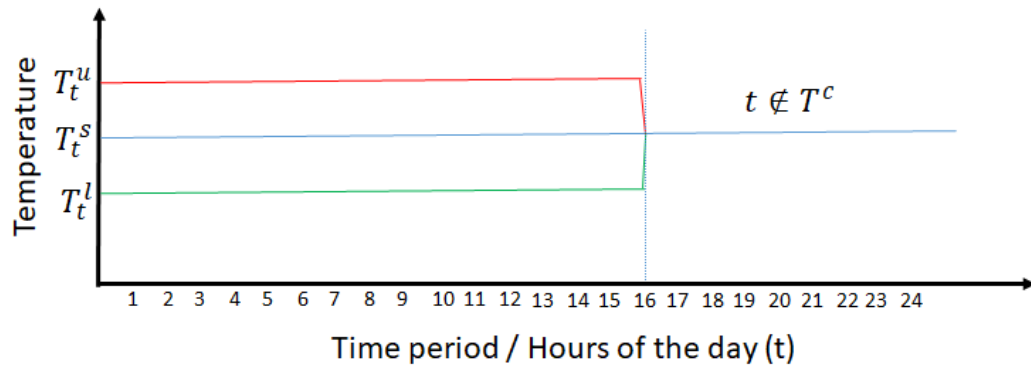


Figure 20. Time restriction of flexibility activation

The necessary constraint for the above restriction is

$$\delta_{l,t}^{SH,run} = 0, \quad \forall l \in L^{sh}, \forall t \notin T^c \quad (55)$$

where  $T^c$  is the subset of periods where heater control is allowed

### 6.8 Identification for ‘start’, ‘run’ and ‘end’ of flexibility activation

To identify the ‘start’ and ‘end’ conditions, the additional constraints are

$$\delta_{l,t}^{SH,run} - \delta_{l,t-1}^{SH,run} = \delta_{l,t}^{SH,start} - \delta_{l,t}^{SH,end}, \quad \forall l \in L^{SH}, \forall t \in T \quad (56)$$

$$\delta_{l,t}^{Sh,start} \in \{1,0\}, \quad \forall l \in L^{sh}, \forall t \in T \quad (57)$$

$$\delta_{l,t}^{SH,end} \in \{1,0\}, \quad \forall l \in L^{sh}, \forall t \in T \quad (58)$$

The flexibility activation should not start and end at the same time. Therefore,

$$\delta_{l,t}^{SH,start} + \delta_{l,t}^{SH,end} \leq 1, \quad \forall l \in L^{sh}, \forall t \in T \quad (59)$$

**Table 7: Example of binary values for start, run and end conditions.**

Time period	1	2	3	4	5	6	7	8	9	10	11	12	13	14	15
$\delta_{l,t}^{SH,run}$	0	0	0	0	1	1	1	1	1	1	1	0	0	0	0
$\delta_{l,t}^{SH,start}$	0	0	0	0	1	0	0	0	0	0	0	0	0	0	0
$\delta_{l,t}^{Sh,end}$	0	0	0	0	0	0	0	0	0	0	0	1	0	0	0

### 6.9 Maximum duration of flexibility activation constraint

The maximum duration of flexibility activation as described in Section 2.1 and as shown in Figure 21 can be limited by the following constraint

$$\sum_{i=t}^{t+D_l^{SH,max}} \delta_{l,i}^{SH,end} \geq \delta_{l,t}^{SH,start}, \quad \forall l \in L^{sh}, \forall t \in T \quad (60)$$

Where  $D_l^{SH,max}$  is the maximum duration of flexibility activation.

For example, if  $D_l^{SH,max} = 7$  as shown in the Table 7 and if the flexibility activation starts at time period  $t=5$ , as per Eq. (60), ( $i$  ranges from 5 to 12 )

$$\left( \delta_{l,5}^{SH,end} + \delta_{l,6}^{SH,end} + \dots + \delta_{l,12}^{SH,end} \right) \geq \delta_{l,5}^{SH,start} \quad (61)$$

## 6.10 Minimum duration between successive flexibility activation constraint

There should be a minimum resting period between two successive flexibility activations as defined by the user. It is illustrated in Figure 21.

$$\delta_{l,t}^{SH,end} + \sum_{i=t}^{t+D_l^{SH,min}-1} \delta_{l,i}^{SH,start} \leq 1, \quad \forall l \in L^{sh}, \forall t \in T \quad (62)$$

Where  $D_l^{SH,min}$  is the minimum duration between two successive activations

In the above example, if  $D_l^{SH,min} = 4$ , as per Eq. (62),  $\delta_{l,13}^{SH,start}$ ,  $\delta_{l,14}^{SH,start}$ ,  $\delta_{l,15}^{SH,start}$  ( $i$  ranges from 13 to 15) will be forced to 0 as  $\delta_{l,12}^{SH,end} = 1$ , to respect Eq. (62) and the expression is

$$\left( \delta_{l,12}^{SH,end} + \delta_{l,13}^{SH,start} + \delta_{l,14}^{SH,start} + \delta_{l,15}^{SH,start} \right) \leq 1 \quad (63)$$

Therefore, next possible flexibility activation can be only at  $t=16$  as shown in Table 7.

## 6.11 Maximum number of flexibility activation constraint

The number of flexibility activations should be limited to a maximum number as described in Section 2.1 and as shown in Figure 21.

The maximum number of flexibility activation can be limited by the following constraint

$$\sum_{t \in T} \delta_{l,t}^{SH,start} \leq N_l^{SH,max}, \quad \forall l \in L^{sh}, \forall t \in T \quad (64)$$

Where  $N_l^{SH,max}$  is the maximum number of activations allowed.

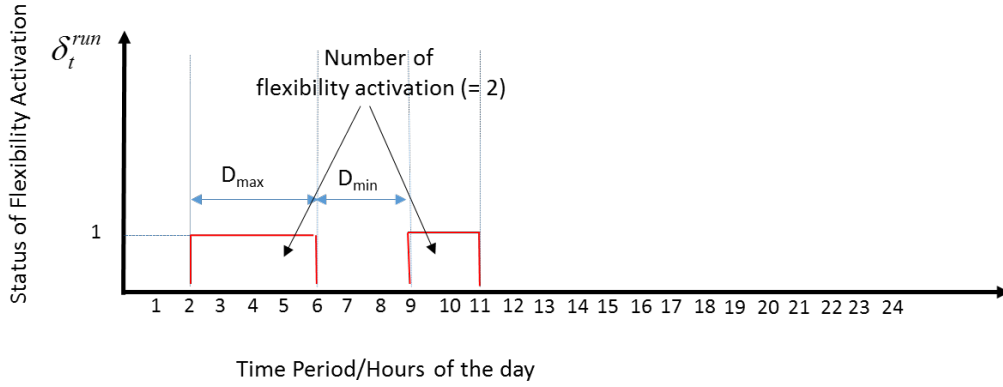


Figure 21. Timing constraints and number of flexibility activation.

## 6.12 Flexibility contract cost

If  $p^{flexibility\_period}$  is the cost for flexibility activation per period, then the total cost for flexibility activation  $\zeta^{SH}$  is

$$\zeta^{SH} = \sum_{l \in L} \sum_{t \in T} P^{SH, flex} \cdot \delta_{l,t}^{SH, run} \quad (65)$$

## 6.13 The complete model

The sub-chapter includes the complete model formulation, to show the overall implementation of space heating model. This includes time restriction of flexibility activation, maximum duration of flexibility activation constraint, and minimum duration between successive flexibility activation as well as maximum number of activations constraints. The objective function is to minimize the electricity bill for the prosumer. The objective functions have already presented in D5.3, and the heater consumption,  $\omega_{l,t}^{SH}$ , in the following equation is in the demand part of the energy balance equation for the given prosumer.

$$w_{l,t}^{SH, r} = w_{l,t-1}^{SH, r} + \omega_{l,t}^{SH} - W_{l,t}^{SH, out}, \quad \forall l \in L^{sh}, \forall t \in T \quad (66)$$

$$0 \leq \omega_{l,t}^{SH} \leq W_{l,t}^{SH, h}, \quad \forall l \in L^{sh}, \forall t \in T \quad (67)$$

$$\begin{aligned} \delta_{l,t}^{SH, run} \cdot W_{l,t}^{SH, l} + (1 - \delta_{l,t}^{SH, run}) \cdot W_{l,t}^{SH, s} &\leq w_{l,t}^{SH, r} \leq \\ \delta_{l,t}^{SH, run} \cdot W_{l,t}^{SH, u} + (1 - \delta_{l,t}^{SH, run}) \cdot W_{l,t}^{SH, s}, &\quad \forall l \in L^{sh}, \forall t \in T \end{aligned} \quad (68)$$



$$\delta_{l,t}^{SH,run} = 0, \quad \forall l \in L^{sh}, \forall t \notin T^c \quad (69)$$

$$\delta_{l,t}^{SH,run} \in \{0,1\}, \quad \forall l \in L^{sh}, \forall t \in T^c \quad (70)$$

$$\delta_t^{run} - \delta_{t-1}^{run} = \delta_t^{start} - \delta_t^{end}, \quad \forall t \in T \quad (71)$$

$$\delta_{l,t}^{SH,start} \in \{1,0\}, \quad \forall l \in L^{sh}, \forall t \in T \quad (72)$$

$$\delta_{l,t}^{SH,end} \in \{1,0\}, \quad \forall l \in L^{sh}, \forall t \in T \quad (73)$$

$$\delta_{l,t}^{SH,start} + \delta_{l,t}^{SH,end} \leq 1, \quad \forall l \in L^{sh}, \forall t \in T \quad (74)$$

$$\sum_{i=t}^{t+D_l^{SH,max}} \delta_{l,i}^{SH,end} \geq \delta_{l,t}^{SH,start}, \quad \forall l \in L^{sh}, \forall t \in T \quad (75)$$

$$\delta_{l,t}^{SH,end} + \sum_{i=t}^{t+D_l^{SH,min}-1} \delta_{l,i}^{SH,start} \leq 1, \quad \forall l \in L^{sh}, \forall t \in T \quad (76)$$

$$\sum_{t \in T} \delta_{l,t}^{SH,start} \leq N_l^{SH,max}, \quad \forall l \in L^{sh}, \forall t \in T \quad (77)$$

### 6.14 Illustrative example

Here, we present an illustrative example of testing the above model for the period of 24 hours with each time period representing a duration of 1 hour. The objective function for this example is to minimize the electricity cost for heating demand  $\omega_t$ , which can be explained by the below equation:

$$\min \left( \sum_{t \in T} P_t^{buy} \cdot \omega_{l,t}^{SH} + P^{SH,flex} \cdot \delta_{l,t}^{SH,run} \right) \tag{78}$$

The list of parameters to the space heating model are listed in Table 8.

Table 8. Parameters of the model.

Parameters	Time period																							
	1	2	3	4	5	6	7	8	9	10	11	12	13	14	15	16	17	18	19	20	21	22	23	24
$W_{l,t}^{SH,u}$ (kWh)	1.5	1.5	1.5	1.5	1.5	1.5	1.5	1.5	1.5	1.5	1.5	1.5	1.5	1.5	1.5	1.5	1.5	1.5	1.5	1.5	1.5	1.5	1.5	1.5
$W_{l,t}^{SH,s}$ (kWh)	1	1	1	1	1	1	1	1	1	1	1	1	1	1	1	1	1	1	1	1	1	1	1	1
$W_{l,t}^{SH,l}$ (kWh)	0.7	0.7	0.7	0.7	0.7	0.7	0.7	0.7	0.7	0.7	0.7	0.7	0.7	0.7	0.7	0.7	0.7	0.7	0.7	0.7	0.7	0.7	0.7	
$W_{l,t}^{SH,out}$ (kWh)	0.5	0.5	0.5	0.5	0.5	0.5	0.5	0.5	0.5	0.5	0.5	0.5	0.5	0.5	0.5	0.5	0.5	0.5	0.5	0.5	0.5	0.5	0.5	
$P_t^{buy*}$ (€ cent/kWh)	10	10	10	10	20	20	40	50	50	40	30	30	20	20	30	40	40	50	50	50	30	20	20	15

In addition to the above table we have the following input parameters to the model

$$N_l^{SH,max} = 5, D_l^{SH,max} = 5, D_l^{SH,min} = 2, T_l^{SH,c} = \{1, \dots, 15\}, W_l^{SH,h} = 4 \text{ kW}, P^{SH,flex} = 1 \text{ € cent/kWh}$$

The output results of the optimization algorithm are presented in Table 9.

Table 9. Output results of the model.

Output	Time period																							
	1	2	3	4	5	6	7	8	9	10	11	12	13	14	15	16	17	18	19	20	21	22	23	24
$w_{l,t}^{SH,r}$ (kWh)	1	1	1	1.5	1.5	1.5	1.5	1	1	0.7	1	1	1	1.5	1.5	1	1	1	1	1	1	1	1	1
$\omega_{l,t}^{SH}$ (kWh)	0.5	0.5	0.5	1	0.5	0.5	0.5	0	0.5	0.2	0.8	0.5	0.5	1	0.5	0	0.5	0.5	0.5	0.5	0.5	0.5	0.5	0.5
$\delta_{l,t}^{SH,run}$	0	0	0	1	1	1	1	0	0	1	0	0	0	1	1	0	0	0	0	0	0	0	0	0
$\delta_{l,t}^{SH,start}$	0	0	0	1	0	0	0	0	0	1	0	0	0	1	0	0	0	0	0	0	0	0	0	0
$\delta_{l,t}^{SH,end}$	0	0	0	0	0	0	0	1	0	0	1	0	0	0	0	1	0	0	0	0	0	0	0	0

Energy cost (without optimization) = 352.5 € cent

Optimized energy cost = 319.5 € cent

Flexibility cost = 7 € cent

Objective function value = 326.5

The electricity price and the optimized space heater consumption are shown in Figure 22. The room is preheated at low price hour t=4 (10 € cent/kWh) to reduce the consumption at the high price hour t=8 (50 € cent/kWh). The room temperature for the time periods t = 4, 5, 6 and 7 will be at higher temperature ( $T_{l,t}^{SH,u}$ ), as the energy level in the room is at higher level ( $W_{l,t}^{SH,u}$ ) as shown in the Figure 23. Further the room is precooled at the time period t=10 when the price relatively higher (40 € cent/kWh) as there is relatively low price at time period t=11 (30 € cent/kWh). Another preheating is activated at low price hour t=13 (20 € cent/kWh) to reduce the consumption at the relative high price hour t=16 (40 € cent/kWh).

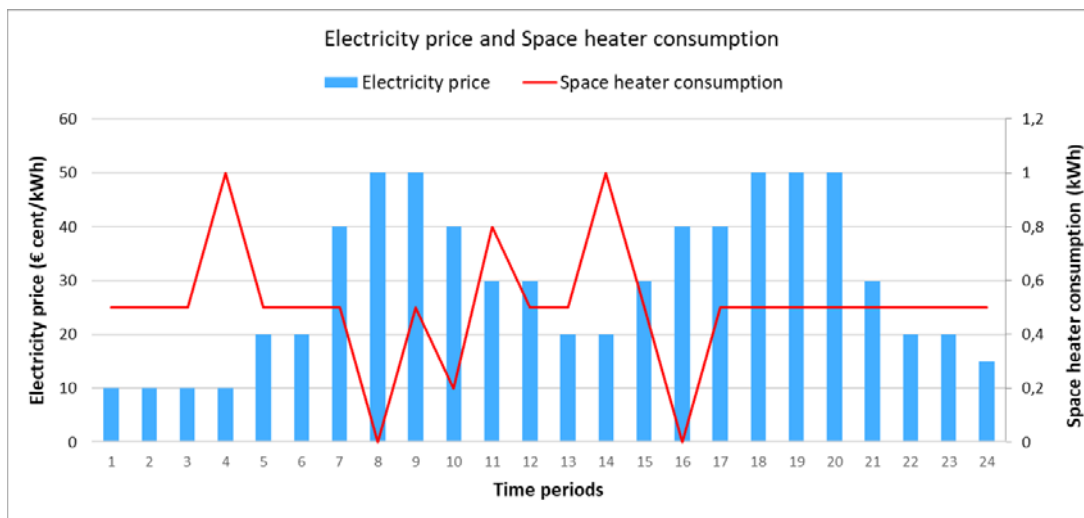


Figure 22. Electricity price and optimized space heater consumption over 24 time periods.

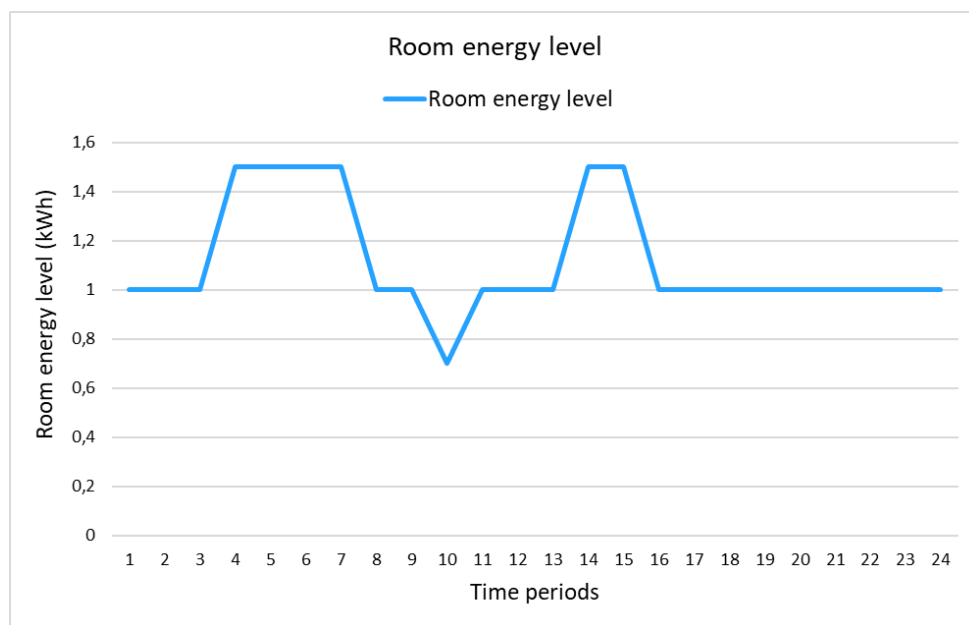


Figure 23. Room energy level representing temperature.

The flexibility activations happen only between the allowable time periods 1 and 15, though there is relative price variation during the time periods  $t=16$  and  $t=24$ . It is shown in Figure 23, in which the room energy level  $w_t^r$  stays at the set value  $W_{l,t}^{SH,s}$ . Therefore the room temperature also stays at the setpoint value  $T_{l,t}^{SH,s}$ , during the time periods between  $t=16$  and  $t=24$ .

## 7 Information structure and the planning process

### 7.1 Introduction

In D5.3, chapter 4 elaborates about different planning approaches, information structure, length of horizon, and time resolution for different services. This chapter will discuss the approach adapted for planning in detail.

### 7.2 Length of planning horizon

The optimization horizon will include historic and forecasted periods. The number of historic and future periods will vary depending on information provided by the INVADE platform. The optimization framework is developed to adopt different historic and forecaster periods as an input from the INVADE integrated platform. In the given example in the following sections, the total optimization horizon stretches for 3 days, in which first 24 hours are historical values and the rest 48 hours are the timeline for optimization with forecasted parameters. At the beginning of a day, the electricity prices are known for 24 hours. Therefore, the planning horizon could have been only 24 hours. As the EV charging schedule overlaps between 2 days (from the first day evening till next day morning), it was decided to keep one day in addition in the planning horizon with forecasted electricity prices to avoid EV charging schedules unserved. Similarly, to accommodate the EV schedule started on the day before and to keep the optimization framework generalized, all the time periods in the previous day is included in the historical data. Thus the planning horizon get stretched for 3 days by considering the day before (as history) and after in the optimization framework.

### 7.3 Time resolution

The general consideration for time resolution is 15 minutes as the electricity metering is done at the main meter with 15 minutes resolution. The optimization framework is developed to adopt different time resolution as an input from the INVADE integrated platform, for example 1 hour, where the metered and forecasted parameter are available with 1 hour time resolution. But the basic requirement is that all the metered and forecasted parameters must have same time resolution for a given optimization instant and the result of optimization also will follow the same time resolution. In addition, in the prosumer case with kWmax subscription, the consumption above subscribed limit is calculated hourly basis. The optimization model adopts to this scenario even if the input data is with 15 minutes time resolution.

### 7.4 Receding and rolling process

In the optimization process for the given planning horizon, the receding horizon method is used. The problem is solved for a given window. The default horizon length is 3 days with one historic day in which the variable are fixed with actual metered values.

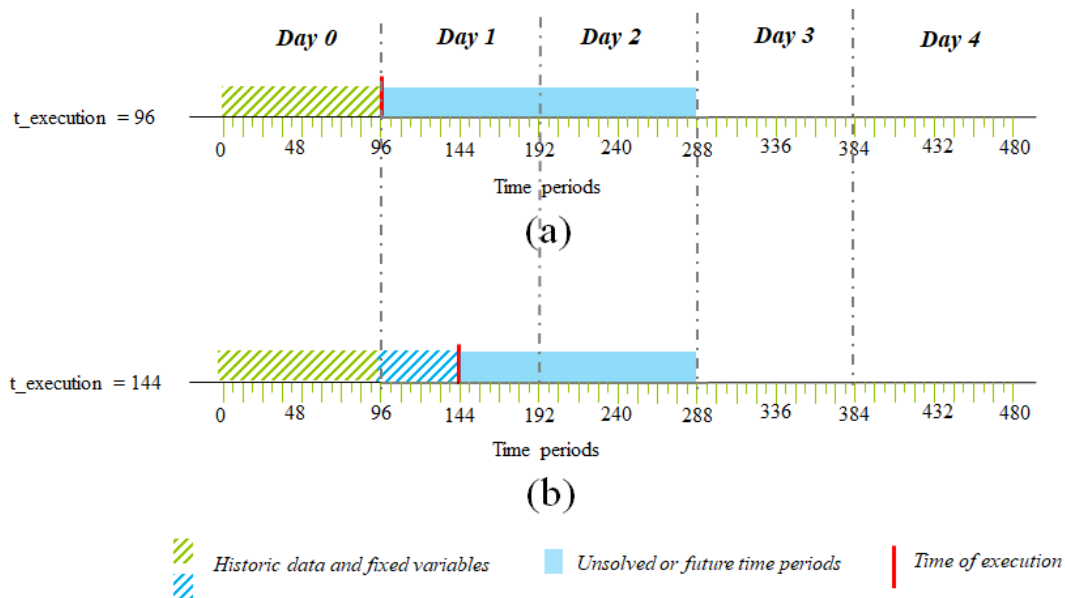


Figure 24. Receding horizon approach within planning horizon.

The receding process is illustrated in the Figure 24 with 15 minutes time resolution. Figure 24 (a) shows the planning horizon at the beginning of the day with 288 periods, when the time of execution ( $t_{\text{execution}}$ ) is 96. The green shaded bar for the first 96 time periods which represents the historic values from the previous day. The optimization problem is solved for the remaining horizon length of 2 days (192 time periods), and the

control signals are applied only for one time period after  $t_{\text{execution}}$ . The current time is entitled as  $t_{\text{execution}}$ . After solving for each  $t_{\text{execution}}$ , the variables values for the  $t_{\text{execution}}$  are fixed similar to the historic values and the  $t_{\text{execution}}$  is incremented and moved forward. By doing that, the horizon is fixed for 3 days but the solver only has to solve for the periods between the current  $t_{\text{execution}}$  and the end of the planning horizon as shown in Figure 24(b). For example, the number of periods to solve in each iteration decrease from 192 (at the beginning of each day) to 144 at the mid of the day when the execution is 144.

After the end of each day, the optimization horizon is rolled forward by one day ahead. A new planning horizon is formulated by including a new day ahead, discarding the oldest day in the previous planning horizon and considering the previous day for historic values. The  $t_{\text{execution}}$  is reset to 96 as it is the beginning of the new day. This can be seen in Figure 25 (a) and (b).

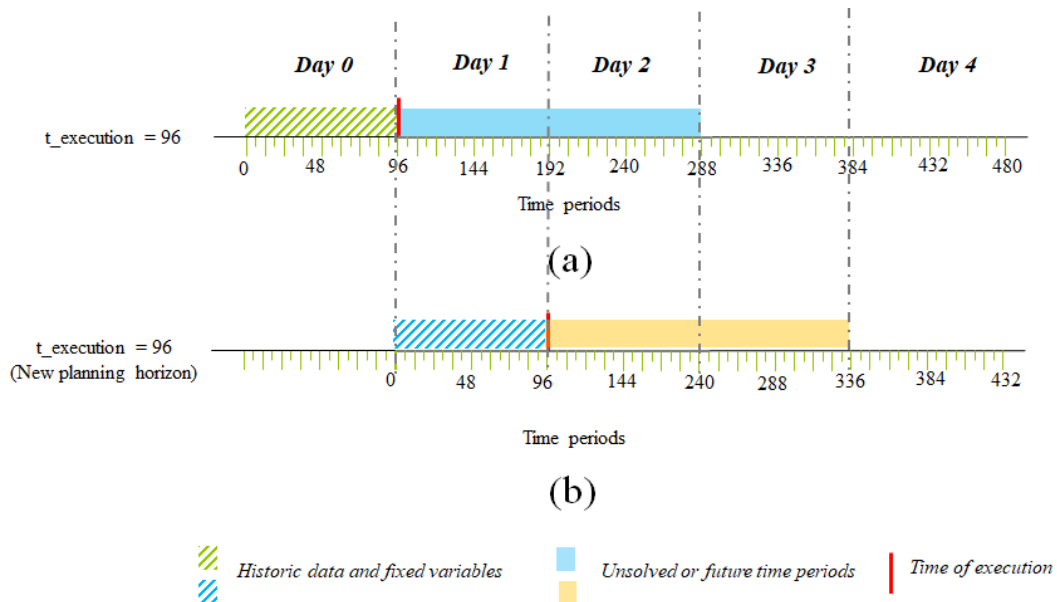


Figure 25. Rolling horizon approach to extend the horizon

## 7.5 Overall framework

The modelling framework is developed in the programming language Python using the software package Pyomo<sup>4</sup>. The framework is developed in 3 layers as shown in the Figure 26. This figure is only for the illustrative purpose. The actual name of the files may be slightly different depending on the version and Pilot user case. The fundamental layer

<sup>4</sup> <http://www.pyomo.org/>

(layer 1) is built on multiple python (.py) files representing every flexibility resource. For example, the “Battery.py” contains the mathematical formulations corresponding to the battery model. For example, the equations representing SOC development, constraints related to charging and discharging powers and SOC capacity, cost functions for degradation are represented in the “Battery.py” file. Similarly other flexibility resource models’ mathematical representations are coded in their respective python files. Though there is a generic representation of thermal load in the Figure 26, the different thermal load types, i.e., domestic water heater and space heater are represented separately. The different types of curtailable and shiftable loads also represented in the similar fashion like thermal loads.

The second layer contains the files related to optimization input output handling, model building and solving the instance. The optimization model can be built with multiple similar flexibility resources represented in the first layer in any combination based on the user case input data. The third layer provides the overall information about the user case and the interfaces with the INVADE integrated cloud platform. This layer contains the ‘main’ function which is invoked by the IIP and the ‘main’ function calls other functions in the other files to build the model, solve the instance and pass the results to the IIP.

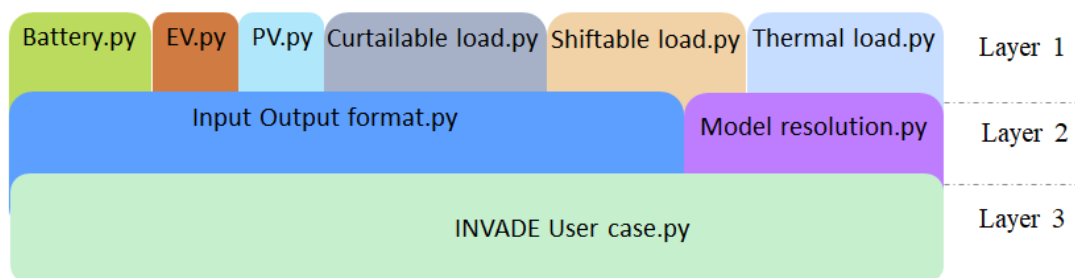


Figure 26. Optimization model file structure

### 7.5.1 Program control flow

The IIP invokes optimization program with the prepared input for the parameters with calculated, forecasted and metered data corresponding to the whole planning horizon. The IIP also provide the information about the time of execution ( $t_{\text{execution}}$ ). The time of execution represents the time period number in the horizon below which the time periods are historic and the parameters and variables are either calculated or metered. And the time periods from time of execution till the end of horizon, the parameters are forecasted and the variables are yet to be solved by the solver during the optimization process.



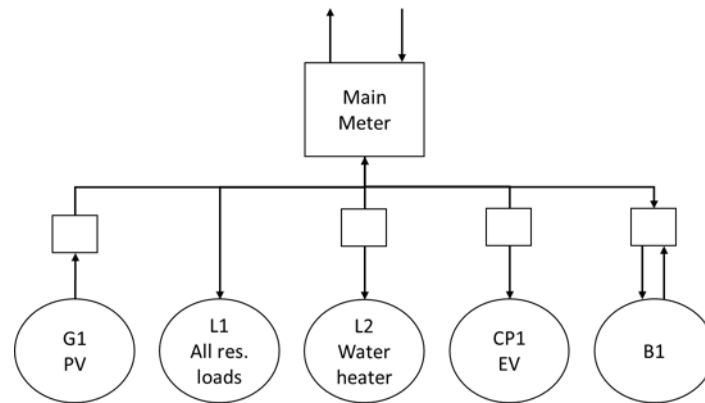


Figure 27. Prosumer site configuration example.

The steps in optimization process are,

1. Optimization model creation

The optimization model is based on the combination of flexibility resources for the given use case with constraints and an objective function for which the result has to be minimized or maximized based on the problem. For example, a prosumer site configuration shown in the Figure 27 has 5 elements namely PV, battery, EV, water heater (thermal load) and all other loads as inflexible loads. The objective is to reduce the electricity import from the grid. The optimization model will be built by adding the resources' to an empty model optimization model based on the input data provided about the resources by the IIP as shown in the flow chart in Figure 28. If there is any problem in building optimization model due to insufficient or wrong information, the program will report the error and terminate the process.

2. Variables fixing for the historic time periods

While creating the optimization model, the parameters are loaded. The second step in the process is to fix the variables and parameters for all time periods less than  $t_{\text{execution}}$  as they represent historic events. Variable fixing problem and the different solution approaches are explained in the Chapter 8

3. Initiate solving process

The third step is to initiate the solving process and wait for the solver to provide solution status. If the optimization problem is solved successfully, the solver provides the status as 'OK'. The optimization result can be formatted as needed

in IIP. In case, if the optimization problem is not solved, other possible solver statuses reported by Pyomo are listed in the Table 10.

**Table 10. Solver status.**

Status	Reason
'warning'	Termination with unusual condition
'error'	Terminated internally with error
'aborted'	Terminated due to external conditions (e.g. interrupts)
'unknown'	Unknown (an uninitialized value)

If the solver reports any status other than 'OK', the status is reported to the IIP, and the results are not valid. The IIP will decide further actions either to execute the optimization process again with new set of forecasted values or use the results from the optimization process executed in the previous time period.

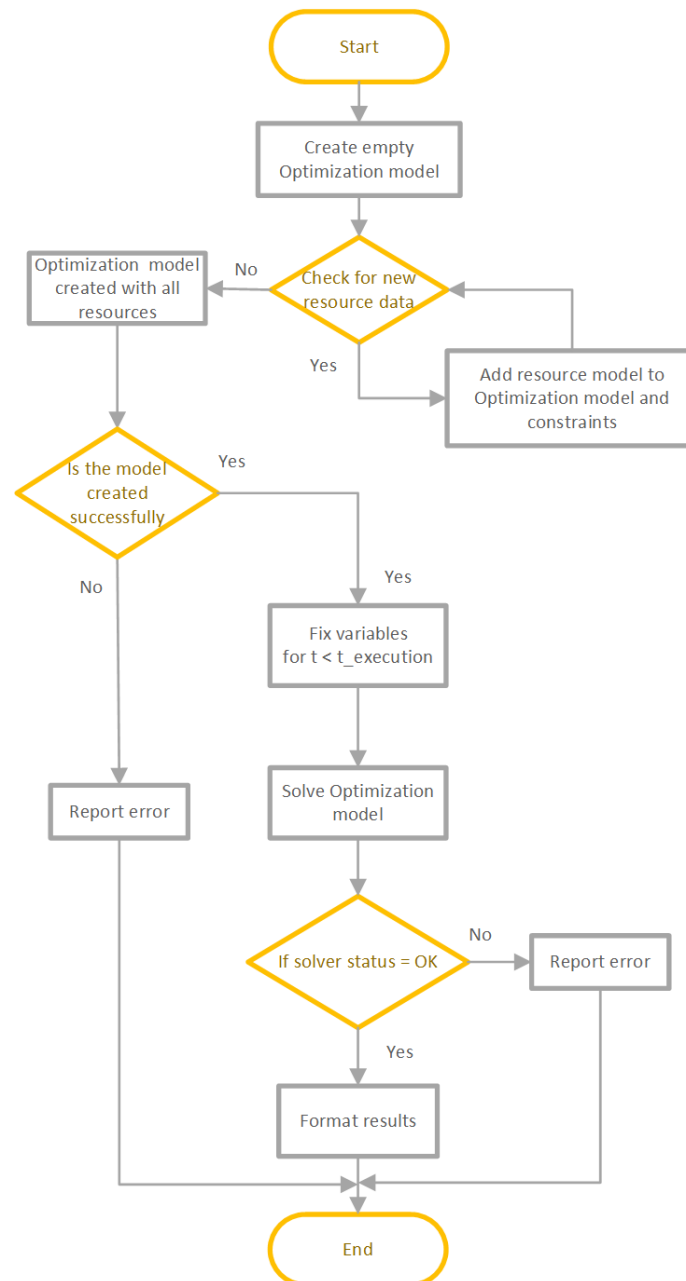


Figure 28. Optimization program flow diagram

## 8 Variable freezing techniques

### 8.1 Problem description

Variable fixing is an issue that appears when operating in a rolling/receding horizon environment. The basic idea is that the algorithm will be run for the same planning horizon many times, but for each iteration, a new period will be historic. When iterating

through a two-day forecasted time horizon and one historic day (288 time periods if programming time units are fifteen minutes), one part of the time horizon is in the past, and the other is in the future for which the optimization problem is solved. The past values (both decision variables and parameters) need to be included in the optimization algorithm using either previously calculated values or metered values from the end-user devices.

Uncertainty is a key factor in variable freezing related issues. Because there always will be deviations from forecasted data to actual metered data, a solid approach has to be chosen in order to deal with these deviations. For example, load consumption is stochastic by nature, meaning that no matter how well our prediction models will perform, we will never be able to predict the exact realized value which is metered.

Mainly, there are two issues related to variable fixing.

1. Parts of the planning horizon is in the **past** and hence, the decisions cannot be freely chosen, since they have already been implemented. So the **decisions must be fixed/frozen** according to decisions made in earlier iterations. This problem stems from the rolling horizon concept. The problem can be divided into the following time segments:

For $t + n$ , where $n \geq 0$ :	All decisions can be treated by the model without any fixing.
For $t - 1$ :	All decisions must be fixed according to the decisions from the previous iteration.
For $t - x$ , where $x \geq 2$ :	All decisions must be fixed, some according to a decision in an earlier iteration (the iteration from which the decision was implemented), some according to a metered value.

2. We in retrospect receive **meter values** for some of the **parameters** and some of the **variables**. The problem with this is that these meter values will be different from the parameters used as input to a previous iteration of the flexibility algorithm (e.g. a prediction or any fixed parameter). In addition, the decision variables decided and implemented in a previous iteration of the flexibility algorithm. The problem can be divided into the following time segments:

For $t + n$ , where $n \geq 0$ :	All parameters are based on predictions and some other assumptions (NB! The latest updated ones).
For $t - 1$ :	All parameters must be fixed according to the predictions used in the previous iteration
For $t - x$ , where $x \geq 2$ :	Some parameters are fixed to metered values (or perhaps we should say that the prediction is substituted with a meter value) and some are fixed according to calculations where meter values are included.

Variable fixing is key in order to ensure feasibility. The goal of this document is to assess what possible approaches exist, analyse their pros and cons, and therefrom decide an approach which is to be implemented.

Some example of situations where variable fixing is needed are listed below:

- Constraints where we need to **keep track of information** such as maximum number of activations, maximum activation or resting time for flexible loads such as disconnectable, reducible and shiftable loads.
- When **metered and calculated values differ**, such as the battery state of charge. This problem could occur due to multiple reasons such as charger efficiency, constant current charging range, overheating etc. As the model is simplified by compromising certain non-linear effects, the metered state of charge may differ from the calculated value.
- In the case of subscribed power (on an hourly basis), uncertainty in inflexible load prediction results in sub-optimal use of flexibility resources. By metering and updating the real conditions, the algorithm can “recover” from such disturbances.

The three above suggested situations also apply to other elements and parameters, such as generation, EV charging etc.

Another issue is what we call the “t-1” issue described in Figure 29. Every 15 minutes, control dispatch signals are sent from the INVADE platform to the local systems as an end result of the previous iteration. When the new iteration starts, predicted and metered data are sent to the platform in order to start the optimization with as new information as possible.

The problem has a horizon of 288 periods in which 192 periods are forecasted. The first iteration will be run some minutes before the start of the 96th period (15 minutes are chosen in this example). The algorithm is free to decide the decision variables for all periods, and all uncertain parameters are represented by their predicted values. The integrated INVADE platform then sends the decisions to the local systems, and the decisions for period 96 are implemented.

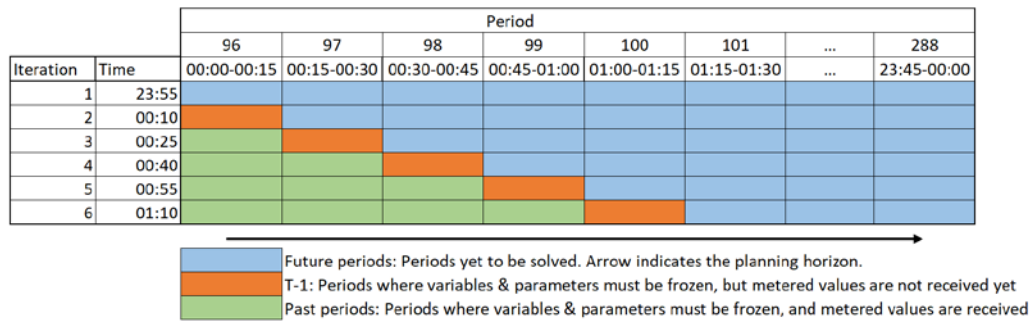


Figure 29: Description of variable and parameter fixing for past time periods.

Then we move to the second iteration, which takes place a few minutes before the start of period 97 (5 minutes). We then are inside period 96. For period 96 we already have decided what to do (in iteration 1). These decisions are also implemented, so when we call the optimization algorithm once more, the variables for period 96 must be fixed to the decisions we already made. The results from iteration 2 are sent to the local systems and decisions for period 97 are implemented. Notice that the decisions for period 96 from iteration 2 are identical to the decisions from iteration 1 (because we force them to be).

Then we move to the third iteration, and here we get a new situation, because a few minutes after the end of period 96 receive meter values for period 96. The idea is that when we initialize the optimization model for iteration 3, we freeze the decisions from iteration 2 for period 97. In addition, for period 96 we substitute some of the predictions and some of the decision variables with metered values. We need to describe in detail which parameters and variables this is relevant for. Anyway, for all further iterations, we will have some historic periods with meter values (the green ones in the figure), we will have one current period where decisions are made, but no meter values are received yet (the orange ones) and a number of future periods, where no meter values exist (obviously), and where no decisions are frozen yet.

## 8.2 Variable freezing approaches

Here we propose two approaches for variable fixing and discuss their pros and cons. The approach 1 is selected for implementation.

### 8.2.1 Approach 1: Running constraints for the entire time horizon

This approach suggests that constraints are run for all time periods in the time horizon from  $t=97$  to  $t=288$ , independent of what time period we are in. By doing this, we are able to run constraints as they are designed in D5.3 (probably) without any major alterations. The optimization is done for the entire time horizon in every time period, but variables will be fixed for all previous periods and updated to their metered values when subject to new iterations of the optimization. This could create problems as we do not know if the metered values will match what we have calculated. Infeasibility issues are described in the next paragraph.

#### Infeasibility issues associated with constraints

A major issue when running constraints for previous time periods, is that the initially feasible problem now is updated with new, metered values for past periods, which can lead to infeasibility.

##### 1. Energy balance (equality constraint).

In a prosumer case with only a battery, the energy balance looks like this (we ignore efficiency for simplicity):

$$\chi_t^{buy} - \chi_t^{sell} = W_t^{inflex} + \sigma_{b,t}^{B,ch} - \sigma_{b,t}^{B,dis}$$

Because this is an equality constraint, any change in values that leads to an inequality will cause infeasibility. One example is shown in Table 11, where we in ( $t=t_{execution}$ ) predict and calculate the decision variables. In ( $t=t_{execution} - 1$ ), we have moved one time step further but we still do not have the metered values and therefore we are still using the calculated values. In this case, it means that we still are buying 5 kW, where 3 kW go to inflexible load and 2 kW go to charging the battery. However, in ( $t=t_{execution} - 2$ ), we receive metered values from that time period, and update the variables and parameters with the values metered in the pilot. However, the metered values now show that we do not have a balance anymore, and we experience an infeasibility. It is worth noting that the equality constraint could be violated by a 100, 1 or 0,001 kW and infeasibility would still happen. As meter readings never will be perfect, this is a significant issue.

Table 11: Example case for prosumer with battery where metered data do not add up in the energy balance.

Energy balance	$\chi_t^{buy}$	$\chi_t^{sell}$	$W_t^{inflex}$	$\sigma_{b,t}^{B,ch}$	$\sigma_{b,t}^{B,dis}$	Imbalance
( $t=t_{execution}$ )	5 (calculated)	0 (calculated)	3 (predicted)	2 (calculated)	0 (calculated)	0
( $t=t_{execution} - 1$ )	5 (calculated)	0 (calculated)	3 (predicted)	2 (calculated)	0 (calculated)	0
( $t=t_{execution} - 2$ )	5,5 (metered)	0 (metered)	3,5 (metered <sup>5</sup> )	2,1 (metered)	0 (metered)	0,1 <i>(infeasibility)</i>

2. A second infeasibility case is whenever an activation of a disconnectable load (space heater) did not perform as expected. An example could be a disconnectable load described in Table 12. In this case, the algorithm scheduled a disconnection in time periods 97-99. As we are in time period 97, the disconnection has already happened and we are starting to plan for time period 98.

Table 12: Disconnectable load example. We are in time period 97 indicated by the orange colour.

t	96	97	98	99	100
$\delta_{l,t}^{start}$	0	1	0	0	0
$\delta_{l,t}^{run}$	0	0	1	1	0
$\delta_{l,t}^{end}$	0	0	0	0	1

When reaching time period 98, the disconnection has failed and the meter which represents the disconnectable load has a meter reading indicating that it is not disconnected<sup>6</sup> (e.g. same as on level of an electric water heater). We now have the situation displayed in Table 13. Because we have not yet received meter values from the meter in time period 98,  $\delta_{l,t}^{SH,run}$  is still 1 in  $t = 98$  as was calculated by the optimization algorithm.

<sup>5</sup> To be specific, it is not metered, but **calculated** as the difference between all other elements in the energy balance.

<sup>6</sup> Note that delta values are not metered. The assumption is that they are derived from the meter readings and are fed into the algorithm as an input.



**Table 13: Disconnectable load example. We are in time period 98 indicated by the orange period. However, the meter reading from time period 97 indicates that the disconnection did not happen in period 97 and is therefore reported as 0 to the flexibility algorithm.**

t	96	97	98	99	100
$\delta_{l,t}^{start}$	0	0	0	0	0
$\delta_{l,t}^{run}$	0	0	1	1	0
$\delta_{l,t}^{end}$	0	0	0	0	1

We see that  $\delta_{l,t-1}^{SH,start}$  which originally was 1, is now measured to be 0 due to the updated meter reading of the disconnectable load. In the equation below, the constraint would in time period 98 have a result of  $0 + 0 = 1 + 0$  which would lead to infeasibility.

$$\delta_{l,t-1}^{SH,start} + \delta_{l,t-1}^{SH,run} = \delta_{l,t}^{SH,start} + \delta_{l,t}^{SH,run}$$

This kind of problem applies to most state variable dependent constraints (constraint with deltas representing the start, running or end of an activation).

3. A third example goes for violation of maximum charging and discharging power in the battery. Batteries are complex, the maximum charging power of a battery can change depending on temperature and other conditions. An example is shown in Table 14. Numbers are shown in %. Due to battery limitations, the SOC can maximum change 50 % per time period. This is shown in the equation below.

$$\sigma_{b,t}^{B,ch} \leq Q_b^{B,ch} = 50\%$$

**Table 14: Battery SOC example. We are in time period 98 indicated by the orange colour. All numbers are shown in %.**

t	96	97	98	99
$\sigma_{b,t}^{soc}$	50%	30%	70%	70%
$\sigma_{b,t}^{ch}$	0%	0%	50%	0%
$\sigma_{b,t}^{dis}$	0%	20 %	0%	0%

When moving to the next time period (t=99), we receive metered values from t=98. The meter readings are shown in Table 15.

**Table 15: Battery SOC example. We are in time period 99 indicated by the orange colour. All numbers are shown in %. An infeasibility is shown by the red colour after receiving metered values.**

t	96	97	98	99
$\sigma_{b,t}^{soc}$	50%	30%	72%	72%
$\sigma_{b,t}^{ch}$	0%	0%	52%	0%
$\sigma_{b,t}^{dis}$	0%	20%	0%	0%

Due to the battery's local management system, a higher charging power was allowed. However, when this was metered and sent to the platform and became subject to the constraint above, infeasibility occurred.

### Problem types associated with approach

In general, we can find the following type of problems:

1. Infeasibility in equality constraints with linear variables, shown in example 1. This is a major issue as a meter reading being imprecise or wrong in any way will lead to infeasibility, exemplified by the energy balance constraint. These types of constraints have to be skipped or relaxed with this approach.

Relaxation of the constraint for previous time periods is done by adding a slack variable on one side of the equation which has no meaning to the actual physical system. This slack variable is only part of the equation for previous time periods.

$$if (t > t_{exec}) : \chi_t^{buy} - \chi_t^{sell} = W_t^{inflex} + \sigma_{b,t}^{B,ch} - \sigma_{b,t}^{B,dis}$$

$$else : \chi_t^{buy} - \chi_t^{sell} = W_t^{inflex} + \sigma_{b,t}^{B,ch} - \sigma_{b,t}^{B,dis} + \varepsilon_t^{EB,slack}$$

By adding  $t_{exec} - 1$ , the last period is still not subject to the slack variable  $\varepsilon_t^{EB,slack}$  as metered values are not yet available for this time period.  $\varepsilon_t^{EB,slack}$  is within the *Reals* domain and can take any positive or negative value depending on which side the imbalance is skewed towards.

2. Infeasibility in inequality ( $\leq$  or  $\geq$ ) constraints with linear variables shown in example 3. This issue might be easier than the above, as a meter reading which deviates from the calculated/predicted value could also lead to feasibility, depending on which direction the meter reading is wrong.

It is possible to relax the constraint for past time periods to “ignore” inconsistent meter-to-calculation deviations. This is done similarly as in the equality constraint issue explained above.

$$\text{if } (t > t_{exec} - 1) : \sigma_{b,t}^{B,ch} \leq Q_b^{B,ch}$$

$$\text{else} : \sigma_{b,t}^{B,ch} \leq Q_b^{B,ch} + \varepsilon_t^{B,slack}$$

Just as above,  $\varepsilon_t^{EB,slack}$  is still within the *Reals* domain and can take any real value to absorb errors in calculated values.

3. Infeasibility when meter readings are different from calculated **binary** values as described in example 2. When a disconnection did not take place, the binary value (delta) got a different value when interpreted by the cloud/algorithm from the meter reading, and lead to infeasibility in the state variable constraints.

This issue is more complicated because it occurs when metered values do not match the binary decision value. This is typically only subject to state variables (on/off). In this case, the constraint can be skipped for past time periods (similar to approach 2 described in 8.2.2). However, this requires an overall evaluation of all constraints that need to be configured.

4. Constraints where slack variables will only solve infeasibility problems, but interrupt the constraint purpose. One example is Eq. 32 from D5.3: For each charging session interval  $I$  the sum energy volume delivered to the EV must equal the sum baseline forecast.

$$\sum_{t=T_{v,n}^{CP,start}}^{T_{v,n}^{CP,end}} \theta_{v,t}^{CP,ch} = \sum_{t=T_{v,n}^{CP,start}}^{T_{v,n}^{CP,end}} W_{v,t}^{CP}$$

When subject to metered values (in past periods), this equality constraint is problematic because the meter readings might (probably never will) match the predicted baseline consumption. By adding a slack variable, we can avoid infeasibility as the slack variable absorbs any deviation between metered and calculated values. However, this also means that we might have a case where the EV load is not served appropriately. One solution is to skip the constraint for previous time periods. However, then we cannot know if the load has been served or not.

**8.2.2 Approach 2: Running constraints (only) for current and future time periods**

Contrary to the approach described in 8.2.1, this approach describes a method where previous time periods are indirectly taken into account by only running constraints for future (and t-1) time periods. Because constraints are not run for previous time periods, we avoid problems such as infeasibility when updating calculated values with metered values. However, information that is gained through running constraints for previous time periods are not taken into account.

As described in D5.3, future decisions depend on previous events. E.g., if a disconnectable load can be activated (disconnected) twice a day, the algorithm needs to keep track of how many times the load has been activated previously in the day. With this approach, information of what has happened in previous time periods needs to be included by storing data in parameters and including them in the constraints.

**Infeasibility issues associated with constraints**

We illustrate the constraints with an example by showing a possible load curtailment and by analysing all constraints related to the curtailable load to see how they are affected by the described approach.

A load unit is curtailed in periods 96 to 99 and 102 to 103. The values of the binary variables are then as shown in Table 16. We are in time period 98 as shown by the **green** colour. The **orange** cells are previous time periods and the **blue** are future periods which are to be optimized. The first curtailment starts in period 96, hence  $\delta_{l,1}^{SH,start}$  is set to 1. The curtailment continues in periods 97, 98 and 99, and the  $\delta_{l,t}^{SH,run}$  are set to 1. The curtailment stops in the beginning of period 100 (or actually, in the end of period 99) so that  $\delta_{l,5}^{SH,end} = 1$ .

**Table 16: Example of curtailable load and how to keep track of information related to the activation. Orange is the time period we are in (t-1), green are past periods and blue are future periods yet to be optimized.**

t	96	97	98	99	100	101	102	103	104
$\delta_{l,t}^{start}$	1	0	0	0	0	0	1	0	0
$\delta_{l,t}^{run}$	0	1	1	1	0	0	0	1	0
$\delta_{l,t}^{end}$	0	0	0	0	1	0	0	0	1

With this approach, the constraints have to be analysed and altered, skipped or kept as they are in order to assure proper operation. All constraints subject to the example above will be described below with the suggested approach.

With the example in Table 16, Eq. (79) will run as normal, as it only requires values from period  $t$ , meaning that the variables in the equation are not connected to past and future time period values. It makes sure that the activation only happens in permitted periods.

$$\delta_{l,t}^{SH,start} + \delta_{l,t}^{SH,run} = 0, \forall l \in L, t \notin T^c \quad (79)$$

Eq. (80) also runs as normal, as it only requires values from period  $t$ , meaning that the variables in the equation are not connected to past and future time period values.

$$\delta_{l,t}^{SH,start} + \delta_{l,t}^{SH,run} + \delta_{l,t}^{SH,end} \leq 1, \forall l \in L, t \in T \quad (80)$$

In Eq. (81), the situation changes because we require  $\delta_{l,t-1}^{SH,start}$  and  $\delta_{l,t-1}^{SH,run}$  from the previous time period. In this case,  $\delta_{l,t-1}^{SH,start}$  and  $\delta_{l,t-1}^{SH,run}$  has to be stored somewhere in order to fulfil the constraint. When the values are stored,  $\delta_{l,t}^{SH,run}$  and  $\delta_{l,t}^{SH,start}$  will be decided by the algorithm.

$$\delta_{l,t-1}^{SH,start} + \delta_{l,t-1}^{SH,run} = \delta_{l,t}^{SH,start} + \delta_{l,t}^{SH,run}, \forall l \in L, t \in T \quad (81)$$

Eq. (82) ensures that activation does not last longer than  $D_l^{SH,max}$  periods. In the example above, if  $D_l^{SH,max} = 4$  in  $t = 98$ , the constraint will go from  $t = 98$  to  $t = 102$ . However, because  $\delta_{l,t}^{SH,start}$  is in the past, the optimizer could break the initial schedule and keep the load activated as both  $\delta_{l,t}^{SH,start}$  and  $\delta_{l,t}^{SH,end}$  could be 0 for all those periods. To avoid long activations,  $D_l^{SH,max}$  has to be updated in all time periods inside the activation. After it has to be reset to its original value (in  $t = 99$ ).

$$\sum_{i=t}^{t+D_l^{SH,max}} \delta_{l,i}^{SH,end} \geq \delta_{l,t}^{SH,start}, \forall l \in L, t \in T \quad (82)$$

Eq. (83) has the same issue as Eq. (82), and  $\delta_{l,i}^{SH,start}$  and  $\delta_{l,t}^{SH,end}$  have to be stored for  $D_l^{SH,min}$  time periods in the past.

$$\delta_{l,t}^{SH,end} + \sum_{i=t}^{t+D_l^{SH,min}-1} \delta_{l,i}^{SH,start} \leq 1, \forall l \in L, t \in T \quad (83)$$

Finally, Eq. (84) makes sure that the maximum number of curtailments does not exceed  $N_l^{SH,max}$ . In this case,  $N_l^{SH,max}$  needs to be updated after each curtailment. In the example above (we assume  $N_l^{SH,max} = 2$ ),  $N_l^{SH,max}$  must be set to 1 in  $t=96$  after the first activation. Depending on the contract,  $N_l^{SH,max}$  is reset after 1 day is finished (typically 96 time periods).

$$\sum_{t \in T} \delta_{l,i}^{SH,start} \leq N_l^{SH,max}, \forall l \in L^c, t \in T \quad (84)$$

Finally, such an analysis has to be done for all types of flexibility and all constraints which belong to the flexibility elements. This could be quite time consuming. In addition, we do not know if we have covered all outcomes, especially when input data is missing or is wrong.

### Problem type associated with approach

In general, we see the following type of problems:

1. Constraints where we sum over time periods in the past and in the future at the same time. These constraints need to be modified to work by storing information in the cloud/algorithm.
2. Constraints where we sum over current and future periods. We might face a scenario where we have to skip some constraints or store values for future periods. This is discussed in the explanation of Eq. (82) above.
3. It is unlikely that we are able to correctly adjust all constraints for all kinds of scenarios regarding variable fixing. Basically if something is not fixed properly, the algorithm may lead to infeasibility or not run at all.

### 8.3 The t-1 issue

In order to have a data value more realistic than the old metered value (from  $t-1$ ), we suggest to utilize the calculated value of the previous optimization algorithm solution. For instance, the battery could at 12:00 have 50 % SOC and is told by control dispatch to discharge to 40 % by 12:15. In this case, the metered value is 50 %, but by the 12:15 the real value will be 40 % which will not be metered in time for the new control dispatch. Thus it makes more sense to use the calculated value for the 12:15 control dispatch. Note that the real value at 12:15 potentially could be wrong (e.g. 38 %) due to external conditions. If such an error occurs consecutively, the real SOC development could

deviate significantly from the calculated values as the errors might potentially stack on top of each other.

Because the SOC equation only depends on the SOC of the previous time period (which is always a calculated value), the errors will stack on top of each other also when we update the variables with metered values. In short: the metered values never “catch up” to the equation.

Note that the stack of errors potentially reset (are removed) when the battery SOC reaches minimum or maximum SOC, but not necessarily.

## **8.4 Overall evaluation of approaches**

First, we evaluate approach 1 described in 8.2.1, then approach 2 described in 8.2.2. Note that approach 1 was chosen in INVADE.

### **8.4.1 Approach 1**

#### **Pros:**

- Constraints stand as they are for all time periods, however, many are given slack variables in order to deal with deviations between meter readings and calculated values.
- As we solve for the entire time horizon in every time period, variables and parameters that are necessary to keep track of, do not need to be stored outside the flexibility algorithm. Past decisions are easily taken into account.

#### **Cons:**

- More tests are needed than in other options to ensure that it works for all situations, especially when metered values are missing or with high errors in forecasting.

### **8.4.2 Approach 2**

#### **Pros:**

- No need to solve time periods that are in the past.
  - Avoid complications in freezing parts of data time series. This requires a time series where the state of charge of a battery is frozen from all

previous time periods, but optimized for all future time periods (incl. present).

- There will not be any infeasibility problems in constraints that are run after the metered values are included in the optimization problem. This is a big advantage.
- We spend less time solving the problem as we do not optimize for previous time periods. This is a minor point as the algorithm must be solved for all time periods at some point either way.

#### Cons:

- It is more difficult to **bring information from all previous time periods**. E.g. how many times have we activated a disconnectable load? For all constraints that run over both past, present and future time periods, information from the previous time periods must be saved somehow to assure correct execution of the flexibility element.
- **Every constraint has to be checked and evaluated for possible issues** connected to variable fixing. This especially applies to constraints where time periods in the past are included, and constraints where parameters must be saved in the cloud in order to keep track of mechanisms such as minimum resting time between activations ( $D^{\min}$ ), maximum activation time ( $D^{\max}$ ) and max amount of daily activations ( $N^{\max}$ ). Such evaluation of the constraints are expected to be quite time consuming and does not guarantee a perfect outcome.

## 9 Pilot structures

### 9.1 Introduction

This chapter will include the details of the Norwegian pilot (Lyse pilot), Dutch Pilot, and Bulgarian Pilot as well as contains agreed information needed to be implemented in the flexibility management algorithm. On the other side, this is also about making the pilots aware about what they need to discuss and clarify. This chapter continues the initial discussion in D 5.3, and has been updated based on new information we have received from the discussions between eSmart and the INVADE pilots. Detailed description of the



remaining pilots in INVADE can be found D4.3, which will be released in similar time as this deliverable.

## 9.2 Norwegian case study

The Norwegian pilot structure and specification is explained in D 10.1.

### 9.2.1 Structure information and historic meter values

The structure information is data that is rarely changed. According to D5.3, the three different types of pilots can be illustrated as in the figures below, i.e., Figure 30, Figure 31 and Figure 32 for the Norwegian pilot.

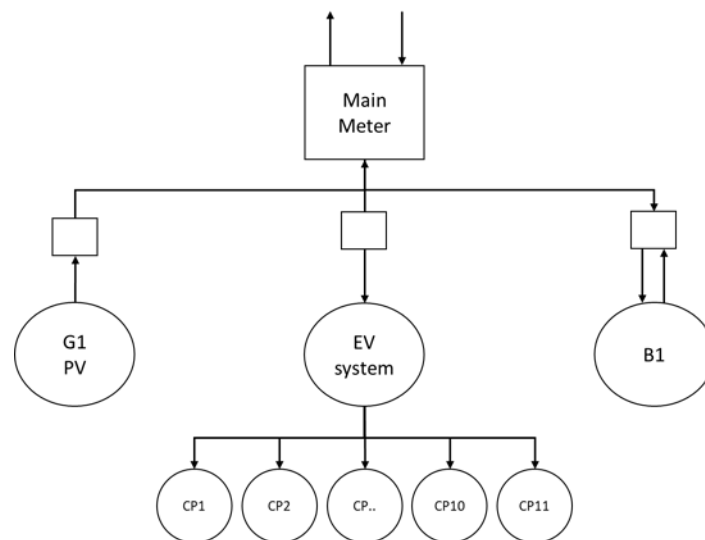


Figure 30. Illustration of Lyse headquarter

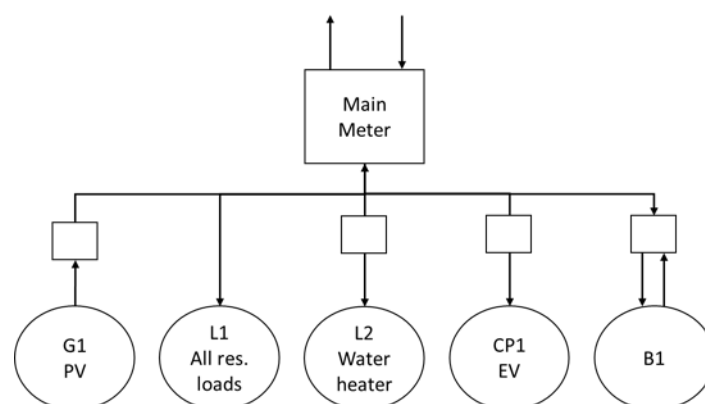
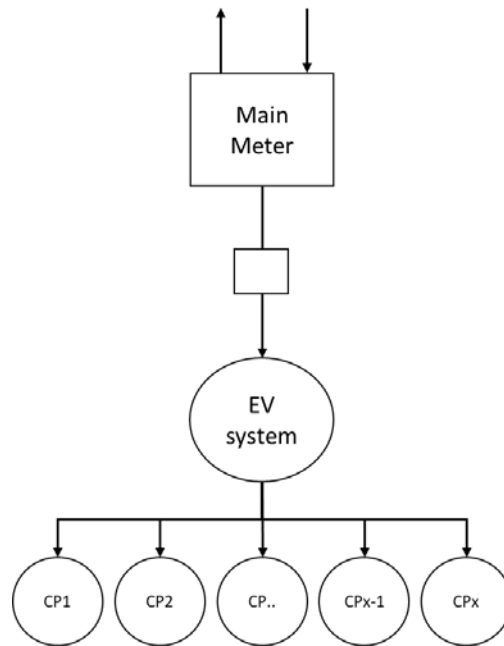


Figure 31. General illustration of Lyse households



**Figure 32. General illustration of Lyse cooperatives**

Integrated INVADE Platform (IIP) will receive information about each specific site, which means each specific household and each specific cooperative, to establish models as illustrated above. The list of input combined in the Norwegian pilot is available in D10.1.

### 9.2.2 Commercial/agreement information

Since the Lyse pilot focuses on the prosumer services ToU optimization, kWmax control and Self-balancing, and since these are closely connected to the terms in the retail contract and the grid contract, information about these contracts must be given at a very detailed level.

All customers/prosumers are connected to Lyse Elnett's grid, hence, all will have grid contract with Lyse Elnett. A working assumption is also that all prosumers will have Lyse as retailer.

### 9.2.3 Grid contract

All prosumers will have the same type of grid contract, which will be based on the principle of subscribed power. The principle is illustrated in Figure 33, and it completes the open discussion from D5.3 on "subscribed power" type of grid contracts.

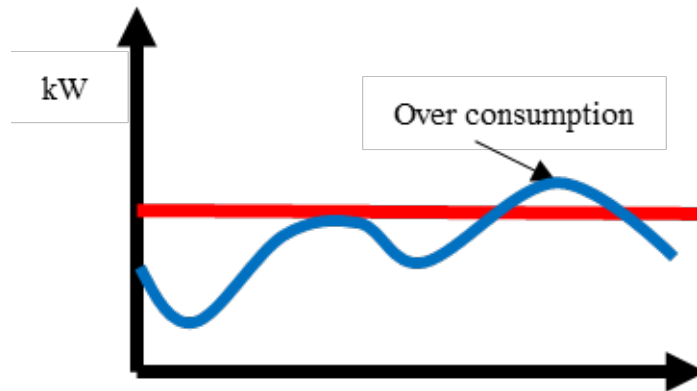


Figure 33. Illustration of the subscribed power concept

A prosumer subscribes to a certain power level, say 5 kW. A fixed fee is paid according to this level. The price increases with increasing power level. The contract has a low energy fee (NOK/kWh) as long as the consumption is below the subscribed level. On the other hand, the energy price is much higher for volumes above the subscribed level. Notice that all meter values still are hourly, so instant power is not considered, only average power over 1 hour, or in other words: energy per hour, metered in kWh/h. This means that the instant power may be above the subscribed power level for some time, but as long as the total energy over the hour is below, the high price does not considered.

An example from a presentation by NVE, the Norwegian regulator, is Figure 34.

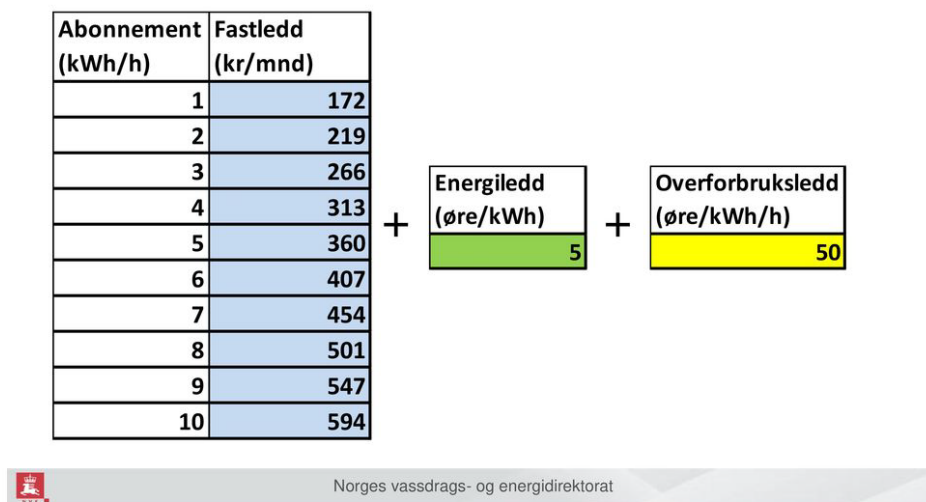


Figure 34. Example of prices for subscribed power

To the left, the figure shows the fixed price in NOK/month for different subscription levels between 1 and 10 kWh/h. To the right, the energy fees are shown for volumes up to the

subscribed level (5 øre/kWh) and for volumes above the subscribed level, also called over consumption. In the example this price is 10 times the energy fee price.

The example does not say anything about energy fee for hours with surplus electricity.

#### **9.2.4 Retail contract**

All prosumers in the Norwegian pilot will have a retail contract with Lyse. A detail of retail contracts based on Nord Pool electricity spot-price was presented in D5.3. For buying electricity, the consumers are supposed to pay electricity spot price plus a mark-up which is different for private consumers (3,9 øre/kWh) and commercial consumers (4,6 øre/kWh).

The remuneration for selling back surplus electricity is twice the Nord Pool spot price. In combination with the low energy fee at the subscribed power grid tariff, the incentive for self-consumption is highly reduced.

#### **9.2.5 Flexibility**

The Lyse pilots will include the following types of flexible devices:

- Batteries
- EV charging points
- Water heaters
- Space heating

In flexibility management algorithm, each device will be modelled and treated separately, which means that meter values and control signals will be for each single device. In other words, there will be no flexible resources at aggregated levels.

To be able to utilize the flexibility in an optimal way and without inducing any loss of comfort or other disadvantages, flexibility properties must be defined in detail. This also includes rules, agreements and interaction with involved people at the site, and which information that will be available at what times. Each type of flexible device will be handled below.

##### **9.2.5.1 Batteries**

Batteries will be involved in the office building (Profile H), in some of the households (Profile C, D and E) and possibly in some of the cooperatives (Profile F). The working assumption is that all of them can be treated similarly, when it comes to flexibility

management and data to and from the batteries. More details of the battery models are available in Chapter 3.

#### 9.2.5.2 EV charging points

EV charging points will be involved in the office building (Profile H), in some of the households (Profile B, E, G), and in the cooperatives (Profile F). The pilot in Norway will use smart chargers from Schneider, and all chargers uses the OCPP standard.

For some EV charging points the charging power (kW) can be controlled at each separate point. In other cases, power can be controlled at a grouped level. Then local systems will distribute the decisions down to each charging point.

Each EV charging point will have fixed data for maximum charging power continuously between 0 and a maximum level. Dependent on the car that connects, the maximum power that the car takes can be lower than the maximum level at the charging point. In addition, there will be a lower level, which is decided by the car.

In some cases a Smartly app might be involved. The main function in this context is that the EV driver can provide information that the charging session is not flexible, i.e. it cannot be controlled. In other words, this session is of type urgent or high priority.

In addition, it should be considered, at least at some of the sites, to get more information from the driver, also through the app. Relevant information could be:

- In advance of a connection: The driver sends information about what time she expects to connect and disconnect, and the expected charging demand.
- When connecting: The driver sends information about real charging demand or battery SOC (in % or remaining number of km) and expected disconnection time.

The benefit of this is that it the information as input to the optimization will be more accurate/correct.

If the EV driver knows that it will be disconnected in a given hour and sends this information through the app, the decisions from the optimization will be adjusted accordingly.

The output of the optimization algorithm will be a charging set-point for each period. The set-point will either be an average power level (kW) or energy (kWh). Implementation of the set-point then will be performed locally, i.e. by the Electric Vehicle Supply Equipment (EVSE) or Smartly.

### 9.2.5.3 Water heaters

Controllable water heaters will be involved in some of the households (Profile A and G). Each water heater will have fixed parameter for installed capacity (kW). The water heaters in the pilot will have 1.95 kW.

Meter readings for the energy to the water heater should be retrieved at the same interval as the rest of the meter readings (15 minutes or smaller). However, according to Smartly, this might not be possible. This is a big issue, since it then is very difficult to add any intelligence. Therefore, the prediction algorithm should provide some estimation about this information. In the further, we assume that these meter readings are available.

The water heater control is based on a set of timing restrictions that will be input to the optimization algorithm:

- d. For each period, a parameter says whether it is allowed to disconnect the water heater or not (e.g. disconnection is allowed at any time, except from between 19:00 and 22:00).
- e. A maximum disconnection duration is given (e.g. if the water heater is disconnected, it must at the latest be reconnected after 1 ½ hour)
- f. A minimum duration (rest time) between two disconnections is given (e.g. if a water heater is reconnected after a disconnection, it cannot be disconnected again before at least 3 hours)

The output from the optimization algorithms is a set of disconnection and reconnection periods. The control signals will be “off” and “on” with a given time (e.g. “off” at 12:15, and “on” at 12:45). NB! This information will have the granularity equal to the length of the periods, e.g., 15 minutes, which means that the connections and disconnections will be set to these time points, and not at any minute inside a 15 minutes’ interval. More details of this model are presented in Chapter 5.

### 9.2.5.4 Space heating

Space heating will be involved in some of the households (Profile A). Space heater may be floor heating cables or panel ovens. Smartly supports temperature control to these customers. The user can change the set-point for the temperature in each room.

The same issue for available meter readings is valid here, as for water heaters. According to Smartly there might be the case that we will not get meter readings for the

space heater, which leaves us in a black box situation. Probably it will be difficult to add any intelligence.

If space heating control shall be involved in the pilot, it must be decided how the flexibility can be treated. One option is to have the same approach as for water heaters: that the heating is controlled “off” and “on”, based on timing constraints. This might lead to inconvenience situations for the end-users. Another approach is to be able to control the temperature set-points. This approach is explained in details in Chapter 6.

### 9.2.6 An illustrative example

Assume we have a prosumer with a PV panel, a controllable water heater (2 kW), a room with controllable temperature (1 kW), an EV charging point (3 kW) and a battery (10 kWh, up to 5 kW charging and discharging power).

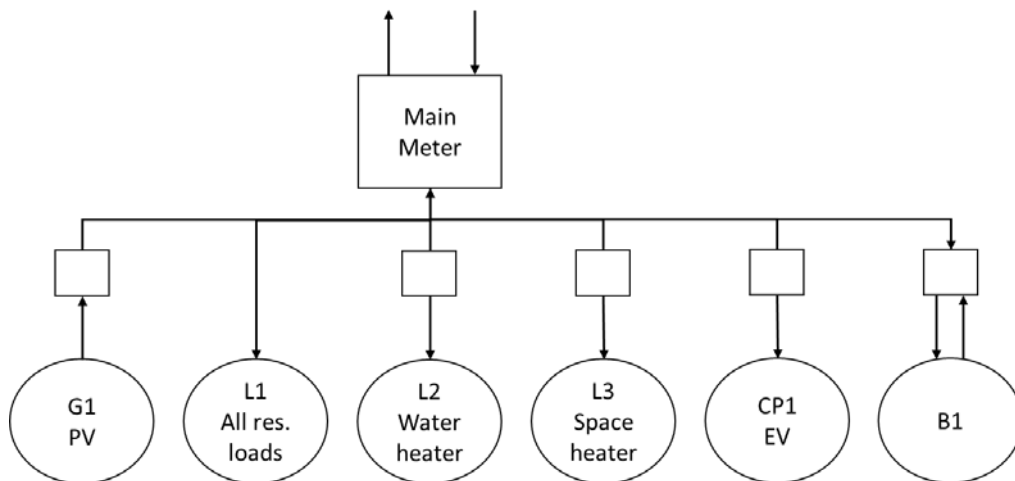


Figure 35. Prosumer and resources

The prosumer has a grid contract with 6 kW subscribed power. For a given day, the day-ahead spot (Elspot) prices are according to Figure 36.

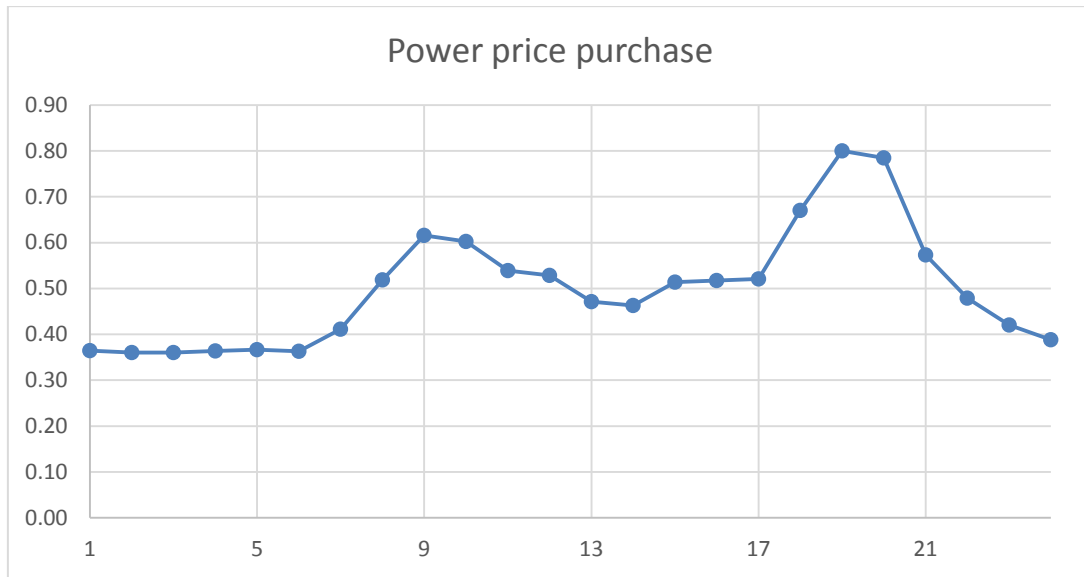


Figure 36. The day-ahead spot prices (Elspot)

The predictions for the electric loads are shown in Figure 37:

- The residual load has a peak 6 kWh/h in the afternoon
- The water heater has high consumption in the morning and early and late in the evening and with long “off” periods
- The space heater is surging electricity all the time, but varying between almost 0 and 1 kW
- The EV is charging twice, in the morning and in the early evening

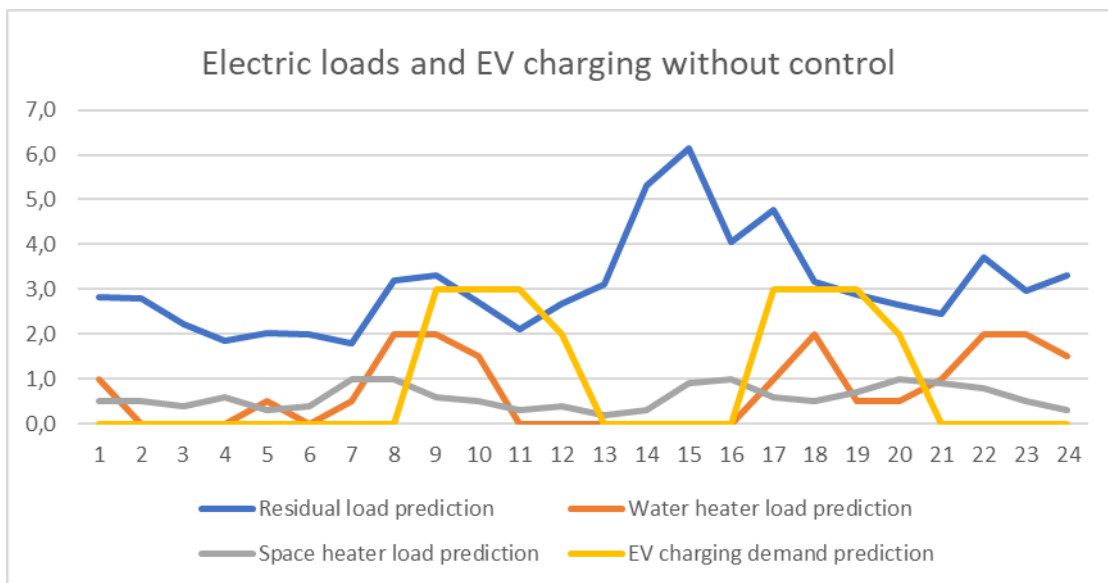


Figure 37. Predicted consumption for water heater, space heater, EV charging and residual loads



The PV production is predicted as shown in Figure 38.

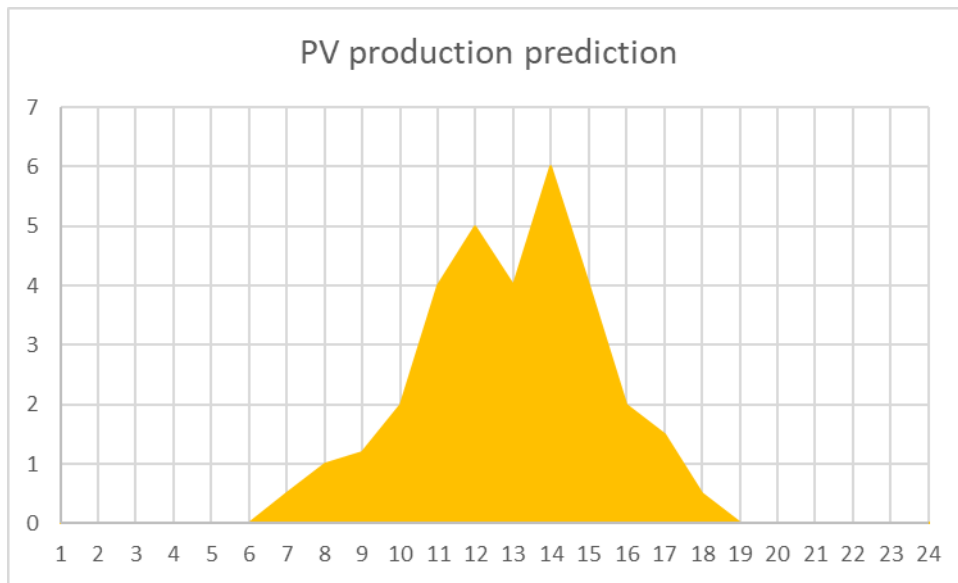


Figure 38. Predicted production from the PV panels

In total, this gives a net exchange with the grid as illustrated in Figure 35. We see that over consumption occurs in the morning, early in the evening, and slightly late in the evening. Further we see that the profile's peaks coincide with the price peaks. This gives a total net cost of 75 NOK for the day.

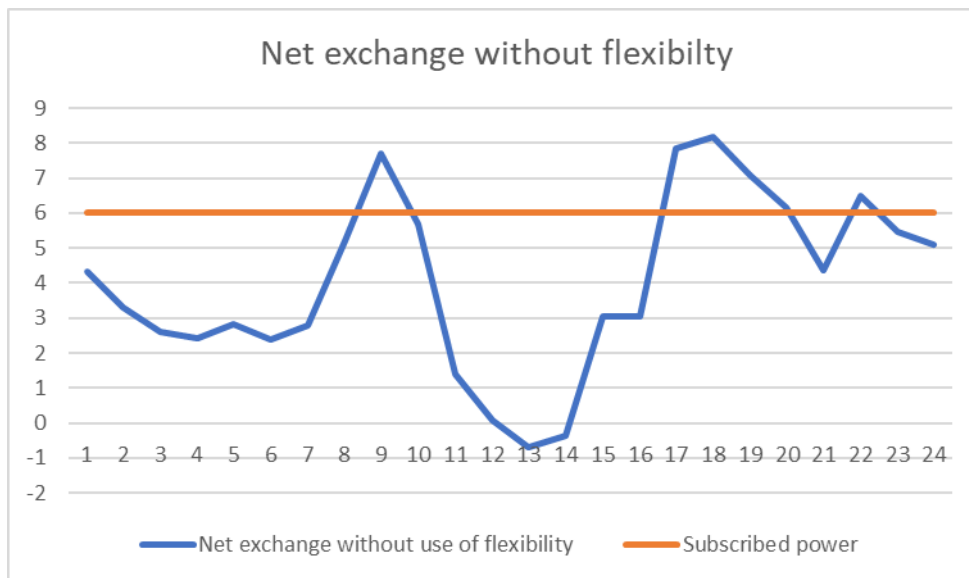


Figure 39. Net exchange without flexibility and subscribed power level

The cost can be reduced with almost 20 % by utilizing flexibility. Then the EV charging is moved in time from morning to the middle of the day and from early evening to the night. Further, the water heater and space heater consumption (which are not large) are slightly shifted.

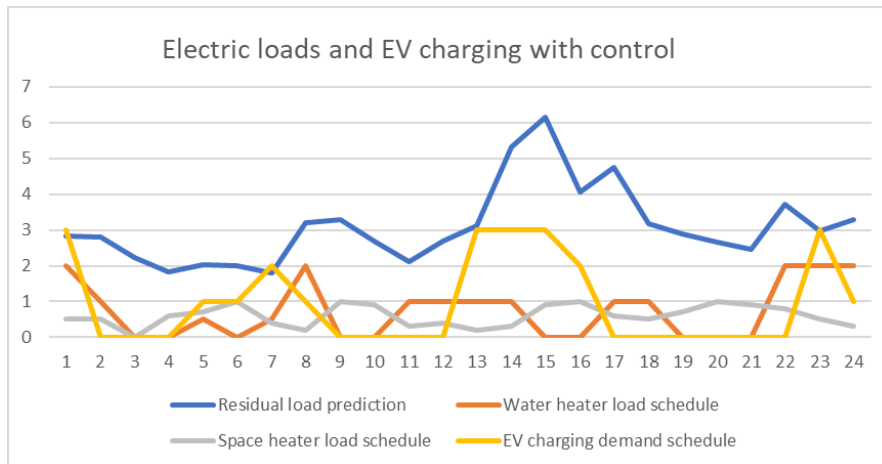


Figure 40. Loads after control

Finally, the battery is the source providing most flexibility in this example. We assume that the initial state of charge is 5 kWh and that this should be the state of charge at the end of the day. Then, the state of charge is developing according to Figure 37.

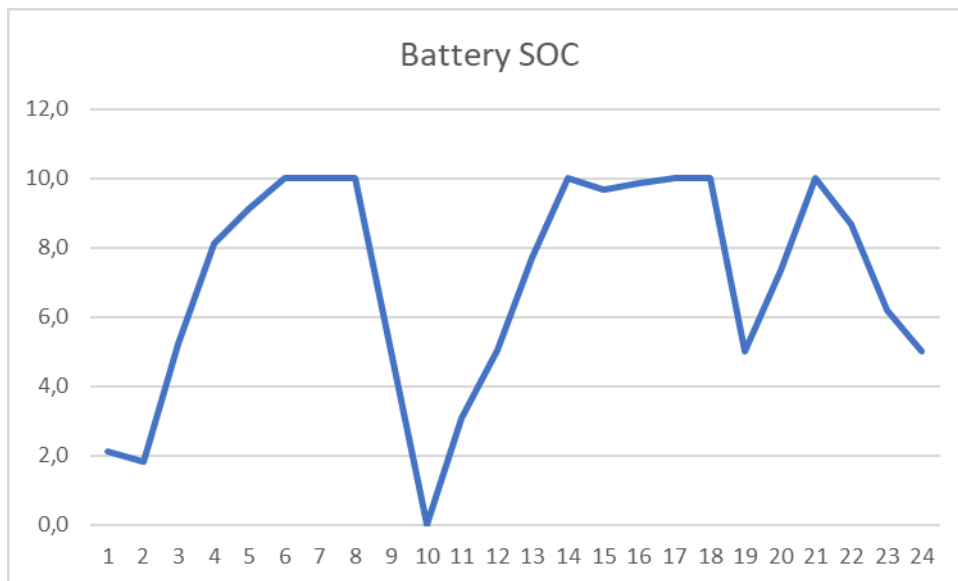


Figure 41. Battery filling development

We see that the battery is charged during the night, and discharged fully during two hours in the morning, when consumption and prices are high. Then it is charged in the middle of the day, when the prices are low, and consumption is low and production is high. Finally it is discharged again during the high price hours in the evening. The net resulting net exchange is illustrated in Figure 42.

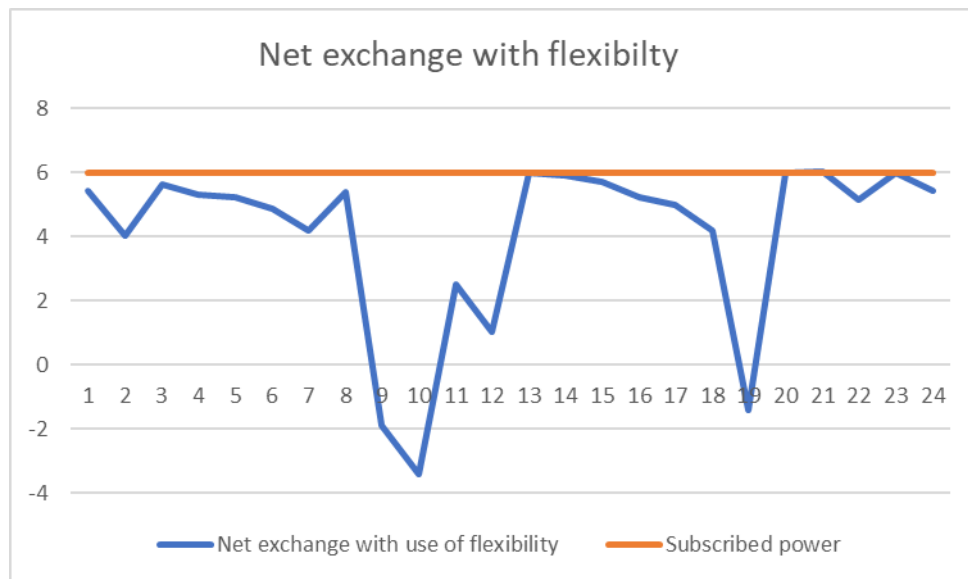


Figure 42. Net exchange after activation of flexibility

We see that over consumption is avoided and that the profile is completely changed so that electricity is bought in cheap hours. Notice also that we now have got sales of surplus electricity in two hours in the morning and one in the evening. According to the self-balancing/self-consumption principle this may seem a bit strange, but remember that in this case, the prosumer gets double price for selling. In addition, the subscribed power tariff has a very low cost for normal consumption.

### 9.3 Dutch case study

#### 9.3.1 Introduction

According to D10.1, Dutch pilots will consist of four different types of sites:

1. **Home charging** with approximately 25 homes and known, private users. 3 homes will have 2 charging points, the rest will have 1.
2. **Large scale offices and parking lots** with semi private/public situations and unknown users. This type will include 25 office buildings and parking lots with app 300 charging points.
3. **Small scale office** sub-pilot with known users, probably also with energy storage and V2X capability. This type includes only one site, which is the Elaad office building.
4. **Large scale public charging** with 500 – 1000 charging points spread over the whole country and unknown users.

All pilot sites will have a GreenFlux and ElaadNL installations, which means that exchange of data in all cases will be between the IIP and GreenFlux/ElaadNL.

According to D4.2 the pilots in the Netherlands will include the following flexibility services:

- DSO
  - Congestion management
  - Voltage/Reactive power control
- Prosumer
  - ToU optimization
  - kWmax control
  - Self-balancing

The DSO services will be treated simply as a capacity constraint for a site or a group of sites.

### 9.3.2 Structure information and historic meter values

A general illustration of the Dutch pilot sites is given Figure 43. Each square illustrates a point from which meter readings are received or to which control signals are sent.

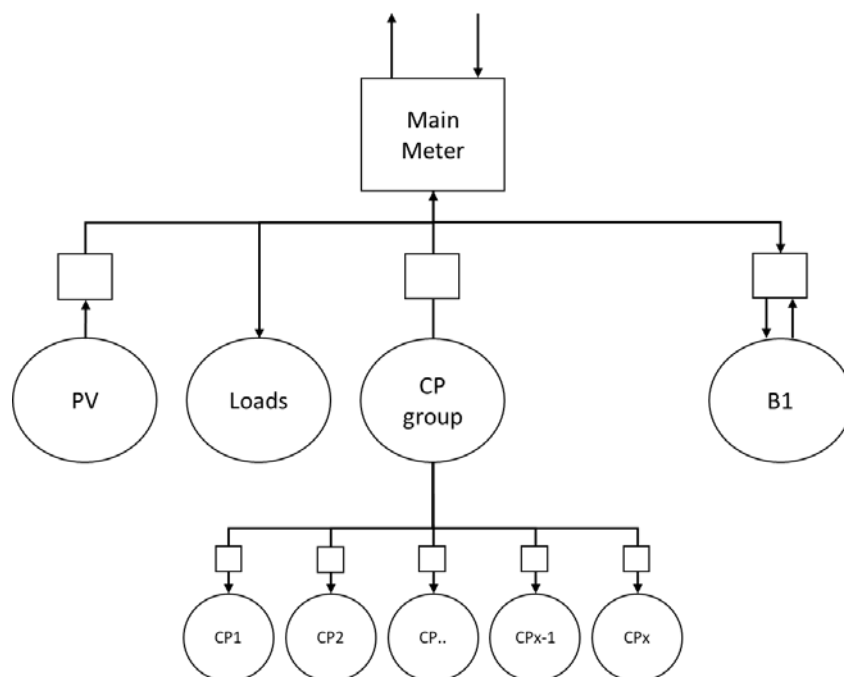


Figure 43. General illustration of the Dutch pilots

All the sites will have at least one charging point. An EV system (not visible in Figure 43) will control each charging point in real time. At some sites the charging points may be grouped with a capacity limit for each group. The pilot site of type 3, i.e., small scale office, will have all components in the illustration. Private homes (type 1) will have load and one or two charging points. In addition, some of these sites will have a PV panel. Finally, large scale offices and parking lots (type 2) will have charging points (up to 80) and load. Some of these sites will also have PV panels.

### 9.3.3 Objectives

Although the pilot types are different, it is a target to define all of them into a common framework. In fact revenue optimization is not the main focus of the Dutch pilot is to learn if steering could be a good control mechanism to ensure grid stability, not optimize revenue. So for grid stability we defer or reduce charging. And yes, the moments that such things are necessary probably correlate to higher APX prices.

It is assumed that electricity is bought on retail contracts based on hourly prices from the APX (EPEX SPOT Power NL Hourly<sup>7</sup>), although the real customers do not necessarily have such a contract. An example of such prices is shown in Figure 44, where prices have been downloaded on February 28<sup>th</sup>, 2018.

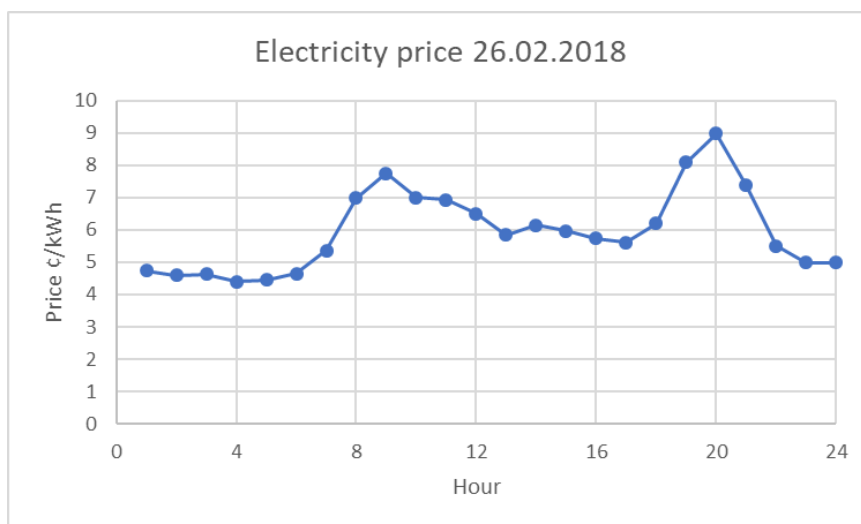


Figure 44. Example of APX spot prices for one specific day

<sup>7</sup> <https://www.apxgroup.com/market-results/apx-power-nl/dashboard/>

We see that for this specific day, the prices vary from hour to hour, with a morning peak in hour 9:00 and an afternoon peak in hour 20:00. The most expensive hour has a cost approximately 100 % higher than the cheapest one.

Sales of surplus electricity is assumed to be done to a price lower than the purchase price. If possible, it will then be profitable to shift EV charging to hours with surplus electricity. This is according to the overall idea to “drive, charged by the sun”.

Finally, since the primary interest of Greenflux and ElaadNL is to ensure grid stability, different capacity limitations can be defined for a site, internally at a site or for a group of sites.

For a simplified and illustrative example (though unrealistic), let a private household has a solar panel, loads and two charging points that can charge up to 3 kW each. The main fuse has a limitation of 5.5 kW. The resource overview is shown in Figure 45.

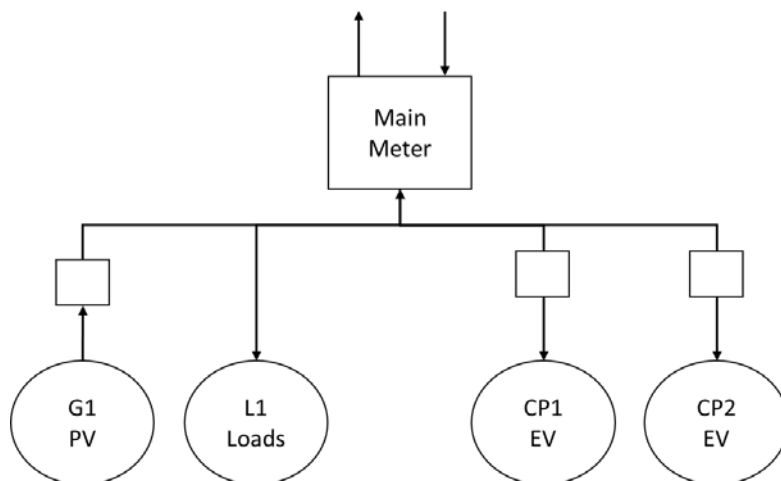


Figure 45. Resource overview of example household

Figure 46 shows possible values for PV production, load and EV charging demand. The blue curve shows net exchange with the grid, where positive values represent purchase and negative represent sales. The net exchange is below the 5.5 kW limitation in all hours.

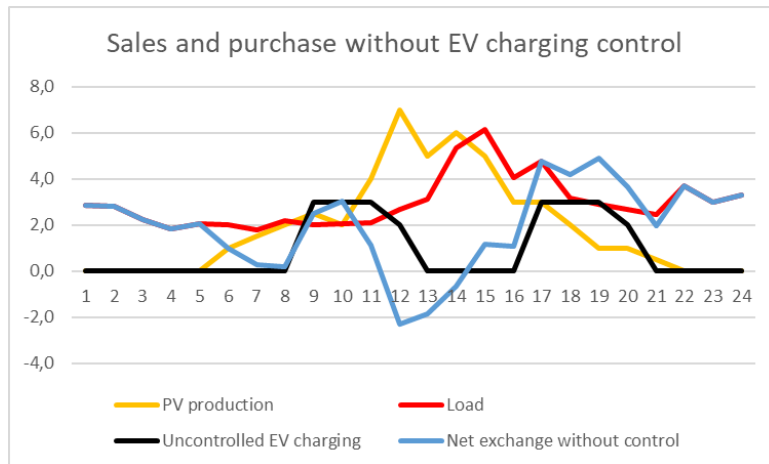


Figure 46. Example of PV production, load and EV charging for a household for one specific day

Further, assume that the revenues from selling surplus electricity is 50 % of the APX price. The total costs sum up to EUR 314, while the total revenues from sales sum up to EUR 15. Net cost then becomes EUR 299.

Now, assume that we are able to control the EV charging by delaying parts of it. As described above, a profitable strategy will be to shift charging away from the peak price periods and to shift into the surplus periods. A possible solution is shown in Figure 47.

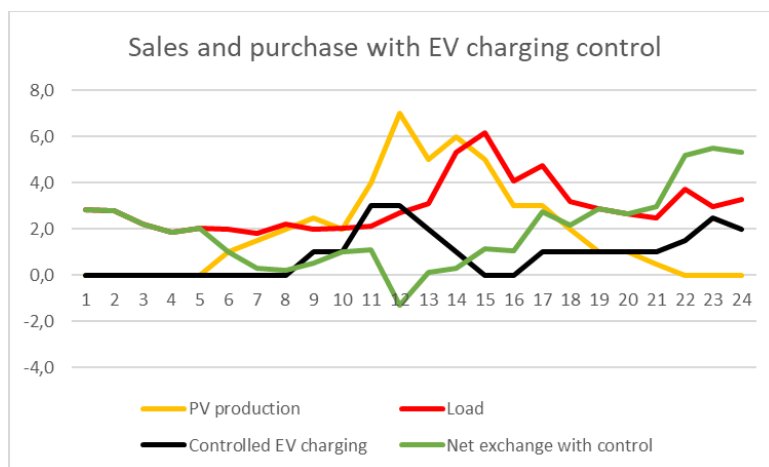


Figure 47. Example of possible strategy when EV charging can be delayed

Purchase in the morning and evening peak hours is now reduced. Purchase in the latest hours is increased, but is not violating the 5.5 kW main fuse constraint. Finally, the sales in the middle of the day is almost eliminated. This strategy gives total costs at EUR 276, total revenues EUR 4 and the resulting net cost EUR 272, which represents a cost saving of EUR 27 compared to the situation with no control. A comparison of the net exchange with and without control is presented in Figure 48.

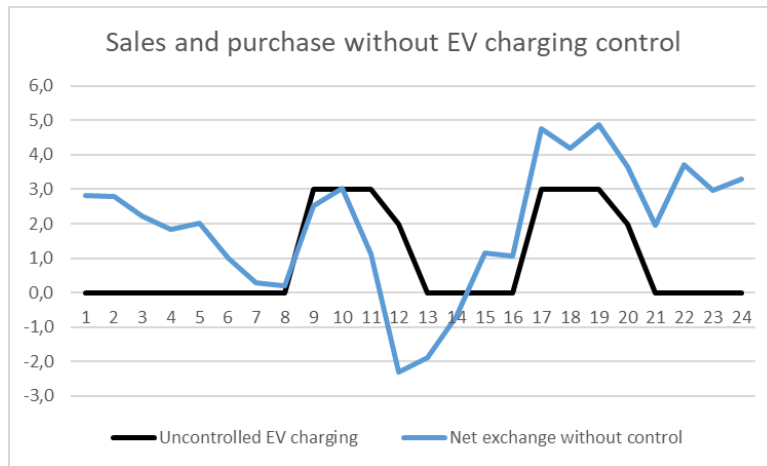


Figure 48. Comparison of the net exchange with and without EV charging control

### 9.3.4 Flexibility and decisions

The main source for flexibility in the Dutch pilots is the control of the EV charging. In addition, batteries may be involved. However, in this document we focus on the EVs.

Meter readings for each charging point will be received in an Open Charge Management Protocol (OCMP) message every 15 minutes. Similar to the Norwegian pilot, the message will contain meter counter values (accumulated kWh) per charging point and charging session. When a new charging session starts, meter values starts coming. For each period, accumulated values will be sent. This continues until the charging session stops, which means that the car disconnects from the charging point. By getting this information, the IIP also gets information about historic connection and disconnection periods, which can be used to train prediction algorithms about potential flexibility in terms of possibility to shift charging in time.

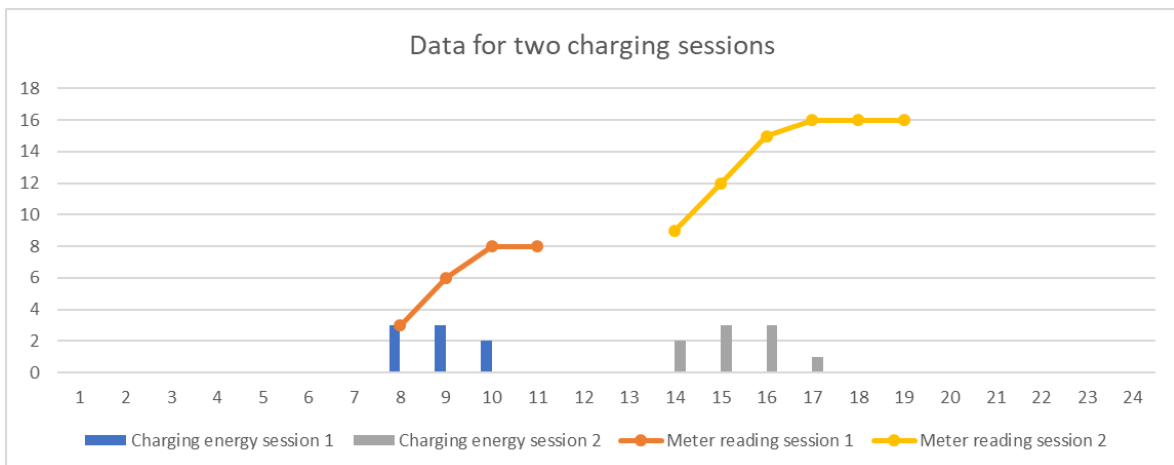


Figure 49. Example of meter readings and delivered charging energy for two charging sessions



Figure 49 shows an example of two charging sessions at the same charging point. The orange and yellow curves illustrate the meter readings received, while the blue and grey bars show the charging energy delivered in each period. The example has hourly time resolution. The charging point is first connected sometime in hour 8. After hour 8, meter reading will be received, and the charging energy can be calculated. The electric vehicle stops charging somewhere in hour 10, but it stays connected until somewhere inside hour 11. Then the charging point is disconnected and no meter reading is sent in hour 12 and 13. Next, the charging point is reconnected somewhere in hour 14. A meter reading is received when hour 14 is over. The counter continues from the last value for the previous session. We see that the EV charges in hours 14, 15, 16 and 17, but it stays connected until somewhere in hour 19. For the rest of the day, no car is connected to the charging point.

NB! An issue to consider here, is that the charging points use a small amount of power (a few watts) even if not connected. For long time intervals where the point is not connected, the counter value may increase. This energy is not related to any charging session, and must be handled, somehow.

The example above shows historic values. Furthermore, this will be used to make predictions, i.e., to predict when the charging point will be connected and disconnected and the related energy need. These predictions will be used as input to the optimization model, which in turn may change the charging profile within the predicted time when the charging point is connected, constrained by the maximum power level. Following the example above (which shows uncontrolled charging), the charging schedule from the optimization could look in Figure 50.

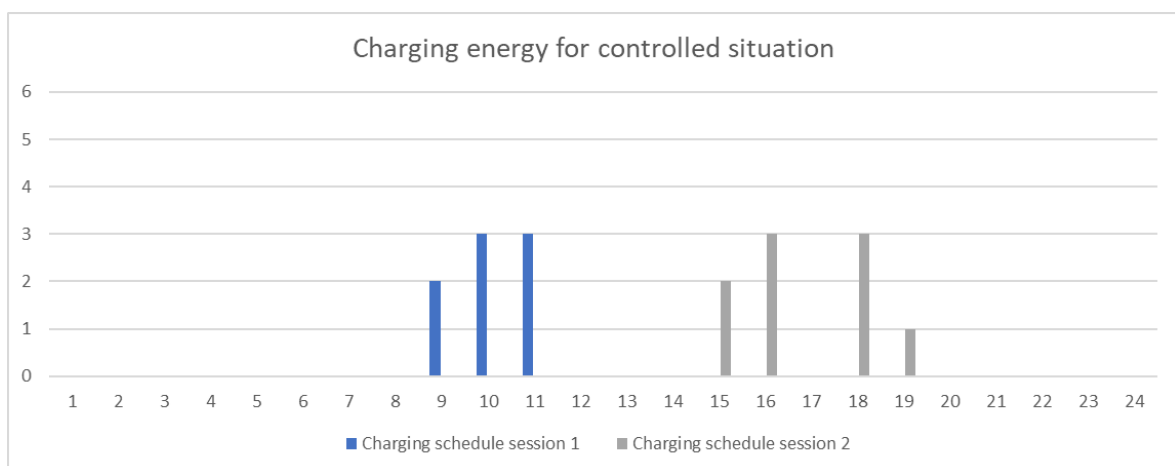


Figure 50. Example of charging energy for two charging sessions when it is controlled

Observe that the first session is delayed one hour, and the profile is changed. For the second session, a delay is also introduced (now starting 1 hour later and finalizing 2 hours later), and the profile is also changed. For instance no charging is done in hour 17.

In the household pilots, the users are known. This means that in normal cases information about car type, maximum charging power, battery capacity etc. can be available. However, this assumption can be violated in situations where a different car like a visiting guest uses the charging point. At some pilot sites, the users can have an app where they have the possibility to select prioritized charging when connecting to a charging point, which means that they do accept the charging to be delayed.

All this represents information that will be used both to predict charging demand and to predict available flexibility.

The nature of our problem is that some information is not known with certainty at the moment where we make the decisions, and further, that information will be revealed successively. To handle this situation, we have selected to use a rolling horizon principle, which implies that the process of receiving fresh data, updating predictions, making decisions and sending these to the local systems. This process is repeated for each time-slot. More information about this can be found in Chapter 7.

In the Dutch pilot OCMP will be used for sending information between GreenFlux/ElaadNL and the IIP in both directions. These messages basically consist of three types of information:

- Meter readings sent from GreenFlux/ElaadNL to IIP
- Available capacity sent from GreenFlux/ElaadNL to IIP as Maximum Capacity Forecast. This contains the capacity limitations (kW) for a time block, defined by a start time and an end time. The capacity is valid for a group, which can be a group of charging points, one site (household, commercial building or charging site) or an aggregation of sites (The aggregation will probably be implemented by use of standard zone-functionality in the IIP).
- Results from the optimization algorithm sent from IIP to GreenFlux/ElaadNL as Optimal Capacity Forecast with the same levels as the Maximum Capacity Forecast. GreenFlux/ElaadNL calculates how this shall be met at the detailed level (down to each charging point) and implements this.

To illustrate this concept, we continue with some simple examples.

#### 9.3.4.1 Example 1: One household

Example 1 follows the example in Sub-chapter 9.2.3.

First, the IIP receives the Maximum Capacity Forecast from GreenFlux. In this example, this will be the capacity limitation for the example household, which will be one time block from 00:00 to 24:00. The value will be 5.5 kW.

Next, the flexibility algorithms will be run. For simplicity, assume that hourly time resolution is defined. In this example, we skip the description of the rolling horizon and pretend that we are running a one-shot planning just before a day starts. Then the planning horizon goes from hour 1 to hour 24.

In a preparatory stage, the IIP performs the following steps:

- Solar production from the PV panel is predicted for each of the hours in the 24 hours' horizon (H1 – H24)
- Consumption for the loads is predicted for each of the hours in the 24 hours' horizon
- EV charging demand for the two charging points is predicted for each of the hours in the 24 hours' horizon.
- Prices from APX are collected. At this stage all prices are known, so a prediction is not needed.
- Maximum capacity forecast for the household is retrieved

It is now possible to calculate the numbers in Figure 46, including costs and to detect whether the capacity limit for the site is violated.

Now, we need to have information about what flexibility that exists for the flexible resources, which in this case are the charging points. Based on historic values (+ potentially some input from apps), charging demand including connection and disconnection times are predicted.

The flexibility algorithm makes decisions at the level of each of the charging points, aggregates the decisions and builds the Optimal Capacity Forecast. This is then sent to GreenFlux, which makes detailed plans for each charging point. Figure 51 illustrates the uncontrolled and controlled situation. The green curve then constitutes the Optimal Capacity Forecast.

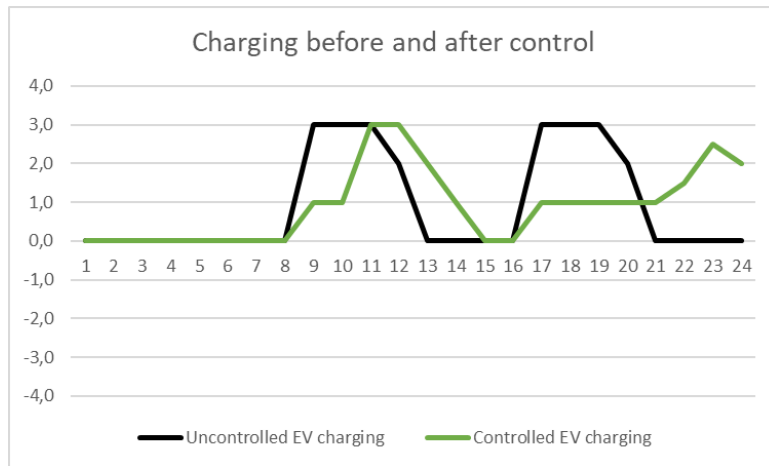


Figure 51. Comparison of charging demand before and after control

9.3.4.2 Example 2: Several households

Now, assume that we expand example 1 with another household, with one charging point and loads. The two sites (households) form a zone because they are connected to a line or transformer with a capacity limit.

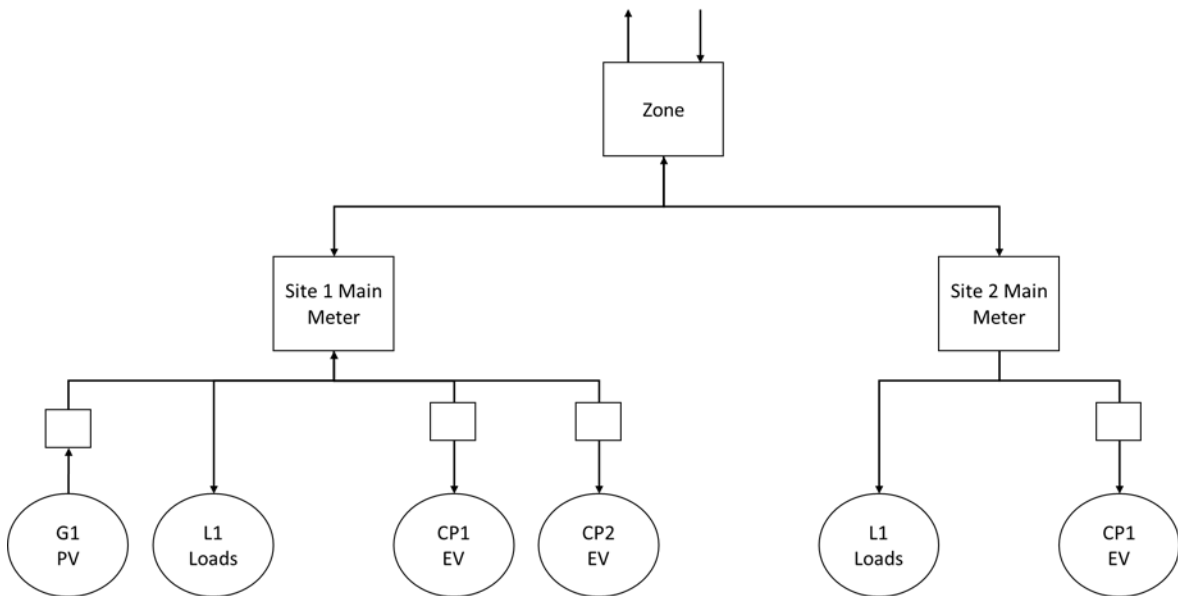


Figure 52. Two households in a zone

The key question now is whether the flexibility algorithm should optimize for the zone or for each of the households.

Optimization for the zone: This approach will ensure that the zone capacity limit is not violated. Further the flexibility will be used to ensure cost minimization for the zone. However, this does not guarantee that the solution is optimal for each of the households.

Optimization for each household: This is in accordance with example 1, but in addition, we now have an additional constraint: The sum net purchase for the two households must be below the capacity limit for the zone. In cases where the optimal solutions for each of the two households lead to violation of the limit, some corrective actions must be performed. One possible approach could be to reduce the household capacity limits pro rata according to main fuse size or something.

Each of these options have pros and cons: Optimization for the zone is easiest to implement, but may have some odd effects that may be perceived as unfair between the households.

#### 9.3.4.3 Example 3: Office charging with 4 charging points

Consider an example with a site outside an office building with 4 charging points.

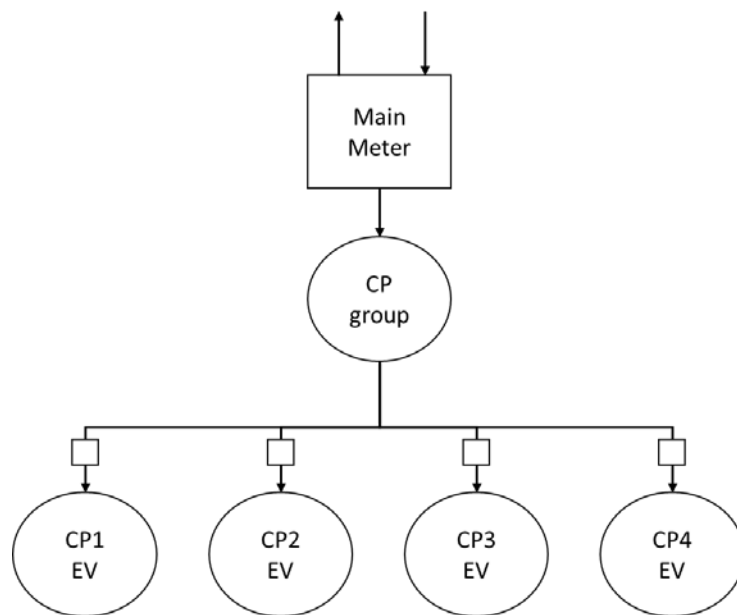


**Figure 53. Four charging points outside an office building**

Charging points 1, 3 and 4 can deliver 3 kW, while charging point 2 can deliver 8 kW. The total capacity at the site is 10 kW (defined in the Maximum Capacity Forecast), which means that all points cannot charge at full power simultaneously. We receive meter readings from each of the CPs. Further, assume that the prices are according to Figure 44.

Based on historic data for each CP, the following situation has been predicted:

- CP1 is connected from hour 8 to 14 with a charging demand of 8 kWh

- CP2 is connected from hour 10 to 15 with a charging demand of 26 kWh
- CP3 is connected from hour 9 to 16 with a charging demand of 11 kWh
- CP4 is connected from hour 10 to 17 with a charging demand of 8 kWh

With no control of the charging process, the following situation will occur (given that the predictions are right):

Baseline case. No flexibility activated								
t	CP1	CP2	CP3	CP4	Sum charging	Grid limit	Price	Cost
1					0	10	4,73	0,00
2					0	10	4,60	0,00
3					0	10	4,63	0,00
4					0	10	4,41	0,00
5					0	10	4,46	0,00
6					0	10	4,64	0,00
7					0	10	5,36	0,00
8	3				3	10	6,99	20,97
9	3		3		6	10	7,75	46,47
10	2	8	3	3	16	10	7,01	112,16
11		8	3	3	14	10	6,94	97,10
12		8	2	2	12	10	6,51	78,08
13		2			2	10	5,85	11,70
14	(departure time)				0	10	6,15	0,00
15		(departure time)			0	10	5,98	0,00
16			(departure time)		0	10	5,74	0,00
17				(departure time)	0	10	5,61	0,00
18					0	10	6,21	0,00
19					0	10	8,10	0,00
20					0	10	8,98	0,00
21					0	10	7,38	0,00
22					0	10	5,50	0,00
23					0	10	4,99	0,00
24					0	10	4,99	0,00
	8	26	11	8	53			366,49
					Grid limit reached			

Figure 54. Example of uncontrolled situation

The sum charging will violate the 10 kW grid limit in the hours 10, 11 and 12. At the same time we see that the prices are high in the hours 8, 9, 10 and 11. We want to find a schedule that relieves the capacity violation, reduces the charging costs and at the same time meets the charging demand.

We enter this information into the flexibility algorithms. Notice that we here make the plans based on predicted departure time. Hence, we know what (predicted) flexibility that exists. This approach will probably only work in cases where the charging follows some kind of pattern, i.e. it is not very random.

Based on the input information, the flexibility algorithms will make optimal decisions at the level of each charging point. An example of a solution is presented in Figure 55. We

observe that there is no violation of the total capacity, that the cost has decreased from EUR 366 to 337 and that all cars have got all energy needed.

t	CP1	CP2	CP3	CP4	Aggregated decision	Cost
1					0	0,00
2					0	0,00
3					0	0,00
4					0	0,00
5					0	0,00
6					0	0,00
7					0	0,00
8					0	0,00
9	2				2	15,49
10	3				3	21,03
11	3	6			9	62,42
12		8	2		10	65,07
13		7	3		10	58,50
14	(departure tin	5	3	2	10	61,53
15		(departure tin	3	3	6	35,86
16			(departure tin	3	3	17,22
17				(departure tin	0	0,00
18					0	0,00
19					0	0,00
20					0	0,00
21					0	0,00
22					0	0,00
23					0	0,00
24					0	0,00
	8	26	11	8	53	337,13

Figure 55. Example of results from the flexibility algorithm

The IIP sends the aggregated decision to GreenFlux/ElaadNL. Based on this information, GreenFlux/ElaadNL distributes this to each charging point.

Some comments:

- The distribution down to each charging point performed by GreenFlux/ElaadNL will probably be different from the ones calculated by the flexibility algorithms. In worst case it will lead to situations where some cars do not get fully charged. An option could be that also the detailed solutions are sent to GreenFlux/ElaadNL as additional input. Another option is that GreenFlux/ElaadNL sends back to the IIP the detailed distribution
- The algorithm believes 100 % in the predictions. We see in the example that no charging is performed in hour 8 and only small volumes in hour 9 and 10. A constraint (minimum value) could be added to avoid situations where no car gets any charging and leaves earlier than expected.

- The approach builds on the assumption that it to a certain extent is possible to predict the charging.
- How to handle situations where an EV connects earlier than predicted, in periods where no car is predicted to be connected (see Chapter 9-variable freezing techniques ).

## **9.4 Bulgaria case study**

### **9.4.1 Introduction**

The Bulgarian pilot (Albena pilot) will consist of one single pilot site, the Flamingo Grand hotel, with an electric battery, a solar PV installation, a number of charging points and two central water boilers.

The site will have a SCADA-system delivered by Schneider. All exchange of data, both meter readings and control signals, will be between the Integrated IIP and this SCADA-system.

According to D10.1 all BRP flexibility services are listed (Day-ahead portfolio optimization, intraday portfolio optimization and self-balancing portfolio optimization) as well as all prosumer flexibility services (ToU optimization, kWmax control, self-balancing and controlled islanding).

Here, we only focus on the prosumer flexibility services, since we assume that these will be implemented first once the pilot becomes live. Furthermore, we interpret the prosumer flexibility services according to the definition in D5.3 as stated above.

### **9.4.2 Structure information and historic meter values**

According to D5.3, the pilot site can be illustrated as in Figure 56.



Bulgaria, Hotel Flamingo Grand

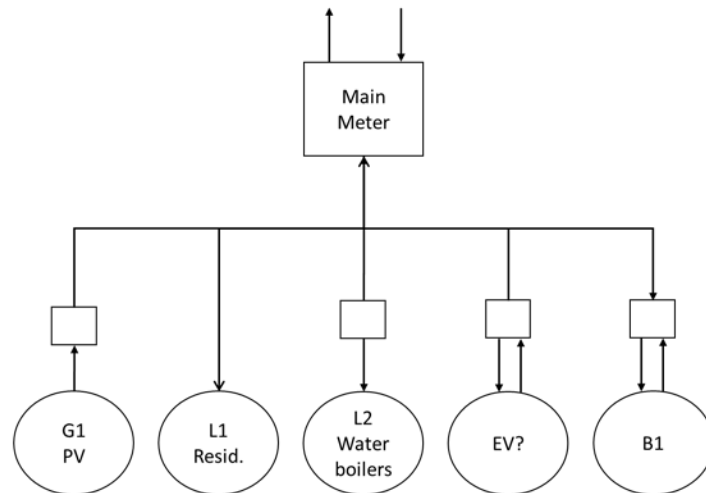


Figure 56. Illustration of resource model for the Bulgarian pilot site

IIP needs structure information about the site and resources to establish the model as illustrated above. Some of the potential necessary data from this pilot to flexibility management algorithm are listed as bellow (time granularity should be hourly or finer):

- Net consumption (purchase) from the main meter .
- Consumption at the water boilers
- Outside temperature and cloudiness data

Since the solar panels and charging points are not installed yet, historic data will not be available yet.

### 9.4.3 Real-time meter values in general

In line with the definitions in D7.2, the IIP will receive the following data from the Schneider SCADA system:

- Net consumption (purchase) for the main meter
- Net production (sales) for the main meter, if relevant
- Charging energy consumption for each charging point
- Consumption for each of the water boilers

All this information will be received as meter readings (i.e. counter values) every 15 minutes or more often. The granularity must be further discussed, but 15 minutes is a working assumption. If values are to be received more often, they must be fit to 15 minutes' intervals, for instance every 5 minutes or every 1 minute.

#### 9.4.4 Commercial/agreement information

Since the December 2018, Bulgarian pilot has a retail contract for electrical energy based on the day-ahead prices of the Independent Bulgarian Energy Exchange (IBEX). An overview of prices variation for delivery day Friday 14/12/2018 is presented in Figure 57.

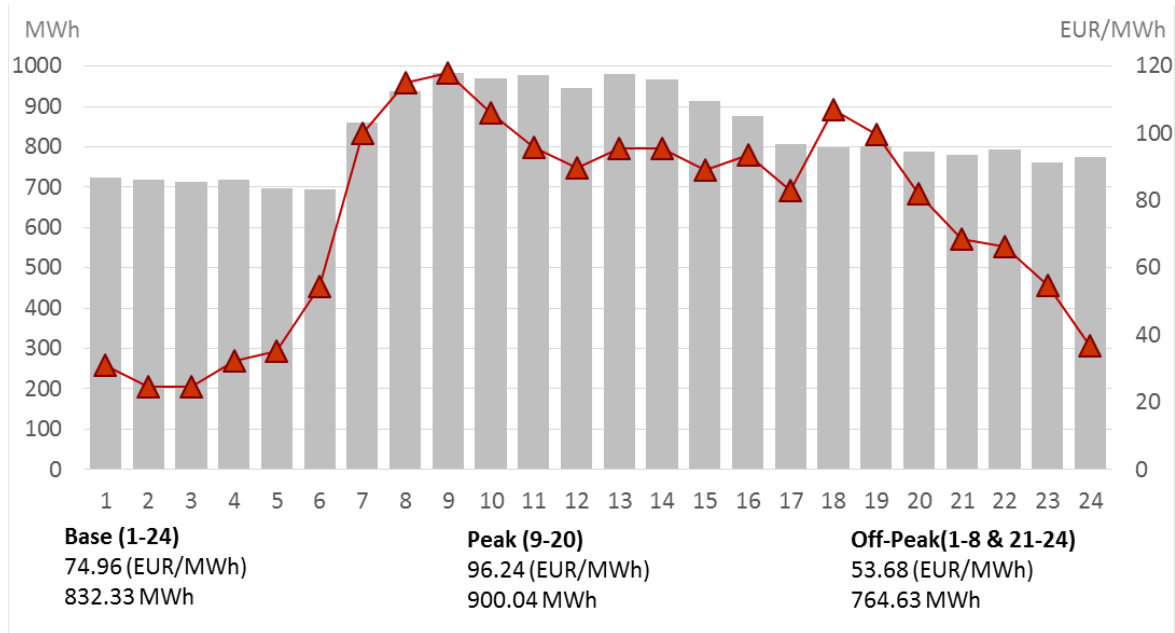


Figure 57. Day-ahead prices from Bulgarian energy exchange (14/12/2018) source (<http://www.ibex.bg/en>)

#### 9.4.5 Flexibility

The Albena pilot will include the following types of flexible devices:

- Battery
- EV charging points
- Water boilers

According to D5.3, the flexible devices will be used in the following way:

*For the prosumer the flexibility in the Bulgarian pilot will be used to shift consumption from peak to off-peak periods. A combination of the following options will be utilized to obtain this objective:*

- *To charge the battery during off-peak hours and to discharge during peak hours*
- *To shift as much as possible of the water boiler consumption from peak to off-peak hours*

- *To shift as much as possible of the EV charging from peak to off-peak hours*

*The flexibility will also be used to keep the maximum outtake/purchase below a given limit (kW<sub>max</sub>) and finally to avoid feeding surplus electricity back to the grid.*

To be able to utilize the flexibility in an optimal way and without inducing any loss of comfort or other disadvantages, flexibility properties must be defined in detail. This also includes rules, agreements and interaction with involved people at the site, and which information that will be available at what times. Each type of flexible device will be handled below.

In chapter 9.3.3 it is stated that a working assumption is that meter readings will be received every 15 minutes. This is closely linked to the time resolution of the optimization algorithms, which also are assumed to have 15 minutes time intervals. This means that every decision (output from the algorithms) has the granularity of 15 minutes. Implementation of these decisions in real-time is the responsibility of the local systems. As an example, the optimization algorithm can decide that a battery is going to charge 5.0 kWh in a given 15 minute time slot. How this is implemented inside the time slot is left to the local system, which in this case might be the local Battery Management System (BMS).

#### 9.4.5.1 EV charging points

EV charging points will be installed at Albena. It is assumed that meter readings will be received from each charging point and that the charging power (kW) can be controlled at each separate point. The alternative is that meter values are received at the aggregated level (for all charging points summed) and/or that control signals are sent at an aggregated level, and that the local system will distribute the power between the charging points.

Each EV charging point will have fixed data for maximum charging power continuously between 0 and a maximum level. Dependent on the car that connects, the maximum power that the car takes can be lower than the maximum level at the charging point. In addition, there will be a lower level, which is decided by the car. Information about the car type will not be available at the Albena pilot, since different cars will connect.

Meter values for charging energy will be received for each EV charging point with the granularity of 15 minutes or smaller. The optimization algorithm output will be a charging set-point for each period. The set-point will either be an average power level (kW) or energy (kWh). Implementation of the set-point will be performed locally, i.e. by the EVSE or SCADA.

#### 9.4.5.2 Water boilers

There will be two disconnectable water boilers, each with 144 kW installed capacity. They are connected under the same meter, which means that the meter value will be at an aggregated level. We assume that the meter only meters water boiler consumption, but this must be verified.

The water heater control is based on a set of timing restrictions that will be input to the optimization algorithm:

- a. For each period, a parameter says whether it is allowed to disconnect the water heater or not (e.g. disconnection is allowed at any time, except from between 1900 and 2200).
- b. A maximum disconnection duration is given (e.g. if the water heater is disconnected, it must at the latest be reconnected after 1 ½ hour)
- c. A minimum duration (rest time) between two disconnections is given (e.g. if a water heater is reconnected after a disconnection, it cannot be disconnected again before at least 3 hours)

In the EMPOWER project, before a disconnection is executed, a message was sent to the user, and she could have the possibility to decline. This was regulated in the contract between the FO and the user. We assume that this functionality will not be included in the Albena pilot, but that might be reconsidered.

The output from the optimization algorithms is a set of disconnection and reconnection periods. The control signals will be “off” and “on” with a given time (e.g. “off” at 12:15, and “on” at 12:45). NB! This information will have the granularity equal to the length of the periods, probably 15 minutes, which means that the connections and disconnections will be set to these time points, and not at any minute inside a 15 minutes’ interval.

An illustrative (probably unrealistic) example is given below. Again, the time resolution in the example is one hour. The blue bars show the predicted consumption, while the orange line shows the consumption based on the output from the optimization algorithm.

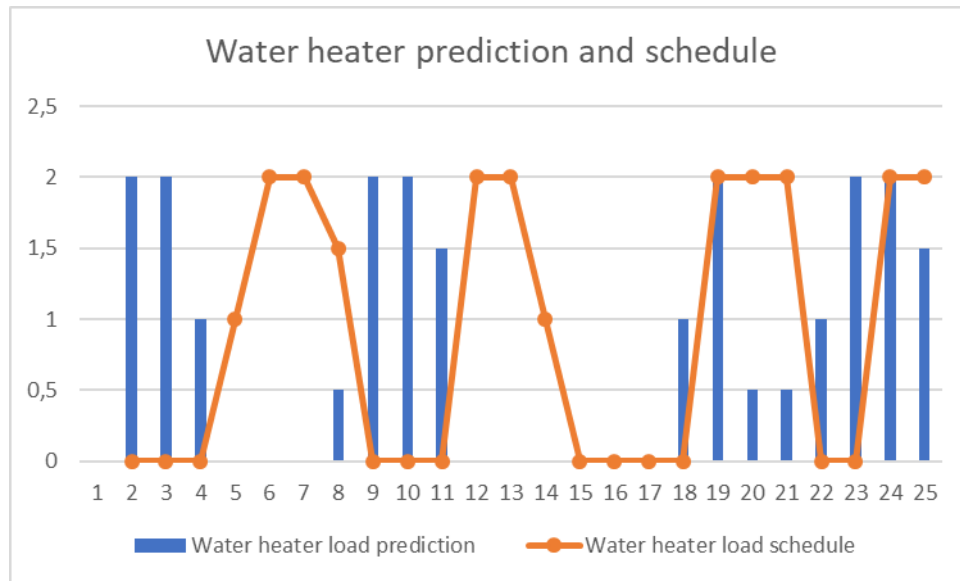


Figure 58. Example of predicted energy consumption at a water heater and the resulting consumption when controlled

#### 9.4.6 An illustrative example

This chapter contains a simple example to illustrate how the flexibility algorithms might work. Assume we have the setup as in Figure 56, with the following parameters:

- The solar panels have installed capacity 100 kWp
- The water boilers have installed capacity 288 kW and can be disconnected for maximum 1 hour between 12 and 17
- There are 2 EV charging points, each with maximum charging power 11 kW, where charging can be delayed maximum 2 hours for each point
- The battery has installed capacity 200 kWh, with 100 kW maximum power in and out and round-trip efficiency equal to 1.0

For simplicity, we use hourly time resolution in the example. The predicted solar PV production is shown in Figure 59.

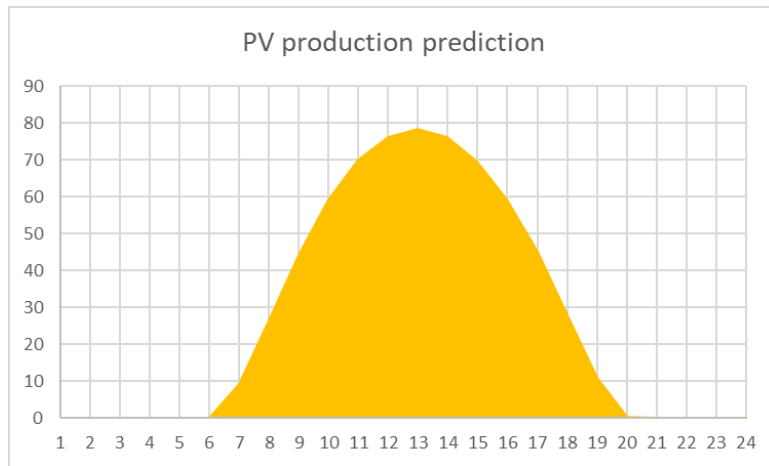


**Figure 59. Example of predicted energy consumption at a water heater and the resulting consumption when controlled**

The load predictions for the EV charging points, the water boilers and the residual load is shown in the figure below.

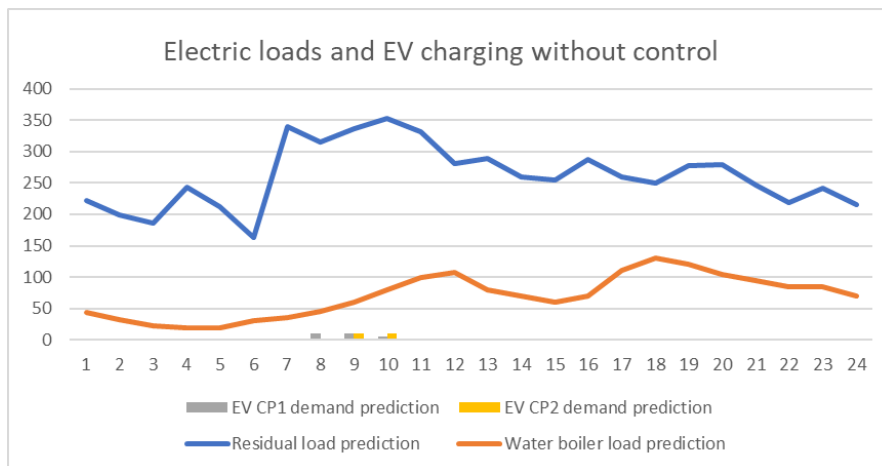


**Figure 60. Example of predicted energy consumption at the water boiler, the charging points and the residual loads without control**

Altogether, this gives the following net profile in Figure 61.

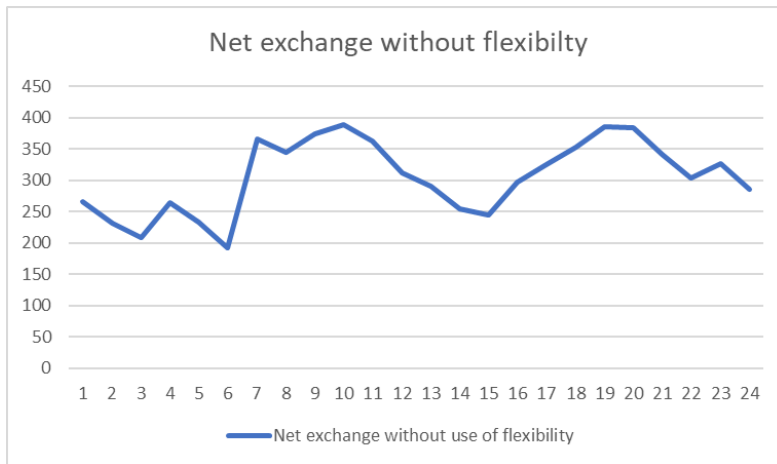


**Figure 61. Net load when no flexibility is utilized**

We see that there is a morning and an afternoon peak. These should be reduced by shifting loads and utilizing the battery.

A possible strategy is shown in Figure 62.

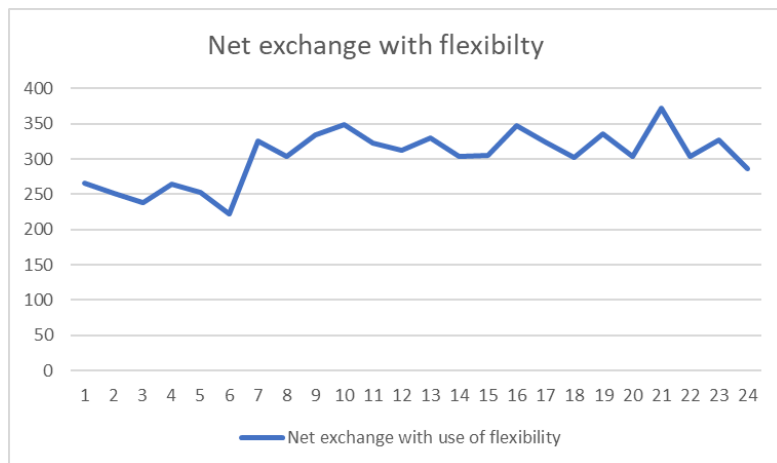


**Figure 62. Netload when flexibility is activated**

We see that the profile is flattened, by reducing the morning and afternoon peaks and by filling the valley between 13:00 and 15:00. Compared to the pilots in Norway and the Netherlands, where electricity cost is a direct input to the algorithm, no cost is calculated here. The target is only to flatten the profile.

## 10 Prosumer objective functions

In this chapter, we discuss issues regarding the objective functions for the prosumer services in different pilots in INVADE. We have not included the German pilot since our information about this new pilot is limited.

### 10.1 Norwegian case study

As it has been already explained, subscribed power tariff will be taken effect in Norwegian pilot. It is deemed that prosumers may turn to energy storage solutions rather than pay the heavy premiums if their energy needs exceed their present levels.

In cases with subscribed power, there will be no demand charge, but an additional energy fee for energy levels above the subscribed value. The tariff will still have a fixed fee and an ordinary energy fee, the latter will cover marginal grid losses. But in addition, an overconsumption fee will be included. It works like this: The prosumer subscribes to a certain power level (actually energy per hour, kWh/h) and pays a fixed fee according to this value. In hours with consumption larger than the subscribed level, an overconsumption fee must be paid for the part above subscribed level. The figure below illustrates the concept, where a prosumer subscribes 7 kW. For the hours 1, 18, 19, 20, 21, 22 and 24, she must pay a cost equal to the overconsumption price multiplied with the overconsumption amount:

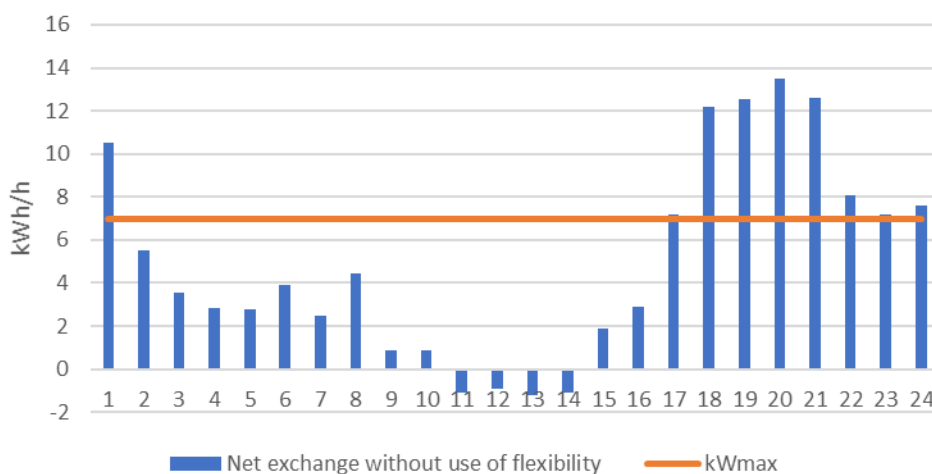


Figure 63. Illustration of overconsumption where subscribed power is 7 kWh/h

The objective function then becomes:



$$\min z = \sum_{t \in T} [(P_t^{\text{retail-buy}} + P_t^{\text{grid-buy}} + P_t^{\text{tax}}) \cdot \chi_t^{\text{buy}} \cdot P^{\text{VAT}} - (P_t^{\text{retail-sell}} + P_t^{\text{grid-sell}}) \cdot \chi_t^{\text{sell}} + P^{\text{overcons}} \cdot \chi_t^{\text{overcons}} \cdot P^{\text{VAT}}] + \zeta^{\text{flexibility}} \quad (85)$$

where

$$\chi^{\text{overcons}} = \chi_t^{\text{buy}} - X^{\text{subscribed}}, \text{ if } \chi_t^{\text{buy}} - X^{\text{subscribed}} > 0, \text{ else } 0 \quad (86)$$

### 10.1.1 Periods smaller than 1 hour

As a working assumption we will have 15 minutes' time slots, which means that we will have 4 periods per hour. This will have certain implications.

First, energy and power cannot be used interchangeably. For instance, charging of 4 kW in one period will give 1 kWh. So, energy and power terms must be used carefully and in a unified way. According to D5.3 all decision variables (e.g.  $\chi_t^{\text{buy}}$ ) are defined as energy values. We then also might need to introduce average power variables and introduce some simple constraints defining the relation between energy and average power. This is probably needed since it is usual to talk about EV charging in kW (or A), which means that charging at 4 kW gives 1 kWh per 15 minutes.

This is also important to capture the peak value related to demand charge. Since this is an hourly value, the  $\chi_t^{\text{buy}}$  cannot be used directly, but must be summed over all periods in one hour. Somehow, we must handle relation from period to hour, like:

$$\chi_h^{\text{buy}} = \sum_{t=1}^4 \chi_t^{\text{buy}}, \forall h \in H \quad (87)$$

And then it is the  $\chi_h^{\text{buy}}$  that must be the basis for the calculation of the peak.

The same issue is valid for the over-consumption amount, since it based on hourly values. Although a prosumer subscribes for instance 5 kW, it is possible to go beyond the average power level for some of the quarters without getting a penalty, as long as the hourly value is below.

## 10.2 Dutch pilot

The objective functions for the different Dutch pilot sites will be formulated in the following sections.

### 10.2.1 Pilot 1: Home charging

The objective is to minimize the total electricity cost for the household. These costs include:

- Grid contract based on maximum outtake (kWh/h) over the year
- Retail contract with supply/retail. In this respect, the more locally produced ‘own’ energy is used, the lower the amount that needs to be paid to the retailer.

The objective function is explained by the following equation, which includes both the retail contract and grid contract.

$$\min z = \sum_{t \in T} [(P_t^{\text{retail-buy}} + P_t^{\text{tax}}) \cdot \chi_t^{\text{buy}} \cdot P^{\text{VAT}} - (P_t^{\text{retail-sell}}) \cdot \chi_t^{\text{sell}}] + P^{\text{peak}} \cdot \chi^{\text{peak}} \cdot P^{\text{VAT}} \quad (88)$$

As discussed above, the pilot has two contracts, i.e., the grid contract and the supply/retail contract.

The grid contract is based on a peak demand charge for the year ( $P^{\text{peak}}$ ). This indicates that it is an incentive to reduce this peak (hourly value) as much as possible.

The supply contract for buying electricity is normally an average fixed price for a full period (1 or 2 years). This pilot is using contract where energy retail prices are based on hourly prices at EPEX Spot<sup>8</sup> without any mark-up or other fees that are relevant for the flexibility algorithm. This contract also regulates the price for sales of surplus electricity sales. This price is 0.18 €/kWh on average. The price change per hour. The homeowner pays the average price and get a refund or surplus at the end of a period depending on the real prices and usage.

The formulation covers grid tariffs with peak demand charges. One issue here is to decide  $\chi^{\text{peak}}$ , which again can be split into two issues:

1. The charge may be based on several models
2. The basis for the charge may not fall inside the planning horizon

The most common model is that the basis for the charge is the highest hourly outtake over a month. Currently, we do not know what type of regime we will have in the pilot, but we assume that monthly demand charge must be covered. We leave this issue for now, but need to have it in mind as the pilot details get clarified.

<sup>8</sup> <https://www.apxgroup.com/market-results/apx-power-nl/dashboard/>

### 10.2.1.1 Peak hour not necessarily in planning horizon

The basis for the demand charge is related to a horizon longer than the planning horizon. To illustrate the issue, assume that we have a 48 hours' planning horizon, and that we first we are going to plan for a 48 hours' horizon in the beginning of a month, see Figure 64.

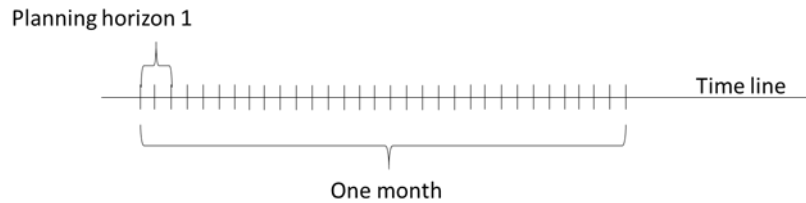


**Figure 64. Illustration of a planning horizon in the beginning of a month**

If the variable  $\chi^{peak}$  is decided as the largest  $\chi_t^{buy}$  in the planning horizon, suboptimal decisions will most likely be the result (in retrospect), since the real monthly peak will realize later in the month. Then the model will try to reduce the maximum  $\chi_t^{buy}$  in the planning horizon, which in reality does not give any cost savings. On the contrary, flexibility could be used better to reduce other cost elements in the objective function, and we might induce unnecessary flexibility costs. The question is then how to deal with this problem in the most efficient way. One way is to estimate/predict the monthly max and somehow set a limitation – in other words to constrain the value  $\chi^{peak}$  from below. This approach is described in eq. (7) in [1].

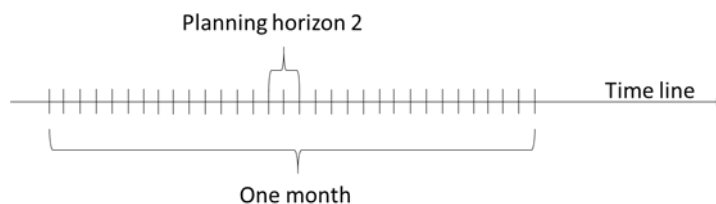


**Figure 65. Illustration of a planning horizon in the middle of a month**

Next assume that we are going to make an optimization in the middle of the month, see Figure 65. Then we already have a monthly max (so far in the month), which can be seen as a sunk cost. But still new peaks can realize in the rest of the month.

Finally, assume that we are running an optimization for the last two days in the month. Then we have all information available: Realised peak so far and planned values for the rest of the month.

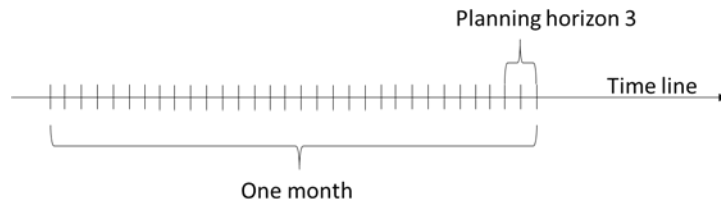


Figure 66. Illustration of a planning horizon in the end of a month

Consequently, this means that we need to introduce a parameter, i.e.,  $M^{peak}$ , that constrain the  $\chi_t^{buy}$  from below:

$$\chi_t^{peak} \geq M^{peak}, \forall t \in T \quad (89)$$

Then,  $M^{peak}$  must be updated before each optimization run based on a combination of predictions and realized peaks.

#### 10.2.1.2 Peak cost

Another issue is how to handle the peak cost. Recall that the optimization algorithm is run for a planning horizon. Assuming that this covers two days, the objective function value will cover two days with costs. However, the peak cost is for a month. One approach could be to multiply this term in the objective function with the fraction that these two days contribute in the given month (e.g. 2/31). On the other hand, a new peak will have a large impact.

Another way is to view the peak cost so far this month (or predicted peak cost) as sunk and only include the additional cost. This means that we do not use the  $\chi^{peak}$  directly, but the delta, for instance:  $\Delta\chi^{peak} = \chi^{peak-new} - \chi^{peak-old}$ . Still, it should be considered if the full “delta-cost” should be included. This represents an increase in monthly cost, while the rest of the cost elements cover two days’ costs.

#### 10.2.2 Pilot 2: Large scale offices and parking lots

The objective is to minimize the total costs for the building owner or prosumers by controlling EV charging. These costs include:

- Grid contract based on maximum outtake (kW) over the year
- Retail contract with costs for purchase based on hourly EPEX Spot price
- Flexibility contract on using charging flexibility services to the EVs

The objective is to maximize the total delivered charging by controlling and balancing charging in such a way that none of the capacity limitations are violated. This way cost of energy consumption can be reduced and extension of the grid connection can be prevented.

There are three contracts that are involved in this pilot: The grid contract, the supply/retail contract and the “flexibility contract” with the EV to deliver charging energy. The objective function can be explained as below.

$$\min z = \sum_{t \in T} [(P_t^{retail-buy} + P_t^{tax}) \cdot \chi_t^{buy} \cdot P^{VAT} - (P_t^{retail-sell}) \cdot \chi_t^{sell}] + P^{peak} \cdot \chi^{peak} \cdot P^{VAT} + \zeta^{flexibility} \quad (90)$$

The grid contract is based on a peak demand charge for the year. This means that it is an incentive to reduce this peak (hourly value) as much as possible.

The supply contract for buying electricity is based on hourly prices at EPEX Spot<sup>9</sup> without any markup or other fees that are relevant for the flexibility algorithm, which is similar to the Pilot 1. This contract also regulates the price for sales of surplus electricity sales. This price is 0.05 €/kWh on average, but it is not known whether this is fixed or varying over the day.

Finally, there is an income from selling charging energy to the EVs. This is a fixed price of 0.29 €/kWh and goes is paid by the EV-driver, via its service provider and charge point operator, to the owner of the charging station.

### 10.2.3 Pilot 3 Small scale office

The objective of the Small scale Office pilot is local capacity management on EVSE while gathering real-time information on the energy use of both the other EVSEs and other loads on the local site. Three optimization levels are considered ranging as a) locally behind the connection point b) locally congestion in agreement with the local DSO c) national level; flexibility is provided to BRP and TSO

Control on the first level will be done based on self-balancing needs. Since this is a single site where ElaadNL performs this local load within the site there are no external parties involved at this level. At this level, the objective function is similar to Pilot 2, and the

---

<sup>9</sup> <https://www.apxgroup.com/market-results/apx-power-nl/dashboard/>

constraints will be added at site asset grouping. The scheme has been proposed by eSmart and is under development.

On the second level there is no price / product / tariff in place at the DSOs (yet). This is part of the R&D work within the DSO's

At the third level flexibility can be priced as the combination of the prices on the potential markets given before ((short term) wholesale; day-ahead and intra-day (like EPEX) and ancillary markets FCR and aFRR) and the own current (im)balance position of the BRP. We will explain the objective function in Chapter 11.

#### 10.2.4 Pilot 4 Large scale public

This pilot focuses on the function of controlling EVSEs and their energy supply to EVs, connected to a management system of the CPO. It is planned to conduct experiment with large scale public charging in the Netherlands, using grid congestion management and BRP services (possibly containing frequency containment reserve support). More specifically, this pilot will follow the steps researching the extent to which charging stations are capable of providing BRP support using by central control.

A new grid tariff type is the “Dynamic capacity” which works like this:

- The customer has a given main fuse size, e.g. 3X35 A. Normal tariff rate is a fixed fee, e.g. 800 €/year
- If the customer can guarantee that he/she will not surge above 3X25 A in certain peak hours, he/she will pay a reduced rate, e.g. 200 €/year. Which hour that are included in the definition of peak hours are dynamic, but will be known in advance illustrates the principle. Here, up to 24 kW can be bought in the non-peak hours defined Figure 67. Illustration of the tariff type “Dynamic capacity” by the hours 8 – 10 and 17 – 21. For the peak hours 8 – 10 and 17 – 21, the capacity is reduced to 17 kW.

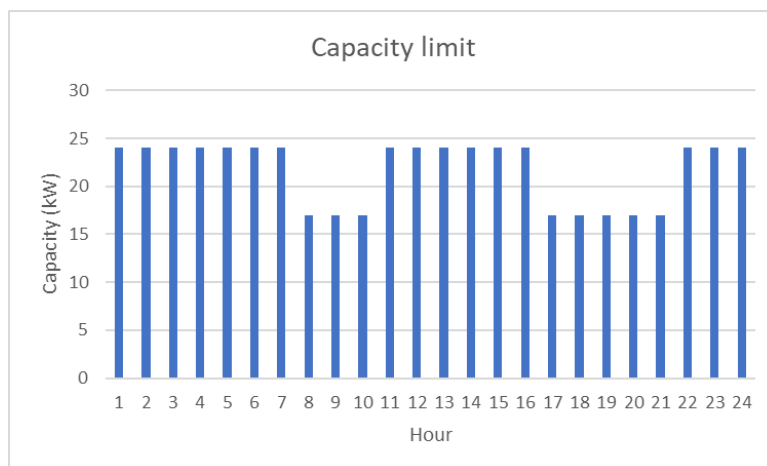


Figure 67. Illustration of the tariff type “Dynamic capacity”

Connections are 3x25A or 3x35A, yearly connection prices are: 225 incl VAT and 816 incl VAT. There are neither volumetric price drivers, nor there is (yet) a contracted capacity component in place. The basis for the objective function of this pilot is explained in the Chapter 11.

### 10.3 Bulgarian pilot

According to the pilot specification in section 9.3, the main objective is to shift as much as possible of the load from the peak-load hours to the off-peak load hours. This can be formulated as:

$$\min z_{Bulg1} = \sum_{t=9}^{20} \chi_t^{buy} \quad (91)$$

An alternative formulation is to maximize the up-regulation in the peak load hours:

$$\max Z_{Bulg2} = \sum_{t=9}^{20} \left( \sum_{b \in B} \sigma_{b,t}^{B,out} - \sum_{b \in B} \sigma_{b,t}^{B,in} + \sum_{l \in L} (W_{l,t} - \omega_{l,t}) \right) \quad (92)$$

Notice that this formulation only covers batteries and flexible loads. Also notice that it presupposes that the battery has no baseline schedule. If other resource types, like EV charging points are added, or batteries have a baseline schedule, the formulation must be changed.

### 10.4 Spanish pilot

The objective function for the Spanish pilot is explained in Chapter 11.

### 10.5 Illustrative prosumer results

This section presents an illustrative example that test the rolling horizon model for a horizon of 24 hours with a resolution time of 15 minutes. This makes a total horizon of 96 periods. The number and kind of devices available in this example are the following: 2 EV charging points, 1 electric water heater (EWH), 1 controllable PV generator and 1 inflexible PV generator, and 2 batteries. This illustrative example can be seen as a subcase of the Norwegian pilot.

The input parameter values of each of the devices are specified below. First, parameters that have constant values are shown in a table and then parameters that vary with time are shown in a graph afterwards.

EV charging points input parameters can be seen at Table 17 and Figure 68.

**Table 17. EV charging points input parameters.**

PARAMETER	VALUE		UNIT
	EV charging point 1	EV charging point 2	
$Q_v^{CP,max}$	3	3	[kW]
$Q_v^{CP,min}$	0	0	[kW]
$P_v^{CP,ns}$	4	4	[NOK/kWh]
$P_v^{CP,shift}$	0.01	0.001	[NOK/kWh]

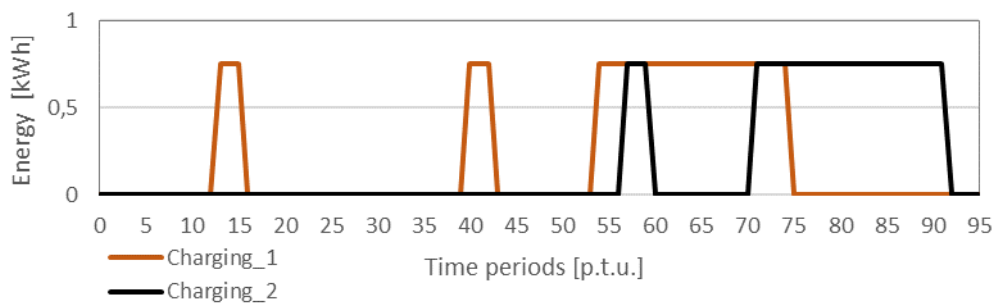


**Figure 68 EV charging points baseline consumption.**

Electric water heater input parameters can be seen at Table 18, Figure 69 and Figure 70.

**Table 18. EWH input parameters.**

PARAMETER	VALUE	UNITS
$D_l^{EWH,max}$	4	[ptu]
$D_l^{EWH,min}$	5	[ptu]
$Q_l^{EWH,max}$	0.5	[kWh]
$Q_l^{EWH,min}$	0.5	[kWh]
$P_l^{EWH,shift}$	0.01	[NOK/kWh]



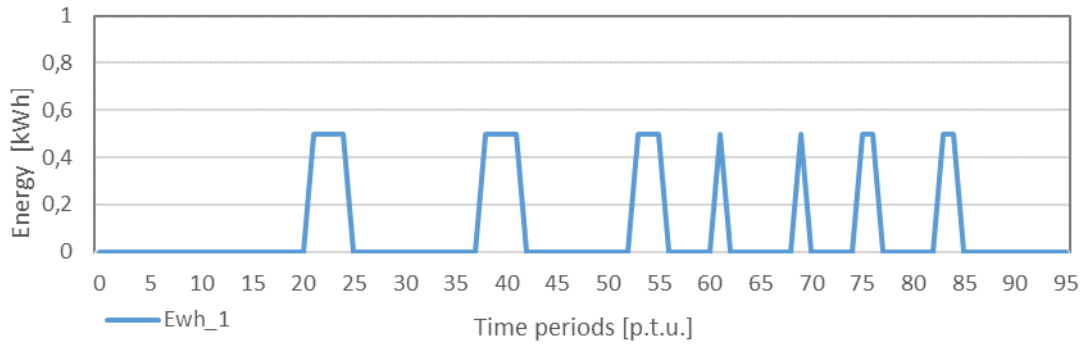


Figure 69. EWH baseline consumption.

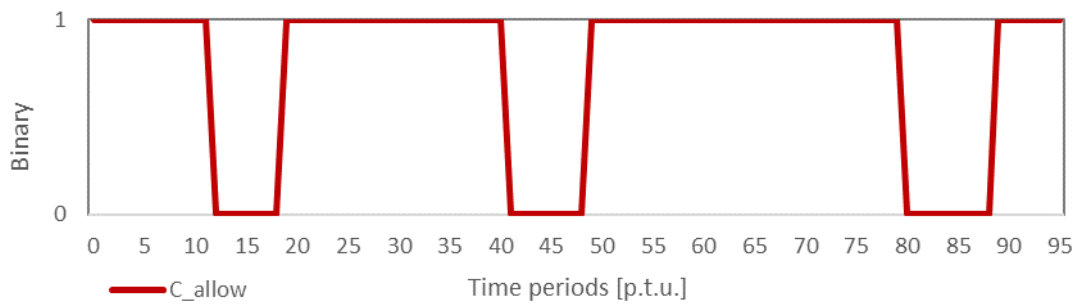


Figure 70. C\_Allow parameter.

PV generation input parameters can be seen at Table 19 Table 18and Figure 71.

Table 19. PV generator input parameters.

PARAMETER	VALUE	UNITS
$P_g^G$	0.5	[NOK/kWh]

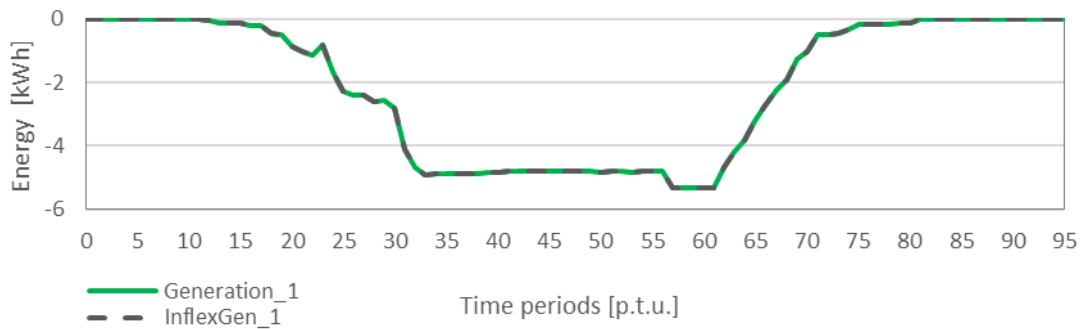


Figure 71. PV forecasted generation.

Input parameters related to the prosumer can be seen at Table 20, Figure 72 and Figure 73.

Table 20. Prosumer input parameters.

PARAMETER	VALUE	UNITS
-----------	-------	-------

$X^{exp-cap}$	100	[kW]
$X^{imp-cap}$	100	[kW]
$p_{tax}$	0.69	[-]
$p^{VAT}$	1.25	[-]
$P_t^{grid-buy}$	0,68	[NOK/kWh]
$P_t^{grid-buy-high}$	1	[NOK/kWh]
$P_t^{grid-buy-low}$	0.21	[NOK/kWh]
$P_t^{grid-sell}$	0	[NOK/kWh]
$p_{peak}$	300	[NOK/kWh/month]

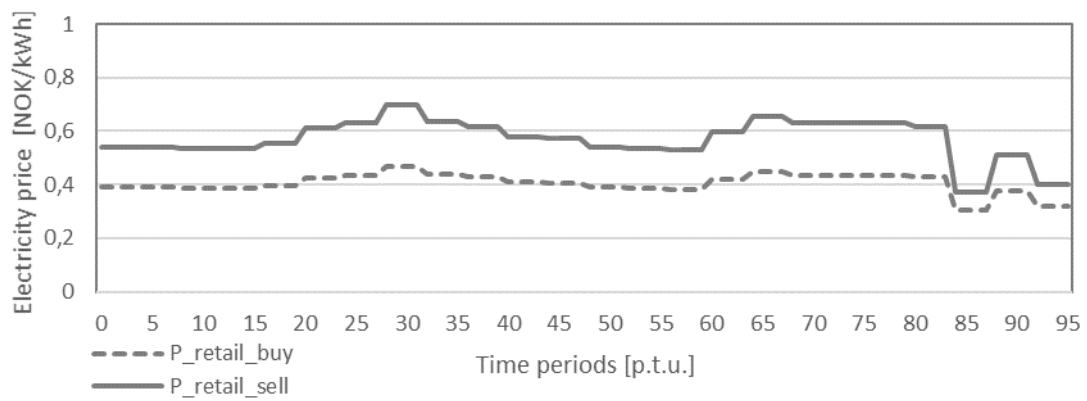


Figure 72. Electricity prices for buying and selling.

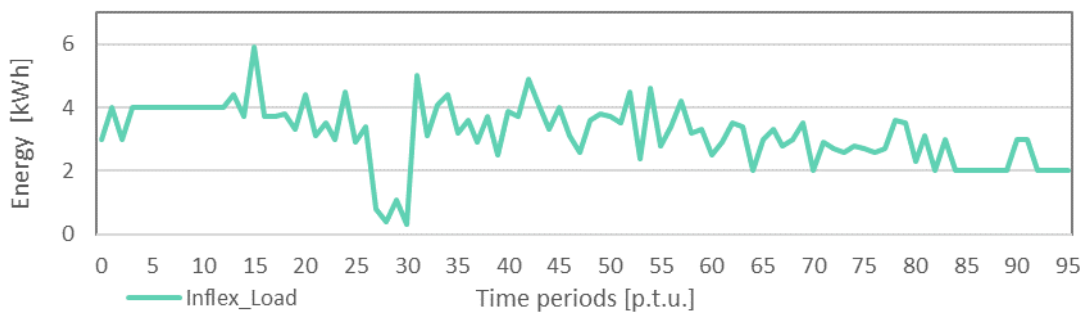


Figure 73. Prosumer Inflexible load.

Battery input parameters can be seen at Table 21 and Table 18.

Table 21. Battery parameters.

PARAMETER	VALUE Battery 1	VALUE Battery 2	UNITS
$A_b^{B,ch}$	0.95	0.9	[-]

$A_b^{B,dis}$	0.95	0.9	[-]
$O_b^{B,max}$	10	20	[kWh]
$O_b^{B,min}$	1	2	[kWh]
$O_b^{B,end}$	5	10	[kWh]
$P_b^{B,ch}$	0.01	0.01	[NOK/kWh]
$P_b^{B,dis}$	0.01	0.01	[NOK/kWh]
$Q_b^{B,ch}$	5	12	[kW]
$Q_b^{B,dis}$	5	12	[kW]
$S_b^{B,ch}$	0.8	0.8	[-]
$S_b^{B,dis}$	0.1	0.1	[-]

Based on all these inputs, the aggregated consumption and generation baseline can be seen at Figure 74.

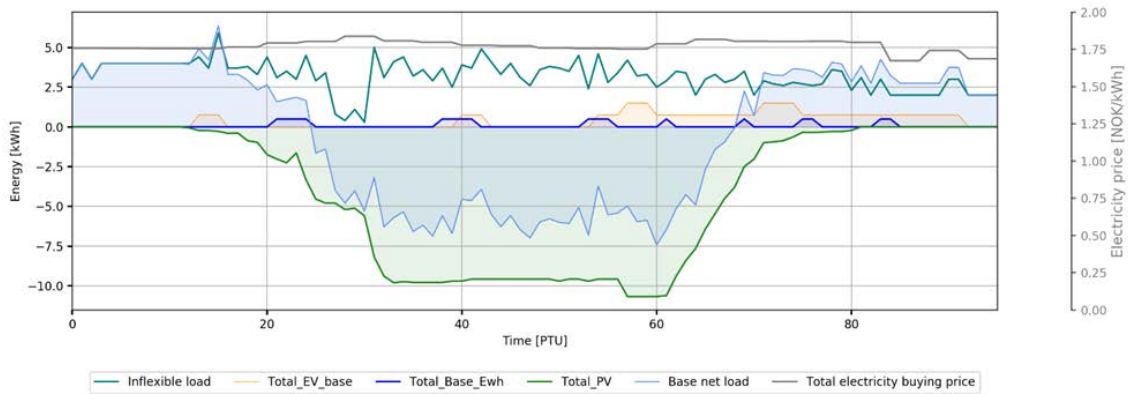
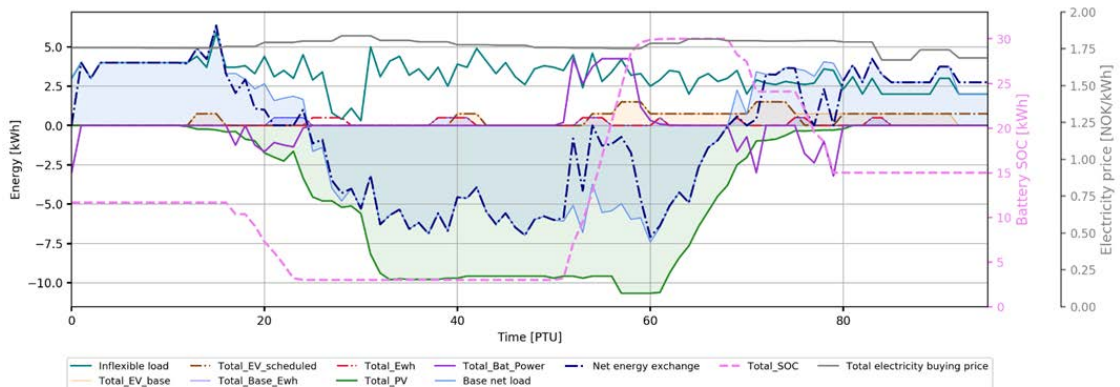


Figure 74. Aggregated baseline consumption and generation.

The results of the optimization can be seen at Figure 75.



**Figure 75. Aggregated optimization results<sup>10</sup>.**

The following points can be observed from these results:

1. Up to period 12, all site consumption is supplied by the grid, except period 0 that indicates batteries are discharging.
2. From period 12 onwards, photovoltaic generation begins. Batteries are discharged from period 19 to 26, because there is enough PV generation forecasted throughout the day, which will be used later to charge the batteries with that surplus power generated. During these periods, the net load is lower than the base load due to battery discharging, which translates into economic savings by having to buy less energy from the grid.
3. EWH consumption in period 21 is postponed to period 25 where there is more PV generation and less inflexible load consumption.
4. In period 51, batteries start charging in order to use that stored energy later in periods where there is no photovoltaic generation thus avoiding having to buy electricity from the grid (Check periods from 69 to 79). See that the net load curve has a lower absolute value than the base load from period 51 to 60. This means that less amount of energy is sold to the grid after the optimization performance. Mainly because batteries need to be charged instead.
5. In the case of EV charging points, some consumption is postponed from the 76 period to the 92, where the price of electricity is lower, because there is no PV generation and all the energy needed is purchased from the grid.
6. Batteries provide the flexibility needed for optimal use of renewable resources. During daylight hours, there is a clear excess of PV generation, which is sold to the grid or used to charge batteries.
7. Storage units end simulation period with the minimum required SOC (5kWh + 10 kWh = 15 kWh).

---

<sup>10</sup> Just as a reminder:

$$\text{Base load} = \text{Inflex load} + \text{EV baseline charging points} + \text{EWH baseline} \\ - \text{total PV forecasted generation}$$

$$\text{Net load} = \text{energy bought} - \text{energy sold}$$

## 11 Aggregated flexibility services

### 11.1 Introduction

This section presents the aggregated flexibility services as centralized and distributed optimization problems. In further stages, the results will be compared. These services are connected with the Spanish and the German pilots. For more information about the problem architecture and agents' interactions, see the D4.3.

### 11.2 Flexibility request prioritization

Under simultaneous flexibility requests (FRs) from two different external agents like DSOs ( $FR_t^{DSO}$ ) and BRPs ( $FR_t^{BRP}$ ), it is necessary to establish a prioritization. Up flexibility means to reduce consumption or increase production and the other way around for down regulation (increase consumption or decrease production).

D4.3 describes this problem in more detail. Figure 76 exposes the prioritization algorithm used. In case of receiving a BRP FR, it is necessary to check if there is any DSO request. In case of simultaneous FRs, the FO takes the minimum if the DSO is asking down-regulation, otherwise it takes the maximum of all FR.

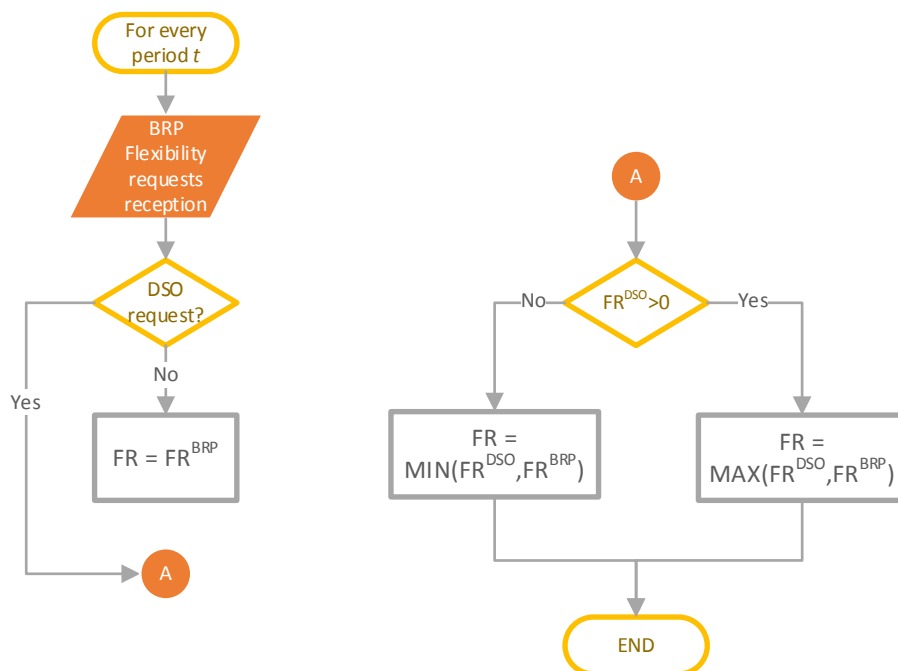


Figure 76 Flexibility request prioritization algorithm

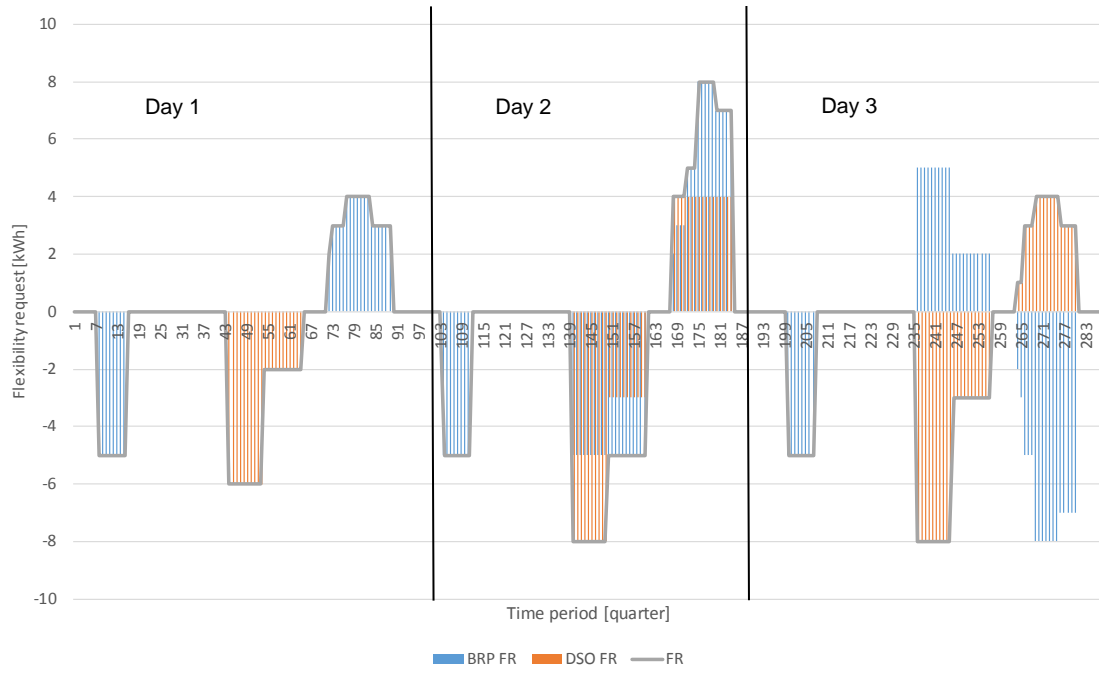


Figure 77 Flexibility requests example and their prioritization

### 11.3 Flexibility availability algorithm

Given a certain FR, it is necessary to know if the FO has enough flexibility in its portfolio to attend the FR. Otherwise the optimization algorithm could be infeasible to be solved. Therefore, it is necessary to verify that the FO portfolio can fully attend the FR.

The algorithm below is in charge of this:

$$\min z = \sum_{t \in T^+} \left( \sum_{p \in P} (\chi_{p,t}^{buy} - \chi_{p,t}^{sell}) - W_t^{baseline} \right) + \sum_{t \in T^-} \left( W_t^{baseline} - \sum_{p \in P} (\chi_{p,t}^{buy} - \chi_{p,t}^{sell}) \right) \quad (93)$$

The  $W_t^{baseline}$  is the FO portfolio total energy consumption or generation in case of providing the prosumer flexibility optimization at site level. Based on this baseline, each prosumer can modify its consumption pattern to attend the FR. During up-regulation periods ( $T^+$ ) the new profile needs to consume less and the opposite during down-regulation periods ( $T^-$ ). The objective function aims to minimize the area between  $W_t^{baseline}$  and the new portfolio consumption after applying the FR.

This objective function is subject to all prosumers constraints and the capacity limitation constraints:

$$\sum_{p \in P} (\chi_{p,t}^{buy} - \chi_{p,t}^{sell}) \geq W_t^{baseline} - FR_t, \quad \forall t \in T^+ \quad (94)$$

$$\sum_{p \in P} (\chi_{p,t}^{buy} - \chi_{p,t}^{sell}) \leq W_t^{baseline} - FR_t, \quad \forall t \in T^- \quad (95)$$

The capacity limitation constraints ensure that the total consumption doesn't

## 11.4 Centralized mathematical formulation

This section describes the mathematical formulation of the aggregated flexibility problem in a centralized approach in generic terms. This problem finds the optimal scheduling that flexibility operators (FO) can apply for attending flexibility requests ( $FR_t$ ). Assuming a certain number of prosumers remotely controlled by the FO, they could provide flexibility in the framework of local flexibility markets described in [17].

The aggregated flexibility algorithm ensures that each prosumer providing flexibility to external agents will be economically rewarded and the FO will schedule the minimum cost flexibility sources at the same time.

Objective function:

$$\min z = \sum \left( \sum_{t \in T} P_{p,t}^{buy} \cdot \chi_{p,t}^{buy} - P_{p,t}^{sell} \cdot \chi_{p,t}^{sell} \right) + \sum_{t \in T} \zeta_{p,t}^{flexibility} + \sum_{h \in H} (P_{p,h}^{low} \cdot \chi_{p,h}^{low} + P_{p,h}^{high} \cdot \chi_{p,h}^{high}) \quad (96)$$

$$P_t^{buy} = P_t^{retail-buy} + P_t^{grid-buy} + P_t^{tax} \quad (97)$$

$$P_t^{sell} = P_t^{retail-sell} + P_t^{grid-sell} \quad (98)$$

Flexibility request constraint:

$$\chi_{t,p}^{aggregated} = \sum_{p \in P} (\chi_{t,p}^{buy} - \chi_{t,p}^{sell}), \quad \forall t \in T \quad (99)$$

$$W_t^{baseline} - FR_t \geq \chi_{t,p}^{aggregated}, \quad \forall t \in T^+ \quad (100)$$

$$W_t^{baseline} - FR_t \leq \chi_{t,p}^{aggregated}, \quad \forall t \in T^- \quad (101)$$

Additionally, every  $p$  has its own constraints for each flexibility device and site as it is shown in the prosumer model.

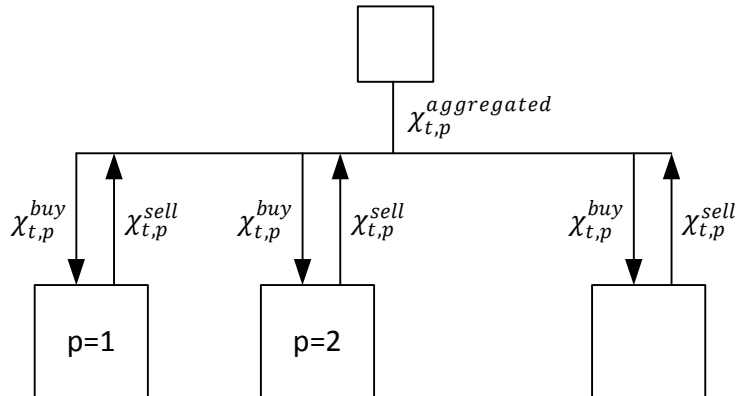


Figure 78 FO portfolio and their energy exchange

### 11.5 Distributed mathematical formulation

The aggregated flexibility services could be formulated as an exchange problem and the formulation presented by Boyd et al.[18]. The exchange problem is a special case of the sharing problem. This is one classic problem in the field of distributed optimization for large amount of data. In case of managing a large number of prosumers, the centralized optimization can be very computational costly. Therefore, it could be necessary to find distribution optimization techniques to find the optimal solution splitting the problem in sub-problems.

The generic distributed exchange problem is formulated as follows:

$$\begin{aligned} \min z &= \sum_p^P f_p(x_p) \\ \text{subject to } &\sum_p^P x_p = 0 \end{aligned} \tag{102}$$

With variables  $x_p$  as the flexibility decisions and  $f_p$  as the electricity cost function of each prosumer  $p$  including its flexibility costs  $\zeta_p^{flexibility}$  in the set P. This minimization function is subject to the energy balance equation. As Boyd et al. [18] states:

*“The goal is to solve the problem above in such a way that each term can be handled by its own processing element, such a thread or processor.”*



## 11.6 Objective functions in pilots

### 11.6.1 Spanish objective function

In this case, the flexibility provider is a single centralized energy storage (CES) units and the consumption costs are simpler than the German pilot. However, this pilot contains two flexibility buyers that could request flexibility simultaneously and the program has to ensure a correct performance.

This formulation is made generic for cases with multiple CES units  $b$ . Eq.(103) is the minimization cost function composed by the electricity costs and the flexibility costs. Eq. (104) and Eq. (105) are the terms that define the electricity buy and sell prices. Eq. (106) is the flexibility cost from CES units for charging and discharging the battery every period.

$$\min z = \sum_{b \in B} \left( \sum_{t \in T} (P_{t,b}^{buy} \cdot \sigma_{t,b}^{ch} - P_{t,b}^{sell} \cdot \sigma_{t,b}^{dis}) + \sum_{t \in T} \zeta_{t,b}^{flexibility} \right) \quad (103)$$

$$P_{t,b}^{buy} = P_{t,b}^{retail-buy} + P_{t,b}^{grid-buy} + P_{t,b}^{tax} \quad (104)$$

$$P_{t,b}^{sell} = P_{t,b}^{retail-sell} + P_{t,b}^{grid-sell} \quad (105)$$

$$\zeta_{t,b}^{flexibility} = P_{b,t}^{B,ch} \cdot \sigma_{b,t}^{ch} + P_{b,t}^{B,dis} \cdot \sigma_{b,t}^{dis} \quad (106)$$

The degradation costs should be included in Eq. (106) if the needed parameters are available.

This objective function is subject to the aggregated flexibility service constraints Eq. (99), Eq. (100) and Eq. (101). In this case, there are no more sites other than the CES. Therefore:

$$\chi_t^{buy} - \chi_t^{sell} = \sigma_{t,b}^{ch} - \sigma_{t,b}^{dis} \quad (107)$$

### 11.6.2 German objective function

The generic model introduced in the section 11.4 fits well for the German case as there are multiple prosumers willing to provide flexibility services to the DSO in collaboration with the CES.

## 11.7 DSO case study

### 11.7.1 Spanish case study

The Spanish pilot site has a single centralized energy storage (CES), and the DSO is one of the flexibility buyers. In Figure 79, the scheme of the MV network can be observed.

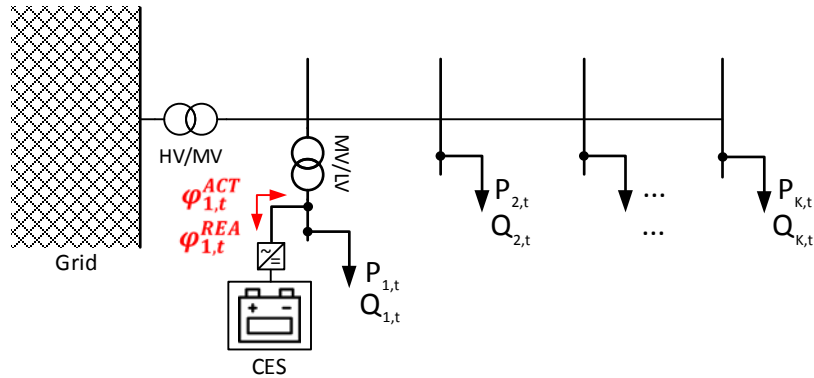


Figure 79: HV-MV pilot site grid scheme

#### 11.7.1.1 DSO flexibility request algorithm

The Spanish case study is based on the distribution grid and a centralized energy storage unit, CES. However, the algorithm is detailed in a generic approach since having more flexibility sources could be a feasible scenario. The problem to solve is mainly an AC-OPF, considering as the objective function the minimization of the total flexibility costs, but also considering the distribution network. In the following subsections the objective function is detailed, as well as all the restrictions related to AC-OPF.

This model is going to work separately from the aggregator algorithms presented above. Since, a completely different and new nomenclature is going to be used to write the algorithm. Below, the sets, the parameters and the variables are detailed.

#### Sets

K	Set of nodes of the MV distribution grid
L	Set of lines of the MV distribution grid

#### Parameters

$B_{i,k}$	Bus susceptance value between nodes $i \in K$ and $k \in K$ [S]
-----------	---

$C_t^{flexibilityDSO}$	Flexibility activation cost accorded between the FO and the DSO for period $t \in T$ [€/kW]
$G_{i,k}$	Bus transversal conductance value between nodes $i \in K$ and $k \in K$ [S]
$I_{i,t}$	Current at node $i \in K$ in period $t \in T$ [A]
$I_l^{MAX}$	Maximum allowed current at line $l \in L$
$P_{i,t}$	Total active power at node $i \in K$ in period $t \in T$ [kW]
$P_{i,t}^{gen}$	Generated active power at node $i \in K$ in period $t \in T$ [kW]
$P_{i,t}^{dem}$	Demanded active power at node $i \in K$ in period $t \in T$ [kW]
$P_{i,t}^{Flex,MAX}$	Maximum active power at node $i \in K$ in period $t \in T$ from the flexibility source. [kW]
$Q_{i,t}$	Total reactive power at node $i \in K$ in period $t \in T$ [kW]
$Q_{i,t}^{gen}$	Generated reactive power at node $i \in K$ in period $t \in T$ [kVAR]
$Q_{i,t}^{dem}$	Demanded reactive power at node $i \in K$ in period $t \in T$ [kVAR]
$Q_{i,t}^{Flex,MAX}$	Maximum reactive power at node $i \in K$ in period $t \in T$ from the flexibility source. [kVAR]
$\underline{S}_{i,t}$	Apparent power at node $i \in K$ in period $t \in T$ [kVA]
$U_{i,t}^{MAX}$	Maximum voltage at node $i \in K$ in period $t \in T$ [kV]
$U_{i,t}^{MIN}$	Minimum voltage at node $i \in K$ in period $t \in T$ [kV]
$U_{i,t}$	Voltage at node $i \in K$ in period $t \in T$ [kV]
$\underline{Y}_{ik}$	Admittance value for line $i - k$ [S]
$y_{1i,k}$	Transversal admittance value for line $i - k$ , first component [S].

$y_{2,i,k}$	Transversal admittance value for line $i - k$ , second component [S]
$\theta_{i,k,t}$	Voltage angle difference between nodes $i, k$ in period $t \in T$ [rad]
$\theta_{i,t}$	Voltage angle at node $i \in K$ in period $t \in T$ [rad]
$\theta_{i,t}^{MIN}$	Minimum allowed voltage angle at node $i \in K$ in period $t \in T$ [rad]
$\theta_{i,t}^{MAX}$	Maximum allowed voltage angle at node $i \in K$ in period $t \in T$ [rad]
$\underline{Z}_{i,k}$	Impedance value for line $i - k$ [ $\Omega$ ]

### Variables

$\varphi_{i,t}^{ACT}$	Total active power injected at node $i$ at time $t$ from flexibility sources [kW]
$\varphi_{i,t}^{REA}$	Total reactive power injected at node $i$ at time $t$ from flexibility sources [kVAr]
$\zeta^{flexibility}$	Total cost for utilizing internal flexibility [€]

#### 11.7.1.2 Objective Function

The objective function is to minimize the total flexibility costs function. This function is based on the price accorded between the FO and the DSO for period  $t \in T$ ,  $C_t^{flexibilityDSO}$ , and the total active power injected by the flexibility resource,  $\varphi_{i,t}^{ACT}$ .

$$\min z = \zeta^{flexibility} = \sum_{t \in T} \left( \sum_{i \in N} C_t^{flexibilityDSO} \cdot \varphi_{i,t}^{ACT} \right) \quad (108)$$

#### 11.7.1.3 Constraints

The constrains listed below ensure the compliance of the AC Power Flow equations and a correct system operation.

#### **AC Power Flow equations**

The AC power flow equations describe the power system network operating point in steady state and are based on complex phasor representation of voltage-current relationship at each node. The active  $P_{i,t}$  and reactive  $Q_{i,t}$  power flow node balance at

node  $i \in K$  in period  $t \in T$ , are formulated below Eq. (109) and Eq. (110). Then, Eq. (111) details the mathematical conversion to express  $\theta_{i,k,t}$  from the voltage angle at each node.

Since the pilot-site is considering sources connected at each node of the grid, the total active power at node  $i \in K$  in period  $t \in T$ ,  $P_{i,t}$ , considers the active power generated, the active power demanded and the active power injected by the flexibility source Eq. (112). Regarding the reactive power, Eq. (113) also considers the reactive power generated at node  $i \in K$  in period  $t \in T$  the reactive power consumed at node  $i \in K$  in period  $t \in T$  and the reactive power consumed or injected by the flexibility source.

Hence, from the admittance equations, it is possible to calculate the apparent flow injected depending on the voltages at all the grid nodes Eq. (114). Consider that the underscore means that the parameter or variable is a complex number. Whether the variable or the parameter is not written with an underscore, a real value is considered.

$$P_{i,t} = U_{i,t} \cdot \sum_{k=1}^K U_{k,t} \cdot [G_{i,k} \cdot \cos \theta_{i,k,t} + B_{i,k} \cdot \sin \theta_{i,k,t}] \quad (109)$$

$$Q_{i,t} = U_{i,t} \sum_{k=1}^K U_{k,t} [G_{i,k} \sin \theta_{i,k,t} - B_{i,k} \cos \theta_{i,k,t}] \quad (110)$$

$$\theta_{i,k,t} = \theta_{i,t} - \theta_{k,t} \quad (111)$$

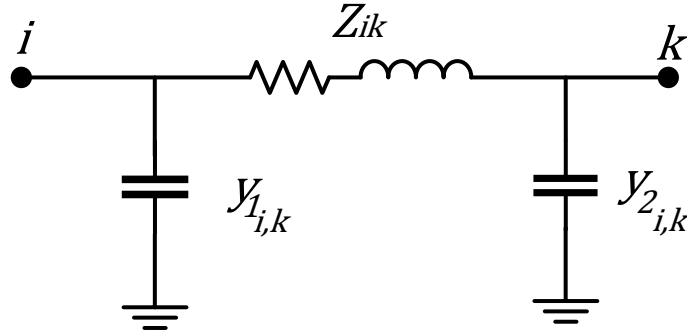
$$P_{i,t} = P_{i,t}^{gen} - P_{i,t}^{dem} + \varphi_{i,t}^{ACT} \quad (112)$$

$$Q_{i,t} = Q_{i,t}^{gen} - Q_{i,t}^{dem} + \varphi_{i,t}^{REA} \quad (113)$$

$$\underline{S}_{i,t} = \underline{U}_{i,t} \cdot \underline{I}_{i,t}^* = \underline{U}_{i,t} \cdot \left( \sum_{k=1}^K \underline{Y}_{i,k} \cdot \underline{U}_{k,t} \right)^* \quad (114)$$

### Line flow constraints

The pilot-site grid is a MV distribution grid, based on underground cables of the type RHZ1. Hence, the line flow constraints follow the  $\pi$ -model of the grid, since both the longitudinal impedance and the transversal capacitance of the line have to be considered. For the sake of clarity, the  $\pi$ -model is shown in Figure 80. Each line of the distribution network is limited to the maximum allowed line current,  $I_i^{MAX}$ .

Figure 80:  $\pi$ -model of the grid

$$\left| \frac{\underline{U}_{i,t} - \underline{U}_{k,t}}{\underline{Z}_{i,k}} + \underline{U}_{i,t} \cdot \underline{Y}_{1,i,k} \right| \leq I_l^{MAX} \quad (115)$$

$$\left| \frac{\underline{U}_{k,t} - \underline{U}_{i,t}}{\underline{Z}_{i,k}} + \underline{U}_{k,t} \cdot \underline{Y}_{2,i,k} \right| \leq I_l^{MAX} \quad (116)$$

### Active Power bounds by the flexibility source

The flexibility sources have both the possibility to inject or consume active power, according to up-regulation or down-regulation commands, to mitigate congestions along the distribution grid. Hence, each source is connected to a node  $i \in K$ , and each node will have an upper and lower active power limitation,  $-P_{i,t}^{Flex,MAX}$  and  $P_{i,t}^{Flex,MAX}$  in time period  $t \in T$ .

$$-P_{i,t}^{Flex,MAX} \leq \varphi_{i,t}^{ACT} \leq P_{i,t}^{Flex,MAX} \quad (117)$$

### Reactive Power bounds by the flexibility source

The flexibility sources connected at node  $i \in K$ , are able to inject or provide reactive power,  $\varphi_{i,t}^{REA}$ . Hence, this variable is restricted between  $-Q_{i,t}^{Flex,MAX}$  and  $Q_{i,t}^{Flex,MAX}$ .

$$-Q_{i,t}^{Flex,MAX} \leq \varphi_{i,t}^{REA} \leq Q_{i,t}^{Flex,MAX} \quad (118)$$

The apparent power limitation  $S$  is not considered in this mathematical formulation. The active and reactive power limitations are considered as technology free. That means that the total amount of reactive and reactive power in each node is limited, but not considering each technology itself. Hence, some sources can provide  $\varphi_{i,t}^{ACT}$  like PV and

batteries and, other sources provide  $\varphi_{i,t}^{REA}$  like DR and EV. The DSO does not consider the technology itself and its capacity limitations. The FO is the entity responsible for that.

### **Voltage Magnitude**

In the AC-OPF algorithm, the nodal voltage is restricted by an upper limit and a lower bound to guarantee the correct operation of the system. In the flexibility requests calculation algorithm, the DSO contracts the flexibility services to prevent and mitigate congestions along the distribution grid. Hence, the DSO aims to minimize the congestion risks throughout the day, which can vary. For this reason, the voltage upper and lower bounds parameters consider also the time period  $t \in T$ , resulting in the following parameters,  $U_{i,t}^{MIN}$  and  $U_{i,t}^{MAX}$ . These parameters will be provided by the DSO based on the level of risk they want to assume on congestions along the network.

$$U_{i,t}^{MIN} \leq U_{i,t} \leq U_{i,t}^{MAX} \quad (119)$$

### **Voltage angle**

To improve the solvability of the problem, the voltage angle constraint is included in this model. The voltage angle at node  $i \in K$ , at time  $t \in T$ ,  $\theta_{i,t}$ , is limited between the minimum value and the maximum,  $\theta_{i,t}^{MIN}$  and  $\theta_{i,t}^{MAX}$  respectively.

$$\theta_{i,t}^{MIN} \leq \theta_{i,t} \leq \theta_{i,t}^{MAX} \quad (120)$$

## **11.7.2 German case study**

The German DSO already has in place an algorithm to forecast the electricity consumption for the day-ahead and they are working in the FR formulation.

## **11.8 BRP case study**

### **11.8.1 Spanish case study**

The Spanish BRP already has in place an algorithm to forecast the hour-ahead consumption and its working in the FR formulation.

## 12 Conclusions

In this part of the report D5.4, advanced operational models of flexibility resources are presented as a complement to D5.3A, where the general simplified models are presented. Chapter 3 detail the battery operational models which includes degradation due to cycle and calendar ageing. Also piecewise linearized efficiency of battery charging and discharging power are detailed. The constraints related to ON-OFF control and charging with minimum and maximum power limits for EV charge points and charging stations are explained in chapter 4. A detailed models of thermal loads which includes EWH and space heating are presented in chapter 5 and 6. The overall framework of optimization and the variable fixing issues and their solution approaches are presented in chapter 7 and 8. Chapter 9 discusses about pilot structures for different pilots. The objective functions of prosumer services are explained in chapter 10. Chapter 11 presents the aggregated flexibility services, which can be offered to external agents on their requests. Chapter 12 concludes the report summary. This report documents the detailed models that will be implemented in integrated INVADE platform. The user manual for the offline version of flexibility algorithm and the list of sets, parameters and variable used in the mathematical formulations are included in the appendix.

.



## References

1. Lloret, P., et al., *Overall INVADE architecture*, in *D 4.1*. 2017: INVADE H2020 project.
2. Lloret, P. and P. Olivella, *INVADE architecture of pilots*, in *D4.2*. 2017: INVADE H2020 project.
3. Bødal, E.F., et al., *Challenges in distribution grid with high penetration of renewables*, in *D 5.1*. 2017: INVADE H2020 project.
4. Korpås, M., et al., *Methods for assessing the value of flexibility in distribution grids*, in *D 5.2*. 2017: INVADE H2020 project.
5. Ottesen, S.Ø., et al., "*Simplified Battery operation and control algorithm*", in *D5.3*. 2017: INVADE H2020 project.
6. Gjerløw, P., *Pilot Specifications (version 3)*, in *D 10.1*. 2018: INVADE H2020 project.
7. Lloret, P. and P. Olivella, *Overall INVADE architecture final*, in *D4.3*. 2018: INVADE H2020 project.
8. Xu, B., et al., *Factoring the Cycle Aging Cost of Batteries Participating in Electricity Markets*. IEEE Transactions on Power Systems, 2018. **33**(2): p. 2248-2259.
9. He, G., et al., *An intertemporal decision framework for electrochemical energy storage management*. Nature Energy, 2018. **3**(5): p. 404-412.
10. Atwa, Y.M. and E.F. El-Saadany, *Optimal Allocation of ESS in Distribution Systems With a High Penetration of Wind Energy*. IEEE Transactions on Power Systems, 2010. **25**(4): p. 1815-1822.
11. Mohseni, A., et al., *The application of household appliances' flexibility by set of sequential uninterruptible energy phases model in the day-ahead planning of a residential microgrid*. Energy, 2017. **139**: p. 315-328.
12. Mouli, G.R.C., et al., *Integrated PV Charging of EV Fleet Based on Energy Prices, V2G and Offer of Reserves*. IEEE Transactions on Smart Grid, 2018: p. 1-1.
13. Bacher, P. and H. Madsen, *Identifying suitable models for the heat dynamics of buildings*. Energy and Buildings, 2011. **43**(7): p. 1511-1522.
14. Bacher, P., et al., *Short-term heat load forecasting for single family houses*. Energy and Buildings, 2013. **65**: p. 101-112.
15. Gomez, J.A. and M.F. Anjos, *Power capacity profile estimation for building heating and cooling in demand-side management*. Applied Energy, 2017. **191**: p. 492-501.
16. Suganthi, L. and A.A. Samuel, *Energy models for demand forecasting—A review*. Renewable and Sustainable Energy Reviews, 2012. **16**(2): p. 1223-1240.
17. Olivella-Rosell, P., et al., *Local Flexibility Market Design for Aggregators Providing Multiple Flexibility Services at Distribution Network Level*. Energies, 2018. **11**(4): p. 822.
18. Boyd, S., et al., *Distributed Optimization and Statistical Learning via the Alternating Direction Method of Multipliers*. Foundations and Trends® in Machine Learning, 2011. **3**(1): p. 1-122.

## 13 Appendix: Offline software testing manual

### 13.1 Introduction

This document provides the procedure to run a test case, placement of relevant input data and their file structure for a test case and placement of results provided by the optimization. The second part of the document explains about building a specific model configuration built from the input data automatically. Further the last section of the document details the contents of the input and output data files.

### 13.2 Building a test case and running

The offline model is provided in a root folder named “*Invade*” which is a copy of the bit bucket repository. It contains all relevant working models and their old versions which are not in use. (The repository will be cleaned and all unnecessary files will be removed later after the development work is completed)

In the “*Invade*” folder, as shown in the Figure 81 there is a subfolder named “*master\_RH*” where the file for execution “*Offline\_example.py*” (“*Invade/master\_RH/Offline\_example.py*”) placed.

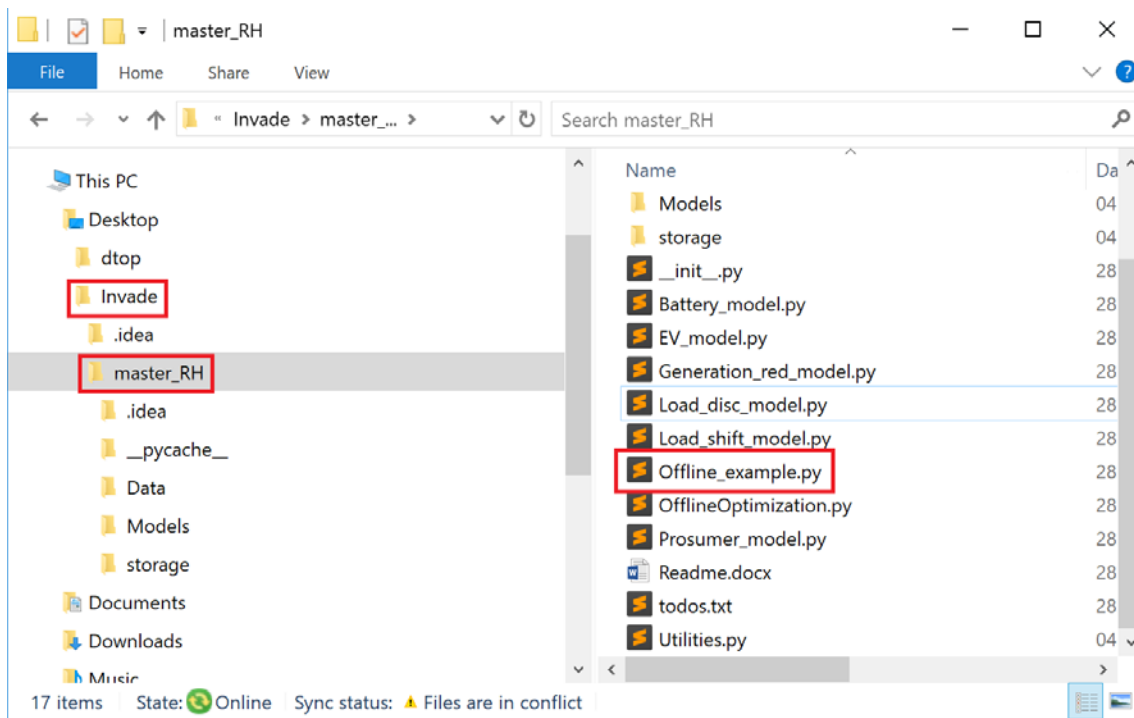


Figure 81: Folder structure of root folder

The same file has the path for input data (“*Invade/master\_RH/Data/TestCaseSite1*”) and the path for output destination folder (“*Invade/master\_RH/Data/Output*”) as shown in the Figure 82. The folder structure is shown in the Figure 83. These paths and folder names can be changed as per user convenience.

```

7 ok=True # to print modelling steps if true
8
9 TestCaseFolder=Path(str(os.getcwd())+'/Data/TestCaseSite1')#This is t
10 # This folder contains input excel files.
11 solution=CallOptimization(TestCaseFolder, fromDateTime='2018-05-12T00
12
13 #Report the result to excel files named Site_x_control_signals.xlsx a
14
15 StoredPath = str(Path(os.getcwd() + '/Data/Output'))
16 if solution.ModeType == 'Zero':
17     for i in solution.g:
18         report = ReportSite(solution.g[i], str(i),StoredPath)

```

Figure 82: Path details for input data for optimization (marked in RED (Top)) and output data from the optimization (marked in GREEN (Bottom))

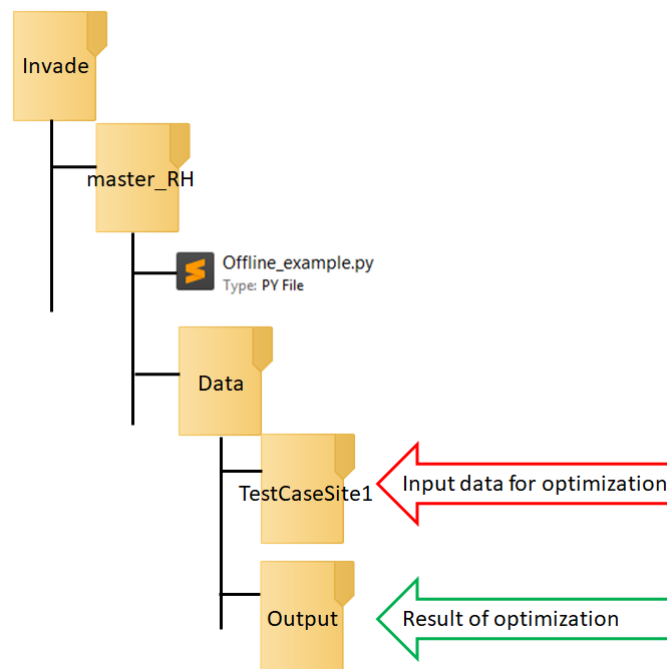


Figure 83. Folder structure for input data and output result from the optimisation

### 13.3 Solver selection and MIP gap input

```
2 from pyomo.environ import *
3 def PrintWhere(ok,s):
4     if ok:
5         print('    Parsing ',s)
6
7
8 def Model_resolution(instance):
9     ### RUNNING MODEL ###
10    import pyutilib
11    pyutilib.subprocess.GlobalData.DEFINE_SIGNAL_HANDLERS_DEFAULT = False
12
13    TransformationFactory('gdp.bigm').apply_to(instance)
14
15    optimizer = pyomo.opt.SolverFactory('gurobi') # Call the Solver (tested)
16    print('solvinggg')
17    optimizer.options['mipgap'] = 10
18    # optimizer.options['timeLimit']=10
19
20    instance.preprocess()
21    instance.write('junk.lp', io_options={'symbolic_solver_labels': True})
22    results = optimizer.solve(instance, tee=False) # , tee=True or False
```

Figure 84: Solver and MIP gap configuration

The user can change the solver and MIP gap in the file **“Utilities.py”** (*Invade/master\_RH/Utilities.py*) as shown in the Figure 84. The given example shows a configuration with a commercial solver ‘Gurobi’ (encapsulated in red). The user can use different solvers for example ‘cplex’, ‘ipopt’ or ‘glpk’ which every is available in their computation and execution platform. The MIP gap necessary for the solution can be configured as per the requirement. The given example shows a configuration with MIP gap = 10 (encapsulated in green).

### 13.4 Automatic model building

The model building is taken care by the input data structure. The input data is organised in a folder and subfolder structure to represent the tree structure of the resource arrangement in a given test case.

At present there are 3 different types are considered, namely 1. Battery (Storage), 2. Charge Point (CP) and 3. PV (Generation).

### 13.5 Site implementation

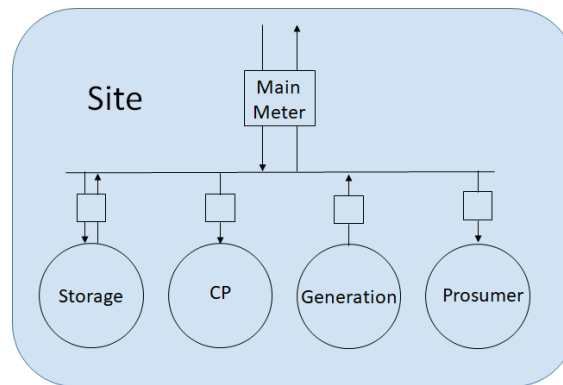


Figure 85. Site implementation

A site is defined as a set of resources under one electricity price structure. For example in the given Figure 85, the site consists of three resources (Storage, CP and Generation). The prosumer part represents the inflexible loads in the site and electricity price information. The input data structure for the site configuration in Figure 85 is as shown in the Figure 86.

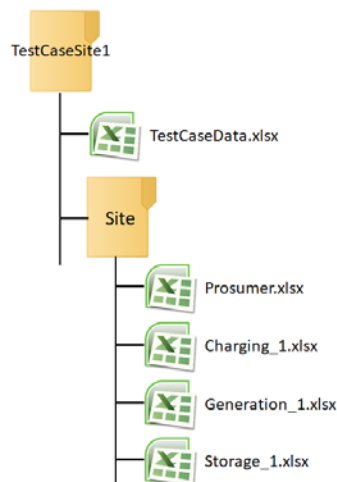


Figure 86. Input data structure to configure the model for a test case represented in Figure 85

The input data files at site level “*TestCaseData.xlsx*” contains the information to build constraints at site level. And each input data files inside the “*site*” folder contains the details corresponding to each resource in the site. A detailed description of input files are given in the further sections.

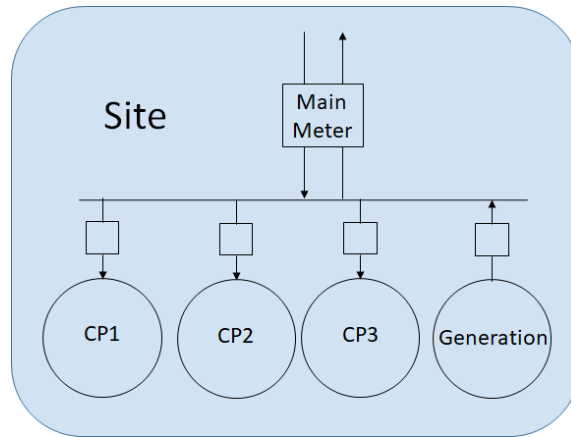


Figure 87. Site configuration without inflexible load.

A site may have any number and any combination of resources with or without inflexible loads. For example, the site shown in the figure 5, has three CPs and a Generation without inflexible load. The input folder structure to configure the site configuration given in the Figure 87 is as shown in the Figure 88. It is to be noted that the configuration still has a prosumer data in the input file “Prosumer.xlsx” which contains the electricity price information and “zero” values for the inflexible loads as the inflexible load parameter is active in the model.

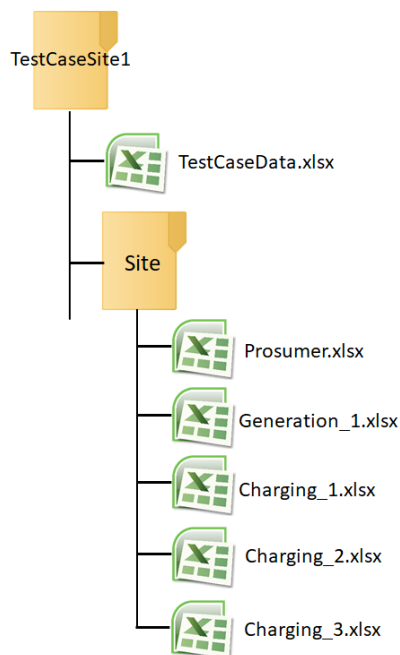


Figure 88. Input data structure to configure the model for a test case represented in Figure 87

In every test case **prosumer data** is mandatory as it has electricity price information.

### 13.6 Input data file structure

The section explains the data arrangement inside the excel files corresponding to different resources, inflexible load and electricity prices and general information applicable to the site.

#### 13.6.1 “TestCaseData.xlsx”

The general information about the site is provided to the optimisation algorithm through the file “TestCaseData.xlsx”. This file is placed at the root input folder (In the above example cases ‘Invade/master\_RH /Data/TestCaseSite1’). The file content and their description are listed in the following Table 22. The Figure 89 shows the arrangement of “TestCaseData.xlsx” and site information inside the input data folder “TestCaseSite1”

**Table 22: Description of contents in the file “TestCaseData.xlsx”**

Column	Content	Description
A		Name of the folder containing resource details inside a site as shown in the Figure 8.
B	<b>CapacityConstraintAppliesToResourceTypes</b>	The site level capacity constraint that applicable for the type of resources at sight level. The possible values at present is “All Resource Types”
C	<b>Capacity constraint resource Key</b>	Capacity constraint resource Key – This information is derived from the INVADE platform. It is not used in the offline test.
D	<b>init_n</b>	Length of time period. Present possible value is “FifteenMinutes”
E	<b>init_p_vat</b>	Parameter that adds VAT to the amount bought $P^{VAT}$ It is mentioned in two files “TestCaseData.xlsx” and “Prosumer.xlsx” as platform provides in both places. The model validate only in the “Prosumer.xlsx”

	A	B	C	D	E
1		CapacityConstraintAppliesToResourceTypes	CapacityConstraintAppliesToResourceTypesKey	init_n	init_p_val
2	Site	All Resource Types	84d5da8d-02e4-4267-be2e-9754136fdcc0	FifteenMinutes	0,25
3					

Figure 89. Site information in the input file “TestCaseData.xlsx”

### 13.6.2 Site configuration and resource information

A site may have any number of resource among the three types 1. Battery (Storage) 2. Charge Point (CP) and 3. PV (Generation). The algorithm understands the type of resource from the file name.

The common file name format for all types of resources is “**ResourceName\_x.xlsx**”, where “\_x” in the file name denotes the resource number.

The possible resource names are

1. “Storage” – for battery
2. “Charging” – for Charge points
3. “Generation”- for PVs

The resource number represents the number among set of same type of resources in the specific site. No two resources of same type in a site can have same resource number. (The same file name to multiple file will restrict this conflict)

For example, if a battery is present in a site, the battery details are present in the input excel file with name “Storage\_1.xlsx”.

The description of each input file is given the following sections.



### 13.6.3 Prosumer.xlsx

The “Prosumer.xlsx” input file contains the site level information including price related information. Each site will have only one “Prosumer.xlsx” file. And therefore it is not numbered.

The description of each column is provided in the Table 23 as well as in the first row of the template file as shown in the Figure 90. The algorithm skips the first row while reading file. The second row serves as the identification string for parsing input data and from the third row onwards the numerical/string values of input parameters are considered.

	A	B	C	D	E	F	G	H
		Maximum export capacity	Maximum import capacity	Limitation of basis for peak fee	Periods per hour	Price at energy part of grid contract for buying electricity in period t	Price at energy part of grid contract for buying electricity in cases with subscribed power in period in period t if bought electricity is above subscribed level	Price at energy part of grid contract for buying electricity in cases with subscribed power in period t if bought electricity is below subscribed level
1		init_exp_cap	init_imp_cap	init_m	init_n	init_p_grid_buy	init_p_grid_buy_high	init_p_grid_buy_low
2								
3	Site	100	100	1	FifteenMinutes			
4	0					0,678250865		1
5	1					0,678250865		1

Figure 90. Image of columns in the input data file “Prosumer.xlsx”

Table 23: Description of columns in the input data file “Prosumer.xlsx”

Column	Content	Description
A		Should be same as the number of time periods in other input files – Do not change the content
B	<b>init_exp_cap</b>	Maximum export capacity [average kW] $X^{exp-cap}$
C	<b>init_imp_cap</b>	Maximum import capacity [average kW] $X^{imp-cap}$
D	<b>init_m</b>	Limitation of basis for peak fee ( $M$ )
E	<b>init_n</b>	Minutes per time Periods. The possible value in the present version “FifteenMinutes”. <b>Do not change</b> . It is mentioned in two files “TestCaseData.xlsx” and “Prosumer.xlsx” as platform provides in both places. The model validate only in the “Prosumer.xlsx”
F	<b>init_p_grid_buy</b>	Price at energy part of grid contract for buying electricity in period t $P_t^{grid-buy}$
G	<b>init_p_grid_buy_high</b>	Price at energy part of grid contract for buying electricity in cases with subscribed power in period in period t if bought electricity is above subscribed level $P_t^{grid-buy-high}$
H	<b>init_p_grid_buy_low</b>	Price at energy part of grid contract for buying electricity in cases with subscribed power in period in period t if bought electricity is below subscribed level $P_t^{grid-buy-low}$
I	<b>init_p_grid_sell</b>	Price at energy part of grid contract for selling electricity in period t $P_t^{grid-sell}$

J	<b>init_p_peak</b>	Price at grid contract for peak fee $p^{peak}$ (As of now it is not used in the objective function. Do not change. Reserved for future use)
K	<b>init_p_retail_buy</b>	Price at energy part of retail contract for buying electricity in period t $P_t^{retail-buy}$
L	<b>init_p_retail_sell</b>	Price at energy part of retail contract for selling electricity in period t $P_t^{retail-sell}$
M	<b>init_p_tax</b>	Sum price for all taxes that are related to buying electricity in period t $P_t^{tax}$ (Only one value is provided in the input, but a time series with same value is created inside algorithm)
N	<b>init_p_vat</b>	Parameter that adds VAT to the amount bought $P^{VAT}$ It is mentioned in two files “TestCaseData.xlsx” and “Prosumer.xlsx” as platform provides in both places. The model validate only in the “Prosumer.xlsx”
O	<b>observed_values</b>	Actual observed inflexible load from prosumer. (As of now it is not used in the objective function. Do not change. Reserved for future use)
P	<b>teXX</b>	Forecasted inflexible load from prosumer $W_{l,t}^{load}$

### 13.6.4 Storage\_x.xlsx

The “Storage\_x.xlsx” input file contains the battery input parameters.

The description of each column is provided in the Table 24 as well as in the first row of the template file as shown in the Figure 91. The algorithm skips the first row while reading file. The second row serves as the identification string for parsing input data and from the third row onwards the numerical values of input parameters are considered. Table 24 describes each input column of the input file Storage\_x.xlsx. The values of the period independent parameters are provided in the last row with a parsing string “Storage” as shown in the Figure 91

	A	B	C	D	E	F	G	H	I	J	K	L	M
t in periods	Not used	Initial SOC value	Efficiency parameter for charging storage unit b - Including battery and inverter	Efficiency parameter for discharging storage unit b - Including battery and inverter	Maximum state of charge allowed for battery b	Minimum state of charge allowed for battery b	Price for charging battery unit b at period t	Price for discharging battery unit b at period t	Maximum charging power allowed for battery b	Maximum discharging power allowed for battery b	Threshold in battery unit b charging process	Threshold in battery unit b discharging process	
	Charging energy	EnergyLevel	init_a_ch	init_a_dis	init_o_max	init_o_min	init_p_b_ch	init_p_b_dis	init_q_ch	init_q_dis	init_s_ch	init_s_dis	
0	0	179											
1	0	179											
2	0	179											
3	0	179											
4	0	179											
5	0	179											
6	0	179											
7	0	179											
89	0	179											
90	0	179											
91	0	179											
92	0	179											
93	0	179											
94	0	179											
95	0	179											
96	0	179											
97	0	179											
98	0	179											
99	Storage		0,95	0,95	200	0	0,01	0,01	100	100	0,8	0,1	
100													

Figure 91. Image of columns in the input data file “Storage\_x.xlsx”

Table 24: Description of columns in the input data file “Storage\_x.xlsx”

Column	Content	Description
A		t in periods – Should be same as the number of time periods in other input files – Do not change the content.
B	<b>ChargingEnergy</b>	Not used in the algorithm. For future use with receding horizon – Do not change
C	<b>EnergyLevel</b>	Fill this column with initial SOC for all rows. Considered as a Time series for future use with receding horizon.
D	<b>init_a_ch</b>	Efficiency parameter for charging storage unit b - Including battery and inverter [p.u.] $A_b^{ch}$
E	<b>init_a_dis</b>	Efficiency parameter for discharging storage unit b - Including battery and inverter [p.u.] $A_b^{dis}$
F	<b>init_o_max</b>	Maximum state of charge allowed for battery b [p.u.] $O_b^{max}$
G	<b>init_o_min</b>	Minimum state of charge allowed for battery b [p.u.] $O_b^{min}$
H	<b>init_p_b_ch</b>	Price for charging battery unit b at period t (Not in D5.3. But implemented as part of simple degradation model.)
I	<b>init_p_b_dis</b>	Price for discharging battery unit b at period t (Not in D5.3. But implemented as part of simple degradation model)
J	<b>init_q_ch</b>	Maximum charging power allowed for battery b [p.u.] $Q_b^{ch}$
K	<b>init_q_dis</b>	Maximum discharging power allowed for battery b [p.u.] $Q_b^{dis}$
L	<b>init_s_ch</b>	Threshold in battery unit b charging process [p.u.] $S_b^{ch}$
M	<b>init_s_dis</b>	Threshold in battery unit b discharging process [p.u.] $S_b^{dis}$

**Note:**

1. The optimization algorithm considers  $O_b^{min}$  as targeted SOC at the last time period in the horizon.
2. The Initial SOC (state of charge) of the battery has to be filled in all the rows of column C. Also the column is reserved for future rolling horizon implementation.

**13.6.5 Charging\_x.xlsx**

The “Charging\_x.xlsx” contains the charge point input parameters.

The description of each column is provided in the Table 25 as well as in the first row of the template file as shown in the Figure 92. The algorithm skips the first row while reading file. The second row serves as the identification string for parsing input data and from

the third row onwards the numerical values of input parameters are considered. Table 25 describes each input column of the input file *Charging\_x.xlsx*. The values of the period independent parameters are provided in the last row with a parsing string “Storage” as shown in the Figure 92

Figure 92. Image of columns in the input data file “Charging\_x.xlsx”

Table 25: Description of columns in the input data file “Charging\_x.xlsx”

Column	Content	Description
A		t in periods – Should be same as the number of time periods in other input files – Do not change the content
B	<b>ChargingEnergy</b>	Not used in the algorithm. For future use with receding horizon – Do not change
C	<b>ChargingPointState</b>	Not used in the algorithm. For future use with receding horizon – Do not change
D	<b>ForecastedChargingPointState</b>	Not in D5.3 status as 10 20 30. Forecasted charging point status
E	<b>Q_cs_ch</b>	Maximum capacity constraint for charging station Not mentioned in 5.3
F	<b>W_cp</b>	Baseline charging schedule for EV x in period t [kWh] $W_{v,t}^{EV}$
G	<b>init_cp_q_ch_max</b>	Maximum charging power allowed for EV unit x $Q_v^{EV,ch}$
H	<b>init_cp_q_ch_min</b>	Minimum discharging power allowed for EV unit x $Q_v^{EV,dis}$
I	<b>init_p_cp_ns</b>	Price for non-supplying 1 kWh of the expected charging demand of EV unit x $p_v^{EV,NS}$

J	<b>init_p_cp_shift</b>	Price for shifting charging for EV unit x with 1 kWh $P_{v,t}^{EV}$
---	------------------------	---

### 13.6.6 Generation\_x.xlsx

The “*Generation\_x.xlsx*” contains the Generation unit (PV) input parameters.

The description of each column is provided in the Table 26 as well as in the first row of the template file as shown in the Figure 93. The algorithm skips the first row while reading file. The second row serves as the identification string for parsing input data and from the third row onwards the numerical values of input parameters are considered. Table 26 describes each input column of the input file *Generation\_x.xlsx*.

	A	B	C	D
1		Price for reducing production for generator unit g in period t	Production (Actual)	Forecasted production
2		<b>init_p_gen_r</b>	<b>observed_values</b>	<b>teXX</b>
3	<b>Generation</b>	0,5		
4	<b>0</b>		0	0,0044236
5	<b>1</b>		0	0,0044236
6	<b>2</b>		0	0,0044236

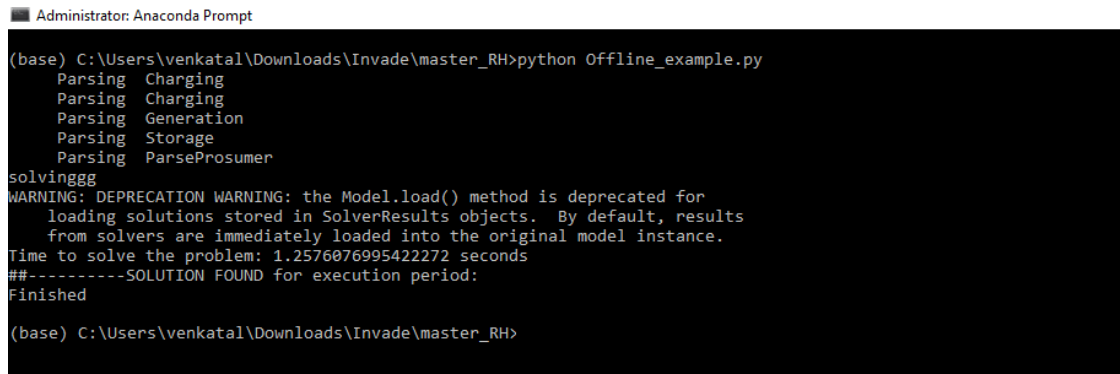
Figure 93. Images of columns in the input data file “*Generation\_x.xlsx*”

Table 26: Description of columns in the input data file “*Generation\_x.xlsx*”

Column	Content	Description
A		t in periods – Should be same as the number of time periods in other input files – Do not change the content
B	<b>init_p_gen_r</b>	Price for reducing production for generator unit g in period t $P_{g,t}^G$
C	<b>observed_values</b>	Not used in the algorithm. For future use with receding horizon – Do not change
D	<b>teXX</b>	Forecasted production $W_{g,t}^{prod}$

### 13.7 Running a test case

The test case built can be run by simply executing the “*Offline\_example.py*” in a “python” environment as shown on the Figure 94. The output files will be generated in the output folder path mentioned in the same file.



```

Administrator: Anaconda Prompt

(base) C:\Users\venkatal\Downloads\Invade\master_RH>python Offline_example.py
Parsing Charging
Parsing Charging
Parsing Generation
Parsing Storage
Parsing ParseProsumer
solvinggg
WARNING: DEPRECATION WARNING: the Model.load() method is deprecated for
loading solutions stored in SolverResults objects. By default, results
from solvers are immediately loaded into the original model instance.
Time to solve the problem: 1.2576076995422272 seconds
##-----SOLUTION FOUND for execution period:
Finished

(base) C:\Users\venkatal\Downloads\Invade\master_RH>

```

Figure 94. Runtime environment and result.

## 13.8 Output file format

The optimization algorithm produces two types of output files namely

1. “Site\_x\_control\_signals.xlsx”
2. “Site\_x\_prosumer\_costs\_and\_energy\_balance.xlsx”

The “Site\_x\_control\_signals.xlsx” file contains the control signals to be sent to the resources. The other file “Site\_x\_prosumer\_costs\_and\_energy\_balance.xlsx” contains the details related to the quarterly and hourly cost related every resources. The following sections will describe the format of each output files.

### 13.8.1 Site\_x\_control\_signals.xlsx

In “Site\_x\_control\_signals.xlsx” file, the control signal for each resource for every time period is listed. The control signals are listed in the following resource order, Charge points (*Charging\_x*), PV (*Generation\_x*) and Battery (*Storage\_x*).

For charge points, the power regulation for every charge point is provided under the column name “EVChargingPowerRegulation\_1”. The “OptimalCapacityRegulation\_1” provides the power limit of the charging station with which the charging point x is associated with. (Do not read “OptimalCapacityRegulation\_1” column, as Site Asset group is not yet implemented - reserved for future use)

After listing control signal related to all charging points, the PV unit control signals are listed under the column name “ProductionPowerRegulation\_x”

Battery charging and discharging schedule are listed after the control signal last PV unit in the site. The charging and discharging schedule for the batteries are listed with the

column names “ChargingPowerRegulation\_x” and “DischargingPowerRegulation\_x”. Table 27 describes the columns in the output data file “Site\_x\_control\_signals.xlsx”

**Table 27: Description of columns in the output data file “Site\_x\_control\_signals.xlsx”**

Column name	Description
<b>t</b>	Time period t
<b>EVChargingPowerRegulation_Charging_x</b>	The Energy delivery schedule at the charge point <i>Charging_1</i>
<b>OptimalCapacityRegulation_Charging_x</b>	Do not read this column reserved for future use
<b>ProductionPowerRegulation_Generation_x</b>	Power schedule for Generation_x
<b>ChargingPowerRegulation_Storage_x</b>	Storage_x charging power
<b>DischargingPowerRegulation_Storage_x</b>	Storage_x discharging power

### 13.8.2 Site\_x\_prosumer\_costs\_and\_energy\_balance.xlsx

In the second file “Site\_x\_prosumer\_costs\_and\_energy\_balance.xlsx”, all costs and their comparison before and after optimization are listed. This file has reports in five different sheets. They are

1. Sheet 1 – “quarterly\_energy\_balance”
2. Sheet 2 – “hourly\_energy\_balance”
3. Sheet 3 – “total\_cost”
4. Sheet 4 – “quarterly\_cost”
5. Sheet 5 – “hourly\_cost\_with\_SP”

Their content and meaning are listed in the further subsections.

#### 13.8.2.1 “quarterly energy balance”

In this sheet, the energy information for every time period (at present the time period resolution is 15 minutes) before and after optimization are given. The energy information includes, main meter level and resource level details. The following Table 28 describes the meaning of each column reported. Table 28 describes the columns in the sheet “quarterly\_energy\_balance” in the output data file “Site\_x\_prosumer\_costs\_and\_energy\_balance.xlsx”



The unoptimized and optimized baseline consumption of flexible resources are listed next to each other. This listing starts after the column name “eb\_inflex\_load”, which lists inflexible load. All the members in one type of resource are listed in the incremental order. The order of resource type in the listing is as follows

1. Charging\_x
2. Generation\_x
3. Storage\_x

**Table 28: Description of columns in the sheet “quarterly\_energy\_balance” in the output data file “Site\_x\_prosumer\_costs\_and\_energy\_balance.xlsx”**

Column name	Description
<b>t</b>	Time period t
<b>energy_baseline</b>	Aggregated energy of all resources (main meter level)
<b>energy_buy_base</b>	Amount of electricity would have been bought in period t [kWh] $\chi_t^{buy}$ without optimization
<b>energy_sell_base</b>	Amount of electricity would have been sold in period t [kWh] $\chi_t^{sell}$ before optimization
<b>energy_buy</b>	Amount of electricity will be bought in period t [kWh] $\chi_t^{buy}$ after optimization
<b>energy_sell</b>	Amount of electricity will be sold in period t [kWh] $\chi_t^{sell}$ after optimization
<b>eb_inflex_load</b>	Prosumer Inflexible load $W_{l,t}^{load}$
<b>eb_EV_baseline_CS_Charging_x</b>	Baseline charging schedule for EV x in period t [kWh] $W_{v,t}^{EV}$
<b>eb_EV_CS_Charging_x</b>	Optimized charging schedule for EV x in period t
<b>eb_pv_baseline_Generation_x</b>	(Forecasted) Baseline production $W_{g,t}^{prod}$ for PV unit x
<b>eb_pv_Generation_x</b>	Optimized schedule for PV unit x in period t
<b>eb_charge_bat_Storage_x</b>	Optimized Charging schedule for Battery unit x in period t
<b>eb_discharge_bat_Storage_x</b>	Optimized Discharging schedule for Battery unit x in period t

### 13.8.2.2 “hourly energy balance”

In this sheet, the energy information for at hourly resolution before and after optimization are given. The energy information includes only main meter level details. The energy exchange details provides values before and after optimization including the details of energy above and below the level of “Limitation of basis for peak fee ( $M$ )”. The following table describes the meaning of each column reported. The following Table 29 describes the meaning of each column reported. Table 29 describes the columns in the sheet



“hourly\_energy\_balance” in the output data file  
 “Site\_x\_prosumer\_costs\_and\_energy\_balance.xlsx”

**Table 29: Description of columns in the sheet “hourly\_energy\_balance” in the output data file  
 “Site\_x\_prosumer\_costs\_and\_energy\_balance.xlsx”**

Column name	Description
<b>t_h</b>	Time period
<b>energy_buy_h_base</b>	Unoptimized total amount of energy buy
<b>energy_buy_low_base</b>	Unoptimized energy imported below “Limitation of basis for peak fee ( $M$ ) without optimization.
<b>energy_buy_high_base</b>	Unoptimized energy imported above “Limitation of basis for peak fee ( $M$ ) without optimization.
<b>energy_sell_base</b>	Unoptimized total amount of energy sell
<b>energy_buy</b>	Optimized amount of total energy buy
<b>energy_buy_low</b>	Optimized amount of energy imported below “Limitation of basis for peak fee ( $M$ )”
<b>energy_buy_high</b>	Optimized amount of energy imported above “Limitation of basis for peak fee ( $M$ )”
<b>energy_sell</b>	Optimized amount of total energy sell

### 13.8.2.3 “total\_cost”

In this sheet, the total cost of energy before and after optimization, and the sum of cost of flexibility of all resources are given. The values give are for the whole optimization horizon. The following Table 30 describes the meaning of each column reported. Table 30 describes the columns in the sheet “total\_cost” in the output data file “Site\_x\_prosumer\_costs\_and\_energy\_balance.xlsx”.

**Table 30: Description of columns in the sheet “total\_cost” in the output data file  
 “Site\_x\_prosumer\_costs\_and\_energy\_balance.xlsx”**

Column name	Description
<b>Total electricity cost</b>	Overall optimized cost of energy at main meter level
<b>Total flexibility cost</b>	Aggregated cost of flexibility of all resources.
<b>Total cost baseline</b>	Unoptimized overall cost of energy at main meter level.

### 13.8.2.4 “quarterly\_cost”

In this sheet, the costs are calculated for energy exchange with grid, cost of flexibility and for the individual time periods.

The flexibility cost of flexible resources are listed after the column name “grid\_sell”, which lists Optimized energy cost with price ( $P_t^{grid-buy}$ ) at energy part of grid contract for buying electricity in period t. All the members in one type of resource are listed in the incremental order. The order of resource type in the listing is as follows

1. Charging\_x
2. Generation\_x
3. Storage\_x – Charging
4. Storage\_x – Discharging

Table 31 describes the columns in the sheet “quarterly\_cost” in the output data file “Site\_x\_prosumer\_costs\_and\_energy\_balance.xlsx”

**Table 31: Description of columns in the sheet “quarterly\_cost” in the output data file “Site\_x\_prosumer\_costs\_and\_energy\_balance.xlsx”**

Column name	Description
<b>grid_sell_base</b>	Unoptimized energy selling cost to grid for the period t
<b>cost_buy_total</b>	Total optimized cost including energy and cost of flexibility (Objective function value)
<b>retail_buy</b>	Optimized energy cost with price ( $P_t^{retail-buy}$ ) at energy part of retail contract for selling electricity in period t
<b>grid_buy</b>	Optimized energy cost with price ( $P_t^{grid-buy}$ ) at energy part of grid contract for buying electricity in period t (Power subscription cost is not included as it is calculated for deviation in hourly values)
<b>taxes</b>	Tax part of the cost.
<b>cost_sell</b>	Sum of retail_sell and grid_sell
<b>retail_sell</b>	Optimized energy cost with price ( $P_t^{retail-sell}$ ) at energy part of retail contract for selling electricity in period t
<b>grid_sell</b>	Optimized energy cost with price ( $P_t^{grid-sell}$ ) at energy part of retail contract for selling electricity in period t
<b>cost_EV_shift_Charging_x</b>	Cost for shifting EV charging associated with charge point Charging_x

<b>cost_pv_Generation_x</b>	Cost of reducing Generation associated with Generation_x.
<b>cost_charge_batteryStorage_x</b>	Cost for charging battery associated with Storage_x
<b>cost_discharge_batteryStorage_x</b>	Cost for discharging battery associated with Storage_x

### 13.8.2.5 hourly cost with SP(With subscription)

In this sheet, the hourly cost for energy buy and sell for a subscribed power limit are listed. The cost for total energy, energy above subscribed limit and energy below subscribed limit for both with and without optimization are listed. The following Table 32 describes the meaning of each column reported.

**Table 32: Description of columns in the sheet “hourly\_cost\_with\_SP” in the output data file “Site\_x\_prosumer\_costs\_and\_energy\_balance.xlsx”**

<b>Column name</b>	<b>Description Description</b>
<b>t_h</b>	Time period
<b>cost_grid_buy_SP_base</b>	Unoptimized cost of energy buy with power subscription limit (M)
<b>cost_grid_buy_low_SP_base</b>	Unoptimized cost of energy buy below “Limitation of basis for peak fee (M)
<b>cost_grid_buy_high_SP_base</b>	Unoptimized cost of energy buy above “Limitation of basis for peak fee (M)
<b>cost_grid_buy_SP</b>	Optimized cost of energy buy with power subscription limit (M)
<b>cost_grid_buy_low_SP</b>	Optimized cost of energy buy below “Limitation of basis for peak fee (M)
<b>cost_grid_buy_high_SP</b>	Optimized cost of energy buy above “Limitation of basis for peak fee (M)

## 13.9 Testing the RH code including variable fixing

To run the RH test, it is needed to make the following changes into the code:

- Changes into the main code file: To add a *for* to iterate between t\_s\_horizon and t\_e\_horizon
- To copy applied values of the current execution time to the next period input Excel file
- To fix the variables for the past periods from 0 to t\_execution (if needed)
- To add metered values from past periods to the baseline production/consumption (merge observed\_values and teXX)

### 13.9.1 Changes into the main code file

The objective has been to add the fewer changes into the current code to be able to test the RH behaviour.

There is a global `t_execution` and an internal `t_execution`. The global includes all the periods during the test while the internal is always from 0 to the end of the optimization window. After the end of each day, internal `t_execution` is reset to 0.

The optimization function is called as an independent process each iteration/period, and it creates a complete new model each time it is executed. The inputs for each period are saved in different folders with the same structure using the name `TestCaseSiteX`, where `X` is the number of the global execution period (see Figure 95).

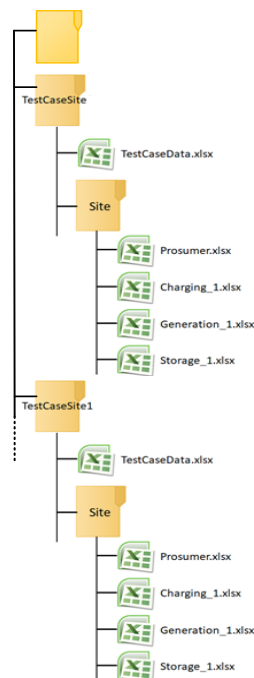


Figure 95: Input data structure to configure the model for a test case.

### 13.9.2 To copy applied values of the current execution time to the next period

It copies the optimization results from the current period to the inputs (observed\_values or similar input parameters) of the next period Excel input.

Generation:

- Copy “eb\_pv” from the output (Site\_X\_prosumer\_cost.s\_and\_energy\_balance.xlsx) to “observed\_values” of the inputs (Generation\_1.xlsx)

InflexGeneration:

- Copy “eb\_pv\_inflex” from the output (Site\_X\_prosumer\_costs\_and\_energy\_balance.xlsx) to “observed\_values” of the inputs (InflexGeneration\_1.xlsx).

#### Storage:

- Copy the result of “eb\_discharge\_bat” - “eb\_charge\_bat” from the output (Site\_X\_prosumer\_costs\_and\_energy\_balance.xlsx) to “ChargingEnergy” of the inputs (Storage\_1.xlsx).
- Copy “eb\_soc\_bat” from the output (Site\_X\_prosumer\_costs\_and\_energy\_balance.xlsx) to “EnergyLevel” of the inputs (Storage\_1.xlsx).

#### Charging:

- Copy “eb\_EV\_CS” from the output (Site\_X\_prosumer\_costs\_and\_energy\_balance.xlsx) to “ChargingEnergy” of the inputs (Charging\_1.xlsx).
- Copy “eb\_EV\_CS” from the output (Site\_X\_prosumer\_costs\_and\_energy\_balance.xlsx) to “ChargingPointState” of the inputs (Charging\_1.xlsx).

#### Prosumer:

- New inflexible load is calculated as the difference in the energy balance of all the other variables from all devices. Copy the result of “energy\_buy” - “energy\_sell” + “eb\_pv” + “eb\_pv\_inflex” + “eb\_discharge\_bat” - “eb\_charge\_bat” - “eb\_EV\_CS” from the output (Site\_X\_prosumer\_costs\_and\_energy\_balance.xlsx) to “observed\_values” of the inputs (Prosumer\_1.xlsx).

In addition to all these input updates, it is needed to update the previous battery SOC at the beginning of the simulation. This previous SOC is currently obtained from the last period of the “EnergyLevel” column of the inputs (Storage\_1.xlsx).

$$\text{init\_o\_min\_initial} = \{\text{'Storage': Input['EnergyLevel']}[timeInput.Nwindow-1]\}$$

For this reason, the last period of the “EnergyLevel” column of the inputs (Storage\_1.xlsx) is always stored in the same column of the input file for  $t_{\text{execution}}+1$  (see Figure 96). In this figure, one day has 24 periods and it takes 1 period to receive the metered values. It makes that in the 2 first periods, initial SOC is not copied directly from the last period of the current “EnergyLevel” column. This last part is not yet implemented into the code, as it depends on how it is done in the platform.

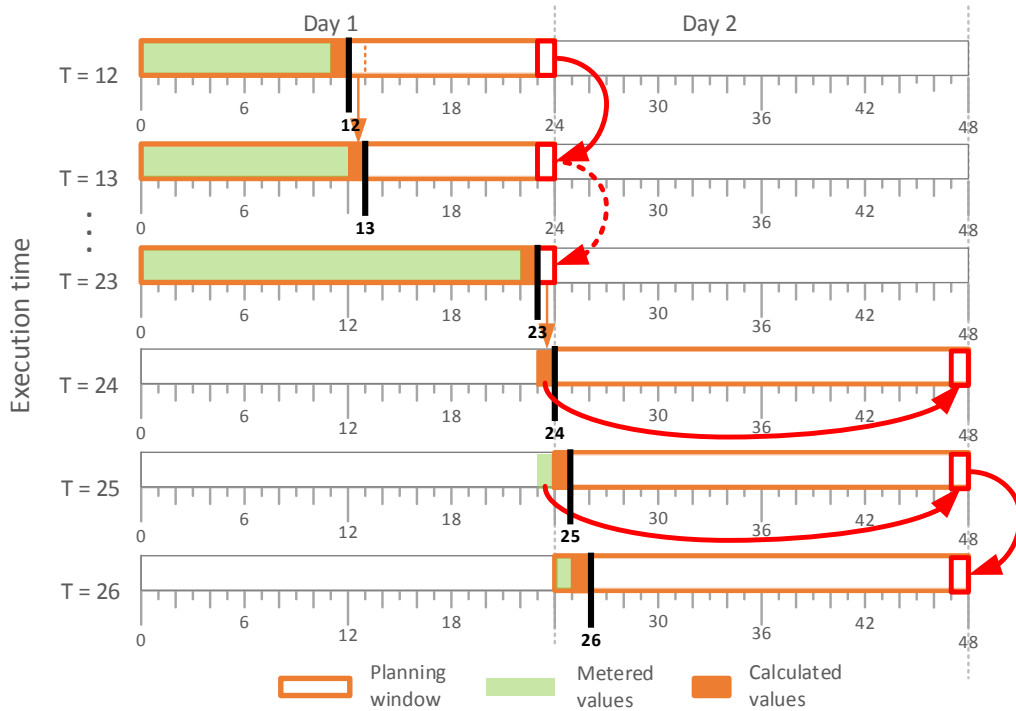


Figure 96: How previous SOC at the beginning of the simulation is saved through the periods of the planning window.

### 13.9.3 To fix the variables for the past periods

Past period values can come from metered or calculated values. Calculated values are those past periods where metered values are not received yet. They can be present in one or more than one period and their values are directly extracted from the results of the optimization.

As a general rule, only variables that have metered values are going to be fixed. The other variables are calculated from these variables or from other input parameters, so they do not need to be fixed.

Device	Variable	Metered values fixed?	Calculated values fixed?	Origin of the fixed value	Additional comments
Battery	sigma_soc	Y	Y	EnergyLevel	
Battery	sigma_ch	Y/N	Y/N	ChargingEnergy	Only fix it if remove SOC constraint for past periods
Battery	sigma_dis	Y/N	Y/N	ChargingEnergy	Only fix it if remove SOC constraint for past periods
EV	theta_cd	N	N		
EV	theta_ch	Y	Y	ChargingEnergy	

EV	theta_es	N	N		
Prosumer	chi_buy	Y	Y	observed_values	
Prosumer	chi_sell	Y	Y	observed_values	
Prosumer	delta_buy	N	N		
Prosumer	delta_sell	N	N		
Prosumer	chi_buy_low_h	N	N		
Prosumer	chi_buy_high_h	N	N		
Generation	psi	Y	Y	observed_values	
InfleGen	psi	Y	Y	observed_values	

- Battery:

The efficiency of charging and discharging is not constant and errors in the calculation of the SOC versus the metered values can cause infeasibilities. To avoid this, two options can be applied:

1. Do not fix sigma\_ch and sigma\_dis
2. Remove SOC constraint for past periods + fix sigma\_ch and sigma\_dis

In the second option, it is needed to remove the SOC constraint for past periods if we also want to fix sigma\_ch and sigma\_dis. Then, errors in the charging/discharging values are absorbed by the inflexible load (see energy balance comment below). We prefer the second option.

- Energy balance constraint:

The only variable/parameter of the energy balance that is not fixed for past periods is the inflexible load of the prosumer (+ battery charge/discharge, if option 1 is chosen).

The inflexible load is calculated as the difference between the main meter (chi\_buy and chi\_sell) and the consumption/generation of each device (sigma\_ch, sigma\_dis, theta\_ch and psi). Thanks to this, all possible deviations can be easily added to the inflexible load “metered” value. It will avoid infeasible solutions due to the energy balance constraint.

#### 13.9.4 To add metered values from past periods to the baseline

It is needed to mix metered, calculated and forecasted values as an input to the optimization algorithm, as it has to solve past and future periods. The current input Excel files only have forecasted and metered values columns. As in the offline test we do not have access to metered values, the metered and calculated values are put together in the metered values inputs, as explained in section 13.9.2. It needs to be adapted to work with the platform.

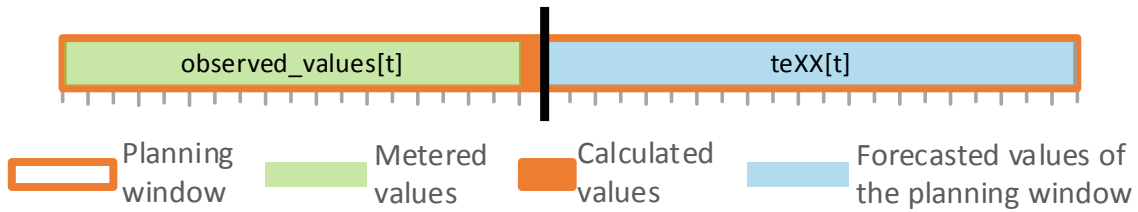


Figure 97: How input parameters are created from metered and forecasted values.

It affects the following models:

- Inflex. Load:

init\_w\_load\_inflex\_RH is made of a mixture of metered and calculated (observed\_values[t] from 0 to t\_execution) and forecasted values (teXX[t] from t\_execution to the end of the optimization window).

- Generation:

init\_w\_gen\_r\_RH is made of a mixture of metered and calculated (observed\_values[t] from 0 to t\_execution) and forecasted values (teXX[t] from t\_execution to the end of the optimization window).

- Infle. Generation:

init\_w\_gen\_inflex\_RH is made of a mixture of metered and calculated (observed\_values[t] from 0 to t\_execution) and forecasted values (teXX[t] from t\_execution to the end of the optimization window).

- EV:

W\_cp\_RH is made of a mixture of metered and calculated (ChargingEnergy[t] from 0 to t\_execution) and forecasted values (W\_cp[t] from t\_execution to the end of the optimization window).

ChargingPointState\_RH is made of a mixture of metered and calculated (ChargingPointState[t] from 0 to t\_execution) and forecasted values (ForecastedChargingPointState[t] from t\_execution to the end of the optimization window). How to deal with differences in the forecasted and metered values of the CP status?? Sessions are obtained from the forecasted CP status. Especially, Tstart is obtained when a new EV is connected AND starts charging, as we forced to charge the EV once it is connected in the forecast.



## 14 Appendix: Overview of sets, parameters and variables

### 14.1.1 Sets

$T$	Set of periods/time slots in the planning horizon
$T^c$	Subset of periods where curtailment is allowed
$B$	Set of battery units
$G$	Set of generation units
$G^i$	Subset of generation units that are inflexible
$G^f$	Subset of generation units that are flexible
$H$	Set of hourly time periods in the planning horizon
$I$	Set of load shift intervals of electric water heaters (EWH)
$K$	Set of charging power segments indexed by $k$
$L$	Set of load units
$L^i$	Subset of load units that are inflexible
$L^{ewh}$	Subset of load units that are EWH
$L^{sh}$	Subset of load units that are space heaters (SH)
$N$	Set of charging sessions per charging point
$V$	Set of electric vehicles
$V^i$	Subset of electric vehicles that are inflexible
$V^c$	Subset of electric vehicles that are fully controllable and interruptible

### 14.1.2 Parameters

Prosumer model parameters

$P_t^{retail-buy}$	Price at energy part of retail contract for buying electricity in period $t \in T$ [€/kWh]
$P_t^{grid-buy}$	Price at energy part of grid contract for buying electricity in period $t \in T$ [€/kWh]
$P_t^{grid-buy-low}$	Price at energy part of grid contract for buying electricity in cases with subscribed power in period $t \in T$ if bought electricity is below subscribed level [€/kWh]
$P_t^{grid-buy-high}$	Price at energy part of grid contract for buying electricity in cases with subscribed power in period $t \in T$ if bought electricity is above subscribed level [€/kWh]
$p_{tax}$	Sum price for all taxes that are related to buying electricity [p.u.]
$p^{VAT}$	Parameter that adds VAT to the amount bought. E.g. 25% is 1.25 [p.u.]
$P_t^{retail-sell}$	Price at energy part of retail contract for selling electricity in period $t \in T$ [€/kWh]
$P_t^{grid-sell}$	Price at energy part of grid contract for selling electricity in period $t \in T$ [€/kWh]
$\chi^{imp-cap}$	Maximum import capacity [kW]
$\chi^{exp-cap}$	Maximum export capacity [kW]
$M$	Subscribed power for the Norwegian tariff structure per hour [kWh]
$N^{hour}$	Periods per hour [p.u.]
$W_{l,t}^{inflex}$	Baseline charging schedule per inflexible load $l \in L^i$ in period $t \in T$ [kWh]

## Battery model parameters

$O_b^{B,min}$	Minimum state of charge allowed for battery unit $b \in B$ [kWh]
$O_b^{B,max}$	Maximum state of charge allowed for battery unit $b \in B$ [kWh]
$O_b^{B,initial}$	Amount of electricity stored in battery unit $b \in B$ at the beginning of period $t = 0$ decided in the previous optimization execution [kWh]
$O_b^{B,end}$	Minimum amount of electricity stored in battery unit $b \in B$ at the end of the planning horizon [kWh]
$Q_b^{B,ch}$	Maximum charging power allowed for battery unit $b \in B$ [kW]
$Q_b^{B,dis}$	Maximum discharging power allowed for battery unit $b \in B$ [kW]
$A_b^{B,ch}$	Efficiency parameter for charging battery unit $b \in B$ [p.u.]
$A_b^{B,dis}$	Efficiency parameter for discharging battery unit $b \in B$ [p.u.]
$S_b^{B,ch}$	Threshold in battery unit $b \in B$ charging process [p.u.]
$S_b^{B,dis}$	Threshold in battery unit $b \in B$ discharging process [p.u.]
$P_{b,t}^{B,ch}$	Price for charging battery unit $b \in B$ at period $t \in T$ [€/kWh]
$P_{b,t}^{B,dis}$	Price for discharging battery unit $b \in B$ at period $t \in T$ [€/kWh]
$w_b^B$	Parameter to control the constant voltage charge/discharge in battery b
$B_{b,k}^B$	End of segment k's x-axis value representing the charging power for segment k in battery b [kW]
$\mu_{b,k}^B$	Slope for segment k in battery b
$R_b^B$	Battery replacement cost of battery b in [€/kWh]

$c_{b,j}^B$	Marginal aging cost of cycle depth segment j in [kWh]
$\sigma_{b,j}^{B,SOC,init}$	Initial state of charge of cycle depth segment j for battery in period t=0 in [kWh]
$\sigma_{b,j}^{B,SOC,end}$	Final state of charge of cycle depth segment j for battery b in period T in [kWh]
$O_{b,j}^{B,max}$	Maximum allowed state of charge of segment j for battery b [kWh]
$T_{Lf}^B$	Battery life time in years
$D_y$	Days per year
$H_d$	Hours per day
$S_h$	Steps per hour
$S_b^{B,0}$	Constant in calendar ageing function
$S_b^{B,SOC}$	State of charge multiplier in calendar ageing function
$\rho_b^B$	Battery degradation tuning factor for battery b, $\rho_b^B \in [0,1]$

## Electric vehicle charging point model parameters

$Q_v^{CP,max}$	Maximum charging power allowed for charging point unit $v \in V^c$ [kW]
$Q_v^{CP,min}$	Minimum charging power allowed for charging point unit $v \in V^c$ [kW]
$Q_t^{CS,ch}$	Total charging power per charging station each period $t \in T$ [kW]
$P_v^{CP,shift}$	Price for deferring 1 kWh energy demand for one time period for charging point unit $v \in V^c$ [€/kWh]

$P_v^{CP,ns}$	Price for non-supplying 1 kWh of the expected charging demand of charging point unit $v \in V^c$ of session $n \in N$ by the end of the charging sessions [€/kWh]
$T_{v,n}^{CP,start}$	First period for charging point unit $v \in V^c$ of session $n \in N$ [p.u.]
$T_{v,n}^{CP,end}$	Departure period of each charging point unit $v \in V^c$ of session $n \in N$ [p.u.]
$V_{v,n}^{CP,start}$	First period of consuming electricity for charging point unit $v \in V^c$ of session $n \in N$ [p.u.]
$V_{v,n}^{CP,end}$	Last period of consuming electricity for charging point unit $v \in V^c$ of session $n \in N$ [p.u.]
$W_{v,t}^{CP}$	Baseline charging schedule for charging point unit $v \in V^c$ in period $t \in T$ [kWh]

Electric vehicle charging point inflexible model parameters

$W_{v,t}^{CP,inflex}$	Baseline charging schedule per inflexible charging point unit $v \in V^i$ in period $t \in T$ and [kWh]
-----------------------	---

Electric water heater model parameters

$C_{l,t}^{EWH,allow}$	Binary parameter equal to 1 if disconnection of EWH unit $l \in L^{ewh}$ is allowed in period $t \in T$ , else 0.
$D_l^{EWH,max}$	Maximum duration of flexibility activation of the EWH unit $l \in L^{ewh}$ in time periods [p.u.]
$D_l^{EWH,min}$	Minimum rest time between two successive shifting intervals $i \in I$ of the EWH unit $l \in L^{ewh}$ in time periods [p.u.]
$Q_l^{EWH,min}$	Minimum power level of EWH unit $l \in L^{ewh}$ [kW]
$Q_l^{EWH,max}$	Maximum power level of EWH unit $l \in L^{ewh}$ [kW]

$P_l^{EWH,shift}$	Price for shifting EWH demand volume for the unit $l \in L^{ewh}$ with 1 kWh [€/kWh]
$T_{l,i}^{EWH,start}$	First period for EWH unit $l \in L^{ewh}$ in shift interval $i \in I$ [p.u.]
$T_{l,i}^{EWH,end}$	Last period for EWH unit $l \in L^{ewh}$ in shift interval $i \in I$ [p.u.]
$V_{l,i}^{EWH,end}$	Last period in EWH shift interval $i \in I$ where the EWH unit $l \in L^{ewh}$ has a baseline consumption [p.u.]
$W_{l,t}^{EWH,c\_allow}$	Baseline consumption of EWH unit $l \in L^{ewh}$ when $C_{l,t}^{allow} = 0$ in time period $t \notin [T_{l,i}^{EWH,start}, T_{l,i}^{EWH,end})$ [kWh]
$W_{l,t}^{EWH,restrict}$	Restricted baseline consumption of EWH unit $l \in L^{ewh}$ in time period $t \in [T_{l,i}^{EWH,start}, T_{l,i}^{EWH,end})$ [kWh]
$W_{l,t}^{EWH}$	Baseline consumption of EWH unit $l \in L^{ewh}$ in time period $t \in T$ [kWh]

## Photovoltaic generator flexible model parameters

$W_{g,t}^G$	Baseline production from flexible generation unit $g \in G^f$ in period $t \in T$ [kWh]
$P_{g,t}^G$	Price of reducing generation output of the unit $g \in G^f$ during period $t \in T$ [€/kWh]

## Photovoltaic generator inflexible model parameters

$W_{g,t}^{G,inflex}$	Baseline production from generation inflexible unit $g \in G^i$ in period $t \in T$ [kWh]
----------------------	---

## Space heater model parameters

$D_l^{SH,max}$	Maximum duration of flexibility activation of the space heater unit $l \in L^{sh}$ in time periods [p.u.]
----------------	---

$D_l^{SH,min}$	Minimum rest time between two successive flexibility activations of space heater unit $l \in L^{sh}$ in time periods [p.u.]
$N_l^{SH,max}$	Maximum number of flexibility activation of space heater unit $l \in L^{sh}$ in planning horizon [p.u.]
$P_l^{SH,flex}$	Price for flexibility activation of space heater unit $l \in L^{sh}$ with 1 kWh [€]
$T_l^{SH,start}$	Starting period where heater control is allowed for space heater unit $l \in L^{sh}$ [p.u.]
$T_l^{SH,end}$	Ending period where heater control is allowed for space heater unit $l \in L^{sh}$ [p.u.]
$W_{l,t}^{SH,l}$	Energy level of the room in kWh for space heater unit $l \in L^{sh}$ corresponding to lower threshold temperature $T_t^l$ in period $t \in T$ [kWh]
$W_{l,0}^{SH,r}$	Energy level inside the room for space heater unit $l \in L^{sh}$ in time interval $t = 0$ [kWh]
$W_{l,t}^{SH,s}$	Energy level of the room in kWh for space heater unit $l \in L^{sh}$ corresponding to setpoint temperature $T_t^s$ in period $t \in T$ [kWh]
$W_{l,t}^{SH,u}$	Energy level of the room for space heater unit $l \in L^{sh}$ corresponding to upper threshold temperature $T_t^u$ in period $t \in T$ [kWh]
$W_{l,t}^{SH,out}$	Heat energy loss from the room for space heater unit $l \in L^{sh}$ in period $t \in T$ [kWh]
$W_l^{SH,h}$	Maximum heat energy delivered by the space heater unit $l \in L^{sh}$ in the given time period [kWh]

## MV network model parameters

$AP_{i,t}^{total}$	Total active power at node $i \in K$ in period $t \in T$ [kW]
$AP_{i,t}^{gen}$	Generated active power at node $i \in K$ in period $t \in T$ [kW]
$AP_{i,t}^{dem}$	Demanded active power at node $i \in K$ in period $t \in T$ [kW]
$RP_{i,t}^{total}$	Total reactive power at node $i \in K$ in period $t \in T$ [kW]
$RP_{i,t}^{gen}$	Generated reactive power at node $i \in K$ in period $t \in T$ [kVAR]
$RP_{i,t}^{dem}$	Demanded reactive power at node $i \in K$ in period $t \in T$ [kVAR]
$U_{i,t}^{MAX}$	Maximum voltage at node $i \in K$ in period $t \in T$ [kV]
$U_{i,t}^{MIN}$	Minimum voltage at node $i \in K$ in period $t \in T$ [kV]
$U_{i,t}$	Voltage at node $i \in K$ in period $t \in T$ [kV]
$\underline{Y}_{ik}$	Admittance value for line $i - k$ [S]
$\theta_{ik,t}$	Voltage angle difference between nodes $i, k$ in period $t \in T$ [rad]
$\theta_{k,t}$	Voltage angle at node $k$ in period $t \in T$ [rad]
$\underline{Z}_{i,k}$	Impedance value for line $i - k$ [ $\Omega$ ]



### 14.1.3 Variables

#### Prosumer model variables

$\chi_t^{buy}$	Amount of electricity bought in period $t \in T$ [kWh]
$\chi_t^{sell}$	Amount of electricity sold in period $t \in T$ [kWh]
$\chi^{peak}$	Basis for calculation of peak fee in cases where this is a part of the grid contract [kW]
$\chi_h^{low}$	Amount of electricity bought in hour $h$ below the subscribed power $M$ [kWh]
$\chi_h^{high}$	Amount of electricity bought in hour $h$ above the subscribed power $M$ [kWh]
$\delta_t^{buy}$	Binary variable = 1 if site is importing/buying electricity in period $t \in T$ , else 0
$\delta_t^{sell}$	Binary variable = 1 if site is exporting/selling electricity in period $t \in T$ , else 0

#### Battery model variables

$\sigma_{b,t}^{B,ch}$	Amount of electricity charged to battery unit $b \in B$ in period $t \in T$ [kWh]
$\sigma_{b,t}^{B,dis}$	Amount of electricity discharged from battery unit $b \in B$ in period $t \in T$ [kWh]
$\sigma_{b,t}^{B,soc}$	Amount of electricity stored in battery unit $b \in B$ at the end of period $t \in T$ [kWh]
$\delta_{b,t}^{B,ch}$	Binary variable = 1 if battery unit $b \in B$ is being charged in period $t \in T$ , else 0
$\delta_{b,t}^{B,dis}$	Binary variable = 1 if battery unit $b \in B$ is being discharged in period $t \in T$ , else 0

$\sigma_{b,t}^{B,ch,bat}$	Power supplied to battery b from the inverter in time step t [kW]
$\sigma_{b,t}^{B,dis,bat}$	Power withdrawn from battery b sent to the inverter in time step t [kW]
$\sigma_{b,t}^{B,ch,inv}$	Power supplied to inverter belonging to battery b in time step t [kW]
$\sigma_{b,t}^{B,dis,inv}$	Power withdrawn from inverter belonging to battery b in time step t [kW]
$\sigma_{b,t,k}^{B,ch,inv}$	Power supplied to inverter belonging to battery b in time step t in segment k [kW]
$\sigma_{b,t,k}^{B,dis,bat}$	Power withdrawn from battery b sent to the inverter in time step t in segment k [kW]
$\gamma_{b,t,k}^{B,ch}$	Binary variable representing activation of charging segment k in battery b in time step t
$\gamma_{b,t,k}^{B,dis}$	Binary variable representing activation of discharging segment k in battery b in time step t
$\sigma_{b,t,j}^{B,SOC}$	Energy stored in segment j in battery b at time step t [kWh]
$\sigma_{b,t,j}^{B,ch}$	Amount of electricity charged to segment j in battery b at time step t in [kW]
$\sigma_{b,t,j}^{B,dis}$	Amount of electricity discharged from segment j in battery b at time step t in [kW]
$\beta_{b,t,j}^{B,cyc}$	Cyclic ageing cost in time step t for battery b in segment j [€]
$v_{b,t}^B$	Binary variable to prohibit simultaneous charging and discharging for battery b in time step t
$\sigma_{b,t}^{B,SOC}$	Energy stored in battery b at time step t in battery b [kWh]

$\beta_{b,t}^{B,cal}$	Calendar battery degradation for battery $b$ in time step $t$ [€]
$\beta_{b,t}^{B,tot}$	Total cycle and calendar battery ageing cost for battery $b$ in time step $t$ [€]

## Electric vehicle charging point model variables

$\theta_{v,t}^{CP,es}$	Amount of electricity supplied to the charging point unit $v \in V^c$ in period $t \in T$ [kWh]
$\theta_{v,t}^{CP,ch}$	Amount of electricity charged to the charging point unit $v \in V^c$ in period $t \in T$ [kWh]
$\theta_{v,n}^{CP,cd}$	Amount of accumulated EV energy during the charging process in the charging point unit $v \in V^c$ in session $n \in N$ (charging demand) [kWh]

## Electric vehicle charging point inflexible model variables

$\theta_{v,t}^{CP,ch-inflex}$	Amount of electricity charged to the inflexible charging point unit $v \in V^i$ in period $t \in T$ [kWh]
-------------------------------	---

## Electric water heater model variables

$\tau_{l,i}^{EWH}$	Weighted average delay of EWH unit $l \in L^{ewh}$ in shift interval $i \in I$ in number of time periods [p.u.]
$\omega_{l,t}^{EWH}$	Amount of electricity consumed from EWH unit $l \in L^{ewh}$ in time period $t \in [T_{l,i}^{EWH,start}, T_{l,i}^{EWH,end})$ [kWh]
$\omega_{l,t}^{EWH,realconsum}$	Real amount of electricity consumed from EWH unit $l \in L^{ewh}$ in time period $t \in T$ [kWh]

## Photovoltaic generator flexibility model variables

$\psi_{g,t}^G$	Amount of electricity produced from generating unit $g \in G^f$ in period $t \in T$ [kWh]
----------------	---

## Photovoltaic generator inflexible model variables

$\psi_{g,t}^{G,inflex}$	Amount of electricity produced from generating unit $g \in G^i$ in period $t \in T$ [kWh]
-------------------------	---

## Space Heaters

$\delta_{l,t}^{SH,start}$	Binary variable equal to 1 if flexibility activation of space heater unit $l \in L^{sh}$ starts in the beginning of period $t \in T^c$ , else 0
$\delta_{l,t}^{SH,run}$	Binary variable equal to 1 if flexibility activation of space heater unit $l \in L^{sh}$ is running in period $t \in T^c$ , else 0
$\delta_{l,t}^{SH,end}$	Binary variable equal to 1 if flexibility activation of space heater unit $l \in L^{sh}$ ends in the beginning of period $t \in T^c$ , else 0
$w_{l,t}^{SH,r}$	Energy level inside the room for space heater unit $l \in L^{sh}$ in period $t \in T$ [kWh]
$\omega_{l,t}^{SH}$	Electrical energy delivered to the space heater unit $l \in L^{sh}$ in period $t \in T$ (Same as the heat energy delivered as the COP of the electric heater is 1) [kWh]

## Flexibility costs

$\zeta^{flexibility}$	Total cost for utilizing internal flexibility [€]
$\zeta^{EV,control}$	Total cost for controlling EV charging [€]
$\zeta^{EV,shift}$	Total cost for shifting EV charging [€]
$\zeta^{EV,non-supplied}$	Total cost for kWh not supplied for EV charging [€]
$\zeta^{EV,charging\ cost}$	Total cost for EV charging [€]
$\zeta^{EWH}$	Total cost for shifting EWH demand volume [€]
$\zeta^{SH}$	Total cost for shifting space heater demand volume [€]
$\zeta^G$	Total cost for utilizing generation flexibility in the planning horizon [€]

$\zeta^B$	Total cost for utilizing battery flexibility in the planning horizon [€]
$\zeta^{B,ch}$	Total cost for charging batteries in the planning horizon [€]
$\zeta^{B,dis}$	Total cost for discharging batteries in the planning horizon [€]
$\zeta^{B,soc-value}$	Total cost for stored energy [€]

## MV network

$\varphi_{i,t}^{ACT}$	Total active power injected at node i at time t from flexibility sources [kW]
$\varphi_{i,t}^{REA}$	Total reactive power injected at node i at time t from flexibility sources [kVAR]



*Smart system of renewable energy storage based on **IN**tegrated **EV**s and **bA**tteries to empower mobile, **D**istributed and centralised **E**nergy storage in the distribution grid*

Deliverable n°:	<b>D5.4 B</b>
Deliverable name:	<b>Flexibility Planning of Distributed Battery Storage in Smart Distribution Networks</b>
Version:	<b>1.0</b>
Release date:	<b>17/12/2018</b>
Dissemination level:	<b>Public</b>
Status:	<b>Submitted</b>
Author:	<b>NTNU – Jamshid Aghaei</b>



**Document history:**

Version	Date of issue	Content and changes	Edited by
0.1	15/10/2018	First outline draft version	Jamshid Aghaei
0.2	26/10/2018	Updated outline	Jamshid Aghaei
0.3	3/11/2018	Introduction description and Chapter 3,4	Jamshid Aghaei
0.4	10/11/2018	New updates in all chapters, chapter 4 is completed	Jamshid Aghaei
1.0	20/11/2018	Final edit	Jamshid Aghaei

**Peer reviewed by:**

Partner	Reviewer
SIN	Jayaprakash Rajasekharan
ElaadNL	Patrick Rademakers

**Deliverable beneficiaries:**

WP / Task
WP5 / Task 5.3 and 5.4
All Pilots
WP6

## Table of contents

<b>Executive summary .....</b>	<b>8</b>
<b>1 Introduction .....</b>	<b>9</b>
<b>2 Modelling of Distributed Battery Energy Storage Systems (BESS) Planning 14</b>	
2.1 Original Single-level Model of Flexibility Planning of BESS	15
2.2 Linearized Model	17
2.3 Simple Modelling of Battery Degradation in Planning Studies	18
2.4 Uncertainty Modelling	21
<b>3 Bi-level Benders Decomposition (BD) Solution Methodology .....</b>	<b>22</b>
3.1 BD Structure	24
3.2 BD Algorithm and Implementation	29
<b>4 Case Study and Discussion.....</b>	<b>30</b>
4.1 Standard test network and data	30
4.2 Simulation Results: Computational Efficiency	32
4.3 Simulation Results: Technical Aspect	36
<b>5 Conclusions.....</b>	<b>46</b>



## Abbreviations and Acronyms

Acronym	Description
ABC	Artificial bee colony
BD	Benders decomposition
BURO	Bounded uncertainty-based robust optimization
DBESS	Distributed battery energy storage system
DE	Differential evolution
DER	Distributed energy resource
DG	Distributed generation
DOD	Depth-of-discharge
DSO	Distribution system operator
ESS	Energy storage systems
FBS	Forward-backward sweep
LP	Linear programming
LV	Low voltage
MILP	Mixed integer linear programming
MINLP	Mixed integer non-linear programming
NLP	Non-linear programming
NRES	Non- renewable distributed energy source
OPF	Optimal power flow
PDF	Probability density function
PV	Photovoltaic
RES	Renewable energy source
RO	Robust optimization
SOC	State of charge
SOCP	Second order cone programing

## Nomenclature

### 1) Indices and Sets

$(b,j), t, l, k, p$	Indices of bus, time, linearization segments of voltage magnitude term, circular constraint and term of degradation of battery, respectively
$\varphi_b, \varphi_t, \varphi_l, \varphi_k, \varphi_p$	Sets of bus, time, linearization segments of voltage magnitude term, circular constraint and term of degradation of battery, respectively
$m, n_f$	Index and total number of the iteration of the primal sub-problem to be feasible, respectively
$r, n_i$	Index and total number of the iteration of the primal sub-problem to be infeasible, respectively

### 2) Parameters

$A$	Bus incidence matrix (if line existed between buses $b$ and $j$ , $A_{b,j}$ is equal to 1, and 0 otherwise)
$A_{min}$	Minimum boundary rate of the stored energy of battery
$c^s$	Annual investment cost (in \$/MWh/year)
$g, b$	Line conductance and susceptance in per unit (pu), respectively
$P^{ch-max}, P^{dis-max}$	Maximum charging and discharging rate of battery in pu, respectively
$PD, QD$	Active and reactive load in pu, respectively
$RES$	The output power of RES in pu
$SG^{max}, SL^{max}$	Maximum loading of distribution line and station in pu, respectively
$T$	Operating horizon, i.e., 6, 12, 24 or 48 hours
$V^{max}, V^{min}, \Delta V^{max}$	Maximum and minimum voltage magnitude, and maximum value of voltage deviation in pu, respectively

$V_{ref}$	Voltage of reference (station) bus in pu
$X, Y$	Horizontal and vertical value of different points of cycle life loss curve, respectively
$\omega_{max}$	Maximum capacity of battery in pu
$\eta_{ch}, \eta_{dis}$	Efficiency parameter for charging and discharging of the battery, respectively
$\lambda^{ch}, \lambda^{dis}$	Charging and discharging price of the battery, respectively in \$/MWh

### 3) Variables: All variables are in per unit (pu)

$D$	Depth of discharge without unit
$E$	Stored energy of battery
$P^{ch}, P^{dis}$	Amount of electricity charged and discharged from battery
$PG, QG$	Active and reactive power of the station, respectively
$PL, QL$	Active and reactive power of lines, respectively
$V, \Delta V, \theta$	Magnitude, deviation (pu) and angle of voltage (in rad), respectively
$\omega$	Capacity of battery
$\lambda_{sub}, \mu_{sub}$	Dual variables of equality and inequality constraints in the primal sub-problem
$\rho, \gamma$	Cycle life loss and auxiliary variable for storage degradation cost, respectively, without unit

### 4) Functions

$f$	Cycle life loss
$J_p, J_{sub}$	Master problem and sub-problem objective functions in pu
$\beta_1$	Operation or charging cost of DBESS in pu

$\beta_2$ 

Revenue of DBESSs due to selling of discharging power in pu

## Executive summary

This report was commissioned to include the flexibility planning of distributed battery storage in smart distribution networks. The objective is to find the cost-efficient placement and sizing of battery storage systems. This leads to an improved efficiency of the existing power system and reduce issues caused by variable renewable energy sources in the physical electricity systems as well as at the electricity markets. The basic battery storage planning strategy principles were already included in D5.3 *Simplified battery operation and control algorithm*. Whereas this deliverable compares two decision strategies in association with distributed and centralized battery optimal siting and sizing. Moreover, this report adds several functionalities such as robust optimization method to deal with uncertainties and the cost of degradation, which are essential for the planning algorithm to make proper investment decisions.

The document contains a detailed explanation of the bilevel robust algorithm for optimal investment decisions on battery storage systems including optimal sizing and placement. The algorithm is implemented from a distribution system operator perspective to increase the network flexibility. In order to explain the battery planning strategy, first, the deterministic planning model of the distributed battery energy storage systems is explained. This is a non-linear problem, which makes it computationally difficult to be solved especially for large-scale systems. Hence, an equivalent linear programming model based on the Benders decomposition approach is proposed. Second, in order to deal with uncertain parameters including forecasted loads, energy and charging/discharging prices and the output power of RESs, a bounded uncertainty-based robust optimization framework is developed. The robust optimization framework represents a tractable uncertainty modeling structure. Finally, the proposed scheme is applied to 19-bus LV CIGRE benchmark grid to investigate the capability and efficiency of the model.

This model is able to help the INVADE pilots, i.e., the German and the Spanish pilot to find the cost-efficient investment decisions.

# 1 Introduction

Variable and uncertain renewable energy sources (RESs) in electricity networks are expected to experience a substantial growth due to emerging market for Green Certificates. This is infact one of the main focus in INVADE project. RESs variable generation along with customers' incoming proactive role in power system operation, and their expanding technology options such as solar photovoltaics panels, the deployment of plug-in electric vehicles and smart appliances, drive the need for higher power system flexibility. The flexibility term defined in INVADE D5.1 as *“the modification of generation injection and/or consumption patterns in reaction to an external price or activation signal in order to provide a service within the electrical system”* [1]. Flexibility could be provided by: supply side, network side, and demand side and storage availability. Indeed, adding flexible resources into the networks can improve the flexibility. Some important flexible resources are demand response programs, distributed battery energy storage systems and non- renewable distributed energy sources (NRESs), e.g., micro-turbines and fuel cells, in the demand and smart distribution network sides. Among these flexible resources, batteries are capable of providing high flexibility due to their inherent fast dynamics combined with fast control based on the power electronic converters [2]. However, allocating more distributed battery energy storage systems (DBESSs) to the smart distribution networks imposes extra costs, accordingly, it is crucial to establish investment planning model to determine how much flexibility from DBESSs might be needed and of where to place them in the network. Finding the optimal investment level requires consideration not only of short-term power system operation procedures, but also long-term investment planning to recover costs. Moreover, the flexibility of DBESSs and their associated costs are system-dependent. Accordingly, it is essential to develop methodologies and procedures to measure economic and technical flexibility benefits of DBESSs and their potential capacity to adequately host uncertain RESs, e.g., photovoltaic (PV) systems and wind power generation. In other words, it is important to make compromise between upgrading the system flexibility levels of DBESSs and escaping extra investment in supply and grid reinforcements. In this regard, the concentration areas of this work are to answer two main questions: *“How does integrating RESs will affect the power system operation and planning procedures?”* and *“How to allocate DBESSs as the flexibility resources to accommodate a higher penetrations of RESs in the distribution grids?”*. To this end, the first step is to determine the optimal location and size of batteries in the distribution networks planning studies [2]. However, the battery planning problem generally is kind of probabilistic or stochastic

optimization problems due to the presence of uncertain parameters that calls for some scenario-based stochastic programming modelling of uncertain parameters that assumes there is a probabilistic description of the uncertainty based on the probability density functions (PDFs). Generally, the scenario-based stochastic modelling of planning problem enforces the high computational burden and calculation time and increase the complexity of the optimization solution methodology. Robust optimization (RO) is a new approach for modelling uncertainty in optimization problems that works with a deterministic, set-based description of the uncertainty to construct a solution that is feasible for any realization of the uncertainty in a given set [3].

Significant research works have been concentrated on the planning of battery energy storage systems requirement as well as evaluating their effects in the power system operation in the presence of RESs. For instance, a two-stage stochastic optimization problem of the integrated investment planning of PVs, battery energy storage systems and gas-fired micro turbines has been proposed in a multicarrier gas and electricity in [4]. The first stage of the proposed framework in [4] deals with the optimal investment planning of the energy storage systems to decide their size and location. Then, according to the results of the first stage, the optimal operation is executed based on the power flow equations in both gas and electricity grids. Different operational considerations of integrating PVs in the low voltage distribution networks have been addressed in [5] including the changes in the voltage profile, reverse power flow, and energy losses. Also, in [5], a localized battery energy storage system has been suggested as a possible solution to improve the system operation conditions in the presence of high penetration of PVs. To this purpose, the battery is charged when production of photovoltaic is more than consumers' demands and discharged when consumers' demands are increased. It is noted that while the investment costs of batteries are high, hence using an objective function based on both economic and environmental goals is important to the placement and sizing of batteries. In addition to the above researches, the optimal sizing of a hybrid photovoltaic and battery storage system has been studied from prosumer viewpoints for residential and non-residential customers in [6]. To determine the optimal sizing and location of battery systems connected to the distribution grids based on AC power flow equations, an optimal planning scheme has been presented in [7]. It has used a relaxation method based on the second order cone programming (SOCP) of the optimal power flow (OPF) algorithm. Also, a relaxation method for the optimal power flow has been used in [8] to decide on the optimal placement and sizing of battery storage systems while considering the uncertain natures of the customers' demands and RESs' generations.

From the perspective of the optimization solution methodology for battery storage planning, different approaches have been conducted in the available researches in the area. For instance, the evolutionary algorithms such as differential evolution (DE) algorithm [9], artificial bee colony (ABC) algorithm [10] have been used for the storage system planning based on AC OPF equations. Also, in [11]-[12], the storage planning is presented based on Benders decomposition (BD) approach wherein the master problem and sub-problem of this scheme, respectively considers the storage planning and the optimal power flow both on the electricity markets [11] and low voltage (LV) distribution networks [12]. Both the proposed BD approaches in [11] and [12], are in the form of mixed integer linear programming (MILP) modelling for a DC OPF and a simple linearized forward-backward sweep (FBS) AC OPF formulations, respectively.

Furthermore, to deal with the uncertainty modelling in the storage planning problems, different frameworks have been adopted. Robust OPF formulations for distribution networks using non-linear adaptive RO and linear bounded uncertainty-based RO have been expressed in [13] and [14], respectively. The proposed non-linear RO in [13] has a complex viewpoint on the duality gap and complementarity (equilibrium) constraints. However, the linear RO in [14] benefits from a simple formulation and a low calculation time. The robust operation problem for energy storage systems (ESSs) considering the uncertainty of load profiles have been presents in [15]. In [16], a developed optimization tool, termed ROSION-Robust Optimization of Storage Investment On Networks, employs the RO to minimize the investment in the storage units that guarantees a feasible system operation without load or renewable power curtailment for all scenarios in the convex hull of a discrete uncertainty set.

To have an overall view on the available researches in the subject of energy storage planning problem, the taxonomy of recent works in the area are listed in Table 1.

As inferred from Table 1, there are different main research gaps for available literature about storage system planning as follows:

- In some researches, the planning problem of the storage system is based on the DC OPF [4]-[6] and [11]. However, the DC OPF is not suitable for the distribution networks while it ignores the power losses and reactive power. Accordingly, the AC OPF has been adopted in [7]-[10] and [12], where [7]-[8] and [9]-[10] are using a relaxation method and evolutionary algorithms, respectively. Nevertheless, these methods are based on the random search iteration methods which are not suitable for the robust modeling. Furthermore, as above mentioned, the simplified linear AC OPF suggested in [12] employs the FBS OPF formulation which fits to the structure



of the radial distribution networks rather than the bidirectional flow ones.

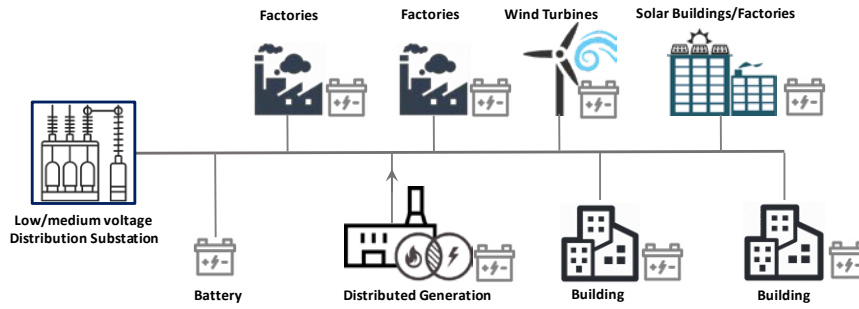
- The robust operation of the distribution networks have been adopted in [13]-[15]. Also, the uncertainty modeling of the RESs have been directed using the robust planning of storage systems in [16].

As a complimentary work to the above researches, this research develops a robust planning of DBESSs from the viewpoint of DSOs to increase the network flexibility. In the first step, a deterministic model of the proposed storage planning problem is formulated based on the structure of distribution grids illustrated in Figure 1. In this step, the difference between the DBESS planning, degradation and operation (charging) costs and revenue of DBESS owing to selling its stored energy to the network is minimized as an objective function subject to the constraints of AC OPF in the presence of RESs and DBESSs, and technical limits of the network, RESs and DBESSs. As shown in Figure 1 (a), the main assumptions of the proposed storage planning problem are as follows:

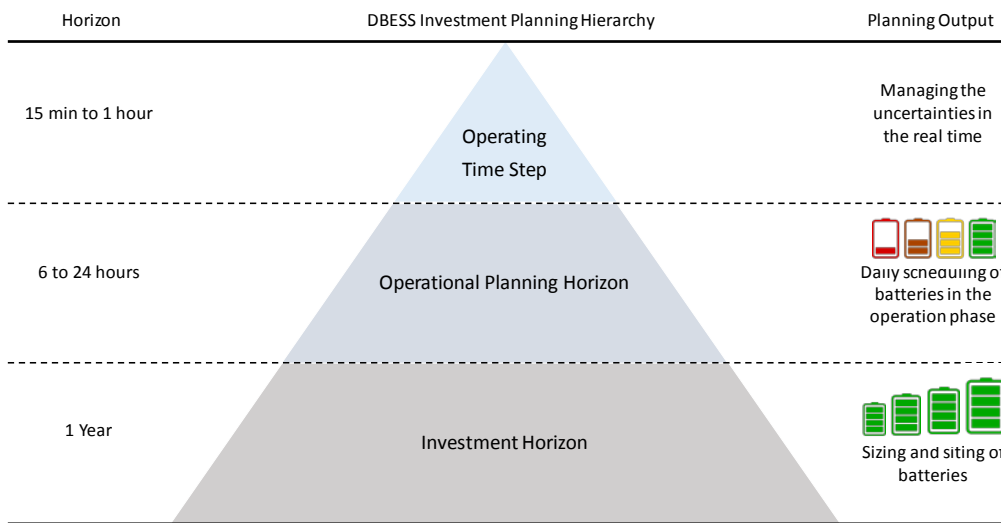
- The network includes different kinds of prosumers with the integrated RESs, e.g., PV systems, as well as flexible and inflexible loads.
- Each bus is a candidate to install battery as shown in Figure 1 (a).

**Table 1. Taxonomy of recent works in the area**

Ref. No.	Flexibility	Robust model	Improve of the network indexes	Power flow		Problem model	Solving method
				AC	DC		
[4]-[6]	No	No	Yes	No	Yes	LP	Simplex method
[7]-[8]	No	No	Yes	Yes	No	LP	Relaxation method
[9]-[10]	No	No	Yes	Yes	No	NLP	Evolutionary algorithms
[11]	No	No	Yes	No	Yes	MILP	Benders decomposition
[12]	No	No	Yes	Yes	No	MILP	Benders decomposition
[13]	No	Yes	Yes	Yes	No	NLP	Benders decomposition
[14]	No	Yes	Yes	Yes	No	LP	Benders decomposition
[15]	No	Yes	Yes	No	Yes	LP	Simplex method
[16]	No	Yes	Yes	No	Yes	MILP	Simplex method
<b>Proposed method</b>	<b>Yes</b>	<b>Yes</b>	<b>Yes</b>	<b>Yes</b>	<b>No</b>	<b>LP based on BD approach</b>	<b>Benders decomposition</b>



(a)



(b)

**Figure 1: a) Low/medium voltage grid, b) different time horizons in planning model of battery sizing and siting.**

Furthermore, the optimal sizing and siting of the DBESSs require the resolution of a temporal and spatial problem based on Figure 1 (b). The temporal problem involves an integrated sequential time intervals to confirm consistency of the battery state of charge (SOC) between different consecutive time intervals, here it is assumed to be one hour for the DBESS planning problem. Therefore, the proposed problem is modeled as a non-convex NLP form that is not suitable for the robust optimization model owing to the high calculation time, consequently, this report suggests an equivalent LP model based on the BD approach by means of the first-order expansion of Taylor's series to linearize power flow equations and develop a polygon for linearization of circular inequalities of the problem. Moreover, to model the uncertainties of active and reactive loads, energy or charging/discharging prices and output power of RESs, a bounded uncertainty-based robust optimization (BURO) framework is proposed. Briefly, the main

contributions of this report with respect to the previous works in the area are summarized as follows:

- Developing a computationally-efficient optimization model for the investment planning of DBESSs in the distribution networks as a LP form based on the BD approach.
- Presenting a robust model based on BURO framework for DBESS planning on account of different uncertainties.

## **2 Modelling of Distributed Battery Energy Storage Systems (BESS) Planning**

The main planning objective of the DSOs is to maximize the distributed generation (DG) or distributed energy resources (DERs) penetration with minimal cost, grid congestion and overvoltage. Accordingly, the conventional practice of DSOs to integrate considerable amounts of DGs is significant investments for the network reinforcement and expansion. The installation of battery storage in the low/medium voltage level is an interesting alternative to fulfill the above planning objective of DSOs because it avoids or at least postpones the need for extensive conventional network reinforcements. Thus, the planning strategy should include both the optimal placement and sizing of batteries complying with grid and storage constraints. To effectively reach this goal, it is necessary to implement multi-period OPF solve the optimal placement and sizing problem, taking into account optimal operation of the battery over a sufficient long operating horizon. The objective of the optimization problem is to calculate revenues from battery operation and find the best maximum net benefit in battery investment in the low/medium voltage grid model shown in Figure 1 (a). The grid consists of a group of prosumers that might have DERs such as PV generators and flexible and inflexible loads. Each prosumer has a meter placed at the connection point to the network. Moreover, it is assumed that each bus is a candidate to install battery shown with dotted red circle in Figure 1 (a).

As we have already discussed, the optimal sizing and placement of battery requires the resolution of a temporal and spatial problem. The temporal problem implies a coupling of multiple time steps to ensure coherence of the battery state of charge (SOC) between each consecutive time step, which is typically one hour for an investment planning problem. On the other hand, in order to find the investment decision that is economic viable we need to compare annual benefit with equivalent annual investment costs. The

long planning horizons and intertemporal coupling (storage) lead to an intractable planning problem if formulated as sub-section 2.1. Hence, in this section, we will explain how we can solve this issue. A typical solution [12] is to decompose the problem with respect to time. The decoupling for battery management algorithm could be chosen to be applied in different operational time horizons, e.g., 6 hours, 24 hours, and the time granularity for the battery management model can range from 15 minutes to one hour. These time horizons are shown in [12] and Figure 1 (b). The coupled time steps of the battery management algorithm are then simulated for each planning horizon in order to successfully complete an annual analysis. Hence, the proposed problem can be written as 2.1 to 2.3.

## 2.1 Original Single-level Model of Flexibility Planning of BESS

In this section, the modelling of the optimal placement and sizing of DBESS is presented in (1). The objective function of the investment planning of DBESS optimization problem is to minimize the difference between the DBESS annual cost and revenue as shown in (1a). The DBESS cost includes the investment and operation terms, and DBESS revenue is equal to the selling of battery stored energy (discharging) to the network. In addition, the proposed optimization problem is constrained by AC power flow equations in the presence of RESs and DBESSs, network operation limits and operation and planning equations of DBESSs. Accordingly, the proposed original model can be written as follows:

$$J = \min \underbrace{\sum_{b \in \varphi_b} c_b^s \cdot \omega_b}_{\text{Annual investment cost}} + \underbrace{\sum_{t \in \varphi_t} \sum_{b \in \varphi_b} \lambda_t^{ch} P_{b,t}^{ch}}_{\text{Operational cost of storage}} - \underbrace{\sum_{t \in \varphi_t} \sum_{b \in \varphi_b} \lambda_t^{dis} P_{b,t}^{dis}}_{\text{Revenue of storage}} \quad (1a)$$

S.to:

$$PG_{b,t} - \sum_{j \in \varphi_b} A_{b,j} PL_{b,j,t} + (P_{b,t}^{dis} - P_{b,t}^{ch}) = PD_{b,t} - RES_{b,t} \quad \forall b, t \quad (1b)$$

$$QG_{b,t} - \sum_{j \in \varphi_b} A_{b,j} QL_{b,j,t} = QD_{b,t} \quad \forall b, t \quad (1c)$$

$$PL_{b,j,t} = g_{b,j} (V_{b,t})^2 - V_{b,t} V_{j,t} (g_{b,j} \cos(\theta_{b,t} - \theta_{j,t}) + b_{b,j} \sin(\theta_{b,t} - \theta_{j,t})) \quad \forall b, j, t \quad (1d)$$

$$QL_{b,j,t} = -b_{b,j} (V_{b,t})^2 + V_{b,t} V_{j,t} (b_{b,j} \cos(\theta_{b,t} - \theta_{j,t}) - g_{b,j} \sin(\theta_{b,t} - \theta_{j,t})) \quad \forall b, j, t \quad (1e)$$

$$\theta_{b,t} = 0 \quad \forall b = \text{reference bus}, t \quad (1f)$$

$$(PL_{b,j,t})^2 + (QL_{b,j,t})^2 \leq (SL_{b,j}^{\max})^2 \quad \forall b, j, t \quad (1g)$$

$$(PG_{b,t})^2 + (QG_{b,t})^2 \leq (SG_b^{\max})^2 \quad \forall b, t \quad (1h)$$

$$V^{\min} \leq V_{b,t} \leq V^{\max} \quad \forall b, t \quad (1i)$$

$$E_{b,t} = E_{b,t-1} + \eta_{ch} P_{b,t}^{ch} - \frac{1}{\eta_{dis}} P_{b,t}^{dis} \quad \forall b, t \quad (1j)$$

$$0 \leq P_{b,t}^{ch} \leq P_b^{ch-\max} \quad \forall b, t \quad (1k)$$

$$0 \leq P_{b,t}^{dis} \leq P_b^{dis-\max} \quad \forall b, t \quad (1l)$$

$$A_{\min} \omega_b \leq E_{b,t} \leq \omega_b \quad \forall b, t \quad (1m)$$

$$E_{b,0} = E_{b,T} \quad \forall b \quad (1n)$$

$$0 \leq \omega_b \leq \omega_{\max} \quad \forall b \quad (1o)$$

The objective function is the difference between the sum of investment and operation cost of storage systems and storage systems revenue as shown in (1a). The constraints (1b) to (1f) represent the load flow equations [17, 18] that include active power balance (1b), reactive power balance (1c), active and reactive power flow of lines (1d) and (1e), and the value of the voltage angle in the reference bus (1f). In this model, DGs or photovoltaic systems (PVs) are considered as PQ buses (the real power |P| and reactive power |Q| are specified which is also known as a *Load Bus*) in different nodes. However, if DGs or PVs are involved in the voltage control strategy, they should be adopted as PV buses.

The system operation limits including bus voltage, line power flow, and substation power have been included in (1g) to (1i) [17, 18]. The constraints (1g) and (1h) refer to avoid the thermal overload of distribution lines and station, while a failure may be occurred due to overloading. Voltage control is typically requested when solar PV systems generate significant amounts of electricity. This will increase the voltage level in the grid. However, in high load situations, there is a risk that the voltage might decrease below the

permissible level, which has a negative consequence on safeguard of operating the system; therefore, constraint (1i) ensures that the voltage levels are maintained within the voltage permissible limits.

The temporal constraints of operating batteries are presented in (1j) to (1n) [11, 12]. The temporal problem implies a coupling of multiple time steps to ensure coherence of the battery state of charge (SOC) or stored energy of battery between each consecutive time step. The spatial problem implies the consideration of all nodes as possible placement locations for storage devices. As we have already discussed a typical operating time horizon can range from six hours to two days. The time steps of  $T$  are then coupled in order to successfully complete an annual analysis. The stored energy of the battery in period  $t$  depends on the stored energy in the previous period, and charging or discharging in current period. These impacts are replicated by (1j). The charging and discharging and the stored energy must be within minimum and maximum limits as expressed in (1k) to (1m). An additional constraint is added to avoid yearly (if  $T$  is 8760 hours) accumulation effects by forcing the stored energy of the first and last time step of the operating time horizon be equal as stated in equation (1n). Moreover, constraint (1o) presents the limitation of storage sizing.

## 2.2 Linearized Model

The original problem, (1), is NLP due to non-linear terms in (1d), (1e), and circular inequality constraints (1g) and (1h). Moreover, NLP problems are intrinsically more difficult to solve compared to linear problems, and there is no guarantee to reach optimal solution. Also, it is not suitable for the robust optimization, and applying BD approach for this case may result in large duality gaps and it needs to use complementarity (equilibrium) constraints in the problem [13], accordingly, solving the proposed problem is hard. Therefore, in the next step, an equivalent linear model is developed as follows:

- The linearized OPF model for the distribution networks is developed based on the first-order expansion of Taylor's series [3, 19]
- Circular inequality constraints are linearized based on a polygon approximation method [3, 14],

Details of the above linearization processes have been explained in [3] and [14], respectively. After applying these linearization techniques, the linear primal sub-problem can be written as follows:

$$J = \min \underbrace{\sum_{b \in \phi_b} c_b^s \cdot \omega_b}_{\text{Annual investment cost}} + \underbrace{\sum_{t \in \phi_t} \sum_{b \in \phi_b} \lambda_t^{ch} P_{b,t}^{ch}}_{\text{Operational cost of storage}} - \underbrace{\sum_{t \in \phi_t} \sum_{b \in \phi_b} \lambda_t^{dis} P_{b,t}^{dis}}_{\text{Revenue of storage}} \quad (2a)$$

S.to:

$$(1b), (1c), (1f), (1j) \text{ to } (1o) \quad (2b)$$

$$PL_{b,j,t} = g_{b,j} \left( \sum_{l \in \phi_l} (m_l - V^{\min}) \Delta V_{b,t,l} - V^{\min} \Delta V_{j,t,l} \right) - (V^{\min})^2 b_{b,j} (\theta_{b,t} - \theta_{j,t}) \quad \forall b, j, t \quad (2c)$$

$$QL_{b,j,t} = -b_{b,j} \left( \sum_{l \in \phi_l} (m_l - V^{\min}) \Delta V_{b,t,l} - V^{\min} \Delta V_{j,t,l} \right) - (V^{\min})^2 g_{b,j} (\theta_{b,t} - \theta_{j,t}) \quad \forall b, j, t \quad (2d)$$

$$\cos(k \times \Delta\alpha) \times PL_{b,j,t} + \sin(k \times \Delta\alpha) \times QL_{b,j,t} \leq SL_{b,j}^{\max} \quad \forall b, j, t, k \quad (2e)$$

$$\cos(k \times \Delta\alpha) \times PG_{b,t} + \sin(k \times \Delta\alpha) \times QG_{b,t} \leq SG_b^{\max} \quad \forall b, j, t, k \quad (2f)$$

$$0 \leq \Delta V_{b,t,l} \leq \Delta V^{\max} \quad \forall b, t, l \quad (2g)$$

In the above problem, the objective function is same to equation (1a), shown in (2a). The constraint (2b) is similar to linear constraints in (1). Also, the constraints of (2c) to (2g) are equivalent linear equations with constraints of (1d), (1e), (1g), (1h), (1i), respectively.

It is noted that based on the reported results in [3, 14], the calculation error of the voltage and power using equivalent LP model with respect to the original NLP is about 0.5% and 2.5%, respectively. It seems these error vales are negligible in planning studies.

### 2.3 Simple Modelling of Battery Degradation in Planning Studies

Degradation stress factors are all the operation practices or circumstances that accelerate the degradation in battery and thus shorten the lifetime of the cell. By identifying the stress factors the battery operating conditions and practices can be optimized within the application limits so that the degradation of the battery is minimized. Therefore, in this section, the simple modelling of the optimal placement and sizing of DBESS considering the storage degradation is written as follows:

$$\begin{aligned}
J = \min & \quad \overbrace{\sum_{b \in \varphi_b} c_b^s \cdot \omega_b}^{\text{Annual investment cost}} + \overbrace{\sum_{t \in \varphi_t} \sum_{b \in \varphi_b} c_b^s \cdot \omega_b \cdot \max(f_b(D_{b,t}) - f_b(D_{b,t-1}), 0)}^{\text{Degradation cost of storage}} \\
& + \overbrace{\sum_{t \in \varphi_t} \sum_{b \in \varphi_b} \lambda_t^{ch} P_{b,t}^{ch}}^{\text{Operational cost of storage}} - \overbrace{\sum_{t \in \varphi_t} \sum_{b \in \varphi_b} \lambda_t^{dis} P_{b,t}^{dis}}^{\text{Revenue of storage}}
\end{aligned} \tag{3a}$$

S.to:

$$D_{b,t} = \left(1 - \frac{E_{b,t}}{\omega_b}\right) \quad \forall b, t \tag{3b}$$

$$(2b) \text{ to } (2g) \tag{3c}$$

The objective function has been expressed in (3a), and as stated above it is equal to the difference between the sum of investment, degradation and operation cost of the storage systems and their revenue. It is noted that the term of  $f$  in the degradation cost equation is cycle life loss that is equal to the inverse of cycle life of battery, and it depends on depth-of-discharge (DOD) as shown in Figure 2 [20], and  $f(D_{t-1})$  is zero at  $t = 1$ . Also, the cycle life is defined the number of cycles, each to the specified discharge and charge termination criteria under a specified charge and discharge regime, that a battery can experience before deteriorating its specified nominal life criteria [2]. In addition, the DOD is calculated based on the constraint (3b), and the constraint (3c) is the same as the constraints of the problem (2).

It is noted that the related equations to the storage degradation cost part in the objective function of (3) and the constraint (3b) are non-linear functions. The term of  $f$  in the storage degradation cost of the objective function is linearized based on the piecewise linearization method [20] according to Figure 2, where details of this linearization process have been explained in [20]. Therefore, the new problem model is as follows:

$$\begin{aligned}
J = \min & \quad \overbrace{\sum_{b \in \varphi_b} c_b^s \cdot \omega_b}^{\text{Annual investment cost}} + \overbrace{\sum_{t \in \varphi_t} \sum_{b \in \varphi_b} c_b^s \cdot \omega_b \cdot \gamma_{b,t}}^{\text{Degradation cost of storage}} + \overbrace{\sum_{t \in \varphi_t} \sum_{b \in \varphi_b} \lambda_t^{ch} P_{b,t}^{ch}}^{\text{Operational cost of storage}} - \overbrace{\sum_{t \in \varphi_t} \sum_{b \in \varphi_b} \lambda_t^{dis} P_{b,t}^{dis}}^{\text{Revenue of storage}}
\end{aligned} \tag{4a}$$



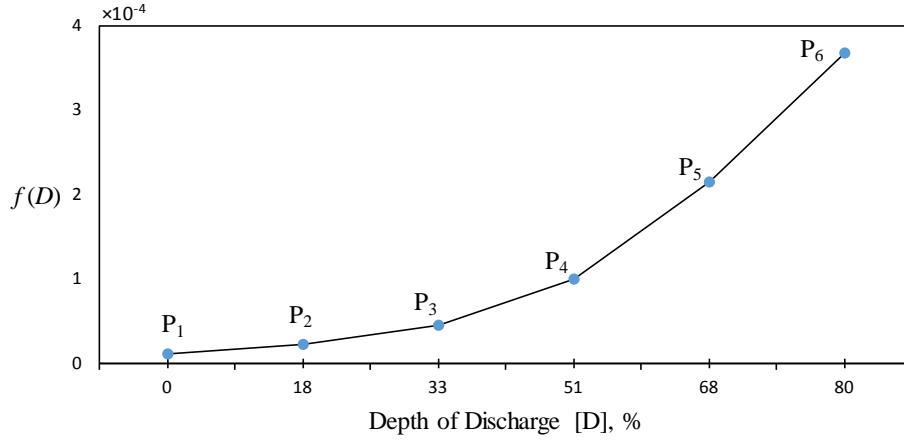


Figure 2: Cycle life loss as a function of the DOD [20].

$$\sum_{p \in P} X_{b,p} w_{b,t,p} = D_{b,t} \quad \forall b,t \quad (4c)$$

$$\sum_{p \in P} Y_{b,p} w_{b,t,p} = \rho_{b,t} \quad \forall b,t \quad (4d)$$

$$\sum_{p \in P} w_{b,t,p} = 1 \quad \forall b,t \quad (4e)$$

$$\gamma_{b,t} \geq \rho_{b,t} - \rho_{b,t-1} \quad \forall b,t, \rho_{b,t-1} = 0 \Big|_{t=1} \quad (4f)$$

$$\gamma_{b,t} \geq 0 \quad \forall b,t \quad (4g)$$

The term  $\gamma$  in objective function is the same as  $\max(f(D_t) - f(D_{t-1}), 0)$  in (3a). Moreover, the constraint of (4b) is similar to the constraints of (3). Also, the storage degradation cost part of (3a) has been replaced (4a) with additional constrains of (4c) to (4g), wherein  $X_p$  and  $Y_p$  refer to the horizontal and vertical axis values of the points  $P_1$  to  $P_6$  in Figure 2, and  $w$  is a continuous variable to choose the right linear segment based on the piecewise linear approximation in Figure 2, where it varies between 0 to 1. Also, The term  $\rho$  is the same as the  $f(D)$ .

It is noted that the problem (4) is non-linear due to the terms  $\omega_b \gamma_{b,t}$  and  $\frac{E_{b,t}}{\omega_b}$ , but these terms are linearized in sub-section 3.1.

## 2.4 Uncertainty Modelling

In the problem of (4), the parameters of active and reactive load,  $PD$  and  $QD$ , charging and discharging price,  $\lambda^{ch}$  and  $\lambda^{dis}$ , and output power of RES,  $RES$ , are as uncertainty. In this section, the BURO model uses for modelling of the uncertainty parameters. Consider the following mixed integer linear programming (MILP) problem [14]:

$$\min/\max_{x,y} \quad c^T x + d^T y \quad (5a)$$

S.to:

$$Ex + Fy = e \quad (5b)$$

$$Ax + By \leq p \quad (5c)$$

$$\underline{x} \leq x \leq \bar{x} \quad (5d)$$

$$y \in \{0,1\} \quad (5e)$$

Where, the elements of matrixes  $A$ ,  $B$ ,  $p$ , i.e.,  $a_{i,m}$ ,  $b_{i,n}$  and  $p_i$ , are considered as uncertain parameters, and these parameters are denoted as  $\tilde{a}_{i,m}$ ,  $\tilde{b}_{i,n}$  and  $\tilde{p}_i$ , respectively. Note that the indices of  $m$ ,  $n$  and  $i$  are used for coefficients of the continuous ( $x$ ) and binary ( $y$ ) variables and uncertain parameter ( $p$ ). Also,  $a_{i,m}$ ,  $b_{i,n}$  and  $p_i$  show the nominal or forecasted values of the uncertain parameters and the terms  $\tilde{a}_{i,m}$ ,  $\tilde{b}_{i,n}$  and  $\tilde{p}_i$  are called “true” values of the uncertain parameters. It is noted that the true values of the uncertain parameters can be defined as follows in the proposed robust model [14]:

$$|\tilde{a}_{i,m} - a_{i,m}| \leq \sigma |a_{i,m}|, \quad |\tilde{b}_{i,n} - b_{i,n}| \leq \sigma |b_{i,n}|, \quad |\tilde{p}_i - p_i| \leq \sigma |p_i| \quad (6)$$

where based on (6), the terms  $\tilde{a}_{i,m}$ ,  $\tilde{b}_{i,n}$  and  $\tilde{p}_i$  are limited by upper and lower limits, and  $\sigma$  is the uncertainty level which is  $\sigma > 0$ . Finally, the solution  $(x, y)$  will be a robust solution if the following conditions are satisfied:

- (i) The original problem, (5), has a feasible  $(x, y)$ ,
- (ii) For the  $\tilde{a}_{i,m}$ ,  $\tilde{b}_{i,n}$  and  $\tilde{p}_i$  based on (6), the inequality constraint, (5c), with an error of at most  $\delta \times \max[i, |p_i|]$  must be satisfied, that  $\delta \geq 0$  is the feasibility tolerance and it allows a small amount of infeasibility in the uncertain inequality (5c) [14].

Therefore, the constraint (5c) for the true value of the uncertain parameter and the worst-

case values of the uncertain parameters are as follows:

$$\sum_{m \notin M1} a_{i,m} x_m + \sum_{m \in M1} \tilde{a}_{i,m} x_m + \sum_{n \notin K1} b_{i,n} y_n + \sum_{n \in K1} \tilde{b}_{i,n} y_n \leq \tilde{p}_i + \delta \cdot \max[i, |p_i|] \quad \forall i \quad (7)$$

$$\tilde{a}_{i,m} x_m \leq a_{i,m} x_m + \sigma |a_{i,m}| |x_m|, \quad \tilde{b}_{i,n} y_n \leq b_{i,n} y_n + \sigma |b_{i,n}| |y_n|, \quad \tilde{p}_i \geq p_i - \sigma |p_i| \quad (8)$$

Wherein,  $M1$  and  $K1$  are the set of indices of  $x$  and  $y$ , respectively, with uncertain coefficients in the  $i$ -th inequality constraint. Thus, (5c) for the worst-case values of the uncertain parameters can be written as follows:

$$\sum_{m \notin M1} a_{i,m} x_m + \sum_{m \in M1} (a_{i,m} x_m + \sigma |a_{i,m}| |x_m|) + \sum_{n \notin K1} b_{i,n} y_n + \sum_{n \in K1} (b_{i,n} y_n + \sigma |b_{i,n}| |y_n|) \leq p_i - \sigma |p_i| + \delta \cdot \max[i, |p_i|] \quad \forall i \quad (9)$$

Note that  $|x_m|$  is defined by  $u_m$  as  $-u_m \leq x_m \leq u_m$  to be added to (9). Finally, the BURO model for (5) with tuning parameters of  $\sigma$  and  $\delta$ ,  $RO(\sigma, \delta)$ , is as follows:

$$\min/ \max_{x,y} \quad c^T x + d^T y \quad (10a)$$

S.to:

$$(5b) \text{ to } (5e) \quad (10b)$$

$$\sum_{m \notin M1} a_{i,m} x_m + \sum_{m \in M1} (a_{i,m} x_m + \sigma |a_{i,m}| u_m) + \sum_{n \notin K1} b_{i,n} y_n + \sum_{n \in K1} (b_{i,n} y_n + \sigma |b_{i,n}| |y_n|) \leq p_i - \sigma |p_i| + \delta \cdot \max[i, |p_i|] \quad \forall i \quad (10c)$$

$$-u_m \leq x_m \leq u_m \quad \forall m \in M1 \quad (10d)$$

It is noted that the proposed equation (4) is non-linear, where its linear form will be presented in sub-section 3.1, and accordingly, the linear form of the proposed robust model, (10), will be discussed more later in the sub-section 3.1.

### 3 Bi-level Benders Decomposition (BD) Methodology

It is noted that the proposed problem can be decomposed with respect to time in order to solve the optimization algorithm in a reasonable computational time. Hence, we can decompose the problem using BD; accordingly, the sizing problem is split into a tractable master problem and sub-problems. The outline of the proposed algorithm is shown in Figure 3.

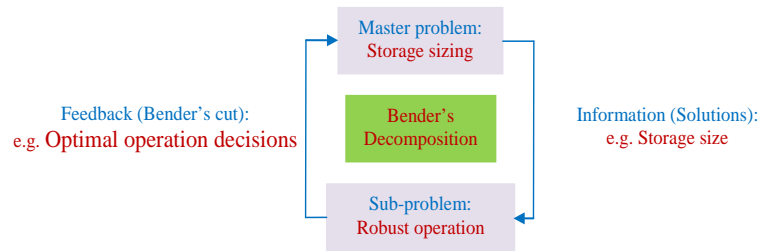


**Figure 3: Applying BD approach for the robust optimal sizing of the DBESSs**

The BD is a commonly used optimization technique. J. F. Benders initially introduced the BD algorithm for solving large-scale MIP problems [21]. The basic idea is to separate integer variables and real variables or relax the tough constraints in the optimization model and treat larger optimization problems via decomposition in order to accelerate the calculation process. The BD algorithm has been successfully used in different ways to take the advantage of underlying problem structures for various optimization problems, such as network design, optimal transportation problem, plant location and stochastic optimization. In applying the BD algorithm, the original problem will be decomposed into a master problem and several sub-problems, based on the LP duality theory. The sub-problems are the LP problems. The process of solving the master problem begins with only a few or no constraints. The sub-problems are used to determine if optimal solutions can be obtained under the remaining constraints based on this solution to the master problem. If feasible, we will get an upper bound solution of the original problem, while forming a new objective function (feasibility cut) for the next calculation of the master problem. If infeasible, a corresponding constraint (infeasibility cut), which is most unsatisfied, will be introduced to the master problem. Then, a lower bound solution of the original problem is obtained by re-solving the master problem with more constraints. The final solution based on the BD algorithm may require iterations between the master problem and the sub-problems. When the upper bound and the lower bound are sufficiently close, the optimal solution of the original problem is achieved [12].

It is noted that the BD approach can be applied to NLP problem, but based on [13], it is possible that there is a duality gap and complementarity (equilibrium) constraints in the problem, and solving the proposed problem is hard. Hence, it is of advantage to apply the BD approach to an LP problem, as the LP model can guarantee to reach global optimal solution. Therefore, the master problem expresses the DBESS planning, but the sub-problem represents the optimal operation of distribution network with an equivalent LP model.

### 3.1 BD Structure

To accelerate the optimization solution procedure, the proposed original optimization model is decomposed by means of BD approach. Accordingly, the sizing problem is split into a tractable master problem and sub-problems based on the illustrated flowchart in Figure 3. The master problem deals with the DBESS investment planning problem and the sub-problem executes the robust optimal operation of distribution networks based on the results of the master problem. Here, it is considered that all buses of the system is capable of installing batteries. Therefore, in the following subsections, the LP model is developed to guarantee obtaining the global optimal solution.

*Master Problem:* The DBESS planning is modelled in the master part as (11) to determine the sizing of DBESS ( $\omega$ ).

$$J_p = \min_{\omega} z_{lower} \quad (11a)$$

S.to:

$$z_{lower} \geq \sum_{b \in \phi_b} c_b^s \cdot \omega_b \quad (11b)$$

$$0 \leq \omega_b \leq \omega_{max} \quad \forall b \quad (11c)$$

$$z_{lower} \geq \sum_{b \in \phi_b} c_b^s \cdot \omega_b + J_{sub}^{(m)}(\lambda_{sub}^{(m)}, \mu_{sub}^{(m)}) \quad \forall m = 1, 2, \dots, n_f \quad (11d)$$

$$J_{sub}^{(r)}(\lambda_{sub}^{(r)}, \mu_{sub}^{(r)}) \leq 0 \quad \forall r = 1, 2, \dots, n_i \quad (11e)$$

The objective function of the master problem has been expressed in (11a) that is equal to the total investment cost of DBESSs in the smart distribution networks based on (11b). Moreover, the constraint (11c) presents the size range of the DBESSs in the network. It is noted that (11b) and (11c) is called the “*initial master problem*”. In the next step, the feasibility cut of (11d) is added to the initial master problem if the primal sub-problem or dual sub-problem is feasible [21], otherwise, the infeasibility cut of (11e) is fed to the initial master problem if the primal sub-problem is infeasible or the dual sub-problem is unbounded [21]. Accordingly, the output decision variable,  $\omega$ , is calculated in the master problem and it is transmitted into the sub-problem as a constant parameter.

*Deterministic Sub-Problem:* The objective function of the deterministic sub-problem is the sum of storage degradation cost, storage operational cost and storage revenue as

mentioned in (4a) that should be minimized subject to (4b) to (4g) without (1o) as constraints. Therefore, the linear primal sub-problem can be written as follows:

$$J_{sub} = \min \underbrace{\sum_{t \in \varphi_l} \sum_{b \in \varphi_b} c_b^s \omega_b \gamma_{b,t}}_{\text{Degradation cost of storage}} + \underbrace{\sum_{t \in \varphi_l} \sum_{b \in \varphi_b} \lambda_t^{ch} P_{b,t}^{ch}}_{\text{Operational cost of storage}} - \underbrace{\sum_{t \in \varphi_l} \sum_{b \in \varphi_b} \lambda_t^{dis} P_{b,t}^{dis}}_{\text{Revenue of storage}} \quad (12a)$$

S.to:

$$PG_{b,t} - \sum_{j \in \varphi_b} A_{b,j} PL_{b,j,t} + (P_{b,t}^{dis} - P_{b,t}^{ch}) = PD_{b,t} - RES_{b,t} : \lambda_{b,t}^p \quad \forall b, t \quad (12b)$$

$$QG_{b,t} - \sum_{j \in \varphi_b} A_{b,j} QL_{b,j,t} = QD_{b,t} : \lambda_{b,t}^q \quad \forall b, t \quad (12c)$$

$$PL_{b,j,t} = g_{b,j} \left( \sum_{l \in \varphi_l} (m_l - V^{\min}) \Delta V_{b,t,l} - V^{\min} \Delta V_{j,t,l} \right) - (V^{\min})^2 b_{b,j} (\theta_{b,t} - \theta_{j,t}) : \lambda_{b,j,t}^{pl} \quad \forall b, j, t \quad (12d)$$

$$QL_{b,j,t} = -b_{b,j} \left( \sum_{l \in \varphi_l} (m_l - V^{\min}) \Delta V_{b,t,l} - V^{\min} \Delta V_{j,t,l} \right) - (V^{\min})^2 g_{b,j} (\theta_{b,t} - \theta_{j,t}) : \lambda_{b,j,t}^{ql} \quad \forall b, j, t \quad (12e)$$

$$\theta_{b,t} = 0 : \lambda_{b,t}^\theta \quad \forall b = \text{reference bus}, t \quad (12f)$$

$$\cos(k \times \Delta\alpha) \times PL_{b,j,t} + \sin(k \times \Delta\alpha) \times QL_{b,j,t} \leq SL_{b,j}^{\max} : \bar{\mu}_{b,j,t,k}^{sl} \quad \forall b, j, t, k \quad (12g)$$

$$\cos(k \times \Delta\alpha) \times PG_{b,t} + \sin(k \times \Delta\alpha) \times QG_{b,t} \leq SG_b^{\max} : \bar{\mu}_{b,t,k}^{sg} \quad \forall b, j, t, k \quad (12h)$$

$$0 \leq \Delta V_{b,t,l} \leq \Delta V^{\max} : \bar{\mu}_{b,t,l}^{\Delta v} \quad \forall b, t, l \quad (12i)$$

$$E_{b,t} = E_{b,t-1} + \eta_{ch} P_{b,t}^{ch} - \frac{1}{\eta_{dis}} P_{b,t}^{dis} : \lambda_{b,t}^e \quad \forall b, t \quad (12j)$$

$$0 \leq P_{b,t}^{ch} \leq P_b^{ch-\max} : \bar{\mu}_{b,t}^{ch} \quad \forall b, t \quad (12k)$$

$$0 \leq P_{b,t}^{dis} \leq P_b^{dis-\max} : \bar{\mu}_{b,t}^{dis} \quad \forall b, t \quad (12l)$$

$$A_{\min} \omega_b \leq E_{b,t} \leq \omega_b : \underline{\mu}_{b,t}^\omega, \bar{\mu}_{b,t}^\omega \quad \forall b, t \quad (12m)$$

)

$$E_{b,0} = E_{b,T} : \lambda_b^{ec} \quad \forall b \quad (12n)$$

$$D_{b,t} = \left(1 - \frac{E_{b,t}}{\omega_b}\right) : \lambda_{b,t}^{dod} \quad \forall b, t \quad (12o)$$

$$\sum_{p \in P} X_{b,p} w_{b,t,p} = D_{b,t} : \lambda_{b,t}^x \quad \forall b, t \quad (12p)$$

$$\sum_{p \in P} Y_{b,p} w_{b,t,p} = \rho_{b,t} : \lambda_{b,t}^y \quad \forall b, t \quad (12q)$$

$$\sum_{p \in P} w_{b,t,p} = 1 : \lambda_{b,t}^w \quad \forall b, t \quad (12r)$$

$$\gamma_{b,t} \geq \rho_{b,t} - \rho_{b,t-1} : \underline{\mu}_{b,t}^y \quad \forall b, t, \rho_{b,t-1} = 0 \Big|_{t=1} \quad (12s)$$

$$\gamma_{b,t} \geq 0 \quad \forall b, t \quad (12t)$$

Noted that the  $\lambda$  and  $\mu$  (in front of the constraints (12)) are dual variables of the constraints. Also, the terms of  $\omega_b \cdot \gamma_{b,t}$  and  $\frac{E_{b,t}}{\omega_b}$  in equations (12a) and (12o) are in the

linear form in problem (12). Because, the term  $\omega$  is a parameter in (12), where it is obtained from the master problem, (11). Therefore, the above dormulation is LP.

**Robust Sub-Problem:** In the proposed deterministic problem, (11) and (12), the charging and discharging price,  $\lambda^{ch}$  and  $\lambda^{dis}$ , active and reactive loads,  $PD$  and  $QD$ , and active power of RESs,  $RES$ , are uncertain parameters. Accordingly, the proposed problem of (11) and (12) should be written as stochastic or robust models. Also, the model (11) includes only variable  $\omega$ , as a “*hear and now*” variable, that is independent of the uncertain parameters [22]. Consequently, the robust model is not implemented on the master problem (11). However, all the variables of the deterministic sub-problem, (12), depend on the uncertain parameters that are called “*wait and see*” [22]. Therefore, the proposed robust model should be applied on the sub-problem. To this end, in the first step, the sub-problem should be converted to the standard form (5) to present the final robust model as follows:

$$J_{sub} = \min \underbrace{\sum_{t \in \mathcal{Q}_t} \sum_{b \in \mathcal{Q}_b} c_b^s \cdot \omega_b \cdot \gamma_{b,t}}_{\text{Degradation cost of storage}} + \underbrace{\widehat{\beta}_1}_{\text{Operational cost of storage}} - \underbrace{\widehat{\beta}_2}_{\text{Revenue of storage}} \quad (13a)$$

S.t:

$$\sum_{t \in \varphi_t} \sum_{b \in \varphi_b} \lambda_t^{ch} P_{b,t}^{ch} \leq \beta_1 : \mu^{\beta_1} \quad (13b)$$

$$\sum_{t \in \varphi_t} \sum_{b \in \varphi_b} \lambda_t^{dis} P_{b,t}^{dis} \leq \beta_2 : \mu^{\beta_2} \quad (13c)$$

$$PG_{b,t} - \sum_{j \in \varphi_b} A_{b,j} PL_{b,j,t} + (P_{b,t}^{dis} - P_{b,t}^{ch}) \geq PD_{b,t} - RES_{b,t} : \mu_{b,t}^p \quad \forall b, t \quad (13d)$$

$$QG_{b,t} - \sum_{j \in \varphi_b} A_{b,j} QL_{b,j,t} \geq QD_{b,t} : \mu_{b,t}^q \quad \forall b, t \quad (13e)$$

$$\text{Eq. (12d) to Eq. (12t)} \quad (13f)$$

Where, equations (13a), (13b) and (13c) are equivalent to the objective function in (12a), because,  $\beta_1$  and  $\beta_2$  are equal to the left side of (13b) and (13c), respectively, while the  $J_{sub}$  is minimized. Moreover, (13d) and (13e) are in the form of  $a \geq b$  that is equivalent to  $a = b$  due to minimization of the objective function. Finally, the robust problem model is based on section 2.4 or  $RO(\sigma, \delta)$  is as follows:

$$J_{sub} = \min \underbrace{\sum_{t \in \varphi_t} \sum_{b \in \varphi_b} c_b^s \omega_b \gamma_{b,t}}_{\text{Degradation cost of storage}} + \underbrace{\beta_1}_{\text{Operational cost of storage}} - \underbrace{\beta_2}_{\text{Revenue of storage}} \quad (14a)$$

S.t:

$$\sum_{t \in \varphi_t} \lambda_t^{ch} \left( \sum_{b \in \varphi_b} P_{b,t}^{ch} \right) + \sigma \sum_{t \in \varphi_t} \lambda_t^{ch} u_t \leq \beta_1 : \mu^{r_{ch}} \quad (14b)$$

$$\sum_{t \in \varphi_t} \lambda_t^{dis} \left( \sum_{b \in \varphi_b} P_{b,t}^{dis} \right) + \sigma \sum_{t \in \varphi_t} \lambda_t^{dis} v_t \leq \beta_2 : \mu^{r_{dis}} \quad (14c)$$

$$-\sum_{b \in \varphi_b} P_{b,t}^{ch} \leq u_t \leq \sum_{b \in \varphi_b} P_{b,t}^{ch} : \underline{\mu}_t^u, \bar{\mu}_t^u \quad \forall t \quad (14d)$$

$$-\sum_{b \in \varphi_b} P_{b,t}^{dis} \leq v_t \leq \sum_{b \in \varphi_b} P_{b,t}^{dis} : \underline{\mu}_t^v, \bar{\mu}_t^v \quad \forall t \quad (14e)$$

$$PG_{b,t} - \sum_{j \in \varphi_b} A_{b,j} PL_{b,j,t} + (P_{b,t}^{dis} - P_{b,t}^{ch}) \geq PD_{b,t} - RES_{b,t} + \sigma |PD_{b,t} - RES_{b,t}| - \delta \max \left\{ t, |PD_{b,t} - RES_{b,t}| \right\} : \mu_{b,t}^{r_p} \quad \forall b, t \quad (14f)$$



$$QG_{b,t} - \sum_{j \in \varphi_b} A_{b,j} QL_{b,j,t} \geq QD_{b,t} + \sigma |QD_{b,t}| - \delta \max \{t, |QD_{b,t}|\} : \mu_{b,t}^{r_q} \quad \forall b, t \quad (14g)$$

$$\text{Eq. (13b) to Eq. (13f)} \quad (14h)$$

The above problem is called primal sub-problem, SP1. It is noted that feasible region of SP1 will be changed by changing the output variables of the master problem [22]. Nevertheless, the dual form of SP1, named SP2, has a feasible region which is not dependent on the output variables of the master problem [22]. Therefore, the dual sub-problem (SP2) is used as follows:

$$J_{sub} = \max_{\lambda, \mu} \left\{ \sum_{b \in \varphi_b} E_{b,0} \lambda_b^{ec} + \sum_{t \in \varphi_t} \left( \begin{aligned} & \left( PD_{b,t} - RES_{b,t} \right) \mu_{b,t}^p + QD_{b,t} \mu_{b,t}^q + P_b^{ch-\max} \bar{\mu}_{b,t}^{ch} + \\ & P_b^{dis-\max} \bar{\mu}_{b,t}^{dis} + \omega_b \bar{\mu}_{b,t}^\omega + A_{\min} \omega_b \mu_{b,t}^\omega + \lambda_{b,t}^{dod} + \lambda_{b,t}^w + \\ & \left( PD_{b,t} - RES_{b,t} + \sigma |PD_{b,t} - RES_{b,t}| \right) \mu_{b,t}^{r_p} + \\ & \left( QD_{b,t} + \sigma |QD_{b,t}| - \delta \max \{t, |QD_{b,t}|\} \right) \mu_{b,t}^{r_q} \end{aligned} \right) \right\} \quad (15a)$$

$$+ \sum_{b \in \varphi_b} \sum_{t \in \varphi_t} \left( \sum_{l \in \varphi_l} \Delta V^{\max} \bar{\mu}_{b,t,l}^{\Delta v} + \sum_{k \in \varphi_k} \left( SG_b^{\max} \bar{\mu}_{b,t,k}^{sg} + \sum_{j \in \varphi_b} SL_{b,j}^{\max} \bar{\mu}_{b,j,t,k}^{sl} \right) \right)$$

S.t:

$$-\mu^{\beta_1} - \mu^{rch} \leq 1 : \beta_1 \quad (15b)$$

$$-\mu^{\beta_2} - \mu^{rdis} \leq -1 : \beta_2 \quad (15c)$$

$$\sigma \lambda_t^{ch} \mu^{rch} + \underline{\mu}_t^u + \bar{\mu}_t^u = 0 : u_t \quad \forall t \quad (15d)$$

$$\sigma \lambda_t^{dis} \mu^{rdis} + \underline{\mu}_t^v + \bar{\mu}_t^v = 0 : v_t \quad \forall t \quad (15e)$$

$$\mu_{b,t}^p + \mu_{b,t}^{r_p} + \sum_{k \in \varphi_k} \cos(k \times \Delta \alpha) \bar{\mu}_{b,t,k}^{sg} = 0 : PG_{b,t} \quad \forall b, t \quad (15f)$$

$$\mu_{b,t}^q + \mu_{b,t}^{r_q} + \sum_{k \in \varphi_k} \sin(k \times \Delta \alpha) \bar{\mu}_{b,t,k}^{sg} = 0 : QG_{b,t} \quad \forall b, t \quad (15g)$$

$$\lambda_{b,j,t}^{pl} - \sum_{b \in \varphi_b} A_{b,j} \left( \mu_{b,t}^p + \mu_{b,t}^{r_p} \right) + \sum_{k \in \varphi_k} \cos(k \times \Delta \alpha) \bar{\mu}_{b,j,t,k}^{sl} = 0 : PL_{b,j,t} \quad \forall b, j, t \quad (15h)$$

$$\lambda_{b,j,t}^{ql} - \sum_{b \in \phi_b} A_{b,j} (\mu_{b,t}^q + \mu_{b,t}^{r_q}) + \sum_{k \in \phi_k} \sin(k \times \Delta\alpha) \bar{\mu}_{b,j,t,k}^{sl} = 0 : QL_{b,j,t} \quad \forall b, j, t \quad (15i)$$

$$\mu_{b,t}^p + \mu_{b,t}^{r_p} + \mu^{\beta_2} \lambda_t^{dis} + \mu^{r_{dis}} \lambda_t^{dis} + \underline{\mu}_t^v - \bar{\mu}_t^v + \frac{1}{\eta_{dis}} \lambda_{b,t}^e + \bar{\mu}_{b,t}^{dis} \leq 0 : P_{b,t}^{dis} \quad \forall b, t \quad (15j)$$

$$-\left(\mu_{b,t}^p + \mu_{b,t}^{r_p}\right) + \mu^{\beta_2} \lambda_t^{ch} + \mu^{r_{dis}} \lambda_t^{ch} + \underline{\mu}_t^u - \bar{\mu}_t^u - \eta_{ch} \lambda_{b,t}^e + \bar{\mu}_{b,t}^{ch} \leq 0 : P_{b,t}^{ch} \quad \forall b, t \quad (15k)$$

$$\lambda_{b,t}^e - \lambda_{b,t+1}^e + \underline{\mu}_{b,t}^\omega + \bar{\mu}_{b,t}^\omega + z_b \lambda_b^{ec} + \frac{1}{\omega_b} \lambda_{b,t}^{dod} \leq 0 : E_{b,t} \quad \forall b, t \quad \& \quad z_b = 1 \quad \forall t = T \quad (15l)$$

$$\lambda_{b,t}^{dod} + \lambda_{b,t}^x \leq 0 : D_{b,t} \quad \forall b, t \quad (15m)$$

$$\lambda_{b,t}^w - X_{b,p} \lambda_{b,t}^x - Y_{b,p} \lambda_{b,t}^y \leq 0 : w_{b,t,p} \quad \forall b, t, p \quad (15n)$$

$$\lambda_{b,t}^y - \underline{\mu}_{b,t}^y + (1-y) \cdot \underline{\mu}_{b,t+1}^y \leq 0 : \rho_{b,t} \quad \forall b, t, y = 1 \Big|_{t=T} \quad (15o)$$

$$\underline{\mu}_{b,t}^y \leq c_b^s \cdot \omega_b : \gamma_{b,t} \quad \forall b, t \quad (15p)$$

$$\left(V^{\min}\right)^2 \left(b_{b,j} \left(\lambda_{b,j,t}^{pl} - \lambda_{j,b,t}^{pl}\right) + g_{b,j} \left(\lambda_{b,j,t}^{ql} - \lambda_{j,b,t}^{ql}\right)\right) + s_b \lambda_t^\theta = 0 : \theta_{b,t} \quad (15q)$$

$$\forall b, j, t \quad \& \quad s_b = 1 \quad \forall b = \text{refrence bus}$$

$$\bar{\mu}_{b,t,l}^{\Delta v} - g_{b,j} \left(\left(m_l - V^{\min}\right) \lambda_{b,j,t}^{pl} - V^{\min} \lambda_{j,b,t}^{pl}\right) + b_{b,j} \left(\left(m_l - V^{\min}\right) \lambda_{b,j,t}^{ql} - V^{\min} \lambda_{j,b,t}^{ql}\right) \leq 0 : \Delta V_{b,t,l} \quad \forall b, j, t, l \quad (15r)$$

$$\lambda = \text{free}, \quad \bar{\mu} \geq 0, \quad \underline{\mu} \leq 0 \quad (15s)$$

Problem (15) is the dual form of LP model of primal sub-problem.  $J_{sub}$  is the objective function of the dual problem, and the constraints (15b) to (15r) represent the dual constraints of the variables in the primal sub-problem which is indicated in the same equation. Constraint (15s) presents the limit of the dual variables which is determined by the constraints of the original problem.

### 3.2 BD Algorithm and Implementation

There are three possible cases after solving SP2 based on the dual problem theory as follows [21]:

(i) SP2 is infeasible, thus, the original problem (4) is either infeasible or has an unbounded objective function. In this condition the process should be stopped.

(ii) SP2 has a feasible solution and its objective function is bounded. For this case, the feasibility cut (16) should be generated and added to the master problem of the previous iteration.

$$\text{Feasibility cut: } z_{lower} \geq \sum_{b \in \phi_b} c_b^s \cdot \omega_b + J_{sub}^{(m)}(\hat{\lambda}_{sub}, \hat{\mu}_{sub}) \quad \forall J_{sub}^{(m)}(\hat{\lambda}_{sub}, \hat{\mu}_{sub}) = Eq.(15a) \Big|_{\hat{\lambda}_{sub}, \hat{\mu}_{sub}} \quad (16)$$

(iii) SP2 has a feasible solution but its objective function is unbounded. Accordingly, thus, SP3, (17) should be solved firstly, and in the next step, the infeasibility cut (18) should be generated and added to the master problem.

$$\text{SP3: } J_{sub} = Eq.(15a) \Big|_{\Omega} \quad (17)$$

$$\forall \Omega \triangleq \left\{ \lambda, \mu \mid Eq.(15a) \text{ to } Eq.(15q), \lambda = [-1, 1], \bar{\mu} = [1, \infty), \underline{\mu} = (-\infty, -1] \right\}$$

$$\text{Infeasibility cut: } J_{sub}^{(r)}(\hat{\lambda}_{sub}, \hat{\mu}_{sub}) \leq 0 \quad \forall J_{sub}^{(r)}(\hat{\lambda}_{sub}, \hat{\mu}_{sub}) = Eq.(17a) \Big|_{\hat{\lambda}_{sub}, \hat{\mu}_{sub}} \quad (18)$$

where  $\hat{\lambda}$  and  $\hat{\mu}$  are optimal values of  $\lambda$  and  $\mu$  in SP2/SP3.

It is noted that the convergence criteria for the BD algorithm is to satisfy  $|z_{upper} - z_{lower}| \leq \varepsilon$ , where  $\varepsilon$  is the BD's convergence tolerance, and  $z_{upper}$  is the value of the objective function mentioned in (19). Noted that, the second part of (19) refers to  $J_{sub}$  for SP2. Also, the value of  $z_{lower}$  is determined in the last iteration based on the results of solving optimization problem of (11). That is, the BD convergence check is obtained if SP2 is feasible. The flowchart of implementing BD for the proposed problem is shown in Figure 4.

$$z_{upper} = \sum_{b \in \phi_b} c_b^s \cdot \hat{\omega}_b + J_{sub}(\hat{\lambda}_{sub}, \hat{\mu}_{sub}) \quad \forall J_{sub}(\hat{\lambda}_{sub}, \hat{\mu}_{sub}) = Eq.(12a) \Big|_{\hat{\lambda}_{sub}, \hat{\mu}_{sub}} \quad (19)$$

## 4 Case Study and Discussion

### 4.1 Standard test network and data

The 19-bus LV CIGRE benchmark grid illustrated in Figure 5 [12] is used for simulation

studies. The grid parameters are shown in Table 2. Also, the problem data is listed in Table 3.

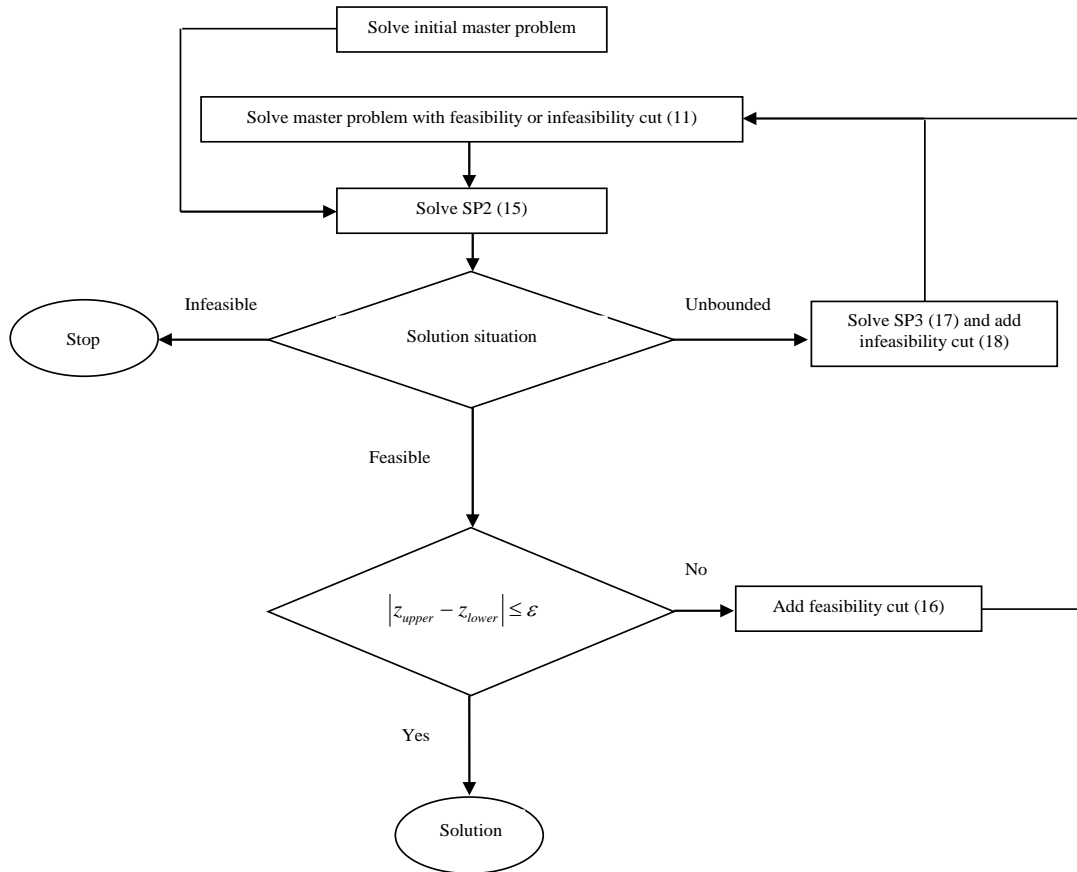


Figure 4: BD algorithm to solve the proposed robust problem.

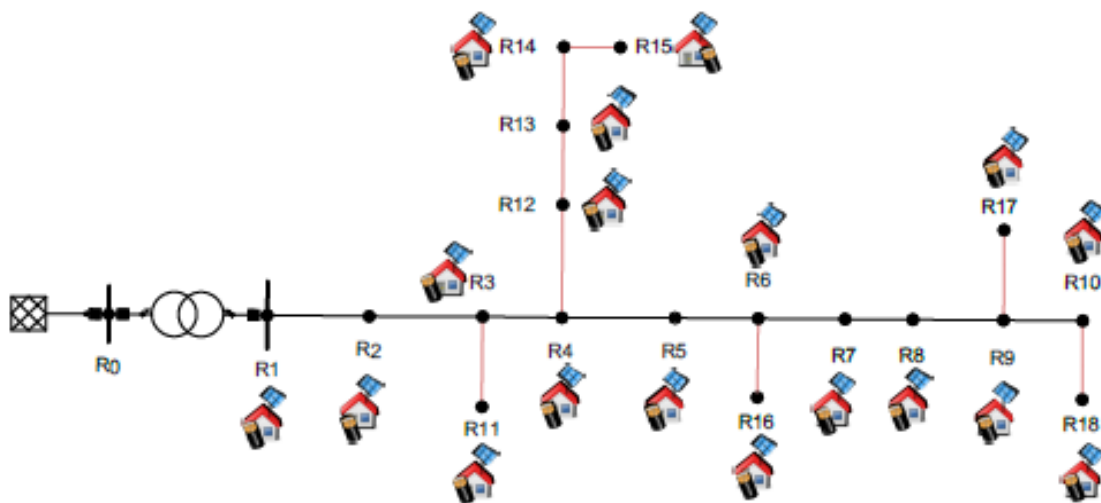


Figure 5: 19-bus LV CIGRE benchmark grid [19].

This research configures the distribution network with a high photovoltaic penetration assuming that it can exploit the full roof top area of a single household based on [12]. Hourly load percent for one year used for a house based on [23]. Also, hourly energy (charging and discharging) price for one year is based on NordPool market in zone of LT [24].

It is noted that in this research, the hourly power percent of PV for one year is based on [25].

## 4.2 Simulation Results: Computational Efficiency

The proposed deterministic and robust models are coded in GAMS 23.5.2 software and they are solved using the CPLEX solver in GAMS [26].

**A. The Results of The Different Deterministic Models:** In this section, the storage maximum capacity and PV capacity are considered 300 kWh and 20 kW, respectively. Moreover, the simulation of the proposed model applied on one year with 8760 hours, and the objective function present the annual profit of all storage systems. Also, number of linearization segments of the voltage magnitude term and circular constraints are equal to 5 and 30, respectively, in the LP model based on BD approach. Results of this section have been presented in Table 4 to compare different cases in NLP and LP based on the BD deterministic models. As shown in Table 4, it can be inferred that:

- The NLP solvers such as CONOPT, COUENNE, IPOPT, MINOS and SNOPT [26] have different results in convergence iteration, calculation time, objective function value and model status, while the total number of equations and variables is the same for all solvers.
- Also, the model status of NLP is locally optimal with the objective function value of 4102.562 EUR/year in the best condition that is occurred in IPOPT solver.
- But, the optimal situation with the lower value of the objective function (3331.220 EUR/year) has been obtained by LP model using BD approach, where the best solver for this case is CPLEX due to the low execution time with respect to the solvers of CBC and CONOPT [26].

- Therefore, the LP model based on BD approach with the CPLEX solver is suitable and reliable for the proposed deterministic or robust problem model based on Table 4.

**Table 2. Line and substation parameters of the LV CIGRE benchmark grid [19].**

Substation parameters					
Start Node	End Node	Resistance [ohm]	Reactance [ohm]	Voltage [kV/kV]	Max power [MVA]
R0	R1	0.0032	0.0128	20/0.4	0.5
Line parameters					
Start Node	End Node	Resistance [ohm/km]	Reactance [ohm/km]	Length [m]	Max current [A]
R1	R2	0.405	0.205	35	398
R2	R3	0.405	0.205	35	398
R3	R4	0.405	0.205	35	398
R4	R5	0.405	0.205	35	398
R5	R6	0.405	0.205	35	398
R6	R7	0.405	0.205	35	398
R7	R8	0.405	0.205	35	398
R8	R9	0.405	0.205	35	398
R9	R10	0.405	0.205	35	398
R3	R11	2.05	0.212	35	158
R4	R12	2.05	0.212	30	158
R12	R13	2.05	0.212	35	158

R13	R14	2.05	0.212	35	158
R14	R15	2.05	0.212	35	158
R6	R16	2.05	0.212	30	158
R9	R17	2.05	0.212	30	158
R10	R18	2.05	0.212	30	158

Table 3. Problem data

<b>Storage units</b>	18
<b>Maximum storage capacity (kWh)</b>	10 to 300
<b>Storage roundtrip efficiency (charging and discharging)</b>	0.88 [12]
<b>Annual investment cost of storage (EUR/MWh/year)</b>	5000 [12]
<b>Charge and discharge rate (kW)</b>	Maximum storage capacity [12]
<b><math>A_{\min}</math> (%)</b>	15%
<b>Prediction horizon (hour)</b>	8760
<b>Year</b>	1 year
<b>Time step (hour)</b>	1
<b>Maximum power of PV (kW)</b>	10 to 20
<b>Power percent of PV</b>	Hourly pattern for one year is based on [25]
<b>Load of house (kW, kVAr)</b>	(5, 1) [12]
<b>Minimum and maximum voltage (per unit)</b>	0.9 and 1.1 [12]
<b>Base power (MVA)</b>	0.5
<b>Base voltage (kV)</b>	0.4

**B. The BD convergence in Different Robust Models:** Figure 6 shows the convergence progress of the proposed BD algorithm for the different cases of the robust distributed storage planning problem. Based on this figure, the BD convergence iteration is 19, 31

and 36 for  $RO(\sigma, \delta) = (0, 0.02)$ ,  $(0, 0)$  and  $(0.1, 0)$ , respectively. Note,  $RO(0, 0.02)$ ,  $RO(0, 0)$  and  $RO(0.1, 0)$  express the impact of the feasibility tolerance ( $\delta$ ) in robust model, deterministic model, and impact of uncertainty level ( $\sigma$ ) on the robust solution. Therefore, it can be said that  $RO(0, 0.02)$  calculates the optimal solution with the lower number of iterations due to increasing feasibility space with respect to the feasibility space of the deterministic model. But, the feasibility space decreases in  $RO(0.1, 0)$  with respect to the feasibility space of the deterministic model due to increased uncertainty level in comparison with the deterministic model. As a result, the number of iterations of the BD convergence is high in this robust model.

**Table 4. Comparison of different solvers results for deterministic model**

Model	Solver	Total number of equations	Total number of variables	Convergence iteration	Calculation time (s)	Objective function (EUR/year)	Model status
<b>NLP</b>	CONOPT	5363547	3009801	390	461.437	5371.324	Locally optimal
	COUENNE	5363547	3009801	-	-	-	Infeasible
	IPOPT	5363547	3009801	54	517.845	4102.562	Locally optimal
	MINOS	5363547	3009801	412	2384.671	4864.483	Locally optimal
	SNOPT	5363547	3009801	-	-	-	Infeasible
<b>LP based on BD</b>	<b>CPLEX</b>	<b>52*</b> , <b>3006324**</b>	<b>20*</b> , <b>7573638**</b>	<b>31</b>	<b>18.013</b>	<b>3331.220</b>	<b>Optimal</b>
	CBC	52*, 3006324**	20*, 7573638**	31	19.438	3331.220	Optimal
	CONOPT	52*, 3006324**	20*, 7573638**	31	22.764	3331.220	Optimal

\* This number shows the number of the master problem's equations or variables (in the iteration that the problem is converged)

\*\* This number shows the number of the sub-problem's equations (variables)



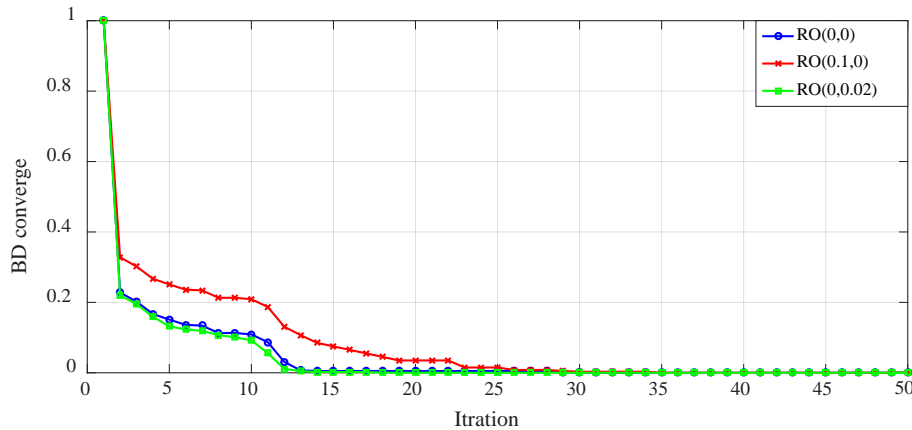


Figure 6: BD converge for different cases of the robust model

### 4.3 Simulation Results: Technical Aspect

**A. The Value of Uncertain Parameters in Different Robust Models:** In this section, the values of the uncertain parameters in the different cases of the robust model are shown in Table 5. Based on the this table, active and reactive loads as well as energy price (active power of PV) are increased (decreases) in the scenario with RO(0.1,0) with respect to the scenario of deterministic model, i.e., RO(0,0). Because, the uncertainty level ( $\sigma$ ) has been increased in RO(0.1,0) in comparison with RO(0,0). It is noted that the proposed objective function, (4a), minimizes (maximizes) the total storage economic loss (profit), hence, it is expected that the profit will be high if discharging revenue of all storages is high and the total storage cost (charging, storage degradation and investment) is low.

It is noted that the discharging revenue of all storages will be increased if the active load and energy price increase and the active power of PV reduces. The reason is that the storage systems have stored the produced energy of their related PVs, thus the revenue is zero in this condition, nevertheless, in the case of supplying loads by the storage systems in the discharging mode, and then the revenue is not zero for such condition. Also, the profit is low in the worst case scenario of RO(0.1,0) if the load and energy price (PV power) are decreased (increased).

In addition, the active and reactive loads as well as energy price (active power generations of PVs) are decreased (increased) in the scenario with RO(0,0.02) with respect to the scenario of deterministic model, RO(0,0), since, the feasibility tolerance ( $\delta$ ) is increased in RO(0,0.02) with respect to RO(0,0). It is noted that increasing  $\delta$  will expand the feasibility region of the proposed problem, thus, it is expected that the profit

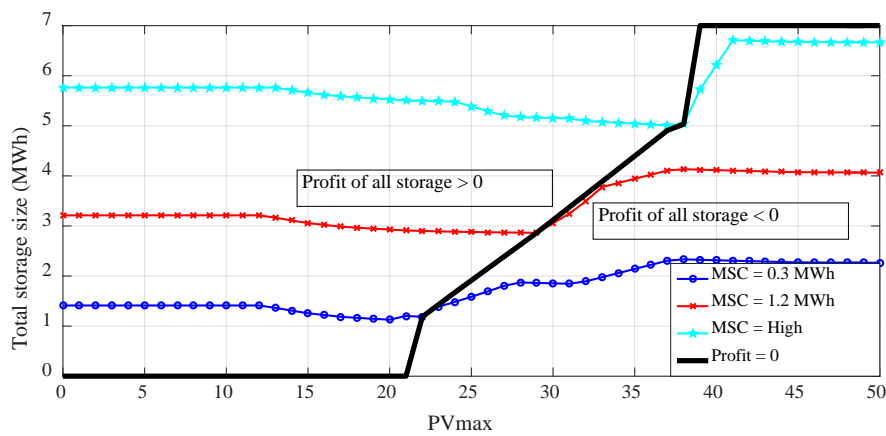
will be improved, i.e., it is increased with respect to RO(0,0). Consequently, increasing  $\delta$  will increase (reduces) the load and energy price (PV power).

**Table 5, The value of uncertain parameters in different robust models for one year with PV capacity of 10 kW**

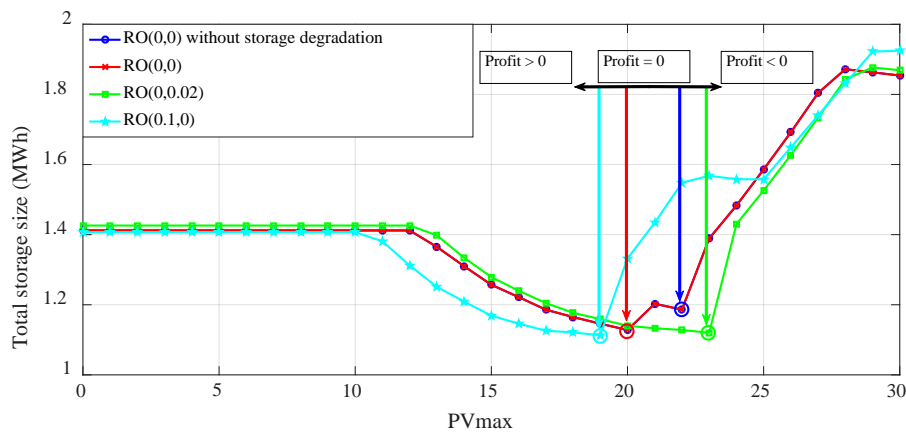
Parameter	RO(0,0)	RO(0,0.02)	RO(0.1,0)
Total active load of network (pu)	5.584	5.695	5.025
Total reactive load of network (pu)	1.117	1.139	1.005
Total average active power of PVs (pu)	4.415	4.327	4.857
Total energy price (EUR/MWh)	446510.88	455441.098	401859.792

**B. Sizing and Placement based on Distributed Strategy:** In the distributed strategy, it is considered that the batteries can be installed in different buses of the system. Figure 7 shows the total size of all distributed storage systems in the network based on the size of each PV and the maximum storage capacity (MSC) for different cases of the robust model. In the case of RO(0,0) without considering the storage degradation as seen in Figure 7 (a), the total size of all distributed storage systems is constant if PV size changes from 0 to 12 kW. However, this value will be reduced for the PV size above 12 kW in the part with “*Profit of Storage* > 0”. For the reason that the system operation limits, i.e., (1g) to (1i), constrain the increment of the size of some distributed storage systems in these conditions. For example, if the system operation limits such as voltage, line flow and station power limits are ignored from the proposed problem, hence, the total size of all distributed storage systems would be equal to  $18 \times \text{MSC}$ , where 18 is the number of storage locations. Therefore, it can be said that the system operation limits are important in specifying the total size of all distributed storage systems. Moreover, it is noted that the charging cost will increase if the PV size is increased, because, the PV energy is more than load energy if the PV size increased. Hence, the excess energy of the PVs will be stored in the storage systems, thus, the charging cost of the storage systems based on equation (4a) will be increased. Also, discharging the revenue of the storage systems will be reduced in this condition, because, the more portion of the supplied energy to loads is generated by PVs. Therefore, it is possible to have negative profit for the storage systems. Accordingly, the larger sizes of the total distributed storage systems would be not suitable in the larger sizes of PVs. This statement has been shown in Figure 7 (a) in the part with “*Profit of Storage* < 0”.

In addition, the total size of all distributed storage systems is increased if the maximum storage capacity increases based on Figure 7. Finally, it is noted that the PV size (PVmax) will be increased if the MSC increases as shown in the section of “Profit = 0” in Figure 7. Because, the profit of the right side of this curve is negative, thus, it can be inferred that in the curve with “Profit = 0”, the PV size is the maximum for different values of MSC. Figure 7 (b) shows the total size of all distributed storage systems in the network versus PV size for different cases of the robust model. Based on this figure, the storage size of the cases RO(0,0) with/without considering the storage degradation is the same. Nonetheless, the storage size will be increased (reduced) if  $\delta(\sigma)$  increased.



(a)



(b)

**Figure 7: Total size of all distributed storage systems in the network versus each PV sizes, a) RO(0,0) without storage degradation, b) robust models**

Also, the maximum PV size is high and low in the cases of RO(0,0.02) and RO(0.1,0), respectively. In other words, according to Figure 7 (b), the profit of the storage is non-positive ( $\leq 0$ ) if the PVmax is more than 22, 20, 23 and 19 kW for the cases RO(0,0) without storage degradation, RO(0,0), RO(0,0.02), and RO(0.1,0), respectively.

In Table 6, the annual investment and charging as well as the degradation cost, annual discharging revenue and annual profit of all distributed storage systems are depicted for different robust model. Based on this table, the annual investment cost of the storage will be increased in the case of higher maximum capacities. But, the annual investment cost and storage size are reduced by increasing the PV size or PV penetration rate in different robust models. Because based on Figure 7, the total size of all distributed storage systems is increased for the higher maximum storage capacities and it would be decreased by increasing the size of PV. In addition, increasing PV penetration rate and maximum storage capacity in the different robust models caused that the annual charging cost and discharge revenue of the all distributed storage systems increased based on Table 6. Indeed, the charging power of storage systems is increased if the PV penetration rate is increased to satisfy the constraints (1g) to (1i), and the discharging power of storage systems is increased to minimize the objective function of (4a) and to satisfy the constraints (1g) to (1i). Moreover, the degradation cost of all storage system is reduced (increased) if PVmax (MSC) increases.

**Table 6, Comparison of economic results for the distributed storages**

Model	RO(0,0) without storage degradation				RO(0,0)			
	0.15		0.30		0.15		0.30	
MSC (MWh)	0.15		0.30		0.15		0.30	
PVmax (kW)	10	20	10	20	10	20	10	20
Investment cost (EUR/year)	5562	4138	7062	5638	5562	4138	7062	5638
Charging cost (EUR/year)	12298	20264	15414	23380	12298	20264	15414	23380
Degradation cost (EUR/year)	-	-	-	-	8	7.2	10.5	10.1
Discharging revenue (EUR/year)	26487	25138	33714	32365	26478	25128	33702	32351
Profit (EUR/year)	8627	736	11238	3347	8610	719	11216	3323
Model	RO(0,0.02)				RO(0.1,0)			

MSC (MWh)	0.15		0.30		0.15		0.30	
PVmax (kW)	10	20	10	20	10	17	10	19
Investment cost (EUR/year)	5674	4202	7125	5702	5243	4128	7232	6145
Charging cost (EUR/year)	12145	19795	15231	22973	12429	16498	16241	23715
Degradation cost (EUR/year)	8	7.2	10.5	10.1	8.2	7.35	10.65	10.26
Discharging revenue (EUR/year)	26873	25469	34233	32840	24451	21771	30966	30224
Profit (EUR/year)	9046	1465	11867	4155	6771	1138	7432	352

In comparison between cases RO(0,0) without and with storage degradation, the investment and charging cost of the storage systems is the same based on Table 6, and the discharging revenue is reduced in RO(0,0) with respect to the RO(0,0) without storage degradation. Because, the discharging mode or contribution of the storage system would be reduced in RO(0,0) with respect to the RO(0,0) without storage degradation due to the second part of equation (4a). Hence, the discharging power,  $P^{dis}$ , and discharging revenue only changes in RO(0,0) in comparison with RO(0,0) without storage degradation. Also, there is a degradation cost in RO(0,0), therefore, the storage systems profit in RO(0,0) is less than RO(0,0) without storage degradation. Moreover, the charging cost of the storage systems reduces/increases in RO(0,0.02)/RO(0.1,0), and the investment cost and discharging revenue of storage systems reduces/increases in RO(0.1,0)/RO(0,0.02). For the reason that the load and energy price/PV power increases with increasing  $\delta/\sigma$  and reduces with increasing  $\sigma/\delta$  based on Table 5. Therefore, charging cost/discharging revenue and investment cost are increased with increasing  $\sigma/\delta$ . Also, the degradation cost is almost the same in cases RO(0,0), RO(0,0.02) and RO(0.1,0).

**C. Sizing and Placement Based on Centralized Strategy:** In this strategy, it is considered that the one battery can be installed in the optimal location of the system. Hence, equation (11c) rewritten as  $0 \leq \omega_b \leq \omega_{max} x_{s_b}$ , where  $x_{s_b}$  is a binary variable for storage installation. Thus, the storage installed if  $x_{s_b} = 1$ , otherwise, it is not installed. Moreover, the constraint of  $\sum_b x_{s_b} = 1$  should be added to the master problem, (11), for

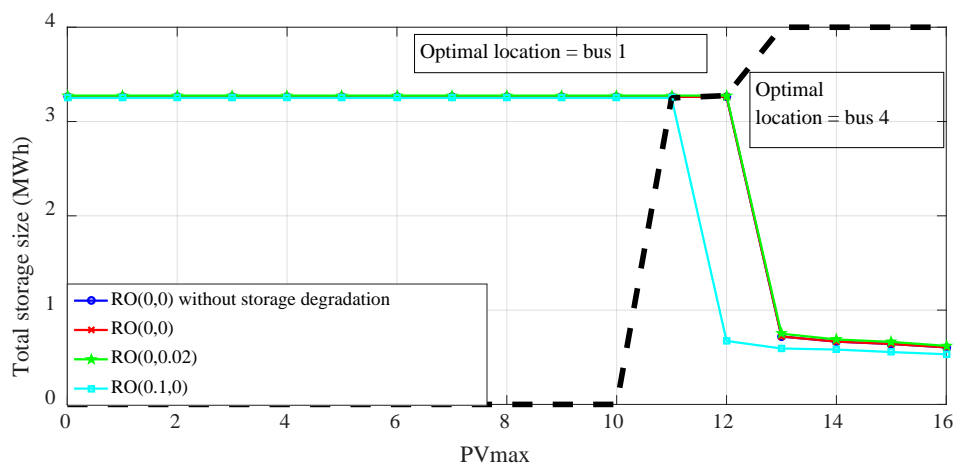
the centralized strategy. Therefore, the output variables of the master problem are  $x_s$  and  $\omega$ . Based on this strategy, the results of the centralized storage systems planning have been expressed in Table 7 and Figure 8. In Table 7, the optimal location of storage system is bus 1 for different cases of the robust model for the smaller sizes of the PVs, but, the location of the storage would be changed to bus 4 in the larger sizes of the PVs for different cases of the robust model. According to the try-and-error approach (similar to the analysis in Figure 7 (b) for the distributed strategy), the maximum PV sizes in the centralized strategy are determined to be 18.3, 18.2, 18.8 and 16 kW for cases of RO(0,0) without storage degradation, RO(0,0), RO(0,0.02) and RO(0.1,0), respectively. Based on these assumptions, as results of Table 7 show, in the case of  $PV_{max} = 10$  kW, the investment and charging cost of the storage systems is the same for the cases of RO(0,0) without storage degradation and RO(0,0), while the discharging revenue has been reduced in RO(0,0) with respect to the RO(0,0) without storage degradation. Also, there is a degradation cost in RO(0,0), therefore, the storage systems profit in RO(0,0) is less than RO(0,0) without the storage degradation. Moreover, the charging cost of the storage systems has been reduced/increased in RO(0,0.02)/RO(0.1,0), and the investment cost and discharging revenue of the storage systems have been reduced/increased in RO(0.1,0)/RO(0,0.02), respectively. Also, the degradation cost is almost the same in cases RO(0,0), RO(0,0.02) and RO(0.1,0). Consequently, as results of Table 7 show the profit of the storage is based on different costs and revenues.

**Table 7, Comparison of economic results for the centralized storages**

Model	RO(0,0) without storage degradation		RO(0,0)		RO(0,0.02)		RO(0.1,0)	
	MSC (MWh)	Inf		Inf		Inf		Inf
PVmax (kW)	10	18.3*	10	18.2*	10	18.8*	10	16*
Optimal location (bus)	1	4	1	4	1	4	1	4
Optimal storage capacity (MWh)	3.262	0.543	3.262	0.545	3.275	0.546	3.250	0.532
Investment cost (EUR/year)	16311	2717	16311	2727	16516	2731	16250	2659

<b>Charging cost (EUR/year)</b>	37587	13900	37587	13668	38249	14326	34223	11733
<b>Degradation cost (EUR/year)</b>	-	-	22.26	24.67	22.2	24.75	22.6	24.47
<b>Discharging revenue (EUR/year)</b>	77447	16658	77440	16586	78842	17109	70383	13432
<b>Profit (EUR/year)</b>	23550	41	23523	168	23995	28	19907	15

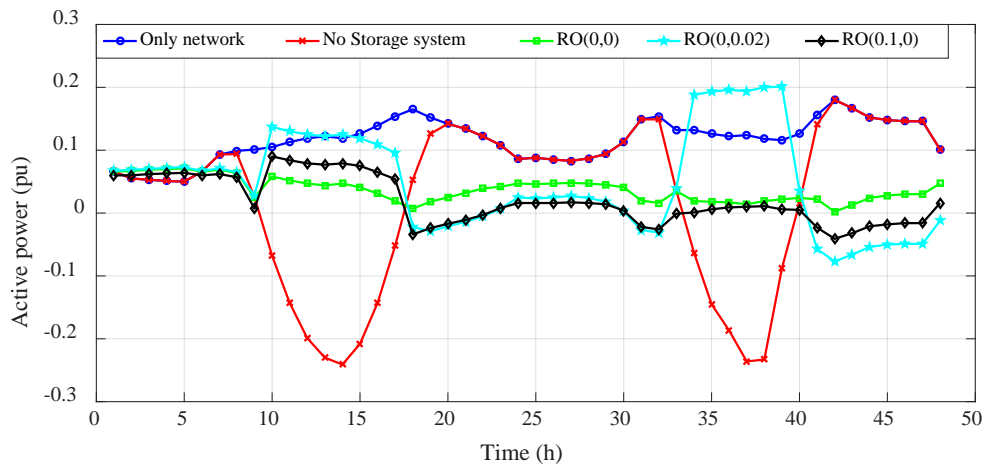
\* Display the maximum value of PVmax in different cases of the robust model



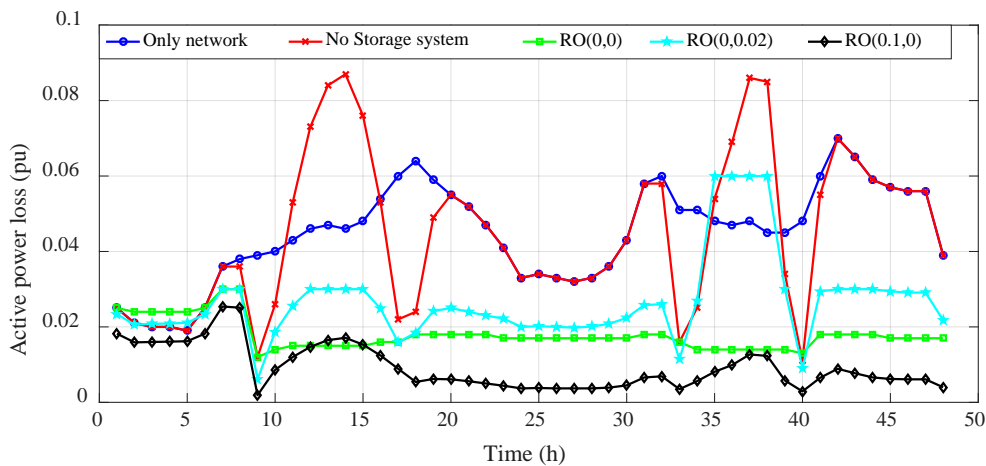
**Figure 8: Size of centralized storage system based on PV size for different robust models**

Figure 8 shows the storage system size versus the PV size for the case that the optimal location of the storage system is bus 1 for the PV size between 0-12 kW at cases RO(0,0) without the storage degradation, RO(0,0) and RO(0,0.02), and it is bus 1 for the PV size between 0-11 kW at RO(0.1,0). Also, the storage size is constant for the PV size between 0-12 kW and 0-11 kW at cases RO(0,0) without storage degradation, RO(0,0) and RO(0,0.02), and RO(0.1,0), respectively. In the Figure 8, the graph has been split to two regions by a dotted line. Indeed, the left side and right side of the dotted line refer to the regions that the optimal location of the storage is bus 1 and bus 4, respectively. Also, it is observed in the figure that the storage size are reduced if the PV size goes above 12 or 11 kW for the cases RO(0,0) without storage degradation, RO(0,0) and RO(0,0.02), and RO(0.1, 0), respectively.

**D. Investigating Network Indexes and Flexibility:** For this purpose, at first, the main assumptions for this study are: maximum size of the storages is 150 kWh for two days (48 hours), the maximum power of PVs is 10 kW, and the energy price, load percent and PV power percent are based on the data of 30 Sept. and 1 Oct. 2017 in [23]-[25]. Also, it is assumed that the objective function of (12a) has been changed to the minimization of the voltage deviation using  $\sum_{b \in \phi_b} \sum_{t=1}^{48} (V_{b,t} - V_{ref})^2$  to investigate the effects of charging/discharging profile of storages on the network indexes. Considering this objective function will affect the storage profile in a way to improve network indexes and enhance PV penetration conditions. Based on the above assumptions, the simulations have been executed and the results have been illustrated in Figure 9 and Figure 10.

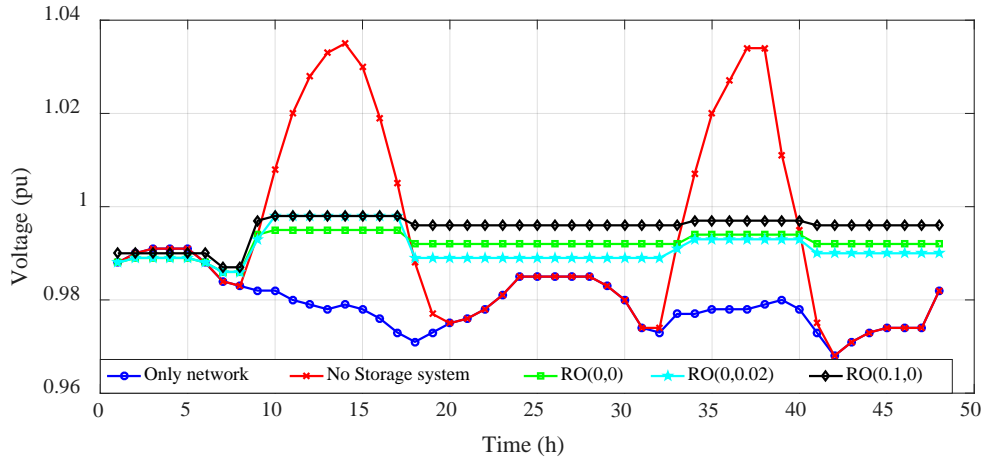


(a)



(b)





(c)

**Figure 9: Effects of storages on the network indexes: a) daily pattern of active power of station bus, b) daily pattern of network active power loss, c) daily pattern of mean voltage of network buses.**

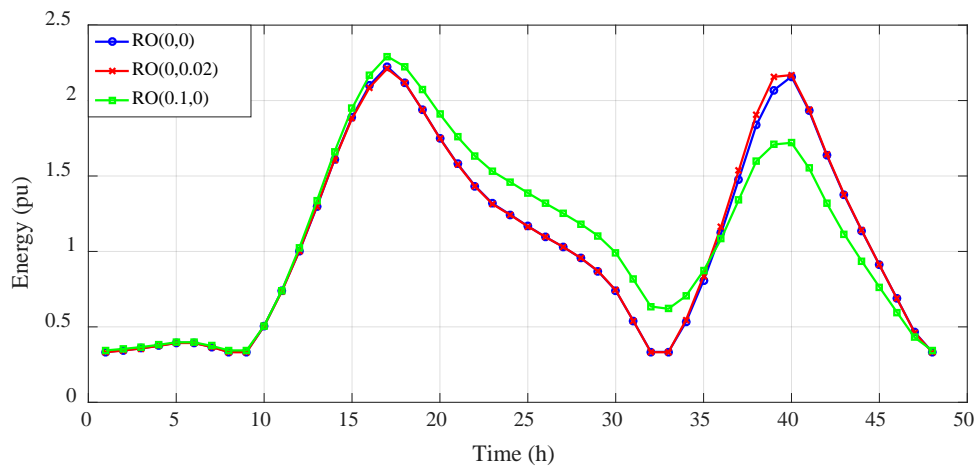


**Figure 10: Daily pattern of the stored energy in all storage systems.**

In this study, four cases are considered: network without PV and storage, network with PV and without storage, and network with PV and storage for RO(0,0), RO(0.1,0) and RO(0,0.02). As shown in Figure 9 (a), the PVs inject their generations in the periods of 10:00–17:00 of 30 Sept. and 9:00–16:00 of 1 Oct. This fact results in the higher network active power loss and increased voltage profile in these periods in case of network without the storage system with respect to the case we have only network as shown by Figures 9 (b) and (c). However, adding storage in cases RO(0,0), RO(0.1,0) and RO(0,0.02), has improved the profiles of the voltage and active power loss and station power as shown in Figure 9. For the reason that, in the low load conditions, the PVs have charged the storage system in the cases RO(0,0), RO(0.1,0) and RO(0,0.02), and the

storages injects back the stored energy to the network in peak load times as shown in Figure 10. Indeed, as Figure 10 shows the storage systems are charged in period of 10:00 to 17:00 of 30 Sept. and 9:00 to 16:00 of 1 Oct. by PVs based on Figure 9 (a). Also, the storage systems inject the energy back to the network in periods of 18:00 of 30 September to 8:00 of 1 October and 17:00 to 24:00 of 1 October. Accordingly, the load profile is flat, where this statement shows the high flexibility in cases RO(0,0), RO(0.1,0) and RO(0,0.02). Also, the storage has been operated in a way that the active power of the station, active power loss and voltage in cases RO(0,0.02) and RO(0.1,0) have been increased with respect to RO(0,0) for some hours, and decreased in some other hours as shown by Figures 9 (a)-(c). This is because of the existing uncertain parameters in different robust models. Also, the daily pattern of the stored energy in all storage systems is almost the same for cases RO(0,0) and RO(0,0.02), but it is increased/decreased at periods 1:00-35:00/36:00-48:00 in RO(0.1,0) with respect to the cases of RO(0,0) and RO(0,0.02).

**E. Comparison between centralized and decentralized BESS planning:** The comparison results of both centralized and distributed strategies of placing storage systems in the network have been addressed in Table 8. As table shows, in the case of unlimited capacity assumption for the storage systems for both strategies, the maximum size of PV is 18 and 38 kW (according to the try-and-error approach), and the total storage size (obtained by the optimization) is 0.583 and 5.033 MWh for the centralized and distributed storage systems, respectively. In addition, the results confirm the superiority of the distributed strategy for placing storage systems in terms of the voltage deviation and energy loss with respect to the centralized storage planning.

**Table 8, Comparison of centralized and distributed storage planning strategies**

Case	Centralized storage planning	Distributed storage planning
Maximum storage capacity (kWh)	Inf.	Inf .
Maximum size of PV (kW)	18	38
Total storage size (MWh)	0.583	5.033
Minimum voltage deviation, i.e., $\sum_{b \in \phi_b} \sum_{t=1}^{48} (V_{b,t} - V_{ref})^2$ , (pu)	0.2231	0.1011
Annual energy loss (kWh)	3476.3	2647.5

## 5 Conclusions

This research presents a robust planning of distributed battery energy storage systems (DBESSs) from the viewpoint of distribution system operator to increase the network flexibility. It is part of T5.3 in INVADE project, which focuses on planning phase of flexibility algorithm. Accordingly, based on the proposed deterministic robust model, the difference between the DBESS planning, degradation and operation (charging) costs and revenue of DBESS due to selling of its discharge power is minimized as the objective function subject to the problem constraints including the AC power flow equations in the presence of RESs and DBESSs, and limits of network indexes, RESs and DBESSs constraints. The original problem is in the form of NLP, accordingly, the equivalent LP model based on the BD approach has been proposed using the first-order expansion of Taylor's series for linearization of power flow equations and the polygon for linearization of circular inequality.

Results imply the LP model based on the BD approach can obtain optimal solution with a satisfactory calculation speed. In addition, to deal with the uncertainty sources (including active and reactive load, energy or charging/discharging price and output power of RESs), the bounded uncertainty-based robust optimization has been developed. The storage system size is high/low in low/high value of PV size. Considering the theoretical properties of the proposed model and the results of the case studies carried out, the conclusions below are in order:

- The obtained results underscore the importance of considering distributed strategy for placing storages in the distribution networks. Therefore, one should be aware that a system with enough storage capacity to cover power mismatches in the case of uncertain renewable energy sources, may not be able to utilize the available storage capacity due to congestions in the network. This is one of the main issues addressed in this report, and is important in INVADE exploitation activities.
- The obtained results illustrate that sizing and sitting of DBESSs highly depend on the adjusting parameters of the uncertainty in the robust models, this should be further included in decisions made by the INVADE pilot planners.
- The results pinpoint the necessity of an accurate AC power flow method for an economically proper system operation.
- Moreover, the distributed storage systems can improve the network and flexibility indexes with respect to the centralized storage system. Indeed, the distributed storage systems can control the network and flexibility indexes locally with dividing

costs between multiple customers or companies in comparison with the centralized storage system. Noted that, this strategy could be a suitable scheme to utilize the possible benefits of the mobile storages of electric vehicles in parking lots which are located in different sites of the INVADE platforms, and in specific in the Dutch and Norwegian pilots.

## References

- [1] Eurelectric, Flexibility and Aggregation Requirements for their interaction in the market, *Eurelectric*, 2014.
- [2] S.Ø. Ottesen, P. Olivella-Rosell, P. Lloret, A. Hentunen, P. Crespo del Granado, S. Bjarghov, V. Lakshmanan, J. Aghaei, M. Korpås and H. Farahmand, “Simplified Battery operation and control algorithm,” Deliverable D5.3, EU-INVADE, 2017.
- [3] S. Pirouzi, J. Aghaei, V. Vahidinasab, T. Niknam, and A. Khodaei, “Robust linear architecture for active/reactive power scheduling of EV integrated smart distribution networks,” *Electric Power System Research*, vol. 155, pp. 8-20, 2018.
- [4] J. Qiu, J. Zhao, H. Yang, D. Wang, Z.Y. Dong, “Planning of solar photovoltaics, battery energy storage system and gas micro turbine for coupled micro energy grids,” *Applied Energy*, vol. 219, pp. 361-369, 2018.
- [5] M.R. Jannesar, A. Sedighi, M. Savaghebi, J.M. Guerrero, “Optimal placement, sizing, and daily charge/discharge of battery energy storage in low voltage distribution network with high photovoltaic penetration,” *Applied Energy*, vol. 226, pp. 957-966, 2018.
- [6] J. Cervantes, F. Choobineh, “Optimal sizing of a nonutility-scale solar power system and its battery storage,” *Applied Energy*, vol. 216, pp. 105-115, 2018.
- [7] E. Grover-Silva, R. Girard, G. Kariniotakis, “Optimal sizing and placement of distribution grid connected battery systems through an SOCP optimal power flow algorithm,” *Applied Energy*, vol. 219, pp. 385-393, 2018.

- [8] M. Bucciarelli, S. Paoletti, A. Vicino, “Optimal sizing of energy storage systems under uncertain demand and generation,” *Applied Energy*, vol. 225, pp. 611-621, 2018.
- [9] Y. Zhang, S. Ren, Z.Y. Dong, Y. Xu, K. Meng, and Y. Zheng, “Optimal placement of battery energy storage in distribution networks considering conservation voltage reduction and stochastic load composition,” *IET Generation, Transmission & Distribution*, vol. 11, no. 15, pp. 3862-3870, 10 19 2017.
- [10] A. Meechaka, A. Sangswang, K. Kirtikara, and D. Chenvidhya, “Optimal location and sizing for PV system and battery energy storage system using ABC algorithm considering voltage deviation and time of use rate,” *9th International Conference on Information Technology and Electrical Engineering (ICITEE)*, Phuket, pp. 1-6, 2017.
- [11] E. Nasrolahpour, S.J. Kazempour, H. Zareipour, and W. D. Rosehart, “Strategic sizing of energy storage facilities in electricity markets,” *IEEE Transactions on Sustainable Energy*, vol. 7, no. 4, pp. 1462–1472, 2016.
- [12] P. Fortenbacher, A. Ulbig, and G. Andersson, “Optimal Placement and Sizing of Distributed Battery Storage in Low Voltage Grids using Receding Horizon Control Strategies,” *IEEE Transactions on Power Systems*, vol. 33, no. 3, May 2017.
- [13] S. Pirouzi, J. Aghaei, M.A. Latify, G.R. Yousefi, and G. Mokryani, “A robust optimization approach for active and reactive power management in smart distribution networks using electric vehicles,” *IEEE System Journal*, pp. 1-12, 2017.
- [14] S. Pirouzi, J. Aghaei, T. Niknam, M. Shafie-khah, V. Vahidinasab, and J.P.S. Catalão, “Two alternative robust optimization models for flexible power management of electric vehicles in distribution networks,” *Energy*, vol. 141, pp. 635-652, 2017.
- [15] J. Kim, Y. Choi, S. Ryu, and H. Kim, “Robust operation of energy storage system with uncertain load profiles,” *Energies*, vol. 10, pp. 1-15, 2017.
- [16] R.A. Jabr, I. Džafić, and B.C. Pal, “Robust optimization of storage investment on transmission networks,” *IEEE Transactions on Power Systems*, vol. 30, no. 1, pp. 531-539, 2015.
- [17] S. Pirouzi, J. Aghaei, M. Shafie-khah, G.J. Osório, J.P.S. Catalão, “Evaluating the security of electrical energy distribution networks in the presence of electric vehicles,” in *Proc. PowerTech Conf, IEEE Manchester*, pp. 1-6, 2017.
- [18] S. Pirouzi, J. Aghaei, “Mathematical Modeling of Electric Vehicles Contributions in Voltage Security of Smart Distribution Networks,” *SIMULATION: Transactions of the Society for Modeling and Simulation International*, (article in press), 2018.

- [19]S. Pirouzi, J. Aghaei, T. Niknam, H. Farahmand, and M. Korpås, “Proactive Operation of Electric Vehicles in Harmonic Polluted Smart Distribution Networks,” *IET Generation, Transmission and distribution*, vol. 12, pp. 967-975, 2018.
- [20]M.A. Ortega-Vazquez, “Optimal scheduling of electric vehicle charging and vehicle-to-grid services at household level including battery degradation and price uncertainty,” *IET Generation, Transmission & Distribution*, vol. 8, pp. 1007-1016, 2014.
- [21]J.F. Benders, “Partitioning procedures for solving mixed-variables programming problems,” *Numer. Math.*, vol. 4, no. 1, pp. 238-252, 1962.
- [22]A.J. Conejo, E. Castillo, R. Minguez, and R. Garcid-Bertrand, *Decomposition Techniques in Mathematical Programming*, Springer, 2006.
- [23]C. Bucher and G. Andersson, “Generation of domestic load profiles – an adaptive top-down approach,” in *Proceedings of PMAAPS 2012*, Istanbul, Turkey, June 2012.
- [24]Nord Pool, <https://www.nordpoolgroup.com/historical-market-data/>.
- [25]M. Malvoni, M.G.D Giorgi, P.M. Congedo, “Data on photovoltaic power forecasting models for Mediterranean climate,” *Data in Brief*, vol. 7, pp. 1639-1642, 2016.
- [26]Generalized Algebraic Modeling Systems (GAMS). [Online]. Available: <http://www.gams.com>.